NOAA Technical Memorandum ERL ESG-15

THE OPERATIONAL METEOROLOGY OF CONVECTIVE WEATHER

VOLUME II: STORM SCALE ANALYSIS

Charles A. Doswell III

Environmental Sciences Group
Boulder, Colorado
April 1985

noaa NATIONAL OCEANIC AND ATMOSPHERIC ADMINISTRATION / Environmental Research Laboratories

NOAA Technical Memorandum ERL ESG-15

THE OPERATIONAL METEOROLOGY OF CONVECTIVE WEATHER
VOLUME II: STORM SCALE ANALYSIS

Charles A. Doswell III
Weather Research Program

Environmental Sciences Group
Boulder, Colorado
April 1985

UNITED STATES
DEPARTMENT OF COMMERCE

Malcolm Baldrige,
Secretary

NATIONAL OCEANIC AND
ATMOSPHERIC ADMINISTRATION

Environmental Research
Laboratories

Vernon E. Derr,
Director

NOTICE

Mention of a commercial company or product does not constitute an endorsement by NOAA Environmental Research Laboratories. Use for publicity or advertising purposes of information from this publication concerning proprietary products or the tests of such products is not authorized.

Preface

> What is the insight with which the scientist tries to see into nature? Can it indeed be called either imaginative or creative? To the literary man the question may seem merely silly. He has been taught that science is a large collection of facts; and if this is true, then the only seeing which scientists need to do is, he supposes, seeing the facts....Science is nothing else than the search to discover unity in the wild variety of nature -- or more exactly, in the variety of our experience. Poetry, painting, the arts are the same search, in Coleridge's phrase, for unity in variety.
>
> -- Jakob Bronowski, **Science and Human Values**

> The scholar must organize; one builds scientific knowledge with facts as one builds a house with stone; but accumulation of facts makes no more a science than a pile of stones makes a house.
>
> -- Henri Poincare', source unknown

> As mathematics, a human invention that parallels but never touches reality, gives the astronomer metaphors through which he may comprehend the powers and the flow of things: so the human sense of beauty is our metaphor of their excellence, their divine nature: -- like dust in a whirlwind, making the wild wind visible.
>
> -- Robinson Jeffers, "The Double Axe"

This second volume is an attempt to summarize the basics of what we know about the topic meteorologists call convection. Since an anticipated third volume in this series is to deal with applications, the emphasis here (as in Volume I) is on science, again without mathematics. To some extent this material is written to stand alone, but it is my hope that some of what I see as the essential unity in all this multi-volume presentation will show through. References internal to these volumes follow an outline structure of the form: **II**.III.B.1.c.ii..., where the leading, boldface Roman numeral refers to the volume. This is omitted for references elsewhere in the same volume.

As I expected, there are already changes in Volume **I** that I would like to make. No doubt the same thing will occur throughout this sometimes painful but always enjoyable writing process. Perhaps even more than in the first volume, the reader is urged to pursue relentlessly the references given here. Since my experience suggests that many operational meteorologists have been poorly prepared in this area, my view of their best action plan is to read widely on the science of meteorological convection. I make no pretense of being totally even-handed in my treatment of these topics, but I hope I haven't been dogmatic. Where views exist which differ from my own, I've tried to include references to alternate viewpoints.

Many of my unacknowledged colleagues may recognize some of their phrases or ideas contained in this text. I hope this can be taken as a measure of my respect for their input. The list of such contributions would be voluminous, but in no way diminishes their individual value. It is the sharing of ideas that makes one's career as a scientist so pleasurable. Thank you one and all.

While I have dwelt at length at times on things we don't know about the problem, I hope the reader will appreciate that there is a considerable understanding upon which we can draw for use in, for example, forecasting. It has been my intent with this series to

draw attention to what we do know, as well as to point out where problems and gaps in that understanding exist.

In acknowledging the host of colleagues who have contributed in some way to this volume, special thanks are owed to Mr. Leslie R. Lemon (Sperry Corp.). His knowledge and enthusiasm are responsible in many ways, not only for this volume, but for contributions to me as a scientist. It has been a privilege and a pleasure to work with him. I also wish to express my gratitude to Prof. Yoshi K. Sasaki (Univ. of Oklahoma) for sharing his profound insights and for his support in my graduate studies, both of which helped make this work possible.

Valuable reviews were provided by: Dr. Joseph T. Schaefer (NWS-CRH/SSD); Dr. Preston Leftwich (NSSFC/TDU); Dr. Richard Rotunno, Mr. Edward Szoke, and Mr. Morris Weisman (NCAR); Mr. Donald W. Burgess and Dr. Robert P. Davies-Jones and Dr. David Rust (NSSL); Mr. Gary Grice and Mr. Alan R. Moller (NWSFO -- San Antonio and Fort Worth, Texas, respectively); and Mr. Leslie R. Lemon. There is no doubt in my mind that this document has been dramatically improved by the reviewers' thoughtful comments, suggestions, and criticisms. As always, any remaining defects are my sole responsibility.

Finally, numerous individuals contributed many of the pieces needed to put all this together. Mr. Donald L. Kelly (NWS-CRH) provided help in obtaining climatological data and Mr. Jose Meitin (WRP) produced plots of those data for analysis. Valuable assistance in obtaining photographs and/or figures was rendered by: Mr. Alan R. Moller (NWS, Fort Worth, TX); Mr. Donald W. Burgess and Dr. Robert P. Davies-Jones (NSSL); Mr. Erik N. Rasmussen (NOW Weather, Inc.); Dr. Robert A. Maddox and Mr. David O. Blanchard (WRP); Dr. Nancy Knight and Mr. Edward Szoke (NCAR); and Mr. John Weaver (NESDIS). Drafting and photographic reproduction were provided by ERL/Weather Research Program. As with Volume I, Mrs. Beverly Lambert (NSSFC/TDU) did a magnificent job with preliminary manuscript preparation, while Chris Anderson and Sandie Chandler (WRP) helped get the final draft ready.

Charles A. Doswell III
Boulder, Colorado
March, 1985

CONTENTS

THE OPERATIONAL METEOROLOGY OF CONVECTIVE WEATHER
VOLUME II: STORM-SCALE ANALYSIS

I. Introduction

> The chessboard is the world, the pieces are the phenomena of the universe, the rules of the game are what we call the laws of Nature. The player on the other side is hidden from us. We know that his play is always fair, just and patient. But we also know, to our cost, that he never overlooks a mistake, or makes the smallest allowance for ignorance.
>
> -- T.H. Huxley, **A Liberal Education**

In the introduction to Vol. **I** (**I.I.**B), considerable effort was expended to provide some motivation for the scale of phenomena to be discussed. When talking of storm-scale events, it becomes more difficult to say precisely what is meant. For operational mesoanalysis, the emphasis was on scales between the Rossby radius of deformation (a length of ~ 1500 km) and a somewhat ill-defined lower limit (~ 100 km), where Coriolis accelerations and ageostrophic advection are both important. One might be tempted to say that by storm-scale, we mean things involving spatial scales below 100 km. This is not completely adequate.

The difficulty here is that convectively-dominated phenomena, which are indeed the processes of interest, can overlap this lower limit somewhat. While individual convective elements almost certainly fall below the 100 km limit, the systems which they create can exceed this by an order of magnitude (Maddox, 1980). Thus, what we have chosen to be "storm scale" falls somewhere well above 100 km at its large end, but descends to perhaps a few km at its small end. That is, items of interest include the range from individual convective elements, to large mesoscale systems which are intimately linked to the convection. While we are as yet relatively ignorant of how convection feeds back to larger scales, it seems that progress is being made. From a theoretical viewpoint, there is more certainty about the small end of "storm scale" events, because we can neglect certain things (like Coriolis force).

It is logical to ask, "Why are convective elements so thoroughly confined to small horizontal space scales?" The answer is, as are most "answers" in meteorology, not available in the sense of a complete understanding. However, one can use an analogy to gain some insight: which is easier to pull quickly up out of the water, a pencil or a pie plate? Naturally, this analogy is not totally satisfactory, since the issue in it is determined by the effects of form drag, which is not the whole problem in convection (although it may play a role). Turner (1973, Ch. 7) has pointed out (see p. 226 ff.) that convection is essentially **intermittent.** Because the atmosphere does not conduct heat very well and is quite transparent to incoming solar radiation, heat tends to accumulate at low levels, where the ground is being warmed by the insolation. Further, except in shallow layers (usually near the surface), the stratification is almost always stable with respect to unsaturated vertical motion. If the heat could always be transported by wide, flat convection cells, the results would be less violent weather, with much less intermittency. Owing to greater stability in the cool season, most convection at that time is via large-scale circulations which are, indeed, wide and flat. With greater heat input and a greater ability to hold moisture at low levels in the warm season, these less violent processes are simply not efficient enough to transfer the input vertically.

Although intense convection is intermittent, and relatively rare at any given location, it is a much more effective vertical heat transfer mechanism than weak,

shallow forms. Why a particular place and time are chosen to be the occasion for this concentrated heat transport is an essential question of this volume. One easily verified notion in atmospheric convection is that the stronger the vertical motion, the smaller the total area occupied by that motion. However, this does not mean that the resulting effects on the surroundings are correspondingly limited in areal extent!

Perhaps it is obvious, but it is useful to understand the importance of convection. In simple terms, convection is the process of vertical transport of air parcels between levels in the vertical. In doing so, convection mixes all the properties of the air (heat, moisture, momentum) in such a manner as to reduce the vertical gradients of those properties. Parcels brought up (or down) to another level are then moved about by horizontal motions (the process of advection) and considerable redistribution of the properties of the atmosphere can result (Hitschfield, 1960). It is this horizontal redistribution which makes definition of storm-scale so difficult, despite the fact that the really intense vertical motions are spatially confined.

As if that were not enough, the redistributions can have a profound influence on the convection itself and its subsequent evolution. Further, the convective processes can alter significantly the conditions controlling the large-scale flow (which is predominantly horizontal by virtue of its spatial scale). The details of how this mutual feedback operates in the real atmosphere are basically unknown. This has obvious implications about our ability to predict the sensible weather -- the features produced by convection can dominate the events which follow, but our knowledge of how the constituent processes interact is severely limited.

The limitations on our knowledge have their origin primarily in the data network's limitations. The data available to an analyst/forecaster from conventional sources (surface and upper-air observations, satellite imagery, radar) are barely adequate for what was called "operational mesoanalysis," (in Vol. I) which involves systems 100's of km in extent, or larger. If the dominant physical processes are at scales below this, there is not much information. What can be seen in the conventional data are isolated pieces of a picture which is vastly more complex. Thus, we find ourselves in the position of the proverbial group of blind men, trying to understand the elephant. Each sees it from the viewpoint of whatever piece of the beast's anatomy happens to be in his grasp.

If this were the totality of the situation, then things would be quite grim. However, there is cause for some optimism in storm-scale analysis. Consider a situation where the men are not blind, but only blindfolded, and already know what an elephant is (not necessarily the same one being sampled). Then their limited sample while blindfolded could lead to considerable insight about their observations, hopefully leading them to conclude that they are dealing with an elephant, even if they might not be able to give an accurate estimate of its height, or whether it has been painted pink. Even this limited perception is an improvement over thinking of the sample in terms of a tree or a rope! In the same way, the research done on convective weather can provide working models with which we can try to piece together what convective systems are doing, even though we can only see a piece of them. We may not be able to give an accurate estimate of the peak pressure, or whether the detail fits the model we carry in our minds, but we are certainly better off than if we had never seen such a system before.

Research on mesoscale aspects of convective weather systems using non-operational, dense data networks has provided us with considerable knowledge of the features common to those systems. Even though those special-purpose data generally are not available to operational analyst/forecasters, the findings are available, and can be integrated into operational forecasting/warning problems. Such knowledge can be used

to infer what is going on, or what is likely to be happening in the future.

This requires some change in emphasis for this volume in comparison to the preceding one, since more stress is necessarily put on the **content** of published research, rather than on summarizing the conclusions. It is the application of conceptual models derived from research efforts which gives us the opportunity to make useful diagnoses and forecasts of storm-scale events based on the limited observations. At the same time, we should be prepared to make serious errors of interpretation, correcting and updating our mental models as new data come in. This process is uniquely human, and no machine is likely to usurp this capability in the foreseeable future. Lest we get too smug about this, it also carries with it the potential for mistakes which no purely objective system would make. In effect, it is a price we pay for the ability to think beyond what computer models can do.

One of the things humans do in their efforts to make some sense of what they see is to **categorize** things. This volume is no different -- a convective storm classification scheme is developed which I think is useful (the only valid test of a classification scheme). No such scheme is going to be universally accepted because, in part, categories usually represent some sort of essentially arbitrary breakdown, whereas the real phenomena do not recognize arbitrary boundaries. If our understanding of the storm-scale phenomena were sufficiently deep, the arbitrary nature of a classification scheme could be reduced; boundaries between classes could then be based on real physical differences. Since definitive knowledge of these phenomena is not available, we shall have to make do with what we have. While not complete, what we have is also not inconsiderable.

In what follows, basic physical concepts, as they are currently known and generally accepted, are emphasized. Naturally, these ideas are subject to change as research and new observations lead to new insights. Readers of the references and current journals are better prepared to include those new findings into the operational routine. Furthermore, they are equipped to **judge for themselves** which of the competing ideas best suit their needs, and don't have to depend on someone else's interpretations. Even more than in Volume **I**, the references should be used in an aggressive program of self-paced study, in order to get the most out of this material. I realize that it is not always easy (or even possible) in an operational environment to find the required time. It is merely my observation that one should not assume that reading this volume will give one all that is needed.

II. Non-Severe Convection

> ...Pearl cumuli over the highest mountains -- clouds not with a silver lining, but all silver. The brightest, crispest, rockiest-looking clouds, most varied in features and keenest in outline I ever saw at any time of year in any country. The daily building and unbuilding of these snowy cloud-ranges -- the highest Sierra -- is a prime marvel...no rock landscape is more varied in sculpture, none more delicately modeled than these landscapes of the sky; domes and peaks rising, swelling, white as finest marble...
>
> -- John Muir, **My First Summer in the Sierra**

A. Cumulus Convection

1. General Concepts

The vast majority of convection is non-severe. Since convection is understood by meteorologists to mean energy transfer in the vertical (Ludlam, 1980, p. 129), most convection therefore involves relatively weak vertical motions. This is consistent with what has been said about large-scale flow -- strong vertical motions are produced only on rare occasions and are invariably limited in space and time. Often, convection is made visible by cumulus (or, more generally, cumuliform) clouds. However, one should be aware that not all convection results in clouds.

It is worthwhile to digress a bit concerning whether or not it is meaningful to make a distinction between severe and non-severe forms of convection. One can argue that deciding whether an event is severe or non-severe is arbitrary, rather than based on physical, dynamical differences between events. There is now good evidence (from numerical simulations) that weak convection can be organized into structures similar to those seen in strong convection. If an otherwise undistinguished thunderstorm produces a single 2 cm (3/4 in) diameter hailstone (and this stone is observed -- see IV. A) is this a severe storm? Is a storm which creates a peak surface wind gust of 49 knots physically distinct from one with a peak gust of 50 knots? These are disturbing thoughts if one wants to make **severe** convection a distinct category.

This argument is particularly telling if one is going to do a scientific analysis of convection. One certainly wants categories to reflect distinct physical entities insofar as this is possible. Thus, I'm in agreement with the argument, at least in principle. However, this volume makes the distinction between severe and non-severe convection for several reasons. First and most important, **whether a storm is severe or not is a distinction which operational forecasters have to make**! In effect, the somewhat arbitrary criteria for deciding whether or not a storm is severe do have significance for the forecasters, scientific subtleties notwithstanding. Also, it is clear that we do tend to find some real physical differences, at least in a statistical sense, between severe and non-severe convection. One certainly sees physical differences among cumulus, ordinary thunderstorms, and supercells. The statistical odds for producing even a nominally severe event change as we move from class to class. While the vast majority of severe weather is associated with certain storm types, there is a non-zero probability that even a cumulus cloud could be associated with a severe event!

Since most significant convective weather phenomena are associated with those somewhat isolated cases of strong vertical motions, one might logically ask, "Why bother to examine the weak convection?" Apart from any general statements about the value of knowledge for its own sake, there are some compelling reasons to understand the problem of non-severe convection.

First, it is desirable to examine what is, after all, the **dominant** form of convection. It is easier to understand the severe forms when we know the basic factors influencing and limiting ordinary convection. Second, in spite of its apparent simplicity, ordinary convection is a rich field of study, full of complexities which have potential application to stronger forms. Third, the sheer numbers of ordinary convective elements allow them to have collective influences far beyond those of any individual element, however violent. Fourth, every severe storm has its origins in what may initially be ordinary convection. Finally, ordinary convection produces much of the convective precipitation, beneficial or otherwise.

Cumulus clouds (of all types) represent the visible manifestation of buoyant plumes or elements. This, as we have discussed to some extent in Volume **I**, is a reflection of the bulk thermodynamic properties of the environment in which convection occurs. If the stratification of the environment is such that a parcel's initial vertical displacement is accelerated, that stratification is termed unstable and convection is possible. Any standard textbook (e.g., Byers, 1959) describes ordinary cumulus convection in these terms. Typically, isolated elements (parcels) near the surface become warmer than their surroundings, perhaps owing to surface "hot spots", which might arise because, say, one underlying surface absorbs solar radiation more effectively than others. If they can remain warmer than their environment, these initially buoyant elements continue to rise and may eventually reach a level where condensation occurs (appropriately called the **lifted condensation level** -- LCL). Since the environment normally shows only modest horizontal variations in the thermodynamic stratification, a field of cumulus clouds has very nearly a uniform base.

If the lapse rate in the environment associated with a field of cumulus were absolutely unstable (i.e., superadiabatic), the cumulus would keep on rising. However, as is well-known, the environmental lapse rate through deep layers is invariably less than adiabatic. This observation is mute testimony to the effectiveness of convection at redistributing heat. Should superadiabatic lapse rates arise somehow, they are modified rapidly by the ensuing convection.

Consider the typical vertical structure as it evolves during a day in which ordinary "fair-weather" cumulus occur. Overnight, a surface inversion has formed, which effectively de-couples the atmosphere above the inversion from the layer that close to the ground.[1] As the sun heats the surface, parcels rising through the inversion have a cumulative heating effect, but their upward penetration is severely limited by the very stable lapse rate. That is, the rising parcels are halted in their ascent by encountering warmer air aloft (which is, after all, the definition of an inversion). Thus, they slow down and stop their ascent before they can reach condensation and no clouds are seen. However, these parcels mix with their surroundings, invisibly preparing the way for their successors to rise even higher. Thus, dry convection is the means by which the nocturnal inversion is eventually eliminated, carrying the heat of insolation upward (Zeman and Tennekes, 1977). The process is depicted schematically in Fig. 2.1.

What sort of lapse rate is created by this process? In detail, the picture is very complex, with heated parcels carried by their momentum into slightly warmer surroundings as they reach the base of the inversion. Since the rising parcels expand and cool dry adiabatically as they mix with their surroundings, the environment as a whole comes to look more like the parcels. The result is a surface-based layer of nearly dry adiabatic lapse rate, through which parcels can rise unimpeded before they encounter the inversion.

---

[1] Of course, this has a dramatic effect on the low-level winds, as described in **I**.III.F.3.

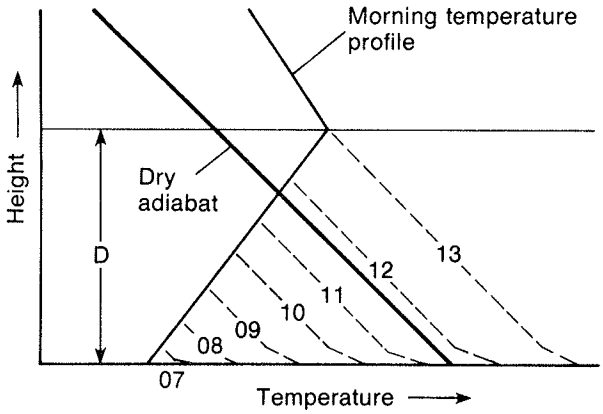

Figure 2.1 Illustrating erosion of surface inversion by heating. Numbers above temperature axis give the hour (in local time) as heating raises the surface temperature and moves the profile toward the right, eventually breaking the surface inversion.

Thus, as dry convection proceeds, the low-level inversion is gradually broken down and lifted, perhaps eventually disappearing altogether. By considering the environmental lapse rate above the inversion (remember, it is most certainly less than dry adiabatic), it can be seen that after the parcels break through the inversion, the stratification above **still** does not permit deep accelerations. Rather, the parcels gradually slow down and end up oscillating about their equilibrium positions (see below for details) as they mix with the environment. Thus, as seen in Fig. 2.2, a new inversion is created by the mixing effect of the convection, at the top of the layer in which convection is occurring.

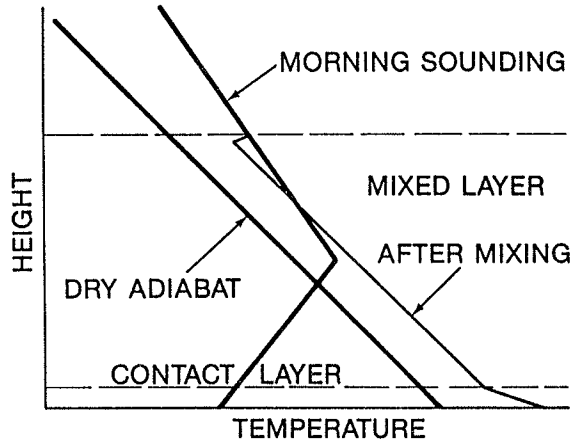

Figure 2.2 Profiles of temperature in the mixed layer before and after mixing. Note the inversion just below the top of the mixed layer, where the dry adiabat (constant θ) characteristic of the mixed layer joins the unaffected temperature profile above the mixing layer.

Further, a shallow "contact" layer often exists very close to the surface in which the lapse rate is indeed superadiabatic.[2] This shallow superadiabatic layer results from the relatively weak conductive ability of air and the lack of strong vertical currents for convection close to the surface. That is, the lowest few tens of meters receive the heat from the surface and are unable to transport it vertically fast enough to prevent the formation of a shallow superadiabatic layer.

---

[2] Detailed observations show that within the lowest few meters, the lapse rate can become "autoconvective". An autoconvective lapse rate is about 34°C km^{-1}. This means the air column is so warm at its bottom that density actually increases with height! The resulting overturning causes mirages and the shimmering effect seen over roads on a sunny day.

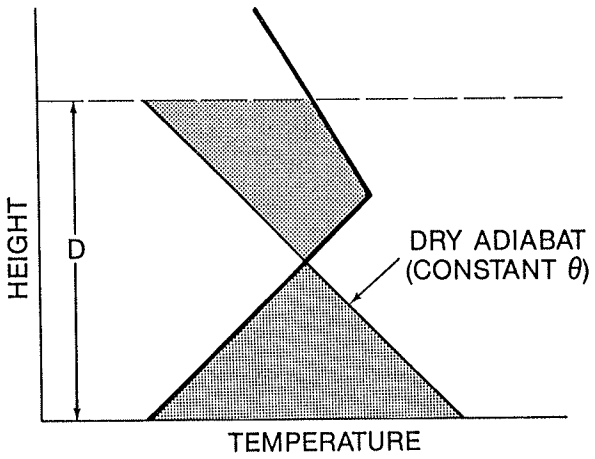

Figure 2.3 Showing how to find the average θ within the assumed depth of the mixed layer (D) by equal areas above and below (stippled), from the morning sounding (thick line).

Therefore, under "fair weather" conditions, the morning sounding is transformed by solar heating such that the resulting **mixed** layer has a nearly constant potential temperature (θ). If solar heating is the only effect, the value of θ in the mixed layer should be greater by evening than the mean value in the morning sounding. That is, if we compare the dry adiabat (constant θ) in the morning which equalizes positive and negative areas across the approximate depth of the mixed layer (as in Fig. 2.3), with that in the following evening, the evening value should be higher (by, say, $\sim 2°C$). Should the afternoon value be the same (or lower), then some process -- probably horizontal advection -- has cancelled (or exceeded) the gain from solar heating.

Up to this point, the formation of clouds has not been mentioned. Since the mixing process can occur with or without moisture, there may not be any obvious visible evidence for the convection just described. Note that convective overturning tends to redistribute moisture, as well as heat. If mixing is sufficiently strong and there are no significant advective processes, the moisture profile should come to resemble one of constant mixing ratio in the mixed layer (Schaefer, 1976; Mahrt, 1977). That is, one might expect the air in the mixed layer to be very nearly uniform in the vertical with respect to heat and moisture.[3] However, if there is no inversion capping the mixed layer, moisture can be dispersed rapidly in the vertical. Thus, deep mixed layers often show a substantial moisture lapse, and tend to be relatively dry throughout, despite having a nearly uniform potential temperature.

If the moisture content is sufficient, thermals rising out of the contact layer can result in cloud formation. This process, shown schematically in Fig. 2.4, gives rise to the **convective condensation level** (CCL). The height of the CCL corresponds quite closely in most instances to the observed base of cumulus clouds. Note that the CCL is not generally equivalent to the lifting condensation level (LCL), which is derived by lifting a parcel with properties defined at a single height level on the sounding (see e.g., Hess,

[3] The mixing process also tends to redistribute momentum, so the wind profile in the mixed layer can be quite uniform, except for a shallow layer near the surface where the wind velocity decreases rapidly to zero. This is complicated somewhat by the considerations of **Ekman layer theory.** The Ekman layer provides the coupling between the friction-dominated surface layer and the essentially frictionless "free atmosphere" above. While the theory is well-developed, predicting a veering wind profile as one rises through the Ekman layer, there are many complications in reality. This is a topic well beyond the scope of these notes, but the reader should consult, e.g., Holton (1979, Ch. 5), Tennekes and Lumley (1972), or Mahrt and Pierce (1980).

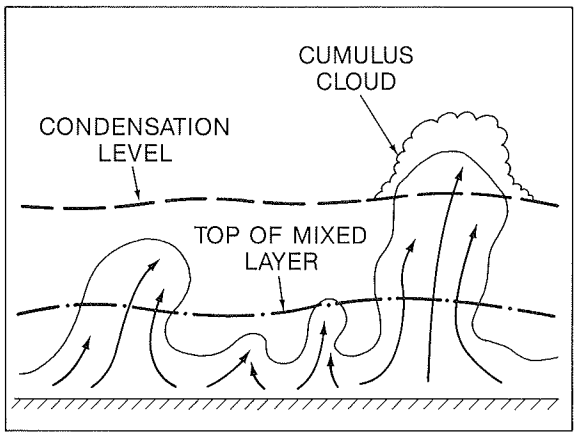

Figure 2.4 Schematic showing formation of cumulus cloud by thermals rising out of the well-mixed layer and reaching condensation. Note that the well-mixed layer rises during the day as solar heating proceeds.

1959, Ch. 4). Of course, late in the afternoon, when mixing is rather thorough, the LCL and CCL are essentially identical. As indicated by Ludlam (1980), actual cloud bases tend to lie a few hundred meters above the calculated condensation level. This can be the result of a variety of processes, including **entrainment.**

Before considering entrainment, we should examine the structure of circulations associated with ordinary cumulus. Since the dominant visual feature of cumulus convection is clouds, it is easy to overlook the fact that mass continuity requires downward motions **outside** the clouds, with downward mass fluxes equivalent to the upward transfer within the clouds. Thus, a key problem is the **distribution** of ascent and descent in space.

For a single convective element, the buoyancy of the initial thermal rising out of the contact layer is generally rather modest (a few °C). Since the environment within the mixed layer is nearly neutrally stratified (i.e., a dry adiabatic lapse rate), the parcel should remain weakly buoyant through its rise toward the inversion capping the mixed layer. Neglecting entrainment, this gives it a weak acceleration. Specifically, the parcel accelerates at about 0.003g for every 1°C of positive temperature excess, where g is the acceleration owing to gravity (9.8 m s^{-2}). Even that amount of acceleration acting on a parcel (initially at rest) for 1 min yields a vertical velocity of about 2 m s^{-1}. Since ordinary cumulus clouds are associated with vertical velocities of a few m s^{-1}, the average temperature excess over the lifetime of the convective element (several min) must be less than 1°C.

When the rising parcel encounters the inversion, it suddenly finds itself colder than its environment by an amount which depends on the strength of the inversion. Therefore, it is decelerated. However, this does **not** mean that the parcel stops dead at the base of the inversion. It has acquired a vertical motion and cannot just come to an immediate halt -- rather, it overshoots the level where it would be in equilibrium (not to be confused with the EL of I.II.C.2) and continues to rise until all its upward momentum has been cancelled by the negative buoyancy.

However, once it has been halted it cannot remain at that level either, since it is now colder than its environment. Hence, it sinks back down (warming dry adiabatically) through the inversion. Such a sinking parcel eventually finds itself once again warmer than its environment, so its **downward** movement is decelerated. Thus, the parcel oscillates about its equilibrium position and these oscillations gradually die out (owing to internal friction). The frequency of these oscillations has a special name: the **Brunt-Väisälä** (B-V) frequency. Theory predicts that the B-V frequency is related to the

stability. For realistic lapse rates (less than dry adiabatic), as the stability increases, the B-V frequency increases (i.e., the oscillations are more rapid). Further, the amplitude (or strength) of unforced oscillations decreases as the frequency increases. Thus, as shown in Table 2.1, as conditions become more stable, the oscillations become more difficult to observe.[4]

TABLE 2.1a

	T_o = 300°K		T_o = 273°K	
γ (°C km^{-1})	N (s^{-1})	p (min)	N (s^{-1})	p (min)
9.0	5.1×10^{-2}	20.5	5.4×10^{-2}	19.5
6.0	1.1×10^{-2}	9.4	1.2×10^{-2}	9.0
3.0	1.5×10^{-2}	7.0	1.6×10^{-2}	6.7
0.0	1.8×10^{-2}	5.9	1.9×10^{-2}	5.6
-3.0	2.0×10^{-2}	5.1	2.1×10^{-2}	4.9
-6.0	2.3×10^{-2}	4.6	2.4×10^{-2}	4.4

Table 2.1a Brunt-Väisälä frequency (N) and period (P) as a function of Lapse Rate (γ). Formula used is $N = \left[\frac{g}{T_o}(\Gamma_d - \gamma)\right]^{\frac{1}{2}}$, *where* $\Gamma_d = 9.8^{o}C\ km^{-1}$ *(the dry adiabatic lapse rate),* T_o *and g is the acceleration owing to gravity. The period p is related to the frequency by* $p = 2\pi/N$.

TABLE 2.1b

	w_o (m s^{-1})				
N	0.1	0.5	1.0	5.0	10.0
5.4×10^{-2}	18.5	92.6	185.2	925.9	1851
1.2×10^{-2}	8.33	41.7	83.3	416.6	833.3
1.6×10^{-2}	6.25	31.3	62.5	312.5	625.0
1.9×10^{-2}	5.26	26.3	52.6	263.2	526.3
2.1×10^{-2}	4.76	23.8	47.6	238.1	476.2
2.4×10^{-2}	4.17	20.8	41.7	208.3	416.6

Table 2.1b Amplitude (z, in meters) of B-V oscillations as a function of initial draft velocity (w_o). *Formula used is* $z = w_o/N$ *(Dutton, 1976, p. 72).*

[4] Anderson (1960) has observed a bimodal oscillation period in cumulus convection. The long-period mode of about 11 min corresponds roughly to an expected B-V oscillation. The short-period mode has a period of about 30 s, which is clearly associated with some much smaller scale phenomenon.

These oscillations, when associated with cumulus clouds, occur within and beneath the cloud layer. It is noteworthy to suggest that, at any given instant, the conditions inside the cloud may well indicate **negative** buoyancy, since the cloud forms near the top of a parcel's ascent. The impact of the small-scale thermals and the associated B-V oscillations implies that the layer in which clouds occur is likely to be pretty turbulent.

Ludlam (1980) states that cumulus cloud heat and moisture contents are characteristic of mixed-layer values, rather than those at the surface. This indicates that the mixing during parcel ascent within the (apparently well-named) mixed layer is rather thorough. Since the cloud-bearing layer contains fewer convective elements (only those which are initially buoyant enough to reach condensation) than in the layer beneath the clouds, the mixing in the cloud-bearing layer is rather less thorough. This is also related to the greater cloud layer stability than that within the mixed layer (recall Fig. 2.2). Further, the dry adiabatic descent (forced by mass continuity) outside the cloud acts to enhance the differences between the cloudy regions and their surroundings. Because the percentage of cloudy versus clear areas can vary widely (depending on the larger-scale nature of the environment), the cloud-bearing layer can show large variations in its horizontal homogeneity. When an area is almost entirely filled with cloud (e.g., stratocumulus), it effectively becomes a "large-scale cloud". In such cases, the convective character of the clouds is less clear -- i.e., it is much more characteristic of layer lifting by larger-scale processes.

The reader should note that the above discussion is most applicable to **mid-latitude, continental** cumulus convection. Although the subject of tropical convection, which is dominated by clouds forming over water, may not be of direct interest to forecaster/analysts in the United States, one should be aware of the differences and similarities between the two convective regimes. Specific comparisons may be found in LeMone and Zipser (1980), Szoke and Zipser (1985) and in the references they cite. In general, tropical oceanic cumulus convection tends to have weaker updrafts, undoubtedly related to weaker convective instability in the tropical oceanic environments. Less is known about the characteristics of tropical continental convection, but it is likely to be characterized by strengths somewhere between the tropical oceanic and mid-latitude continental varieties. Interestingly, as suggested by Szoke **et al.** (1985), the updrafts in tropical cyclones tend to be roughly the same as in tropical oceanic cumulus convection (typically less than 6 m s^{-1}).

2. Entrainment

We have considered the mixing effects produced by ordinary cumulus convection on the environment. It is clear from simple observations of cumulus that mixing occurs on the cloud scale as well. A rising thermal ingests air from its environment, a process known as entrainment. As we have seen, observed properties of cumulus clouds indicate that the dilution of the initial buoyancy occurs as the thermal rises through the mixed layer. Since the ultimate fate of a thermal is determined basically by its buoyancy, this process is worth some examination.

That pure parcel theory is generally inadequate to describe convection (except, perhaps, in the cores of intense updrafts, as we shall see) has been recognized for a long time. This is implicit in the "slice method" of Bjerknes (1938), which accounts for the descending air which surrounds cumulus elements, but not accounting explicitly for the entrainment process. A description of the slice method also can be found in Hess (1959, p. 103 ff.). Since the slice method requires **a priori** estimates of the area ratio of cloudy, rising air to clear, sinking air, it has never been widely used.

Some of the earliest work on entrainment includes that of Stommel (1947), Austin and Fleisher (1948), Malkus and Scorer (1955), Scorer (1957), and others. Our understanding of cumulus convection has benefitted from numerical simulations which typically have incorporated some form of entrainment. The models traditionally have fallen into one of two main classes: **plume** models or **bubble** models. These terms are fairly descriptive of the basic concepts used. A plume convection model assumes a continuous point source of convective elements. This results in a roughly conical plume of entraining convection (Fig. 2.5). Squires and Turner (1962) have presented a typical plume model. In their model, entrainment is assumed to be inversely proportional to the plume radius and the convection is **steady-state** (we will return to this concept later).

By far the most popular convection models are the bubble-like models. Scorer and Ludlam (1953) were among the first to introduce such a model, in which a puff of buoyant air rises, spreading vertically and horizontally, eventually to produce a roughly conical volume which is influenced by the convection. In the bubble models, the **active** portion of the conical volume is confined to a roughly spherical volume at the top. This region contains a vortex ring (Fig. 2.6) with steady erosion of cloud material at the top of the spherical vortex, and non-turbulent entrainment into its wake. Ludlam (1958) has suggested that most of a cumulus cloud actually consists of the "wakes" of previous

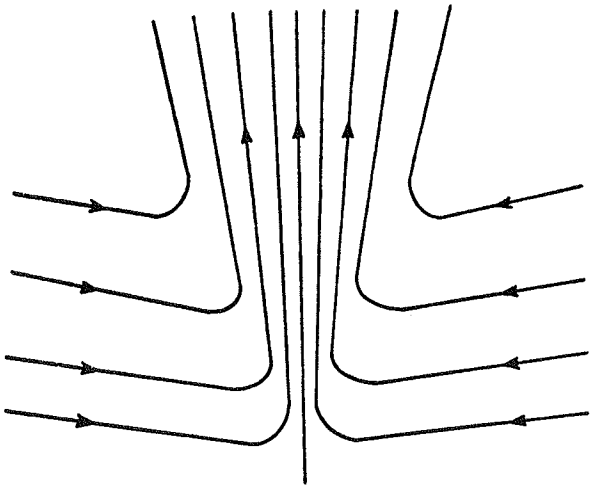

Figure 2.5 Schematic model of a plume-like convective element, showing lateral entrainment (from Stommel, 1947).

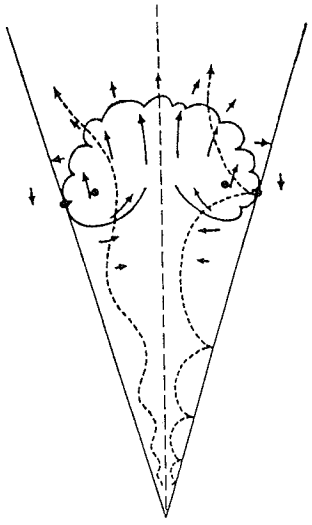

Figure 2.6 Schematic model of a bubble-like convective element, showing the vortex ring circulation (like a smoke ring) at the top and the wake left behind (from Scorer and Ronne, 1956).

bubbles. These are seen as inactive cloud -- i.e., without any significant updraft. Most bubble models are unsteady, and many use entrainment hypotheses which (like Squires and Turner's model) assume entrainment is proportional to the bubble radius.

So which model is right? As is often the case with models, it is not obvious how to answer the "rightness" question -- it appears that weak, fair weather cumulus more closely resemble bubbles, but as they grow into cumulonimbus clouds they become more plume-like (McCarthy, 1974).[5] Both cloud-scale and smaller scale (turbulent) phenomena act to bring environmental air into the convective element. In spite of years of development, numerical simulations still do not seem to have evolved a completely satisfactory means of describing entrainment. It does seem reasonable that large-diameter clouds ought to suffer less entrainment, at least deep in their interiors (McCarthy, 1974). While this idea is the basis of most radius-dependent estimates of entrainment (via mixing into the cloud from its outer boundaries), it omits several key factors, including wind shears and relative flow.

One important observation, first noted by Squires (1958b), is the occurrence within cumulus of **penetrative downdrafts.** If entrainment takes the form of turbulent mixing from the cloud boundaries, then thermodynamic properties across the cloud at any level ought to resemble a bell-shaped curve, with the least dilution at the core and a smooth variation outward. Further, the liquid water content in cumulus should increase with height since, in the lower portions of the cloud, entrainment has had more time to operate. Instead, Squires found that more dry air is observed in the **upper** portions of cumulus. Also, aircraft penetrations of cumulus show a rather sharp transition at the cloud boundaries to cloudy air properties, as well as internal regions (also with sharp edges) where the thermodynamic properties resemble environmental air. These observations are consistent with the notion that a substantial part of "entrainment" into cumulus occurs in the form of penetrative downdrafts. Squires developed a basic theory whereby an unsaturated parcel could enter the upper portions of the rising cloud and be accelerated downward (through the cloud) by evaporating cloud water. This concept has recently been supported by the study of Paluch (1979), who showed that the entrained air within mixed regions of the cloud originates at higher levels. Raymond (1979) has used this notion to develop a successful numerical model which omits the lateral entrainment hypothesis, but includes the possibility for smaller scale "convective turbulence" within the cloud. Emanuel (1981) has presented a detailed theoretical description of this penetrative downdraft process.

In summary, the process of entrainment is still the subject of current research. Lateral entrainment appears to be inadequate to explain some of the basic observed properties of convection. If the penetrative downdraft hypothesis is more nearly correct, then cumulus modelling becomes considerably more complex. Mixing with the environment is an undeniable reality, but the details of the process remain unclear. Some interesting discussions, both scientific and historical, in this area can be found in the review articles by Simpson (1983a,c,d).

---

[5] Turner (1962) has developed a "starting plume" model which combines features of both.

3. Wind Shear and Relative Flows

Environmental wind flow appears to have an important influence on the structure of convection. In an unsheared environment, classic convection may take the form of the so-called **Benard cell,** shown in cross section in Fig. 2.7. The convection in horizontal view appears as a network of polygonal cells (Fig. 2.8), in which sinking motion at the boundaries at the polygons gives way to a core of ascent at their centers. That motions akin to this occur in the atmosphere is regularly verified by satellite imagery (Fig. 2.9). In the atmosphere, the rising motion can be at the center (closed cells), or on the edges (open cells), so one suspects that the atmospheric versions of Benard convection are more complicated than the laboratory models. The details are beyond the scope of this volume (see Agee and Chen, 1973; Mitchell and Agee, 1977).

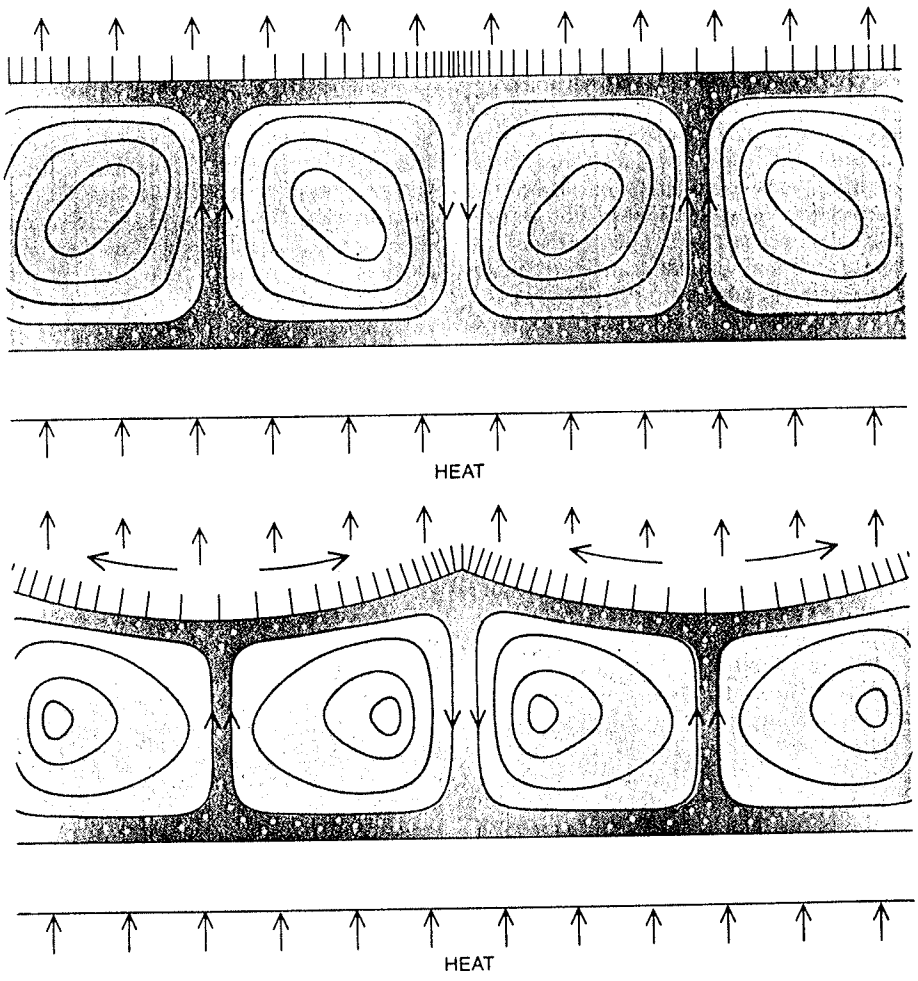

Figure 2.7 Variations in surface tension alter the pattern of convective transport in a fluid with a free surface. The magnitude of the surface tension varies with temperature, being greatest where the fluid is coolest. The magnitude of the tension is represented here by the density of the hatching. Fluid is pulled along the surface toward cooler regions of greater surface tension and is replaced by warmer fluid from below (from Velarde and Normand, 1980).

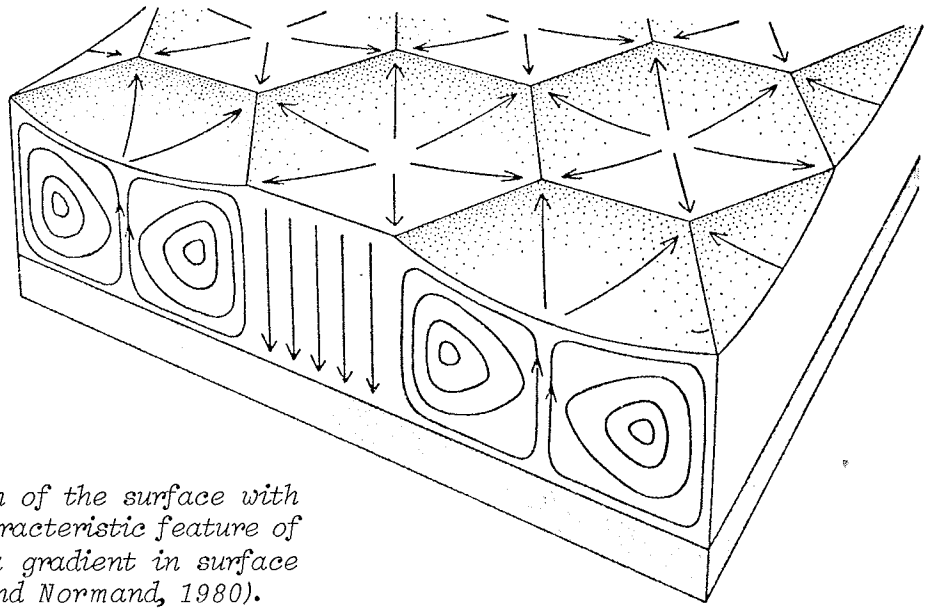

Figure 2.8 Tessellation of the surface with hexagonal cells is a characteristic feature of convection driven by a gradient in surface tension (from Velarde and Normand, 1980).

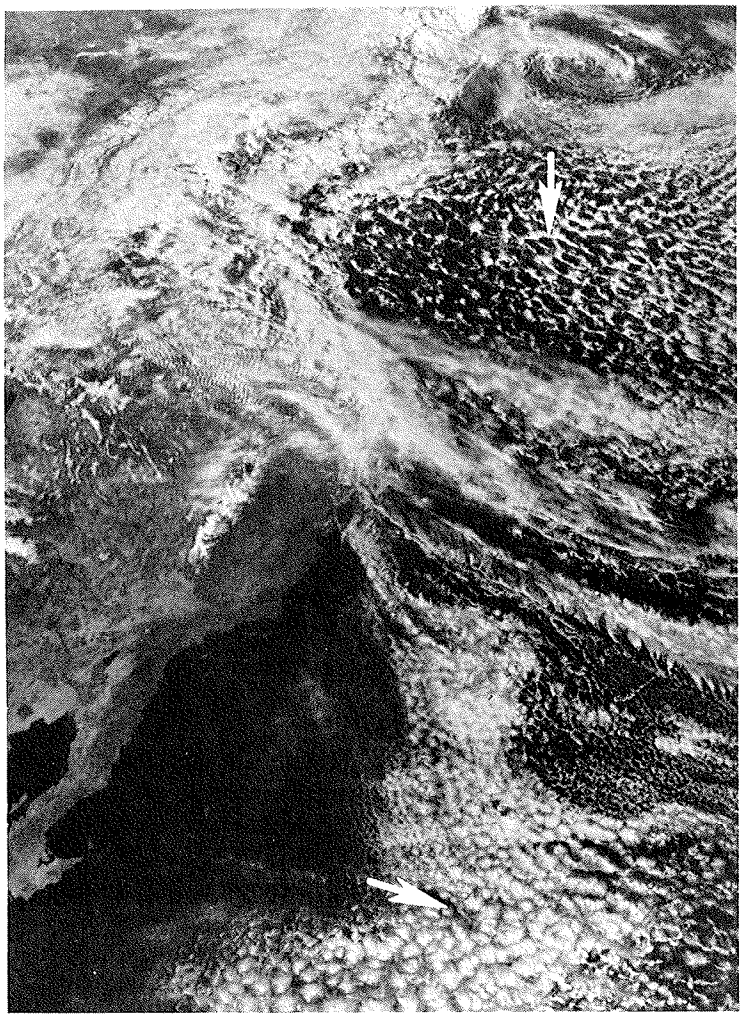

Figure 2.9 Polygonal convection cells over the Pacific Ocean. Note the mostly open cells in the north (top) and the mostly closed cells to the south (arrows).

The restrictive conditions needed for such geometrically regular convection do not apply generally and much atmospheric convection occurs in the presence of enough shear to disrupt this regular pattern. Further, non-uniform heating, topography, etc., diminish the opportunities to develop the polygonal form, especially over land. Once again, classic theory and experiment are able to provide some explanation for the forms that the convection field takes in the presence of shear. The trajectory of a parcel rising through a sheared environment can be determined easily if we know the forces on it resulting from its interaction with the environment. In reality, this is not an easy problem, but to a first approximation, assume that the parcel's horizontal acceleration is given by the product of the vertical shear in the environment and its vertical velocity. The horizontal displacement as it rises through the sheared environment can easily be calculated if the acceleration is constant (see e.g., Resnick and Halliday, 1966, p. 44).

Suppose we determine this displacement for a parcel rising through a 1 km deep layer, over which the horizontal velocity changes by 1 m s^{-1} (a moderate shear value of 10^{-3} s^{-1}). If the parcel is ascending at a constant vertical speed of 1 m s^{-1} with no initial horizontal motion, it is displaced horizontally by 500 m (Fig. 2.10). However, if the ascent rate increases to 10 m s^{-1}, the resulting horizontal displacement is only 50 m (one-tenth as much). Thus, the weaker the updraft, the greater the tilt of the parcel trajectories, for a given amount of shear. As cumulus clouds become increasingly tilted downshear (i.e., in the direction of the shear vector), it is less likely that their updrafts can be sustained. Using relatively simple theory, it can be shown that convection tilted downshear transfers energy to the environment, contributing to its decay. In general, **shear tends to destroy weak updrafts.**

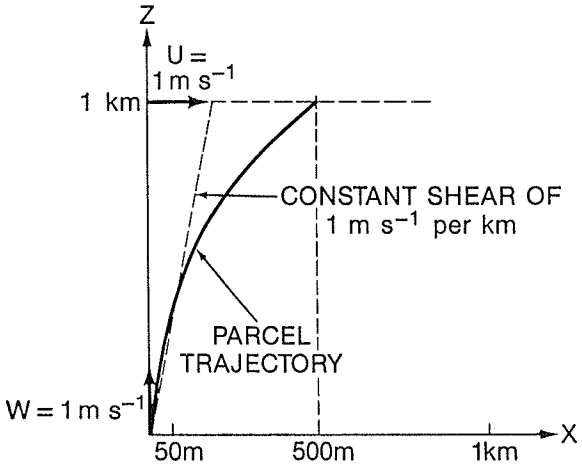

Figure 2.10 Illustration of the trajectory of a parcel rising at constant speed through a layer of constant shear (see text for details).

Note that shear can be important in lateral entrainment -- one might want to assume that entrainment is in some way proportional to the vertical shear. If this is valid, strong shear can also decrease updrafts by reducing the buoyancy.

Hess (1959, p. 112) indicates that bubble theories of convection predict that the moisture-enhanced wake of rising bubbles is tilted downshear, making it easier for thermals on the downshear side of a bubble's ascent to rise. He notes that observations tend to support this for weak convection. It should be remembered also that evaporation of condensed water (in the wake of the bubbles) tends to chill the air aloft on the downshear side. This has two opposing influences. By cooling the air aloft, a more unstable lapse rate results, enhancing the updraft potential on that side of the cloud. On

the other hand, if a cloud-scale downdraft results from this chilling, the updraft potential on the downshear side is suppressed. It appears that either effect can be dominant in a particular situation.

Since the cumulus cloud generally drifts roughly with the mean wind of the layer in which it is contained (normally, this drift is somewhat slower than the mean layer wind speed, as explained below), the subject of **relative flow** becomes important when the clouds begin to develop appreciable depth. If the clouds have depths of even a few km, it is possible for the storm top to be experiencing a substantially different relative flow than the cloud base. In many instances, cumulus clouds form in regions of essentially uniform properties. However, when convection occurs in regions of great vertical and/or horizontal variation of properties, the relative flow direction can be of dramatic importance, as we shall see in the discussion of **severe** convection.

Since convection transports parcels relatively rapidly from low levels to higher levels, the properties of the parcels do not necessarily have time to adjust to their new surroundings. Mixing and entrainment eventually dilute the parcel's original properties, but on scales larger than the cloud, the net effect of convection is upward flux of heat and moisture. Note that since environmental momentum (essentially, the speed of the flow) typically increases upward, convective effects usually produce a net **downward transport of momentum.**[6] Parcels of rising air are usually moving slower than the environment into which they are brought, so a relative flow is developed. This relative flow produces accelerations which act on the parcel. As just mentioned, this interaction is complicated, in general. However, this acceleration is not capable of adjusting the rising parcel's horizontal speed immediately to that of the environment. Thus, the overall cloud (which consists mostly of relatively low-momentum parcels brought up from below) **tends** to move more slowly than the mean wind in the layer of convection. However, one must be cautious in accepting this at face value, as we shall see.

4. Larger Scale Aspects of Cumulus Convection

So far, we have considered only one basic structure for ensembles of convective cells, Benard convection. It appears that the polygonal form may, in part, be an artifact of "surface tension" effects (Turner, 1973, p. 216). The most fundamental form for organized convection in an unstably stratified atmosphere with shear may well be the horizontal roll (e.g., Kuettner, 1971), since theory and experiments given in Turner's text seem to suggest this. Roll-type convection has a cross-section much like Fig. 2.7, but the plan view would be a series of lines along which upward or downward motion dominate. This can result in long lines of cumulus clouds, often called **cloud streets** (Fig. 2.11). These are typically aligned roughly with the low-level flow seem to result from one or more instabilities associated with wind shear (see e.g., Lilly, 1966; Brown, 1972; LeMone, 1973). Figure 2.12 reveals this common organizational structure in a satellite image.

Another way in which something resembling cloud streets may be formed is the so-called **Kelvin-Helmholtz** (K-H) wave. This is an oscillation in the form of horizontal rolls which is produced in sheared flows, with the rolls oriented across the wind (strictly speaking, aligned perpendicular to the shear) as discussed by Haltiner and Martin (1957, p. 373), Drazin and Howard (1966), and Lindzen (1974). This phenomenon is perhaps most familiar in the form of "wave clouds" in mountainous terrain, but can occur wherever

---

[6] This is even the case without clouds, as in the dry, mixed layer convection behind a dryline discussed in I.III.B.5. The reader should be aware that convective momentum flux is **not** always down the momentum gradient (LeMone **et al.**, 1984).

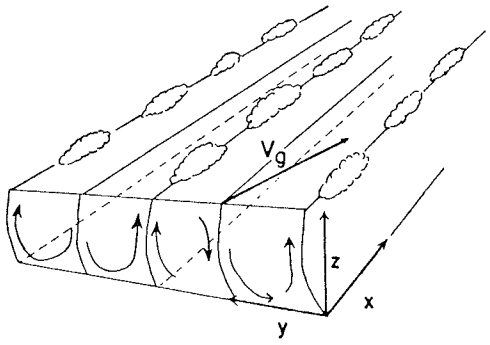

Figure 2.11 Schematic showing roll-type convection which produces cloud streets. The vector V_g is the geostrophic wind vector (from LeMone, 1973).

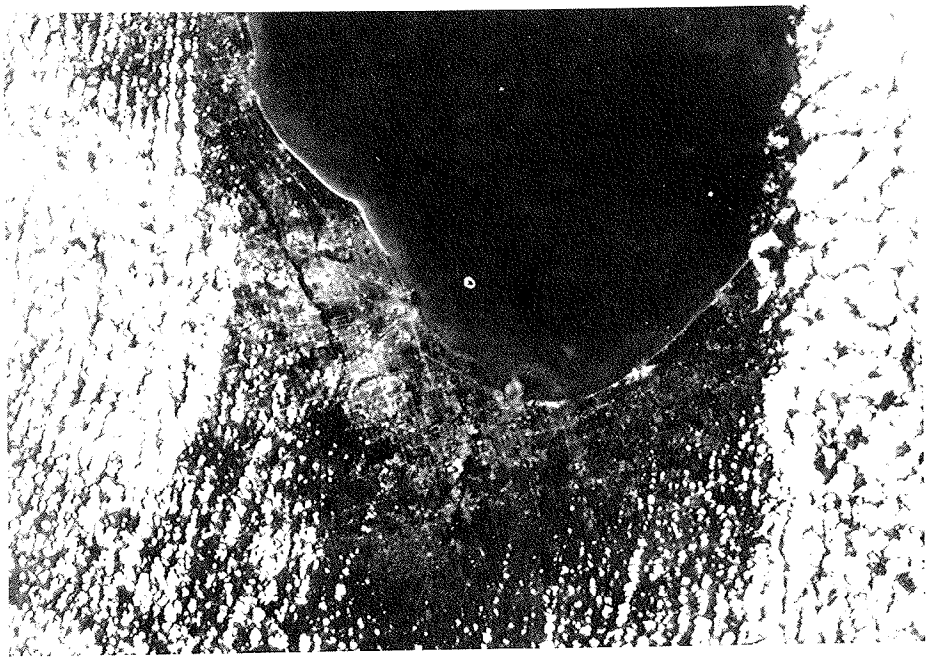

Figure 2.12 Example of cumulus cloud streets, forming to the south of Lake Michigan and Chicago (Photo courtesy of J. Weaver).

there is wind shear in a **stably stratified** environment. Thus, these wave clouds can be present in stratus-type clouds. When cumulus clouds are associated with K-H waves, it is likely that the waves are occurring with a shallow inversion aloft. The ascending branches of the wave provide enough lift for cumulus clouds to develop, whereas the descending branches suppress the clouds.

Asai (1970) has examined the problem of how convection orients itself relative to the basic flow. He has shown that for **weakly unstable,** sheared flow the rolls tend to lie with their axes perpendicular to the shear. For **strong instability,** the rolls are more or less aligned with the shear (cloud streets). Polygons are possible only for a narrow range of combinations of shear and instability (see Asai's Fig. 7).

Cumulus can form in another organized pattern, associated with regions of cold air aloft and/or warm air at low levels (perhaps with origins in a terrain-related "hot spot"), or enhanced low-level moisture in a large-scale area which is otherwise unfavorable for

cumulus convection. One quite commonly observed example of this occurs with a pool of cold air associated with an upper low pressure system. Behind a cold front, a steep lapse rate may be present which can produce a fairly well-defined region of cumulus and, perhaps, some showers. This is shown in Fig. 2.13, where the cumulus and small cumulonimbus clouds in northern Kansas, southern Nebraska and most of Iowa are under a pool of very cold temperatures aloft. The thunderstorms in Wisconsin are along a cold front which extends southwest across Illinois, Missouri, Arkansas, and Texas. An even more common example occurs over the ocean, behind a cold front which has moved over warm waters. Such "cold air cumulus" as shown in Fig. 2.14 are a common feature along the continental margins during winter.

Ludlam (1980, p. 130 ff.) has described the two main circumstances under which large amounts of heat (sensible and/or latent) are transferred to the atmosphere from the surface. One is when cold air moves over warmer waters and the other is when solar radiation results in low-level heating over land. As a basis for reference, the average daily input from the sun at the top of the atmosphere is about 720 cal cm^{-2}, of which about 331 cal cm^{-2} are absorbed by the earth's surface and converted to sensible heat. Ludlam's value for heat transfer to the atmosphere in situations of cold air moving over

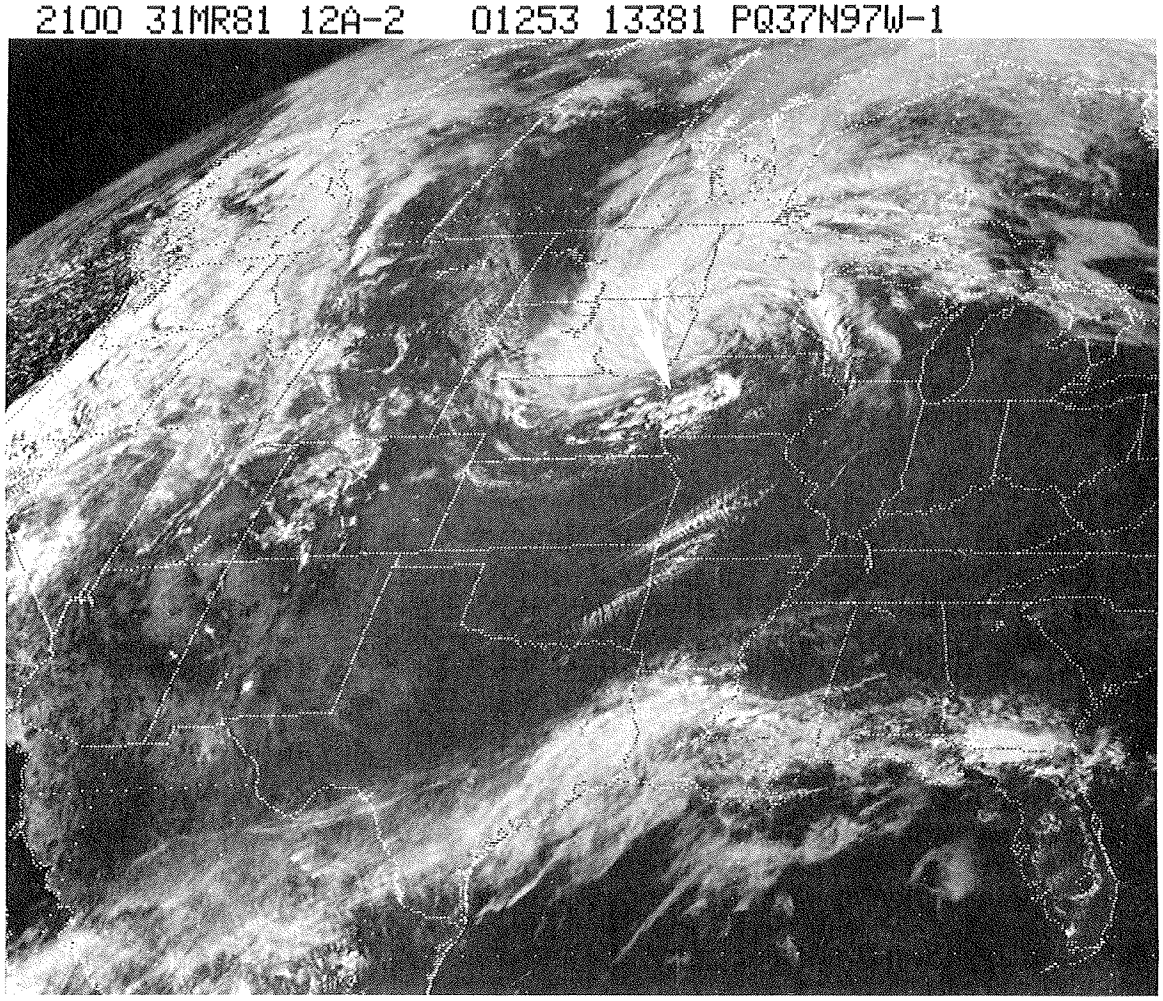

Figure 2.13 Cumulus and cumulonimbus under a cool pool of air aloft (arrow). See text for discussion.

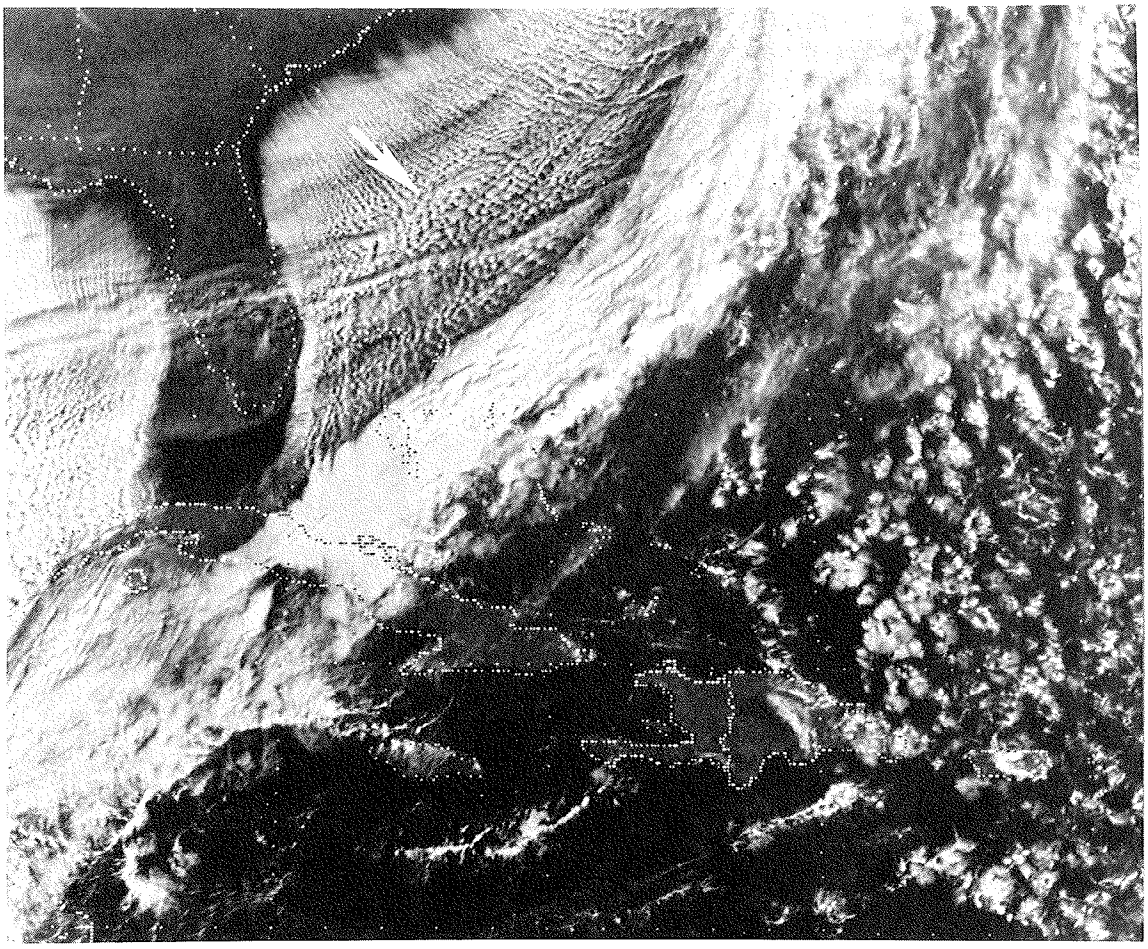

Figure 2.14 Example of cumulus clouds over warm water, usually in the form of cloud streets (arrow), behind a front. Note the change in character of clouds on opposite sides of the frontal cloud band (Photo courtesy of D.O. Blanchard).

warm water is about 600 cal cm^{-2} day^{-1}, of which about half is in the form of latent heat. For solar radiation situations in summer, Ludlam's typical value is about 300 cal cm^{-2} day^{-1}, with the amount of latent heat contribution ranging from 50 to 250 cal cm^{-2} day^{-1}, depending on the moisture content of the earth's surface.[7] These values suggest that convection represents the **primary** source for transfer of solar heat from the ground to the air. Thus, even on days with little or no cumulus cloud activity, convection is still performing an important meteorological function.

A basic feature of ordinary convection is that the heat transfer and vertical motion are distributed rather evenly, in a sense, over a relatively large area. That is, even though the strongest vertical motions are confined to the relatively small fraction of the area actually occupied by cumulus, there is a large population of clouds, all more or less the same. Most of the area **between** rising thermals (and/or cumulus clouds) is characterized by subsidence, usually somewhat weaker than the more concentrated

---

[7] Note that mid-latitude seasonal values of incoming solar radiation ("insolation") range from more than 1000 cal cm^{-2} day^{-1} in summer to less than 400 cal cm^{-2} day^{-1} in winter.

upward motion in thermals. This subsidence also acts to warm the environment by compressional heating. Thus, even though the clouds may only occupy a small fraction of the total area in a cumulus field, the **whole** region is characterized by warming. Weak cumulus activity is, as we have seen, not generally associated with air mass boundaries or areas of large-scale upward motion. When large-scale phenomena act to create regions of relatively concentrated ascent, the intensity of cumulus activity increases dramatically, often to produce thunderstorms. Nevertheless, in the material which follows, cumulonimbus activity should be considered as an extreme example of the more general process of convection which we have been examining.

B. Thunderstorm Cell Structure and Evolution

1. General Remarks

Many authors choose to divide thunderstorms into two categories: "air-mass" and "frontal" storms. Not only is this a drastic oversimplification, but it is misleading as well. As we have seen, "air-mass" convection is most typically of the non-precipitating, fair weather cumulus variety. The air-mass thunderstorm label carries with it the connotation that such convection is more or less random. Examples of pure air mass thunderstorms are difficult, if not impossible to find. While the real thunderstorms which occur under this classification often are not associated with fronts, per se, this does **not** imply that there is not some large-scale phenomenon which is acting to enhance (or suppress) the convection (albeit, still locally) enough to produce thunderstorms in one place (and not in another). It is often possible to determine topography-related influences (local hot spots, upslope flow, sea-breeze fronts, etc.) which are influential in producing thunderstorms in an otherwise uniform (but unstably stratified) environment. Even in the most homogeneous environments (e.g., the tropics), it usually is possible to determine organizing factors for convection (Blanchard and Lopez, 1984), given enough data. **Thunderstorms are not random**! Difficult to forecast, perhaps, but not random.

Further, it often is implied that "frontal" storms are severe while "air-mass" storms are benign. Nothing could be more deceptive, since it has long been recognized that "pre-frontal" storms are more likely to be severe than those on a front. Also, under the right circumstances, storms that might be seen by some as "air-mass" type can be extremely severe. Thus, this sort of terminology generally is not used in these notes and it is hoped that the reader will consider avoiding it.

Material in this section draws heavily from the concepts originally presented in the Thunderstorm Project Report (Byers and Braham, 1949). That study represents a prototype for virtually all subsequent thunderstorm research projects. Its enduring value can hardly be impeached. However, the reader should be aware that more recent research has added substantially to the framework built by that original project. Without suggesting any lack of confidence in the findings of the Thunderstorm Project, this volume emphasizes progress in our knowledge of thunderstorms (particularly severe thunderstorms) since that time. It is assumed that the Thunderstorm Project findings are relatively well-known and only a brief summary of these follows.

As convective activity increases in intensity, the number of convective elements decreases. One does not find large regions more or less uniformly covered with cumulonimbus clouds, as with fields of ordinary cumuli. The amount of mass cycled through the convection may be enormous, but instead of being spread widely over a broad area, the mass flux is concentrated in a few, very intense elements. This is at the heart of the "hot tower" hypothesis (Simpson, 1983b), which was developed to apply to tropical cyclone convection, but is also useful in understanding mid-latitude thunderstorms and their interactions with their environment.

Perhaps the most important concept to come out of the Thunderstorm Project is that **thunderstorms consist of one or more cells.** Each cell has a distinct life cycle, to be described below, but it is important to recognize that the typical, complicated structure and evolution of radar echoes can be understood relatively easily in terms of its building blocks, the constituent cells. This is illustrated by Fig. 2.15. Knight **et al.** (1981), provide an interesting discussion of the cell concept and point out that its application is fraught with confusion. This is typical of non-mathematically defined concepts -- initially they seem straightforward, but if one tries to pin down their details, they become elusive. We hope to avoid the confusion by dwelling on the (hopefully) straightforward aspects.

Once again, the discussion to follow is most applicable to mid-latitude continental forms of convection. It is interest to note that most tropical oceanic convection is found in mesoscale clusters and/or lines, whereas isolated convective cells seem to be more common in continental mid-latitudes (see Szoke **et al.**, 1985).

2. Towering Cumulus Stage

This point in a storm cell's development is considered, somewhat arbitrarily, as the beginning of the cell's life cycle. This is because a cumulus cloud which has attained the cumulus congestus (or "towering cumulus" [TCU]) level of development represents a large change in the nature of the convection. It has a sufficiently strong updraft (of order 10 m s^{-1} or more) to distinguish it from ordinary convection. The standard picture developed in the Thunderstorm Project study remains essentially unchanged (Fig. 2.16).

During this stage in the cell's development, it is dominated by updrafts, although small-scale downdrafts probably exist (recall the entrainment discussion above). The air rising through the cloud converges into the developing cell from miles around, although perhaps not uniformly from all directions. For example, if the cloud is moving across the low level flow (as would be likely if the wind veers from south to west with height), it preferentially ingests air on its right front flank.

For a peak vertical velocity of 10 m s^{-1} at a height of 5 km, this implies an average convergence through the inflow layer of 2×10^{-3} s^{-1}. Since synoptic scale values for convergence are of order 10^{-6} s^{-1}, there must be some mesoscale mechanism which is forcing this convergence. Included in this use of the term "mesoscale" are processes

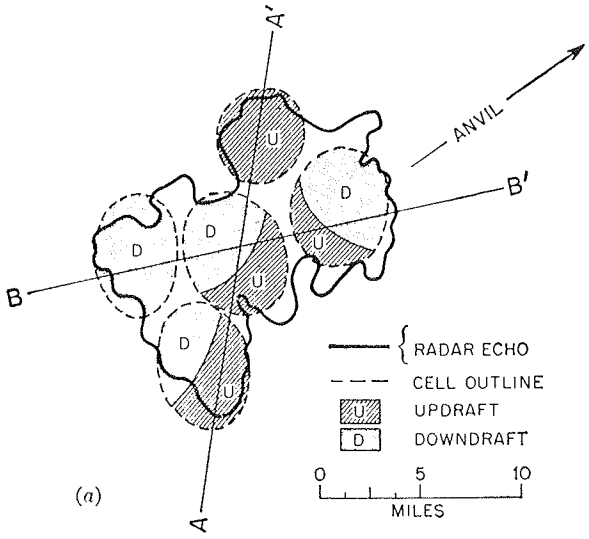

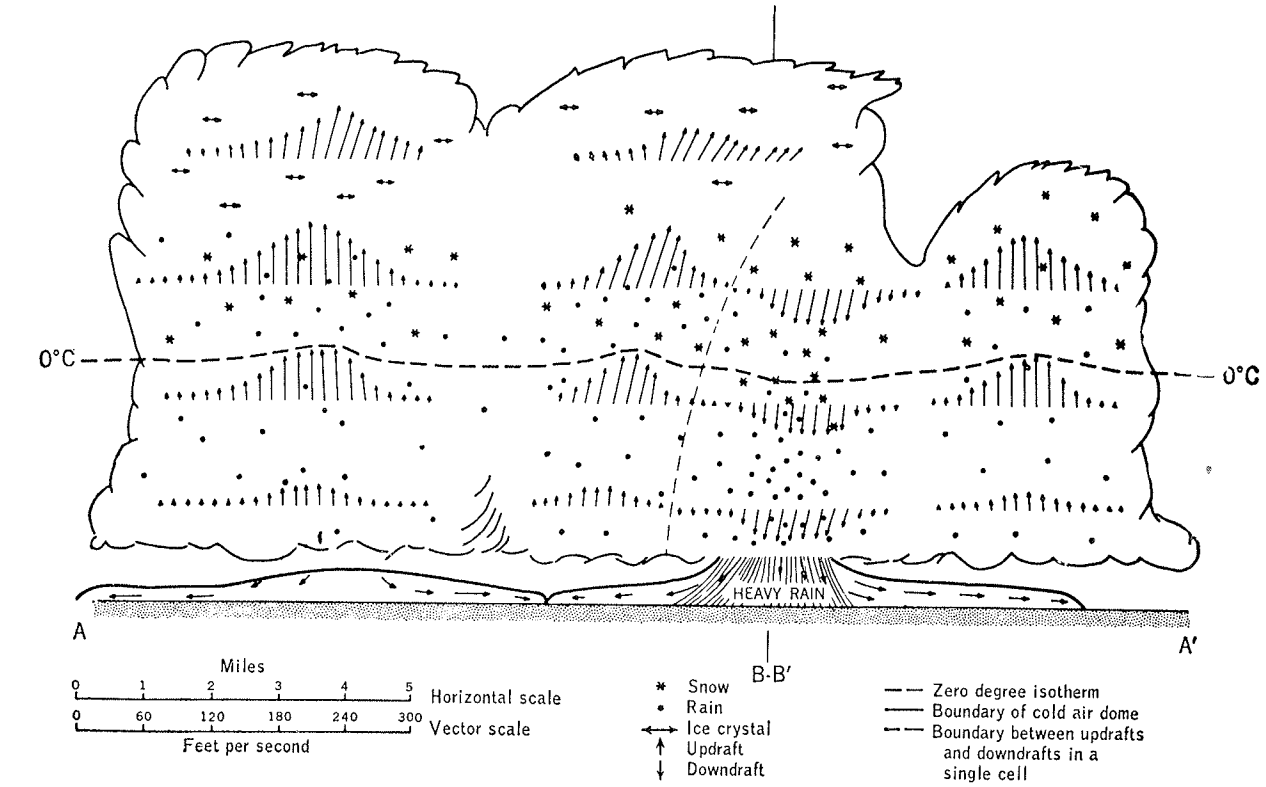

(b)

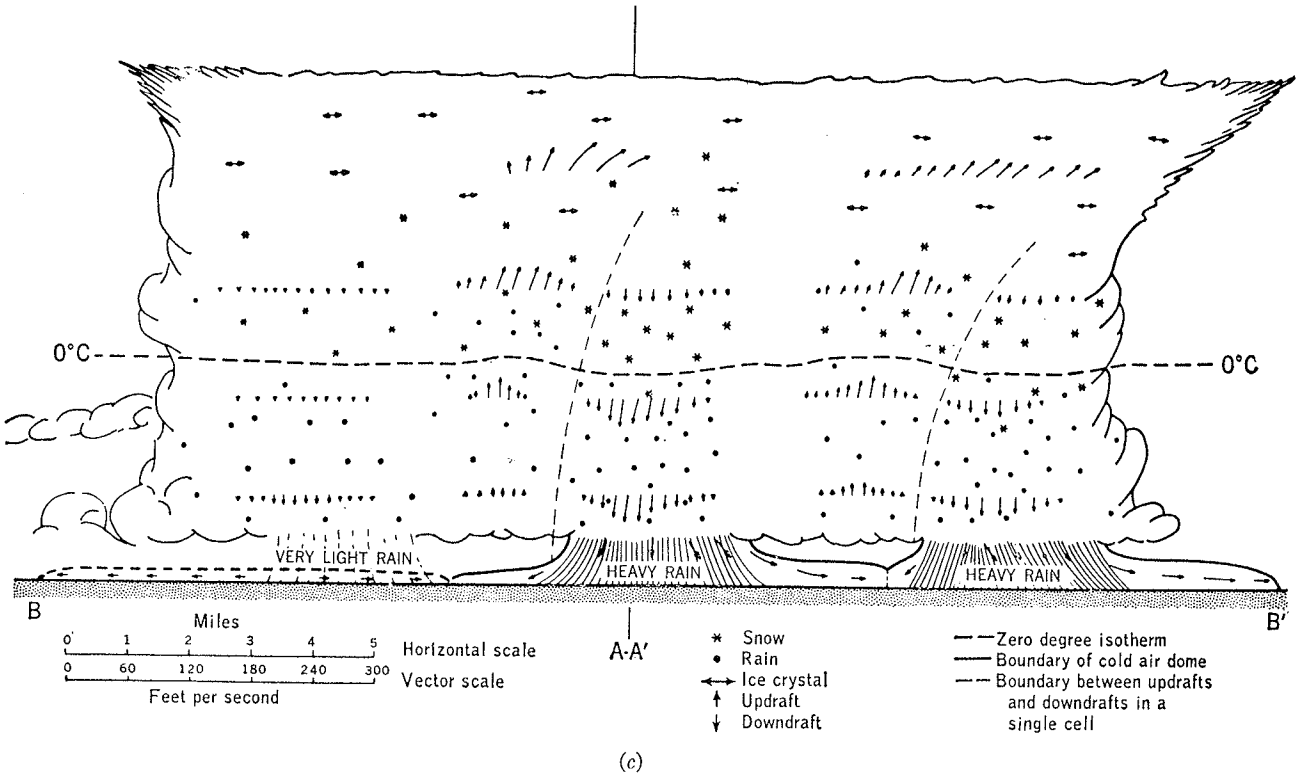

(c)

Figure 2.15 Model of a thunderstorm complex, as envisioned by Byers (1965). In (a) a low-level echo is shown (heavy solid line), with schematic updrafts (U) and downdrafts (D) showing the individual cells. A cross-section along line AA' is shown in (b), while a similar cross-section along line BB' is seen in (c).

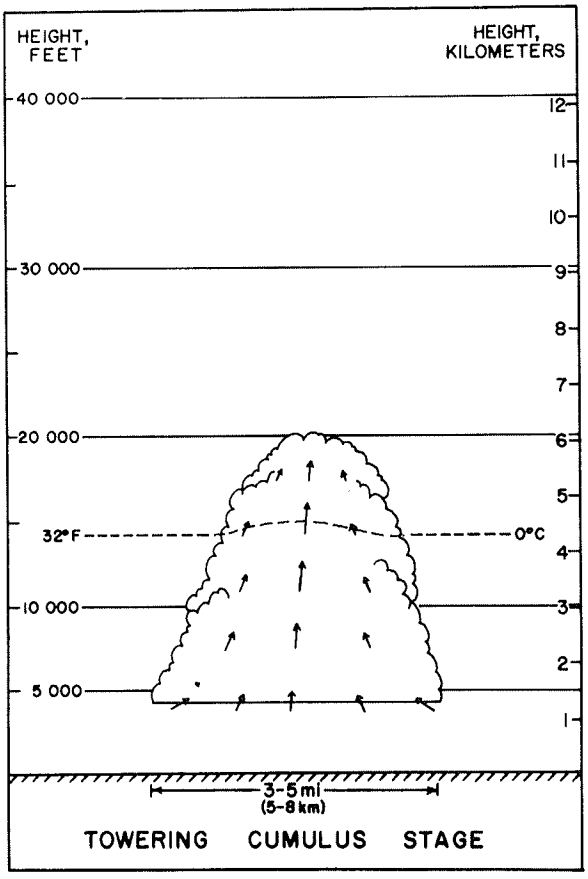

Figure 2.16 Schematic of towering cumulus stage in ordinary thunderstorm cell life cycle.

created by the thunderstorms themselves, especially the convergence associated with outflow from previous cells. Diagnosis of such mechanisms with operational data generally is not possible. See Holle and Watson (1983) for detailed analysis of this process with mesonetwork data.

The speed and size of updrafts in towering cumulus are such that it is possible for undiluted parcel ascent to occur within the cores of the updraft. Actual observations (e.g., Heymsfield **et al.**, 1978) support this. Therefore, simple parcel theory can be applied successfully to predict the vertical velocity in the undiluted cores. Interestingly, the undiluted updraft cores are found preferentially on the upwind side of the cumulus towers, as seen in Heymsfield **et al.** (1978). This may be the result of "erosion" of the diluted portions of the cloud by the relative flow on the upstream side of the cell.

It is during the latter portions of this stage in the cell's life cycle that precipitation begins to form and radar echoes can first be detected. The subject of precipitation formation is discussed in II.C below, but it is noteworthy here to observe that the first radar echo in a common mid-latitude thunderstorm cell typically develops near the freezing level (0°C) within the cloud. While the subject of thunderstorm electricity is also deferred (to Chapter VII in this volume), lightning is seen rarely at this stage.

3. Mature Stage

It is conventional to define the mature stage of a cell as starting when the first precipitation reaches the surface. Perhaps this is as good as any other arbitrary definition. However, a more essential characteristic of the mature stage is the

coexistence of substantial up- and downdrafts within the same cell. The development of a storm-scale downdraft coincides roughly with the beginning of precipitation descent, which may require several minutes before it reaches the surface. Since rain drops have terminal fall velocities of roughly 5-10 m s^{-1} (see II.C.3), it takes about 8-15 min for such drops to reach the surface from 5 km AGL (recall that first radar echoes usually are seen at about the freezing level). Because the rain usually falls in a region of downdraft, the time to reach the surface may be somewhat less than this.

Downdrafts associated with the precipitation arise from two processes: **precipitation drag** and chilling of unsaturated air by **evaporation** of smaller droplets. The drag effect can be substantial, depending on the total amount of liquid water (see IV.C.1). Kessler (1969) has estimated the drag effect of 1 g m^{-3} of liquid water to be equivalent to a reduction in buoyancy of about 0.25°C. During a 10 min descent to the surface, that would produce a downdraft of roughly 5 m s^{-1}, which is about equal to the fallspeed of the particles themselves. Since the particles are falling **with respect to the air**, this effect can make the rate of precipitation descent near the surface exceed that of the particle fallspeed. Clearly, the descent of precipitation from the region where it was formed is a complicated process!

Precipitation which forms in the updraft most typically does **not** fall back directly through the updraft. Rather, it is carried downwind by the winds aloft and may fall into relatively dry (or at least unsaturated) environmental air. Figure 2.17 from Ludlam (1980) illustrates this rather clearly. Divergence aloft (Fig. 2.18) also acts to expel precipitation from the updraft as the storm enters the mature stage. As it is carried away from the updraft and begins to fall relative to the earth, some of the condensed water evaporates. For each g of water which evaporates in a kg of air, the air is chilled by about 3.7°C. Clearly, if this process operates to a significant extent, a substantial downdraft must result. Evaporation depends on the humidity of the environmental air and on the droplet size spectrum (Kamburova and Ludlam, 1966). If a parcel maintains a negative buoyancy of 1°C through a descent from 5 km, it develops a downdraft speed of roughly 15-20 m s^{-1}. Obviously, in non-severe convection, this evaporational cooling is not very substantial, because measured downdraft speeds are usually less than those in the updraft.

In the mature phase, after the downdraft and precipitation descend to the surface, the air brought down in the downdraft spreads out laterally, forming the **gust front** (see discussions in I.III.B.7 and IV.C.1). It is the gust front which marks the boundary of the downdraft outflow. Analysis of the properties of this outflow air indicate that it is usually a mixture of environmental air at mid-storm levels and low-level air, probably mixed out of the updraft (a process of **detrainment**).

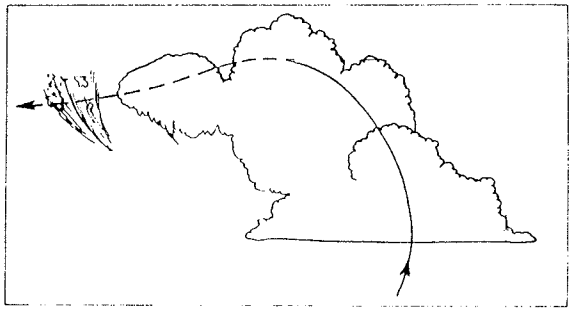

Figure 2.17 Schematic representation of the generation of rain in a cumulus. The line through the model cloud represents an idealized (smoothed) trajectory of air through the cloud; it is drawn continuously through the regions of strong updrafts and greatest concentrations of condensed water, and dashed where evaporation is dominant (after Ludlam, 1980).

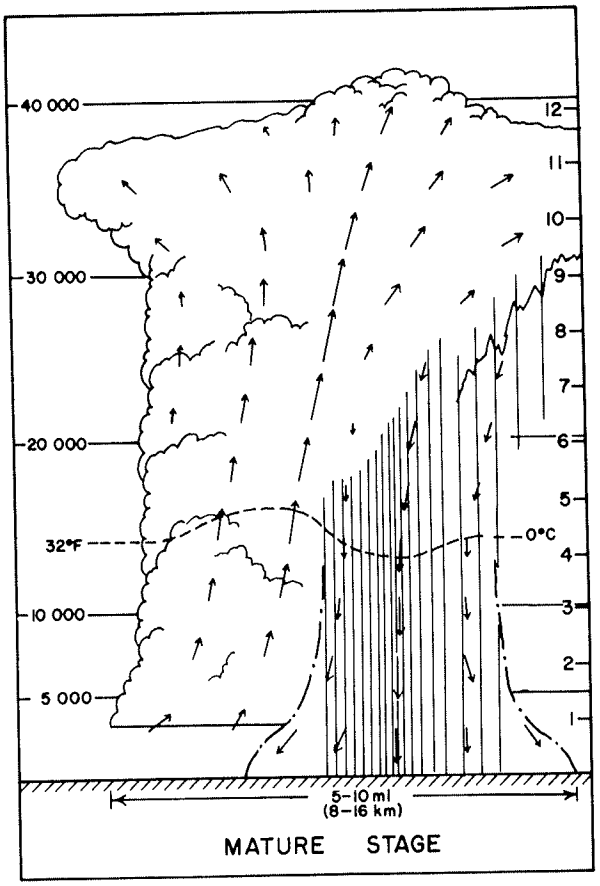

Figure 2.18 Schematic of mature stage of ordinary thunderstorm cell life cycle.

Downdrafts act to dissipate clouds, because clouds are composed of very small droplets (see, e.g., Byers, 1965, p. 145), in the size range of 30 μm (1 μm = 10^{-6} m) or less. Droplets of this size are readily evaporated in the descending air. The descent warms the air through adiabatic compression and thus reduces the relative humidity. Therefore, Fig. 2.18, which illustrates the important features of a mature stage thunderstorm cell, is modified from the equivalent original Byers-Braham model to reflect dissipation of cloud in the downdraft. Further, the anvil top is emphasized more in this model of themature phase, since spreading anvil tops are not confined to dissipating storms.

At this time, the cell is characterized by its greatest vigor in all phases of its activity. Drafts are at their maximum strength, lightning is most frequent throughout the depths of the cell, precipitation is most intense, maximum radar reflectivity is achieved, radar and visual storm tops are highest, and so forth. In non-severe thunderstorm cells, the cell's mature stage is relatively brief, usually on the order of 10 min.

4. Dissipating Stage

Under conditions which yield non-severe storms, the mature stage has already developed the seeds of its own demise. In broad terms, the environment in which such a storm develops is not capable of sustaining the initial impulse or rapidly redeveloping a new cell. The downdraft's low-level outflow spreads out and "undercuts" the updraft, cutting off its source of warm, moist air. Without its buoyancy supply, the updraft cannot be maintained and it rapidly diminishes. Precipitation formed aloft continues to

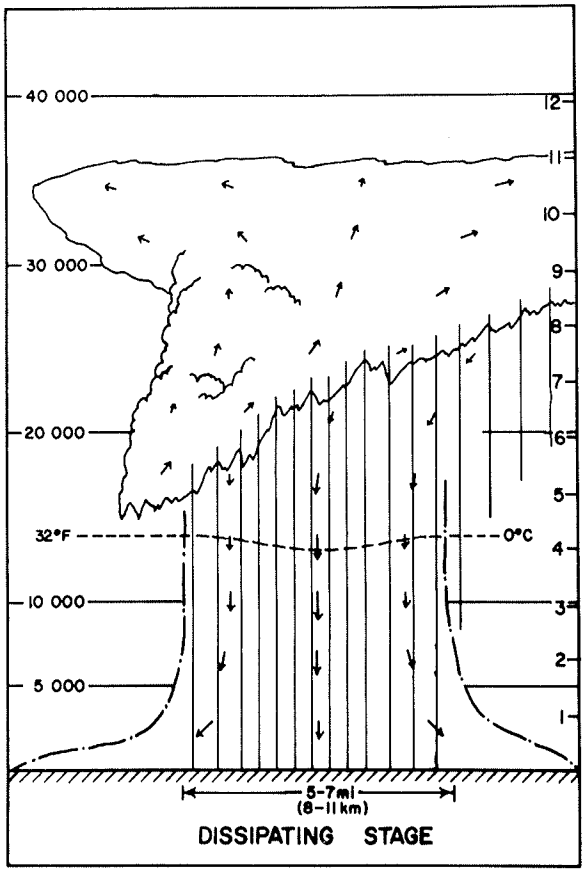

Figure 2.19 Schematic of dissipating stage in life cycle of ordinary thunderstorm cell. Note the absence of cloud in the downdraft area. Compare with Fig. 2.20.

fall out, maintaining a downdraft of decreasing strength. This last stage is dominated by downdraft (Fig. 2.19). Therefore, the cumuliform cloud towers which characterize the first two stages disappear and only ragged clouds remain. Kessler (1969, p. 47) has pointed out that residual precipitation (after the updraft has diminished) can act to scavenge out and dissipate cloud droplets, enhancing the loss of cloud material in downdrafts. The anvil aloft may be the only remnant of a storm cell late in the dissipation stage, sometimes called an "orphan" anvil (Fig. 2.20). Eventually, even this disappears, and precipitation ceases for lack of resupply.

How long does this process of cell formation and decay require? If the storm is the result of an initial, non-sustained impulse of buoyant air, the lifetime should be roughly equivalent to the time required for a parcel to rise to the ultimate height attained by the storm. If it is assumed that the average parcel buoyancy is enough to produce an average updraft speed of 5 m s^{-1} and the storm rises to a height of, say, 35,000 ft (10.7 km), the resulting time estimate is about 30 min. This figure is generally accepted as the typical single cell lifetime.

Most thunderstorms consist of a number of cells at various stages in their development (Fig. 2.21), so the complex can persist for much longer periods than that of an isolated cell. Each cell contributes cloud and precipitation material to the ensemble. Thus, a rather extensive anvil of debris is often created from previous cell developments. It is well-recognized that new cells form in preferred areas of such a complex, rather than haphazardly within it. Such new cells are most common wherever the outflow from the complex can run into and lift previously unaffected, potentially buoyant air. The potential for redevelopment along the gust front depends on the

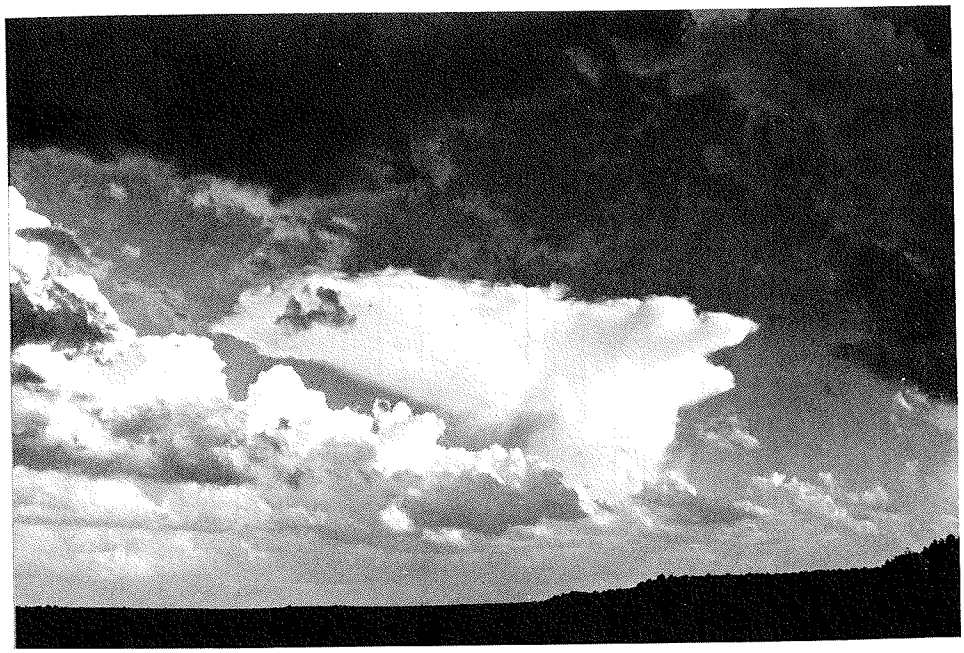

Figure 2.20 Example of an "orphan anvil," which no longer has surface-based updraft. It is merely the last stage of a dissipating thunderstorm. Note new convection in front of and to the left of the dying cell.

Figure 2.21 Series of weak cells associated with a non-severe thunderstorm. Note the precipitation (as an obscuring of cloud base) to the far right, with the oldest cells in this series.

stability of the ambient air and the vertical wind shear structure in the environment (which influences the location and strength of the convergence along the outflow boundary). Clearly, cells which move into areas of convective stability are likely to dissipate rapidly. This process of preferential cell development is especially crucial for severe storms and is explored in detail in that which follows. However, before considering severe convection, we need to review in more detail some aspects of the basic processes involved in forming and distributing convective precipitation.

C. Precipitation Processes

1. Condensation

Up to this point, the implicit assumption has been that condensation of water vapor into clouds occurs as one would expect when working with a thermodynamic diagram (e.g., a skew-T, log p diagram). When such a diagrammatical analysis predicts condensation to begin, the prediction is accurate enough to be of operational value (Rooth, 1960). Of course, mixing, water loading, and other processes can result in the parcel's ascent not being exactly as predicted by pseudo-adiabatic parcel theory (see e.g., Hess, 1959, p. 92 ff.).

In this section very small scale details which can influence condensation are considered briefly. Such details fall under the general heading of **microphysics** and are covered extensively in textbooks (see e.g., Fletcher, 1966; Byers, 1965; Kessler, 1969).

Generally, it can be assumed that condensation within a rising parcel begins when the local relative humidity reaches 100% and that enough water vapor condenses to keep the relative humidity at 100% in a rising parcel once its condensation level is passed. As one might suspect, this is by no means a complete picture. While these notes are not intended to present all the details, some basic concepts are useful.

When water vapor is present in the air, like any other gas, it exerts pressure. This is, logically enough, known as **vapor pressure.** By Dalton's Law of Partial Pressures, the vapor pressure is simply added to the pressure of the "dry air" constituent gases to yield the total pressure. Further, the temperature of the vapor can be assumed to be the same as the air temperature. It turns out that the saturation vapor pressure (the vapor pressure in a saturated parcel) is a function of temperature alone. That is, the amount of water vapor which is present in a parcel (as measured by its partial pressure) at saturation depends only on the parcel temperature. This functional relationship is shown in Fig. 2.22.

Relative humidity can be defined by the ratio of the actual vapor pressure to the saturation value.[8] When this number is not converted to a percentage value, it is called the **saturation ratio,** with a value of 1.0 corresponding to equilibrium.

The process of condensation is one in which water molecules in vapor form "clump together", forming liquid water. Naturally, the water molecules themselves are not

[8] This is also very nearly equal to the quotient of the mixing ratios, which is accepted by the WMO to be the true definition of relative humidity.

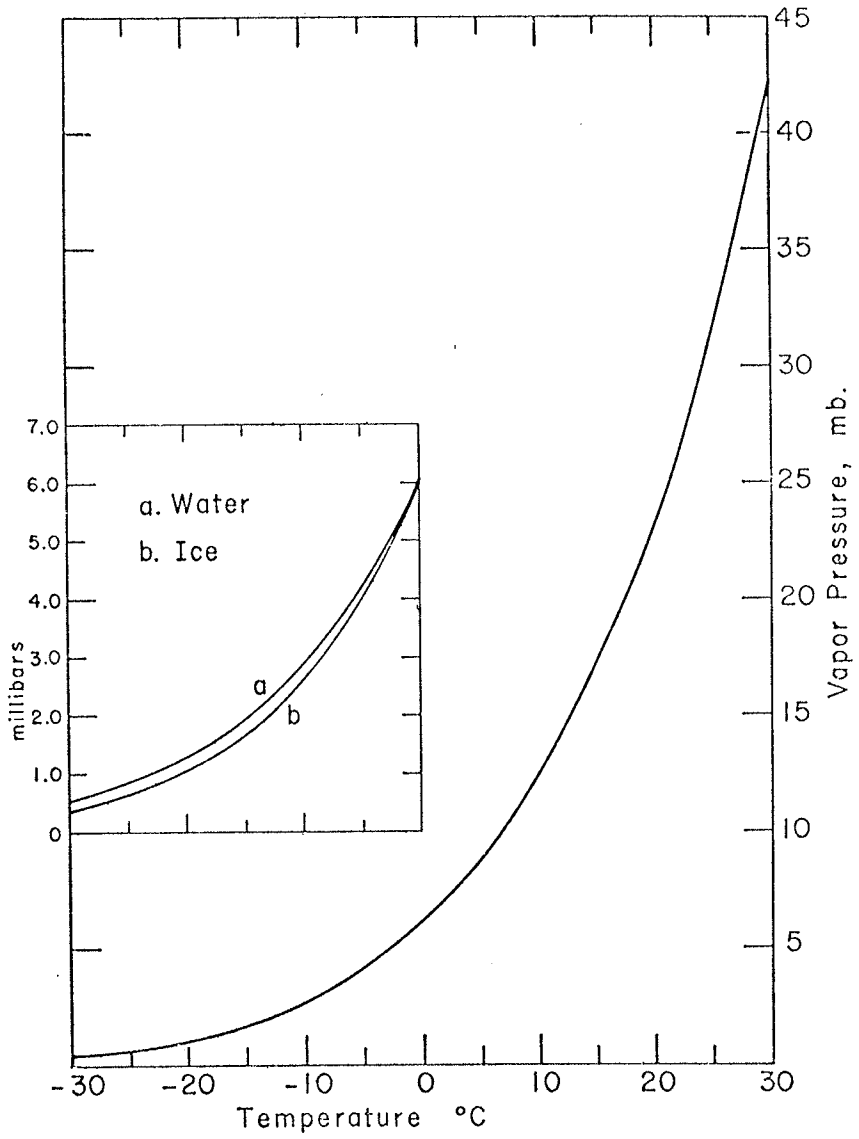

Figure 2.22 Phase diagram for water in the p,T plane. Inset: vapor-ice equilibrium (lower curve) and vapor-liquid equilibrium (upper curve) at subfreezing temperatures (from Byers, 1965).

chemically changed, but they are more tightly bound together than in vapor form.[9] At equilibrium (or saturation), exactly the same number of molecules are being added to the liquid form (condensing) as are breaking away (evaporating) under random molecular agitation. Since there is no net gain to the amount of condensed water at equilibrium (by definition), there must be a slight supersaturation for condensation to occur. Typically, the supersaturation is very small, say at saturation ratios at most of order 1.01-1.03 (or relative humidities of a few percent over 100%).

The process is complicated by several factors. Since it is most common for condensation to begin on small particles called **condensation nuclei,** the chemical properties of the nuclei are important. These particles may come from windborne dust, oceanic salt (resulting when sea spray evaporates in the air), human-created pollution, natural aerosols, etc. In absolutely pure air (no condensation nuclei), the saturation ratio can be driven to values far beyond what is observed in the real atmosphere. However, it is safe to say that in real (impure) air, we are not likely to observe the actual supersaturated state with our rather crude humidity-measuring devices (at most accurate only to a few percent). If the chemical nature of the nucleus upon which the vapor first condenses acts to **lower the equilibrium vapor pressure** of the resulting solution (the nucleus-water solution, that is) then the nucleus is said to be **hygroscopic.** A salt particle (NaCl) is an example of a hygroscopic nucleus. By lowering the equilibrium vapor pressure, the hygroscopic nucleus allows condensation to occur at a much lower saturation ratio. In fact, condensation in the real atmosphere typically begins at apparent relative humidities below 100%, perhaps even as low as 80%!

It is significant that as the water drop grows, the tendency for growth by condensation diminishes (Mordy, 1959). That is, as the amount of condensed water around the hygroscopic nucleus gets larger, the hygroscopic effect is increasingly diluted. For drops larger than 10^{-6} m (or 10^{-4} cm) even relatively large hygroscopic nuclei are of minor significance, and supersaturations are once again required for continued condensational growth. This can be seen graphically in Fig. 2.23. Note that the curves for "solution" drops (i.e., containing a hygroscopic material in solution) have lower saturation ratios than that of pure water (the "pure" curve). However, as the size of the drop increases, for a given amount of hygroscopic material, the solution curves approach the pure curve.

This results in a peak in the supersaturation for each amount of hygroscopic material, at what is called the **critical radius.** When the saturation ratio is lower than the value at the critical radius, drops cannot grow by condensation beyond the size dictated by the given saturation ratio. In the figure, for example, a drop with 5×10^{-15} g of NaCl cannot grow beyond a size of 2×10^{-5} cm (0.2 μm) when the saturation ratio is 0.90 (see the inset). Alternatively, given a saturation ratio of 1.001, a solution drop must have more than 10^{-15} gm of dissolved NaCl in order to grow beyond its critical radius (at about 6×10^{-5} cm = 0.6 μm).

---

[9] By virtue of this more compact structure, the volume of the total water content is rather substantially reduced. If we compare the density of water vapor at typical atmospheric values to that for an equal amount (by mass) of liquid water under comparable conditions, the reduction in volume is by a factor of roughly 10^5! Since the volume occupied by water vapor within a parcel is at most about 1%, when it all condenses, the parcel volume is decreased by roughly the same percentage. That is, by condensing, the water content no longer occupies even that small percentage of the parcel's volume. This can be interpreted as a slight increase in parcel density, since the total mass of the parcel does not change. For many purposes, this effect is completely negligible.

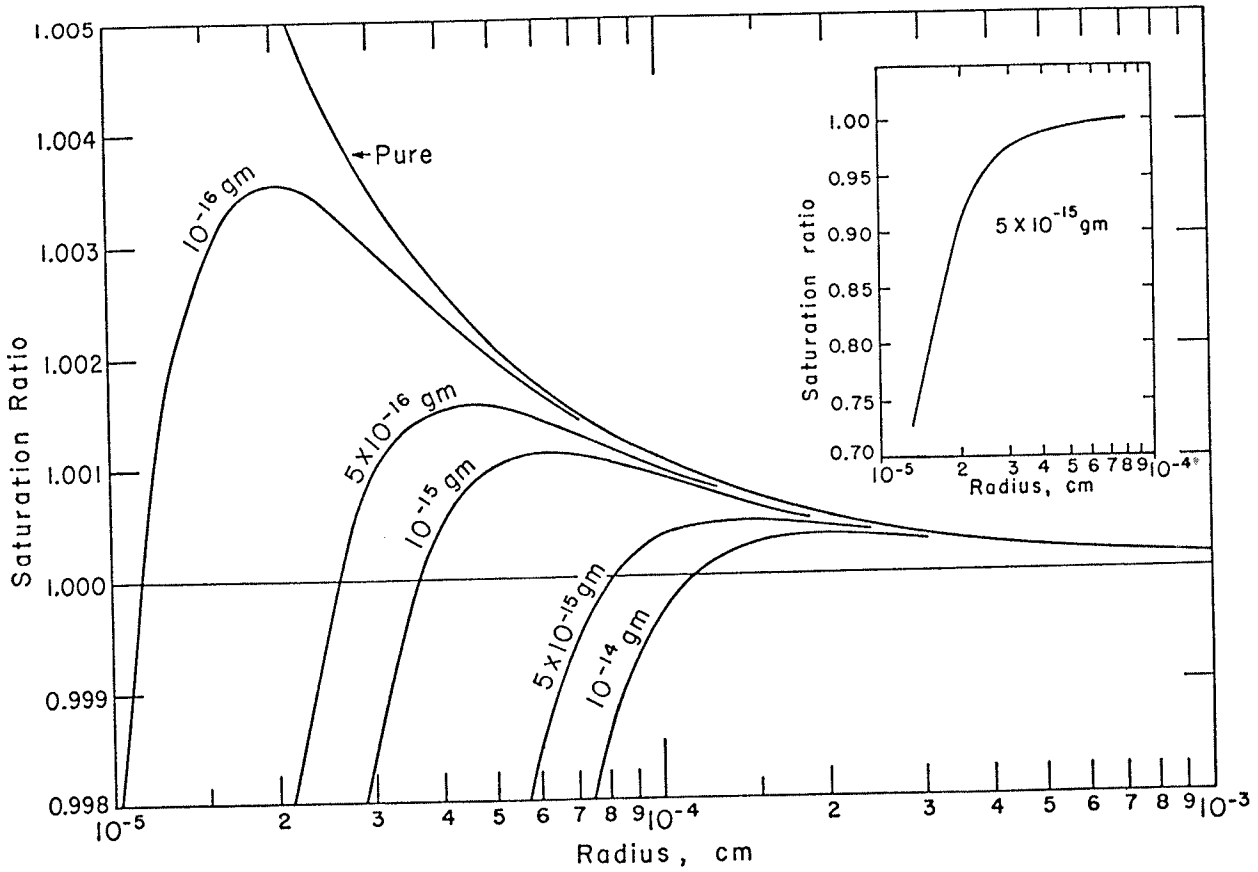

Figure 2.23 Equilibrium supersaturation as a function of droplet radius for water droplets, each containing the given mass of NaCl (salt). The inset is the curve for 5 x 10^{-15} g of salt on a compressed scale. All computations are for a temperature of 25°C, but little variation with temperature is expected (from Byers, 1965).

Once the critical radius has been exceeded by a growing cloud droplet, the implication is that it can grow without limit by "diffusion". For growth by diffusion (i.e., by condensation), an important assumption is that the air surrounding the growing droplet has an infinite supply of water vapor. In reality, the growth rate is directly proportional to the supersaturation but **inversely** proportional to the radius. As the radius of the growing drop increases, its growth rate by diffusion decreases until it becomes so small as to be negligible. This can be understood as a depletion of water vapor in the surroundings by the largest droplets, slowing their growth and preventing smaller droplets from growing at all. It turns out that droplets larger than about 10 μm grow so slowly by diffusion that their growth can be said to have ceased. Since raindrops have typical radii of order 1 mm (10^3 μm), there must be some other means of producing particles of raindrop sizes.

There are two basic processes for continued droplet growth. Even these together are not the whole answer, but they are widely recognized as the dominant mechanisms for growth to precipitation-sized drops.

2. The Bergeron-Findeisen Process

Bergeron (1933) and Findeisen (1938) are responsible for development of a plausible theory for precipitation growth in middle and high latitudes which has come to be widely accepted. It is based on the observation that most precipitation (either convective or stratiform) in mid-latitudes is associated with clouds that reach above the freezing level (see Fig. 2.24).

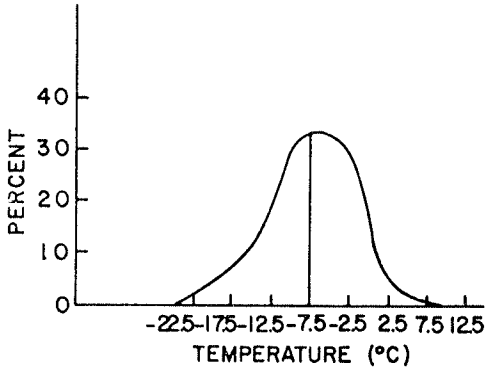

Figure 2.24. Approximate temperatures at heights where first echoes form in non-severe storms in Texas (from Carbone ***et al.****, 1976).*

Although freezing of water is usually thought to occur at 0°C, it turns out that very pure water can be cooled well below that point (or "supercooled") before freezing occurs spontaneously. For freezing to commence at 0°C, another type of nucleus is required, a **freezing nucleus.** The properties of freezing nuclei do not necessarily coincide with condensation nuclei. It is almost as if water needs to be "taught" how to freeze. This is because ice must take on specific crystalline structure in which water molecules are bound. Thus, a freezing nucleus is some substance with a lattice structure similar to the crystalline form (or forms, since ice can have any of several crystalline structures) of ice. Obviously, the best form upon which ice can grow is another piece of ice -- perhaps falling from levels high enough to have already frozen spontaneously.[10] Vonnegut (1949) discovered that silver iodide has a crystal lattice very similar to ice and this substance is widely used to seed supercooled clouds (i.e., those containing unfrozen water droplets at temperatures below 0°C). Seeding with dry ice (see Schaefer, 1946) serves to cool droplets below the point at which even pure water freezes spontaneously ($\sim$ -40°C). For some interesting historical perspectives on the process of cloud seeding, see Byers (1974).

In any case, once a few ice particles are created in an environment containing supercooled water, the Bergeron-Findeisen process can begin. Recall the inset of Fig. 2.22, in which it can be seen that ice has a slightly lower saturation vapor pressure than water at an equivalent temperature. This is because ice, by virtue of its crystal structure, binds water molecules more tightly than liquid water. The rate at which molecules can leave the ice by random molecular agitation is less than that relative to liquid water, lowering the equilibrium vapor pressure. Thus, when the two exist side by side, the ice particles have an advantage in competing for available water vapor needed

---

[10] Since the clouds at anvil level in most situations are at temperatures well below the spontaneous freezing point for pure water, a cumulonimbus cloud can "seed" itself, with ice crystals falling into lower levels. Also, one pre-existing cloud can seed others developing in regions around it, if its ice crystals can enter the newer clouds.

for growth. Clearly, under these conditions, ice crystals can grow at the expense of the water droplets. This allows the ice crystals to reach sizes where they can begin to fall at substantial speeds.

If the freezing level is far enough aloft, the falling ice particles melt on their way to the surface. Droplets grown by this process can attain radii on the order of 100 μm. If no other process occurs, drizzle is produced. Therefore, while the Bergeron-Findeisen process can develop droplets well above cloud droplet sizes, it cannot explain the formation of mm-sized raindrops. Further, the process cannot explain rain from clouds which never penetrate the freezing level, as often is the case with tropical showers (see Langmuir, 1948). However, in mid-latitudes the process which does create large drops needs droplets in the range of 100 μm.

3. Coalescence

In any cloud, a spectrum (or distribution) of drop sizes is found. The typical spectrum shows a trend for decreasing numbers of droplets as the size category increases (Fig. 2.25). That is, the typical cloud contains large numbers of small droplets but only a few large ones. This distribution is important since large droplets fall faster than small ones. In this way, larger droplets can overtake, collide, and merge with smaller ones, a

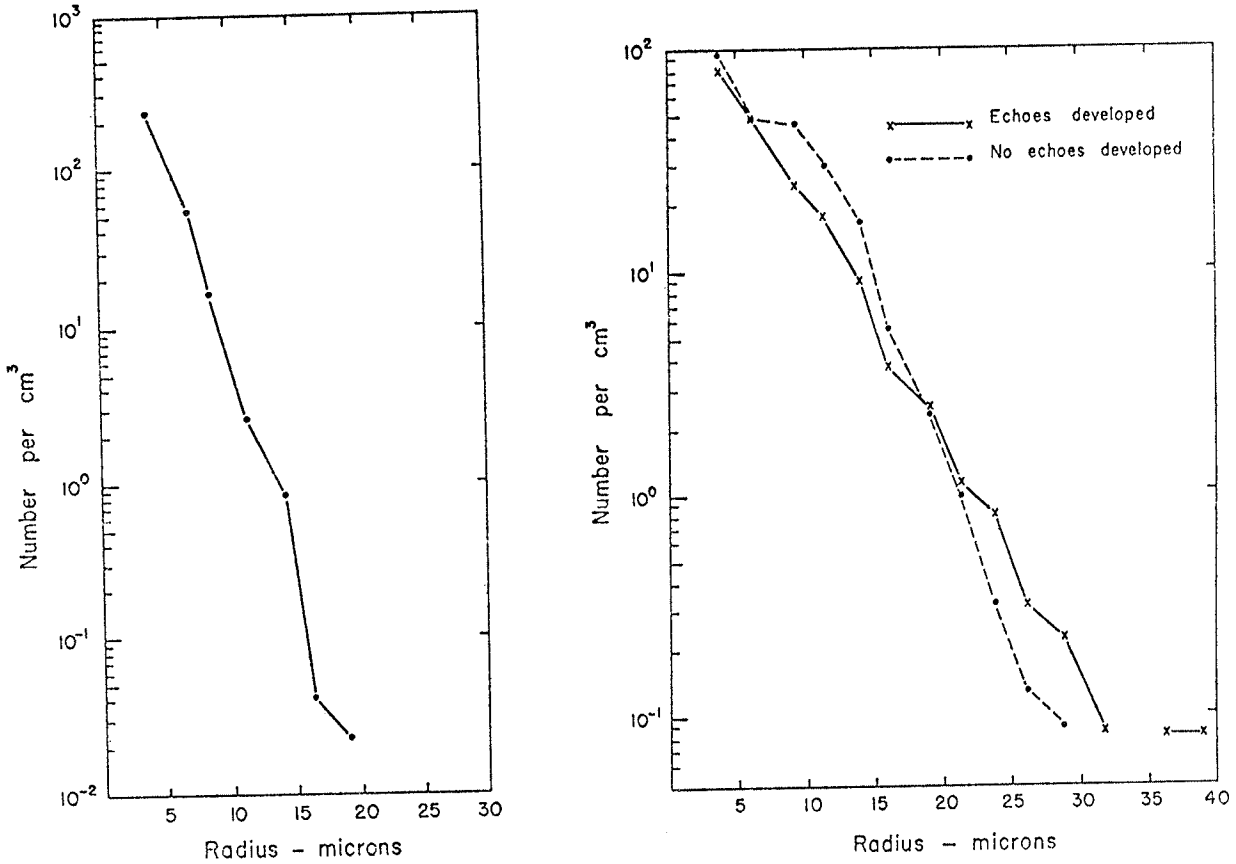

Figure 2.25 Distribution of droplet sizes in summer convective clouds over continental United States: left, fair-weather cumulus, 19 clouds with average number concentration of 293 cm^{-3}; right, cumulus congestus, average droplet concentrations 247 cm^{-3} for arrested growth, 188 cm^{-3} for those growing to echo production (from Byers, 1965).

process referred to as **coalescence**, or accretion. Because droplets much smaller than 100 μm have such slow terminal fallspeeds, they are not very important in the formation of rain, except as a supply of liquid water for the faster falling droplets.

In addition to the textbook treatments, discussions of coalescence can be found in Langmuir (1948), Bartlett (1965), Berry (1967), Scott (1968) and others. It is generally accepted as the means by which precipitation-sized drops are achieved. To a good approximation, for drop radii less than 90 μm, the fallspeed of drops increases as the square of their radius. Clearly, this law is useful only at the start of the coalescence process. Figure 2.26 shows the terminal fall velocity over most of the range of interest. One should also be aware that the terminal fallspeed increases with height, owing to lower air density as one goes up (see Table 2.2).

As a drop falls, it sweeps out a roughly cone-shaped volume (Fig. 2.27), adding to its radius by coalescing with the smaller droplets in its path. Kessler (1969, p. 28) has described this process mathematically. For the purpose of getting a feeling for the numbers involved, consider a droplet which starts at a height of 5 km with an initial radius of 10 μm. It reaches the ground with a final radius of 1 mm. Thus, its radius has increased from 10^{-5} to 10^{-3} m. The volume swept out is about 4.0×10^{-3} m^3 (an average radius during the fall of 5×10^{-4} m). During its fall, the drop has increased its volume by about 4.2×10^{-9} m^3 = 4.2×10^{-3} cm^3, only negligibly different from its final volume. If the droplets swept up have an average radius of, say 2 μm (a volume of 3.35×10^{-11} cm^3), then roughly 10^8 such drops are required! This is not absurd when one examines Fig. 2.28, illustrating how small cloud drops are in comparison to raindrops. In the volume swept out, then, the liquid water content averages about 1 g m^{-3}, which is a realistic value.

Continuing along these lines, consider a cumulonimbus cloud which is 10 km in radius and 10 km deep -- for a total volume of 3.14×10^3 km^3 (or 3.14×10^{12} m^3). If the average liquid water content within the cloud is 3 g m^{-3}, there is about 10^{13} g of liquid water in the cloud (or 10^7 metric tons!). If all this condensate were to fall over the circle 10 km in radius directly beneath the cloud, it would attain a depth of a little over

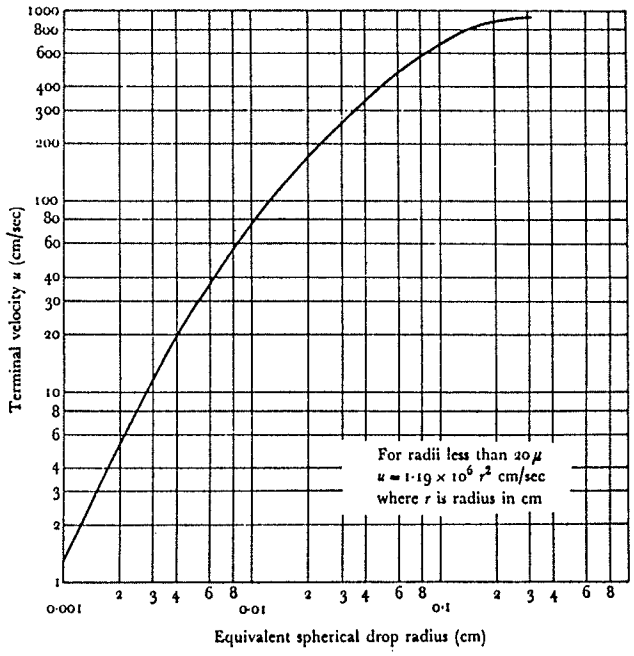

Figure 2.26 The terminal velocity of water drops in air at 760 mm pressure and temperature of 20°C (from Fletcher, 1966).

TABLE 2.2

Height	Pressure	Temp	$f = v/v_o$
kft	mb	°C	
40	190	-58	1.9
35	240	-50	1.7
30	300	-37	1.5
25	375	-22	1.4
20	470	-13	1.3
15	570	-3	1.3
10	700	+6	1.2
5	840	15	1.1
surface	1000	20	1.0

Table 2.2 Increase of terminal fall speed of particles with height in the atmosphere. The factor f is the ratio of fallspeed v to that at 1000 mb, v_o (from Hitschfield, 1960).

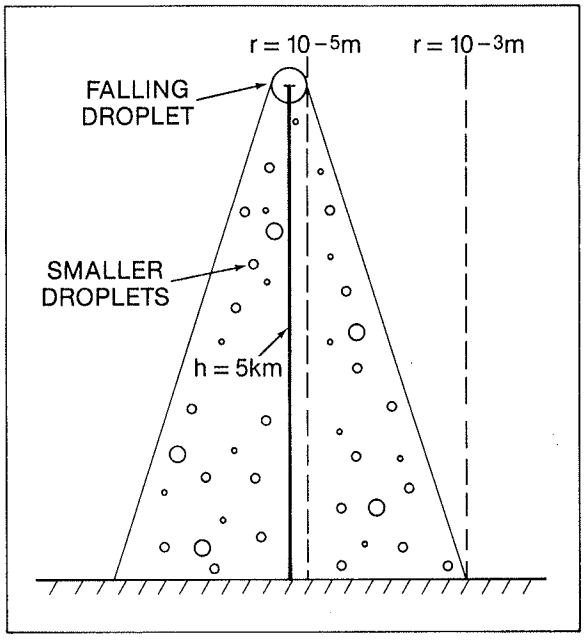

Figure 2.27 Schematic diagram of cone swept out by falling drop as it falls from a height of 5 km, growing from 10^{-5} m (10 μm) radius to 10^{-3} m (1 mm) radius.

3 cm (~ 1.25 in). This is roughly equivalent to values associated with "precipitable water" calculations, which are based on the total water vapor content above a point. The process of formation and fallout of precipitation involves tremendous quantities of water mass, but the efficiency at which it occurs can be rather low.

Thus, coalescence provides the mechanism for growing precipitation-size drops. Further, it can operate (under the right conditions) to produce precipitation from clouds which never reach the freezing level (see Mason, 1959). As noted by Zipser and LeMone (1980), the relatively weak updrafts in tropical oceanic convection can give coalescence alone more time to produce precipitation-size particles.

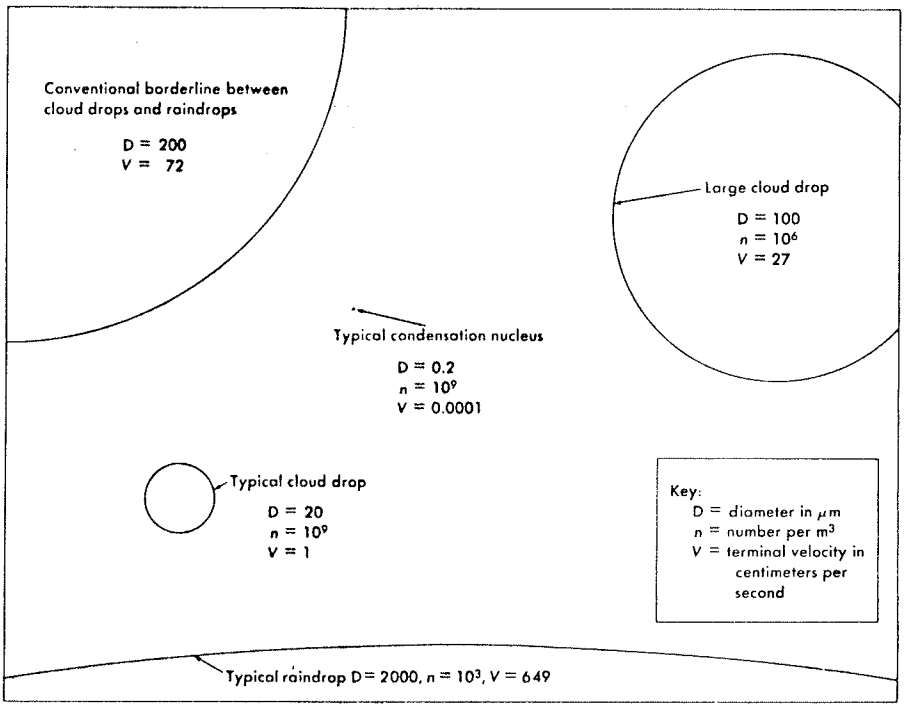

Figure 2.28 Comparative diameters, concentrations, and terminal fall velocities of some particles involved in condensation and precipitation processes. Note particularly the great difference in diameter of a typical cloud drop and of a typical raindrop (from McDonald, 1958).

4. Distribution and Fallout

Efficiencies associated with condensation, coalescence and fallout can have a dramatic effect on the distribution of condensed water within the cloud. Generally speaking, most situations in which parcels rising in an updraft reach their "condensation level" are not hampered by a lack of condensation nuclei. Thus, the formation of cloud droplets is usually efficient enough to produce observed cloud bases which are relatively close to the level where parcel theory predicts saturation. Circumstances can arise which inhibit condensation, but these do not seem to be very common.

Given that cloud has developed and the updraft is maintained, precipitation formation from the available cloud water becomes possible. If it is assumed that enough freezing nuclei are present (perhaps because the updraft is sufficiently strong to reach spontaneous freezing temperatures even for pure water droplets) to allow the Bergeron-Findeisen process to operate, the efficiency of the coalescence process must be considered as well. As with all microphysics, there are many details about the process which are beyond the scope of these notes, but it can be stated that not all the droplets encountered by a falling drop are necessarily collected by that drop. The so-called **collection efficiency** is influenced by such diverse factors as electric fields, surface tension, and the chemical properties of the nucleus-drop solution. For many purposes, it is adequate to assume that this overall collection efficiency is 100%, even though we know that it is not necessarily true (see Fig. 2.29).

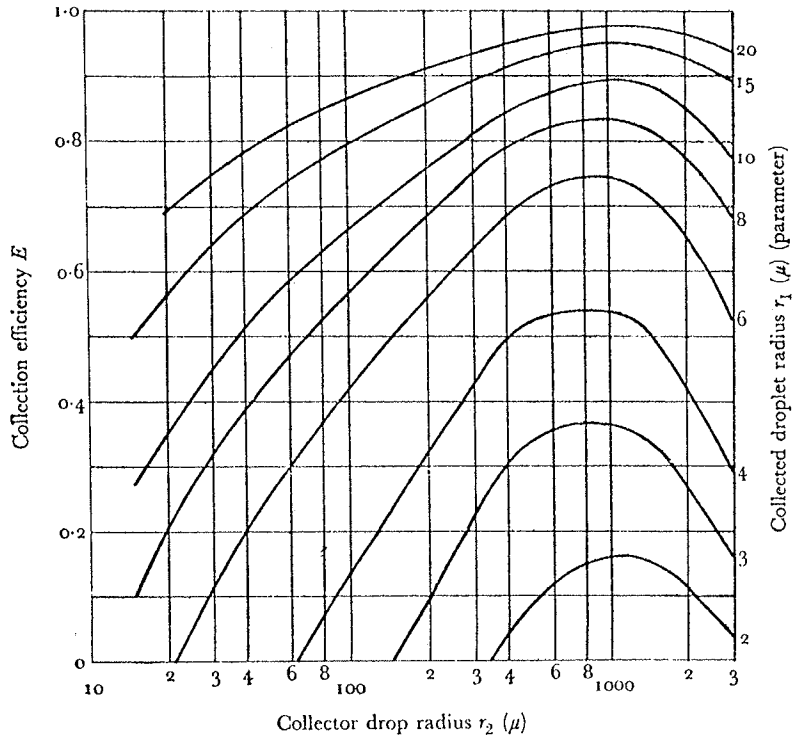

Figure 2.29 Collection efficiency E for a drop of radius r_2 falling through a cloud of droplets of radius r_1 (after Langmuir, 1948).

As noted earlier, for a drop to grow to precipitation-sized radii, generally it must fall through an appreciable depth of cloud air.[11] This takes time (which depends on the cloud water content, among other things) but as long as it is supported by sufficient updraft, the drop itself is rising and growing at the same time. Therefore, one expects to find a greater proportion of larger drops at upper levels in a growing storm.[12] Since total liquid water content (LWC) is most sensitive to the proportion of large drops, one also expects to find higher liquid water contents in those upper levels. Generally, observations and model simulations of **strong** convection confirm this (e.g., Kessler, 1969, p. 52 ff.). Roys and Kessler (1966) have found that liquid water contents high in the storm may be above 10 g m^{-3}, with the extreme value they cite being about 44 g m^{-3}! This high a value is rather questionable, but there is little doubt that values above 10 g m^{-3} do occur. Note that if penetrative downdrafts exist in the upper parts of a given cloud (which is more likely in weak to moderate convection), there may be regions in which the LWC is substantially lower than in surrounding regions (Squires, 1958a). This will result in a net decrease in the overall cloud LWC at those levels.

There are connections between updraft speed and liquid water content since, as we have seen, the liquid water tends to retard the updraft. Also, strong updrafts are typically the result of releasing large amounts of latent heat, which implies large

---

11 Remember that this cloud air is rising, so the drop may be rising relative to the ground, even though it is falling relative to the air.

12 When the updraft is weak and/or the clouds are shallow -- as in stable forms of precipitation -- the drops are smaller (in general) than with deep, strong updrafts.

amounts of available liquid water. The drops themselves never develop radii greater than a few mm, since drops break up into smaller drops if they reach 3-5 mm size. Nevertheless, the total LWC can eventually slow down the updraft and allow the descent of the precipitation. This can result in what Kessler (1969, p. 72 ff.) calls **condensation oscillations,** during which the updraft redevelops after precipitation falls out, only to be slowed again by the development of high liquid water contents, and so on. The periodicity of such oscillations depends on microphysical parameters, as well as updraft strength; in Kessler's model the range of periodicity values is from about 25 to 40 min. It is not certain that observed variations in storm intensity are attributable to this mechanism. As Kessler (1969, p. 73) suggests, since precipitation formation is relatively time-consuming compared to the time it takes a parcel of air to attain high vertical velocity by buoyant accelerations, the development of large liquid water content is delayed to middle and upper cloud levels during the cell's growth phase.

Once the liquid water (and, perhaps, frozen forms of precipitation as well) reaches middle and upper levels, another process can begin to effect the distribution of the hydrometeors (i.e., all forms of condensed vapor). Since the storm cell tends to move somewhat more slowly than the mean winds in the cloud-bearing layer, there are likely to be substantial relative winds in the upper cloud levels, where wind speeds tend to be greatest. These relative winds act on the cloud and precipitation to move it downstream (in the relative wind direction) from the updraft. Divergence in the upper part of the cell augments this, as well. Thus, there is a net movement of hydrometeors out of the updraft into areas of weaker (or non-existent) vertical motion, allowing the descent, relative to the ground, of the hydrometeors.

The general picture just described is consistent with the observation that precipitation is first observed by radar at middle levels (near the freezing level) during the growth phase of the cell as it approaches maturity.[13] Some of the hydrometeors are carried to higher levels by the updraft and some begin their descent near but on the side of the updraft core (see Fig. 2.30). A useful analogy is a water fountain on a windy day -- the smallest particles are carried farthest downwind, while the largest fall close to the updraft. Note that fallspeeds of the largest raindrops are in the range of 5-10 m s^{-1} so that they can fall relative to the ground on the edge of the typical updraft.[14] As the precipitation falls, radar observations indicate that it may descend faster than even a downdraft-aided speed would allow (Byers, 1965, p. 160). An explanation for this phenomenon is not yet available, but Byers suggests that electrical effects may be involved.

As the cell begins to decay, the input of liquid water from the updraft begins to wane, and more of the large drops are found at successively lower levels. This also has the effect of stretching the precipitation column, because the larger particles fall faster (Kessler, 1969, p. 33 ff.). Not only does the input of precipitation from the updraft stop but, at the surface, the precipitation size decreases during the cell's waning stages. The result on radar is a rapid decrease in low-level echo strength. In effect, it is like "shutting off the fountain", so that the remaining precipitation falls out and the cell dissipates.

It is noteworthy that even in the case of non-severe convection, the updraft and downdraft are basically **separate** entities. It has been suggested that severe storms

---

[13] Remember that radar sensing is more heavily influenced by the size of the hydrometeors than by the numbers of particles.

[14] We have not considered hail formation and fallout -- this is described in IV.D.1 below.

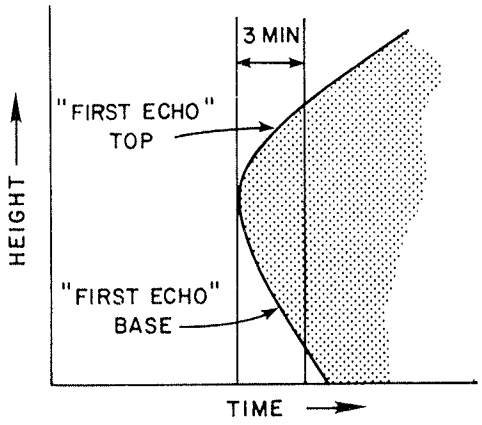

Figure 2.30 Schematic illustration of the time-height evolution of the radar echo from non-severe storms (after Johnson and Dungey, 1978).

differ from the non-severe variety in that their up- and downdrafts are separated, whereas non-severe cells have downdrafts which "fall through" their updrafts. This does not stand up to visual, radar, and logical examination. It appears that the distinction is by the strength and frequency of updrafts (and perhaps by dynamical factors).

III. Severe Storm Classification

> A great thunderstorm; an extensive flood; a desolating hurricane; a sudden and intense blast; an overwhelming snowstorm; a sultry day, -- each of these different scenes exhibits singular beauties even in spite of the damage they cause. Often while the heart laments the loss to the citizen, the enlightened mind, seeking for natural causes, and astonished at the effects, awakes itself to surprise and wonders.
> --St. John de Crevecouer, **A Snow Storm as it Affects the American Farmer**

Numerous passing references have been made that severe storms can be lumped into broad classes which seem to share certain characteristics. We have indicated that the old scheme of "air mass vs. frontal" thunderstorms is no longer considered useful. While it is probable that non-severe convection also could be broken down into categories there is substantially less interest in doing so. A non-severe storm classification scheme is likely to involve even more arguable and subtle distinctions than the proposed severe convection schemes.

Any collection of categories for severe thunderstorms is inevitably "wrong" in some sense. We have already mentioned that even the distinction between severe and non-severe convection has some problems. Certain storms may fit equally well in two (or more!) classes. Others can seem not to fit anywhere. Further, equally qualified people may find it possible to argue almost incessantly over the scheme and where within it a particular storm should lie. This is not necessarily bad, since at least it promotes thought, which may in turn promote new understanding. No scheme should be considered sacred, least of all the one presented here. The value of categories lies in being able to predict, with some reliability, how the members of each class behave (i.e., the weather they produce). Such a prediction must depend on **common physical processes**, shared by the members of that class. If predictions based on it fail more than occasionally, then the scheme is suspect and changes should be considered.

In order to develop a classification structure for severe convection, it is necessary to examine the tools available for observing them and to define what constitutes a severe thunderstorm. In a way, the first step is done -- having already considered the class of **non-severe** thunderstorms. Attention can now be turned to severe thunderstorms.

A. Observation Tools

1. Radar Data

It is probably fair to say that most of our current understanding of thunderstorms is derived from their appearance on radar. This observing tool (originally developed for non-meteorological use in World War II) is sensitive to atmospheric temperature structure and to the presence of particulate matter (e.g., water droplets). While these features are "noise" in terms of military applications, meteorologists quickly recognized this tool's potential use. Excellent summaries of the history of meteorological radar applications, as well as some of the basic theory, can be found in Ligda (1951) and Battan (1973). The Thunderstorm Project (Byers and Braham, 1949) made heavy use of radar in developing the cell concept we have already considered.

It is not possible here to mention all of the literature which applies radar analysis to convection. Rather, the reader is encouraged to examine the references. Further, there are textbooks (Doviak and Zrnic', 1984; Battan, 1973; Skolnik, 1970), review articles (Atlas, 1963; Ligda, 1951; Lemon **et al.**, 1977; Chisolm, 1973; Lemon, 1977) and

numerous preprints available from the AMS conferences on radar meteorology. Recent developments in the application of Doppler radar (see also Wilson **et al.**, 1980) have led to enhanced interest in radar meteorology. Since it is unnecessary for our purposes, these notes do not develop the theory of radar beam propagation. Some basic understanding of conventional and Doppler radar is necessary, however, in order to evaluate their use in storm classification.

It is generally accepted that a radar emitting microwave radiation of about 10 cm wavelength is best for meteorological applications. Shorter wavelengths suffer large losses in beam strength (attenuation) when passing through heavy precipitation, while longer wavelengths only reveal the very largest precipitation particles. It is important to realize that a 10 cm radar only "sees" precipitation, and does not respond well to cloud droplet-sized particles. Only through **inferences** based on the distribution of precipitation can the radar meteorologist visualize the up- and downdrafts which in reality constitute the storm. Since substantial portions of a cumulonimbus do not contain precipitation-sized drops, radar cannot "see" them. It is not unusual for observers watching the PPI scope to refer to the low level (say 0.5° elevation angle) echoes as "the storm" or as "clouds". It cannot be overemphasized that the storm is **more** than its precipitation and the echo is not cloud material. In fact, it has been noted here that precipitation is typically present in areas of thunderstorms dominated by downdrafts, which may not contain clouds!

Radar observers should also be aware that the radar is much more sensitive to the **size** of the particles observed than to their numbers. A relatively small number of very large drops falling into otherwise clear air may produce a substantial return. Another factor which influences radar reflectivity is the surface characteristics of particles in the beam. Ice reflects radio energy differently than water, so the presence of hail can alter the appearance of echoes.

Doppler radars gradually should become operational in the late 1980's (barring budgetary setbacks). However, their widespread use in research already has led to a considerable gain in our understanding of severe thunderstorm air flow. Since a single Doppler measures only the velocity along the beam (i.e., the radial velocity), considerable art is necessary to interpret the single Doppler data (see, e.g., JDOP Staff, 1979; Donaldson, 1970). There are many problems, some fairly straightforward and some rather subtle, in Doppler data analysis, but there can be no question of its value and potential for future applications.

Nevertheless, much of the difficulty in interpretation and application of conventional weather radar also applies to Doppler observations. Beam spreading, sidelobe echoes, ducting, multiple trip echoes, etc., are all included. For Doppler radars, to these are added velocity folding, range-velocity ambiguity, spectral noise thresholds, baseline geometry (with multiple Dopplers), and so on (see Brown **et al.**, 1981). While these may be unfamiliar to some (if not most) readers, it is in their interest to recognize the limitations of the observing system. A study of the references is certainly called for if the analyst is not at least passingly familiar with these concepts.

Most guidelines for operational use of radar have been dictated by empirical rules, without much attention devoted to how storm structure and airflow can influence what the radar reveals. In contrast, Lemon's (1977) work is an effort to apply what we know about (severe) thunderstorms to the problem of radar scope interpretation. This material will be presented in somewhat abbreviated form in Volume **III**. Since Doppler radar data are not yet available routinely, they are not considered further, except where research studies are used to provide knowledge about storm airflow.

2. Satellite Data

While the first TIROS satellite began operations in 1960, it has been the **geostationary** satellites which have provided the potential for near real-time operational applications of satellite imagery. By providing a fixed viewpoint, successive geostationary satellite images (in time) can be projected as a sequence of pictures. This gives the visual impression of movement, which adds dramatically to the value of the imagery. Since this remote sensing tool is relatively new, its ultimate value is far from being realized. An analogy with radar is revealing: it has taken nearly 40 years for the best uses of radar information to become clear. While it can be hoped that the "learning curve" for satellite data will not be so long, there is no guarantee that it shall not be.

Nevertheless, there has been explosive growth in satellite applications (again, analogous with the early history of radar). The opportunity to observe the distribution of clouds in near real-time is truly revolutionary. Like radar, it must be understood what these data actually reveal before they can be applied confidently. An obvious drawback in the area of severe thunderstorms is that a mature thunderstorm usually creates a large, more or less indistinct, mass of anvil debris which can mask the active storm(s) beneath (if any!). This can be partially offset by using infrared imagery to map the cloud-top temperatures and by visual examination for overshooting tops, cloud structures protruding from beneath the anvil, etc.

Much of the current research in satellite-based observing systems focuses on data obtained from regions of the electromagnetic spectrum other than visible light. By using information from different parts of the spectrum, it is possible to construct something like a sounding under the proper conditions. These "soundings" can provide relatively high **horizontal** resolution (say, every 50 km) but presently have limited vertical resolution. There is a rather imposing list of problems yet to be overcome in developing a strategy for the most effective use of these data, but the potential is certainly exciting.

Another use of multispectral satellite data is the imagery in different spectral regions. Petersen **et al.** (1982) offer some very interesting suggestions in this regard. As in the case of satellite-derived soundings, much remains to be learned.

It is not yet clear how satellite images can be applied to the task of classifying a particular storm. If storm severity were determined only by updraft strength, the anvil expansion rate seen in satellite images would be a key classification parameter (see Mack and Wylie, 1982). Unfortunately, things are not that simple. As should be apparent at the end of the examination of storm types, satellite images are more useful when they can be combined with three-dimensional radar displays (and vice-versa!). Users should be aware of potential errors in navigation, positioning errors resulting from the fact that elevated objects (like storm tops) are not directly over the corresponding point on the surface (see Fujita, 1978a, p. 50), and so forth. Also, the nominal resolution (say, 1 km in visual images) only applies at the point on the equator directly below the satellite. As one moves away from the sub-satellite point, image resolution is degraded.

Another limitation of satellite imagery is its timeliness. A photograph takes on the order of 20-30 min to be in the hands of the analyst/forecaster today. This is a relatively long time, compared to the growth and change rates in a thunderstorm. At times, the satellite "scoops" the radar by seeing the developing storms before they have radar-detectable echoes. At other times, the delay in receiving a picture can result in radar echoes being detected before a cloud appears in the available images. A related problem is the normal half-hour time interval between pictures. Dramatic changes can occur

between pictures, with the resulting series of images missing the changes, or only visualizing them roughly. This may be improved upon in the next generation of geostationary satellites. Modern technology is moving in the direction of computerized processing of digital satellite data, which allows much more rapid display and increased timeliness for satellite imagery. Interactive computer systems with direct satellite read-out (e.g., Anthony **et al.**, 1982; or Reynolds, 1982) will eventually replace photographic processing and allow much more flexible use of satellite data.

3. Surface and Rawinsonde Data

As mentioned previously, the surface and upper-air data normally available to the analyst/forecaster are barely sufficient for "subsynoptic" analysis. They are certainly not capable of revealing structures associated with different storm types. However, they do allow the basic identification of **environments** in which particular storm types are likely to develop. This process is hampered by a general insufficiency of data, but there are some useful generalities which are fairly widely accepted (as discussed in Vol. I of this series).

Further, on some occasions, features can be seen in these "conventional" data which are **suggestive** of the effects of a particular storm type. For example, when a squall line type of event occurs, the resulting structures (see III.E.3) can be large enough that the operational data reveal those structures. This type of inference can be risky, unless there are other data (e.g., radar) to corroborate the implied features. As described in I.III.B.7, a knowledge of the structures produced by a particular storm-scale event is valuable for the larger-scale analysis. There can be potentially valuable feedback among different data sources in the process of analysis.

Since high-density mesonetwork data are not routinely available (now or in the foreseeable future), it might be considered appropriate to skip discussion of such data entirely. However, the research results can often depend heavily on the availability of mesonetwork data. That is, many of the features associated with specific storm systems have been discovered by the special-purpose networks. Where it is appropriate, these shall be mentioned.

4. Visual and Aircraft Data

Although the earliest concepts of severe thunderstorms were based almost totally on visual information [see the historical discussion of cumulonimbus models by Ludlam (1963)], this aspect of storm observation has, until recently, fallen on hard times. Since it is difficult to be quantitative with visual data, they are considered by many to be of lesser importance. Ludlam himself (Ludlam, 1976, 1980) has suggested that this is not necessarily a valid position. Doswell and Moller (1985) discuss the observations of storm intercept crews over a period of years. These observations have contributed to vastly improved severe storm spotter training materials (e.g., Lemon **et al.**, 1980), new conceptual storm models (Lemon and Doswell, 1979), and have provided visual confirmation of severe weather events during mesonetwork operations.

Visual observations can be made quantitative by use of **photogrammetry** (see also III.B.3.b,c). In essence, given certain information about the location of the camera(s), their optical properties, and the relationship of the features with respect to them, it is possible to make reasonably accurate measurements of cloud features in space and time (see Lee **et al.**, 1981 and Holle, 1982). Such data are a valuable addition to research studies, especially when used in conjunction with other measurements.

While it seems clear that familiarity with actual, visually-observed severe weather is a substantial benefit for research purposes, one might question its value in operations. A partial justification is in the need for communication with spotters, as will be discussed in Volume III. Further, there are specific visual clues in the storm clouds which are apparently related to the storm type. While this is an area which remains unsettled and needs more study, it should not be overlooked.

Aircraft data can be visual and/or quantitative. Quantitative aircraft observations generally are confined to research-oriented special observing programs. To some extent this may be changing and quantitative aircraft data may become an important routinely collected data base in the future. Some "PIREPS" already routinely collected and distributed can be useful -- e.g., observations of large, isolated CB's, lines of storms, etc. Although these often are not needed in areas of radar and/or satellite coverage, they may be valuable in situations where other data are unavailable. Given that radar and satellite systems are "down" at times, such information may be critical.

McCarthy and Veal (1982) have presented a summary of research-oriented aircraft observations. Aircraft are often the only means of obtaining certain kinds of data needed to understand convection. Recently, Biter **et al.**, (1983) have discussed airborne photogrammetry and its application (also, see Knight **et al.**, 1983).

Again, research findings may depend on non-routine data (as in the dryline traverses described by McGuire, 1962; or Fujita, 1958b). Such data are discussed in what follows, as appropriate. Those familiar with the Thunderstorm Project should recall the vital role played by aircraft in development of the cell concept.

5. "Profiler" Sounding Systems

Within the past few years, some new observing technology has been developed to the point where it is being considered seriously as an operational tool. Most advanced are the techniques for observing vertical profiles of winds aloft, more or less continuously in time (Gage and Balsley, 1978). To a lesser extent, there a similar systems under development to sense temperature and moisture profiles.

The more advanced wind profiling systems employ Doppler radar, and offers considerable potential for meteorological analysis (see e.g., Zamora and Shapiro, 1984). Owing to the relative youth of this technology, it may be several years before the meteorological community understands (a) how best to use it for gaining meteorological insight and (b) how best to deploy it and incorporate the new data in the operational forecasting problem.

At the moment, profiling capability is still several years from operational implementation. In spite of the normal issues which must be dealt with in applying new technology, the possibilities inherent in the systems make the prospects quite exciting.

B. Severe Convective Weather Events

1. Official Definitions

For purposes of the National Severe Storms Forecast Center's Severe Local Storms Unit (NSSFC and SELS, respectively), a severe convective storm is one which produces one or more of the following phenomena:

a. A tornado,
b. Damaging winds, or measured winds >50 knots,
c. Hail, surface or aloft, >3/4 inch in diameter.

While a funnel cloud officially is not considered a severe storm event, an abbreviated record is kept of funnel cloud reports. Also, only waterspouts which move onshore are logged as tornadoes -- otherwise, they are treated in the same manner as funnel clouds.

There are certain semi-official rules for logging severe weather, since a problem arises when a single storm produces a more or less continuous swath of hail and/or wind damage. Reports of the same type of event separated by less than 10 n mi or 20-30 min are not logged as separate events.

SELS maintains a log of reported severe weather, which is updated with Storm Data and follow-up work done by local NWS offices. The updated (or "smoothed") SELS log represents the official NSSFC summary of severe convective weather events. Also, an unofficial "Activity Chart" is kept for each day (and retained by SELS for two years) upon which are noted any reported thunderstorms and convective weather phenomena which are significant, but fail to reach the severe limits defined above. Further, the unsmoothed (or "rough") SELS log reports are plotted on the Activity Chart map and the rough log sheet is attached. Procedures followed by SELS and NSSFC for logging severe weather events are detailed in the Appendix.

2. Other Significant Convective Weather

While the aforementioned smoothed SELS log and **Storm Data** certainly provide the best available records of severe thunderstorm activity, they may not represent the totality of thunderstorms **perceived** as severe. As with any somewhat arbitrary division of real phenomena, the criteria for severe reports may not be entirely satisfactory to everyone.

One class of thunderstorms which fails to fit the criteria, but which certainly is significant, is the **heavy rain-producing storm.** Attention has been drawn to these by some recent devastating flash floods (Maddox **et al.,** 1979; Caracena **et al.,** 1979; Maddox **et al.,** 1978; Hales, 1978; Maddox and Dietrich, 1981; Grice and Maddox, 1983). For those experiencing such a storm, it is hard not to perceive it as anything but severe, even though the official criteria are not met. These storms are considered in more detail in Chapter V, along with some of the distinctions between storms which produce only heavy precipitation and those which become officially severe. Recently, flash floods have been responsible for an average annual fatality rate exceeding that produced by tornadoes or lightning (Mooney, 1983)!

Another officially non-severe storm type is one which produces large amounts of **small** hail. These occur perhaps most frequently in the High Plains region just east of the Continental Divide. However, they can occur virtually anywhere (Robb, 1959) and are undoubtedly seen by many persons as severe storms. Since these events do not fit severe criteria, their climatology is not well-known. Several examples of this are presented in Flora (1956; see plates between his p. 106 and p. 107). In terms of damage production, very large hail can be relatively ineffective except perhaps in populated areas, since the number of large stones per unit area is almost always low. There are some occasional events which produce large numbers of giant hailstones, but these are relatively rare. In contrast, the more common events producing widespread heavy falls of small hail can be incredibly destructive of crops and trees, especially when accompanied by wind (even if the wind itself is also below official severe limits). Although the hailstone size may not be sufficient for official logging, such storms are certainly severe in terms of inflicted damage.

Finally, any thunderstorm producing frequent cloud-to-ground **lightning** is dangerous. Such storms in the western U.S. can ignite costly forest fires. In the plains, electrical storms can cause prairie and structural fires which are hazardous to lives and property. Damage to trees and property can be substantial even without lightning-set fire. Lightning is responsible for an annual fatality total often exceeding that of tornadoes (Mogil, 1977). Since lightning deaths are often singular in nature and can occur with virtually any thunderstorm, there is no unique connection with severe thunderstorms.

Only part of the damages and injuries associated with thunderstorms is sampled by restricting attention to official definitions of severe weather. It is an erroneous notion that all storms which do not fit official criteria are not severe in some sense. Of course, some boundaries must be determined, even if arbitrarily. But do not be deceived into believing that they are meaningful in an absolute sense.

C. The Concept of Storm Steadiness

The cell concept has been developed here previously in connection with the generally non-severe, ordinary thunderstorm. As noted, the updraft in such a storm is essentially a transient event which is rapidly superceded by a similarly transient downdraft as the cell dissipates. The reader may already be familiar with the idea that severe thunderstorms often develop a continuing updraft (and downdraft), thus approximating a steady-state structure. That is, the storm persists for hours with an unchanging circulation structure (Browning and Donaldson, 1963). This **steady-state hypothesis** is considered here and a hierarchy of updrafts is proposed which seems to describe the range of thunderstorm phenomena.

When one observes storms visually (and with high-resolution radar), it becomes clear that superimposed on the overall structure are many small-scale features.[1] At times, this fine-scale detail seems more significant than at other times. Since no storm has lasted forever, no storm has ever attained a true steady state. One disadvantage common to all models is that **pure** examples never occur in reality, so trying to apply the model has risks in the real atmosphere. However, steady-state models are useful approximations. Advantages to making this approximation are (1) it provides a storm model which is relatively easy to understand and (2) the degree to which it applies offers a means of classifying storms.

As a possible means of describing thunderstorm updrafts, we consider three of their properties: **strength, numbers,** and the **time interval** between them. That is, they can be categorized as (a) weak or strong, (b) singular or multiple, and (c) long or short interval. Using these three properties, thunderstorms then can be organized as in Table 3.1. Note that in order for the interval to have meaning, there must be more than a single updraft involved. Further, while there are only two classes for each property, it is possible (or even likely) that these properties are each characterized by a more or less continuous distribution. Thus, for example, the time between updraft pulses may range from only a few 10's of seconds to a few 10's of minutes (or longer), and anywhere between.

Some discussion of the "interval between successive updrafts" is called for, in order to clarify how this notion is used here. As shown in Table 3.1, multicellular storms are considered to have "long" intervals between each updraft pulse. It is this which enables

---

[1] An interesting discussion of how each weather phenomenon is composed of a basic structure with smaller features superimposed can be found in Tennekes (1978).

TABLE 3.1

Class			Example(s)
1.	Weak, Singular	-	Non-Severe: "Byers-Braham" Cell
2.	Weak, Multiple		
	a) Low Frequency	-	Non-Severe: Multicellular
	b) High Frequency	-	Non-Severe: Squall Line
3.	Strong, Singular	-	Severe Cell: "Pulse"
4.	Strong, Multiple		
	a) Low Frequency	-	Severe: Multicellular
	b) High Frequency	-	Supercell, Severe Squall Line, "Dryline"-type

Table 3.1 Classification of updrafts.

observers to distinguish successive updrafts visually and on radar. One might argue that supercells really only consist of a single, long-lived updraft, in which case they belong in the class of singular events of Table 3.1. This also suggests that they are quasi-steady, an approach that cannot be discounted. However, in this text, I prefer to think of a supercell as a process which maintains the appearance of quasi-steady updrafts through a succession of updraft pulses at such short intervals that they are indistinguishable except perhaps via very detailed observations. While I realize that this is an arguable approach, it is one which highlights the **departure** from a steady-state situation. The process which I assume to be governing the rapid production of "new" updrafts also evolves, but on a longer time scale. In effect, this view is similar to that presented by Foote and Frank (1983) and discussed by Burgess and Ray (1984), except that it is **temporal**, rather than spatial intervals between cells which emphasized. This whole area of storm classification is characterized by active debate and research -- I have expressed one interpretation of the data, but others are certainly available (check the references)!

It generally is found that strong updrafts are associated with all severe weather phenomena, with the possible exceptions of lightning and some "downburst" situations (Caracena **et al.**, 1983a). So how strong is "strong"? Generally, an updraft is considered strong when it attains speeds of 30-40 m s^{-1} or more. There is good evidence to suggest that peaks approaching 50-60 m s^{-1} are present in the strongest storms.

The existence of more than a single updraft indicates that there is some mechanism operating to produce updrafts repetitively. The scale of this mechanism may be larger than the individual storm scale. Part of the evidence for such a mechanism is the knowledge (discussed in I.IV.A) that a severe storm processes mass through its drafts much faster than can be re-supplied by synoptic-scale inflow. Thus, some subsynoptic (or

mesoscale) system must be acting to sustain multiple updrafts.[2] Otherwise, the storm quickly uses up the "pooled" energy and there is only a single "pulse" (or relatively short series) of severe weather. Such short-lived events do occur, of course (see F.2).

As discussed in II.B.1, severe storms do not generally occur randomly. There is a rather extensive list of candidate processes which are capable of supplying lift and renewing the source of fresh convectively unstable air for a series of updrafts. When that process is **linear** in character, a squall line often results (as in the case of fronts). At other times, the organizing feature is concentrated in an **area** (e.g., to the northeast of a subsynoptic-scale low pressure system), so thunderstorms resulting form in "blobs", or clusters.

Regardless of how the convective weather system is initiated, convection and the weather system (process) producing it evolve together.[3] The storm's evolution can prduce a wide range of structures during its total lifetime and, as its structure changes, the convective processes can modify their environment substantially. Thus, there can be feedback between the storms and their larger-scale organizing structure. Consequently, the convection may develop as weak, long-period storms, change to strong, short-period activity, and finally decay as a weak squall line. In fact, this is is the sequence of events described by Lemon (1977) as being common for supercell storms.

So how does all of the preceding relate to storm steadiness? Given that thunderstorm events can persist more or less unchanging for hours, the concept of a steady-state approximation is appealing. The proposed updraft hierarchy is one other way to describe the problem. The short-period, multiple updraft examples (supercells, squall lines) derive a long lifetime by virtue of some process, which in comparison to the **convective time scale** (the time required for a parcel to pass through the system), is basically unchanged. The more or less steady (or quasi-steady) period must be long compared to the convective time scale. For a cell reaching heights of 16 km, with updrafts averaging 25 m s^{-1}, this is about 11 minutes, so a "long" time might be anything more than 30 min.

In this sense, even a multicell complex (severe or not) can be considered to be in a steady state. However, if the viewpoint is at convective time scales (as defined), the multicell storm is clearly unsteady while the supercell remains more or less steady-state. Information at time scales less than the convective scale is pretty limited, so updrafts produced much more frequently than the convective time scale are virtually indistinguishable from a truly steady "plume" (i.e., infinite frequency).

The evolution of the storm is governed to some extent by its interactions with its environment. A storm which alters its environment in a way destructive to convection cannot persist. Similarly, an environment which cannot supply energy to convection limits the lifetime of the storms even if they are not destructively altering their surroundings. Our understanding of this interaction is limited, but there is good evidence

---

[2] Furthermore, it is often found that the air rising through the cloud base is actually negatively buoyant (Marwitz, 1972a). Thus, some process must operate which overcomes this for parcels to continue to rise (see I.II.B.2 and I.II.C.2). Such a process may be linked to larger scale features or it may be some storm-scale phenomenon.

[3] In fact, it is tempting (from a philosophical viewpoint) to consider a severe thunderstorm (or most meteorological phenomena) to be a process, rather than a thing. An extensive discussion of this topic is beyond the range of this volume, but it makes interesting food for thought, to be taken up in Vol. III.

that supercell storms, for which the steady-state hypothesis is most often invoked, have some **dynamical** differences from other storm types (Weisman **et al.**, 1983; Lilly, 1983), apart from differences resulting from the resolution of the observing system (or, alternatively, the time scale associated with a particular viewpoint). Thus, storm steadiness may be related to a physically-based difference even at convective time scales. This has important implications for storm classification, should continuing research verify these hypotheses.

For these notes, the convective time scale is used to assess storm steadiness. Thus, storm steadiness (as sensed by current observing systems) is an important criterion for distinguishing storm types. Nevertheless, the reader should recognize that even supercells evolve, but only on time scales which are long in comparison to the convective scale (see e.g., Lemon and Doswell, 1979; Jensen **et al.**, 1983).

D. Storm Motion and the Environment

For most non-severe convection, it has already been noted (II.A.3) that the characteristic form of the convection is influenced by the environmental wind structure, especially in the vertical. In severe convection, the role of shear in the environment is even more apparent. Although not the first (or last) to point this out, Ludlam's (1963) review article has drawn attention to the very close association between the severe storm-prone areas world-wide and middle (and upper) tropospheric jet streams.

Essential to understanding the basic origins of mid-latitude jet streams is the notion of the **thermal wind.** While this was mentioned in I.II.B.2, a brief review is useful here. Since the free atmosphere in mid-latitudes is typically in a state of near-geostrophic balance, the change of the geostrophic wind with height can account, in large measure, for the actual vertical wind change. This geostrophic wind **difference** between pressure levels is the thermal wind, which is proportional to the horizontal gradient in thickness between the pressure surfaces. In turn, the Hypsometric formula relates this thickness to the mean virtual temperature in the layer.

Since it is, in general, more or less uniformly warm to the south of mid-latitudes as well as more or less uniformly cold to the north, the greatest horizontal temperature contrast is in mid-latitudes. Hence, the strongest thermal winds are found in mid-latitudes. The normal orientation of the thermal wind vector (determined by the normal temperature field) is such that westerly winds increase with height. The westerly jet streams of mid-latitudes arise, in large part, through this mechanism. It is a simple outgrowth of this simple argument to see that **severe storm-prone areas are found in regions of relatively strong vertical shear.**

As mentioned in I.II.C.3, this situation represents a paradox. Strong vertical shear can be detrimental to convection and yet observations show clearly that severe convective storms prefer regions of strong vertical shear! Thus, any review of severe thunderstorms must account for how they can thrive in a seemingly destructive environment.

Further, from the earliest observations of severe storms on radar, it became apparent that many severe storms do not travel simply with the flow field in which they are embedded. Since severe storms occur typically in sheared environments, by virtue of their substantial depth, different parts of the storm are within substantially different environmental wind fields. Thus, it is common to compare the storm motion (as seen on radar) to the mean wind vector, averaged over some layer roughly comparable to the depth of the storm (Fig. 3.1). If this mean wind vector is subtracted from the environmental wind at all levels, an approximation to the storm-relative wind profile

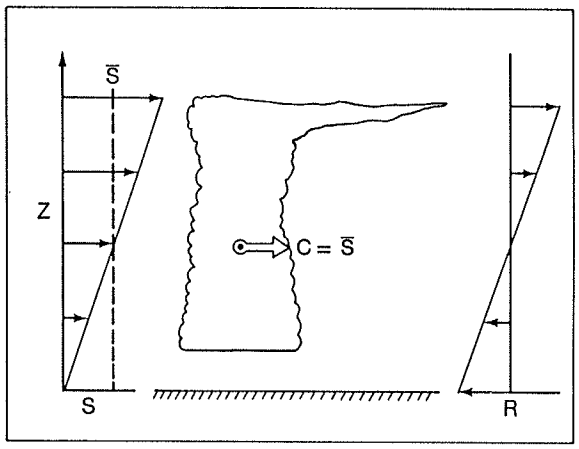

Figure 3.1 Schematic showing relative flow with respect to astorm moving at speed C which equals the mean speed S in the shear layer. Subtracting the storm motion C gives the storm-relative flow, R.

results, provided the storm motion is not substantially different from the mean wind vector. In this simple case, the relative flow brings air in from low levels ahead of the storm, and then forces air out of the storm in upper levels, also ahead of the updraft. For this example, the environmental wind profile is unidirectional (i.e., no direction change with height).

When the storm motion differs from the mean wind, as it often does, the possibilities multiply rapidly. For the severe storm situations described by Darkow and McCann (1977), it is clear that there are definitely preferred relative flow structures, but they are not limited to the "classical" cases of right-moving storms in a sheared environment. Thus, there is apparently a substantial, but not limitless, number of ways in which storms can be structured (in a relative flow context) and still produce severe weather events. It is likely that further research in this area would be fruitful.

Storm motion has been of considerable interest to researchers and forecasters for some time. Newton (1950) devotes considerable effort to explain the differences in squall-line motion between his cases, since the two examples had different speeds and orientations with respect to the upper flow. Tepper (1950) uses an exotic hydraulics argument to explain squall line motion -- an idea explored more recently by Charba (1974) among others. Newton and Newton (1959) point out that thunderstorms can move as a result of preferential new cell development on one flank of the updraft (i.e., **propagation**) -- arising at least in part from the storm's interactions with the environment. This concept is used by Browning and Ludlam (1962), Browning and Donaldson (1963), Fankhauser (1971), Charba and Sasaki (1972), Newton and Fankhauser (1975), and Rotunno and Klemp (1982), as well as a host of others.

The occasionally odd motion of storms, especially severe storms, has puzzled and stimulated meteorologists ever since radar has enabled them to be tracked. Browning's (1964) classic paper on right-moving storms and the more detailed study (Browning, 1965a) from which it is derived, are among the most noteworthy of a large number dealing with severe storm deviate motion. Others include Marwitz's (1972 a,b,c) insightful analyses, Hammond's (1967) study of a left-moving storm, and Fujita's (1965) paper on the lift force produced by rotating storms. Both right- and left-moving storms are often the result of a **storm splitting** process (discussed in III.E.2.b). Splitting storm events have been documented by Achtemeier (1969), Fujita and Grandoso (1968), Haglund (1969), Charba and Sasaki (1971), McCann (1983), and others.

So how do these various storm motions arise? While a completely satisfactory explanation has not been advanced, it is possible to indicate likely avenues for pursuing

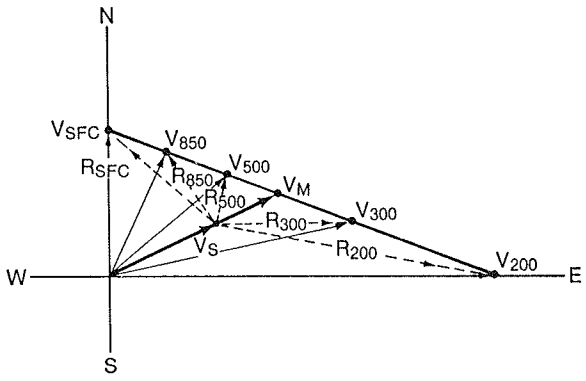

Figure 3.2 Example of straight-line hodograph in a basically southwesterly flow situation (see text for discussion).

the answers. The primary key seems to be the way in which a storm interacts with its environment.

Consider the example in Fig. 3.2, where the line connecting the tips of the plotted environmental wind vectors (i.e., the hodograph) is a simple straight line. The mean wind (V_M) then falls on that straight line. For a storm which moves with a velocity on the hodograph, the storm-relative flow looks very much like Fig. 3.1. The storm motion in such a case may not coincide exactly with the mean wind (V_M), which results in shifting the point of zero relative flow up or down. Nevertheless, a straight-line hodograph with storm motion along the hodograph is essentially the same (relative to the storm) as a case with unidirectional environmental shear. When the motion of the storm is not on the hodograph (e.g., V_S on Fig. 3.2), the relative winds become more complex. In this example, the relative wind vectors (those denoted by R) show relative inflow at low levels on the right flank. That is, because the storm movement is not somewhere **on** the straight line hodograph, an observer travelling with the storm would see low-level inflow from the right side of the storm.

It is important to distinguish between storm motion (e.g., the movement of the updraft, or of the radar echo, which are not necessarily the same!) and the parcel trajectories. It is a common mistake to confuse **storm** motion with **parcel** motion, which seems to arise from thinking of "the storm" as a **thing**, rather than a **process.** At any given instant, the storm is made up of a collection of parcels, but during the lifetime of the storm (especially one which persists as an entity for periods longer than the convective time scale), the constituent parcels are continuously leaving and being replaced by others. The paths taken by the parcels do not define the path of the storm!

During the time of residence within the storm's drafts, parcels are acted upon by processes which may change their momentum. Clearly, parcels which participate in the strong vertical drafts have their **vertical** momentum changed by buoyancy, water loading, and whatever dynamical processes that forced them up (or down) in the first place. Once they are displaced vertically, in a **sheared** environment, their **horizontal** momentum no longer equals that of parcels in the surrounding environment. Thus, forces on the storm's constituent parcels act to alter their horizontal momentum (as mentioned in II.A.3), in cases of non-zero shear.

If we consider what happens to an isolated thunderstorm in zero shear, we end up producing a downdraft which falls right back through the updraft (a pretty unrealistic situation). As the downdraft approaches the surface, it slows down and spreads out

symmetrically.[4] Thus, there is no preferred direction for new updrafts to be developed -- the convergence along the outflow is symmetric. Such a storm must move **with** the environmental flow (which is constant with height, so one possibility is that the storm is not moving at all). Once new storms are initiated along the outflow (**if** they are initiated!), their environments may now contain some vertical shear as a result of the previous storm's effects, so the situation becomes more complex.

Proceeding to a somewhat more realistic approximation, suppose there is vertical shear in the environment, such that the hodograph looks like a straight line (as in Fig. 3.2). Our isolated thunderstorm is now moving parcels up and down which have different horizontal momentum depending on what level of the environment from which they originally came. For the sake of argument, suppose that a parcel's initial horizontal momentum is conserved. This is a reasonable assumption if the horizontal accelerations arising from imbalances with the environment are small and/or if the time which the accelerations have to act on the parcels is brief (as in a strong up- or downdraft). Parcels which participate in the downdraft, whatever their origins, must have the momentum associated with the symmetric outflow added to their original momentum, because the flow must diverge at the surface. Thus, the outflow is no longer symmetric, but becomes elongated in the direction of the parcels' original flow vector. Since the hodograph is a straight line, the difference between velocities brought from some level to another level must fall on that straight line. Thus, the enhanced convergence resulting from momentum transport must result in new cell development so as to yield a propagation effect (and "storm" movement) somewhere **along** the hodograph.

Clearly, a more realistic situation allows for the hodograph to be curved, but it is important to re-emphasize that a straight line hodograph need not require the winds to all be the same direction! Thus, **veering or backing of the winds is not sufficient to infer curvature of the hodograph.** When the hodograph is curved, it is possible to produce storm movement by propagation through momentum transport which does **not** fall anywhere on the hodograph. To see this, consider Fig. 3.3, which shows that, for example, the velocity difference between 300 and 850 mb does not fall on the hodograph. Hence, the propagation effect arising from momentum transport in an environment with a curved hodograph will not fall on the hodograph, in general. As a matter of fact, neither will the vector mean wind! To see this, consider Fig. 3.4. Since the vector mean wind is derived by averaging the u and v components, it must fall somewhere **inside** the curved hodograph. Note that in Fig. 3.4, the winds have been given equal weight in the averaging. It is not uncommon to weight the winds according to pressure or density, so that winds at lower levels are given more weight. This is to account for the fact that at higher pressures, there is more mass per unit volume of moving air, which means that there is more inertia with a given speed at lower levels. Pressure or density weighting will not, in general, change the result that the resulting weighted mean wind does not fall on a curved hodograph.

Up to this point, we have only considered propagation through the mechanism of **momentum transport.** For cases with little or no shear, or linear shear, we have seen that for isolated storms to move with a velocity other than those seen in the environment (i.e., somewhere on the hodograph), there must be some propagation mechanism **besides** momentum transport. While situations with non-linear hodographs are more complicated in terms of their possiblities, anomalous movements unexplainable in terms of momentum transport still arise. There are two other ways to induce new development of updrafts and, therefore, make the storm move via propagation.

---

[4] Do not make the mistake of thinking that vertical accelerations **cause** convergence or divergence. Rather, one should think of them (i.e., vertical motion and divergence) as operating together. That is the point of the mass continuity constraint.

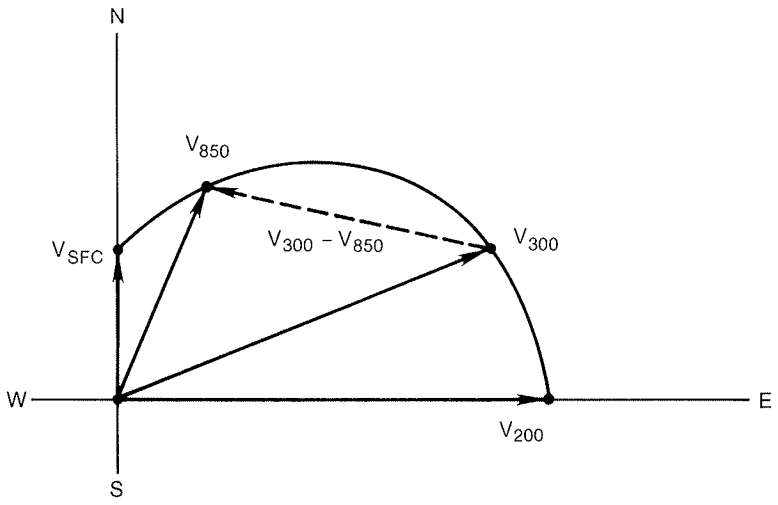

Figure 3.3 Schematic showing the effect of a curved hodograph on the vector difference between levels.

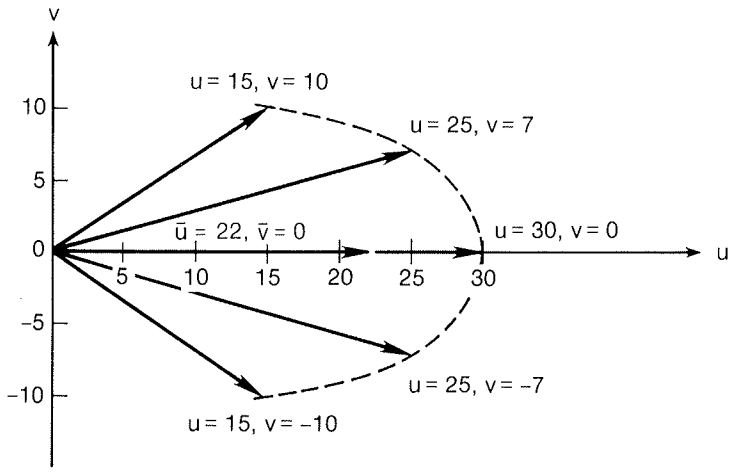

Figure 3.4 A calculation of the mean vector wind with a curved hodograph.

The first such broad category includes the **physical processes created by the storm itself.** That is, the intense vertical drafts, gust fronts, hydrometeors, and so on can have profound effects within the storm and its immediate environment. Without the presence of the storm, these would not be present. Such influences can act to favor new updraft development in some places, while suppressing new convection in other places.

One of the classical studies of this is by Newton and Newton (1959). They suggested that the vertical transport of momentum could result in the storm behaving something like an **obstacle** to the environmental flow field. Naturally, the storm is not really a solid obstacle, but the large horizontal momentum gradients resulting from convection in a sheared environment produce hydrodynamic (i.e., non-hydrostatic) pressures acting to enhance convection on specific flanks of the storm. In their classical two-dimensional depiction of this effect (Fig. 3.5), this argument is actually analogous to the previously-discussed momentum transport arguments. That is, without momentum

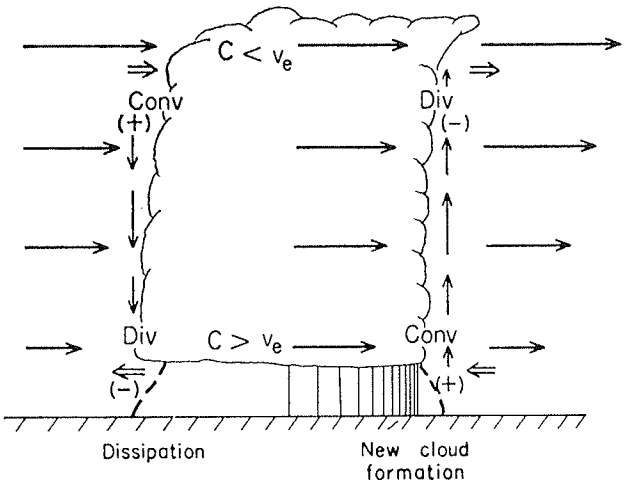

Figure 3.5 Schematic cross section through a squall line or large rainstorm. Lengths of horizontal arrows proportional to wind speed outside and inside cloud system (from Newton and Newton, 1959).

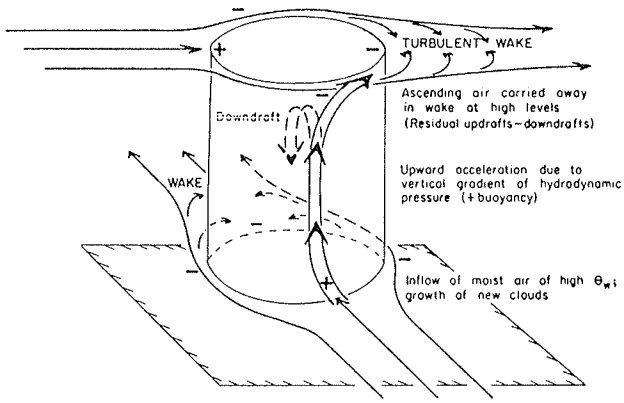

Figure 3.6 Schematic representation of flow at upper and lower levels, relative to rainstorm represented by cylinder. Plus and minus signs indicate positive or negative hydrodynamic pressure (from Newton and Newton, 1959).

transports, the momentum differences which are associated with the hydrodynamic pressure forces could not exist. With directional shear imposed (as well as speed shear), their implied dynamic interaction is shown in Fig. 3.6. Note that they used a non-linear shear profile in developing this concept (see their Fig. 9), with a storm motion off the hodograph.

The discussion by Newton and Newton (1959) and that by others (e.g., Alberty, 1969) concentrated on establishing the applicability of the arguments favoring hydrodynamic pressure as a mechanism for deviate storm motion. More compelling verification had to await fully three-dimensional storm modelling by numerical simulation, about which more will be said.

Another internal mechanism for storm motion was proposed as storm observations began to suggest that intense, supercell-type convection is characterized by storm-scale rotation. As first proposed, the notion borrowed from the concept of a storm as an obstacle to the environmental flow, but one which is rotating. Fujita and Grandoso (1968) or Charba and Sasaki (1971) give representative discussions of this idea. An interesting variation on this theme is found in Lemon (1976b). All of these suggestions draw heavily on aerodynamic experiments which have shown that a rotating obstacle in a flow field produces a horizontal "lift force" (see e.g., Prandtl and Tietjens, 1934).

Lemon's variation is to point out that when an obstacle in a flow field **begins** rotating (or **changes** its rotation rate if initially already turning), a vortex of opposite sign to the obstacle's change in rotation is shed into the environmental flow. Lemon proposed this to explain the observations of splitting storms, apparently with opposite rotation in the resulting pair of storms.

As discussed in Charba and Sasaki (1971), the rotationally-induced lift force could combine with the other hydrodynamic effects to provide a qualitative explanation for the resulting storm motion (Fig. 3.7). As with the hydrodynamic effects, this notion of rotationally-created lift force has awaited three-dimensional numerical storm simulations for a detailed evaluation. Since the most comprehensive evaluations of how internal storm processes affect storm motion (via interactions with the sheared environment) have been done in conjunction with numerical model simulations, the final discussion of these (and other) issues is deferred to Chapter VI.

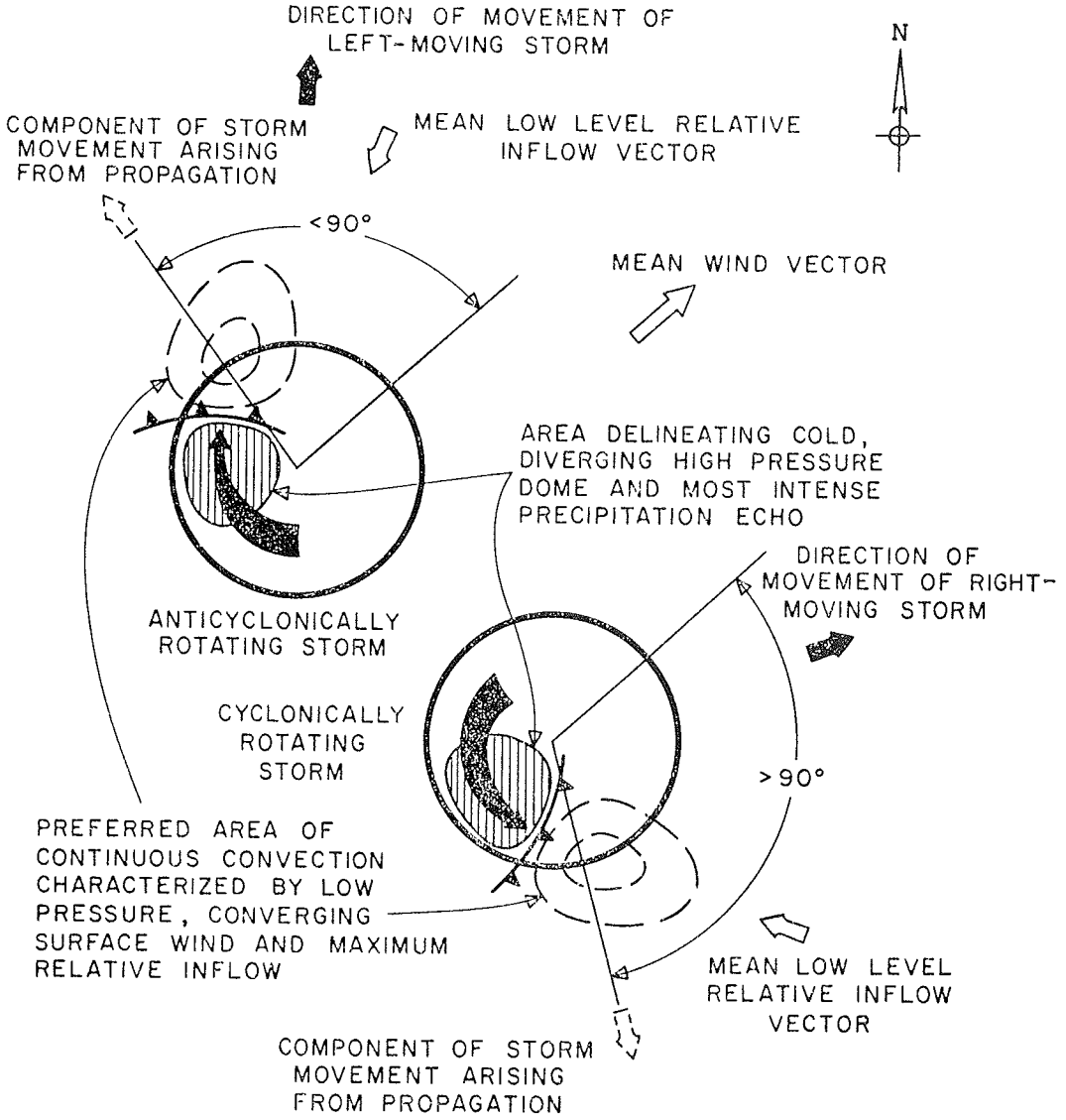

Figure 3.7 Model illustrating the continuous propagation mechanism for left- and right-moving thunderstorms of 3 April 1964 (from Charba and Sasaki, 1971). See text for discussion.

The second category of processes which influence storm propagation includes **physical processes which are independent of the actual convective storm itself.** Of course, one has to be aware that when thunderstorms interact with these processes, they may alter them substantially. Whether or not the convection interacts to modify these external forcing mechanisms, there is a clear distinction whenever other processes are involved, since by definition, they exist in the environment independent of the thunderstorms.

A fine example of this is found in Weaver (1979). The case Weaver examined shows clearly that new convection was developing in a slow-moving subsynoptic area of moisture convergence. Although the radar echo centroid moved slowly northeastward, in association with the overall expansion of the echo mass, the southwestern edge remained nearly stationary, in spite of a substantial westerly mean wind.

Another case of interest is that described by Browning (1965a), in which the storms commenced their deviate motion (Fig. 3.8a) upon encountering a warm front (Fig. 3.8b). The alteration in tornadic storm behavior and motion when running into a pre-existing boundary has been documented by Maddox **et al.**, 1980a).

Of late, **gravity waves** have been suggested by many authors as having some role in thunderstorm propagation (e.g., Uccellini, 1975 or Raymond, 1975). It is perhaps more common to propose gravity wave **initiation** or **enhancement** of convection. However, the studies seem to show a subsequent continuing association of the gravity wave with the convection, once initiated. This suggests that the motion of the convection is being influenced by the gravity wave in some way (perhaps through an unknown feedback mechanism).

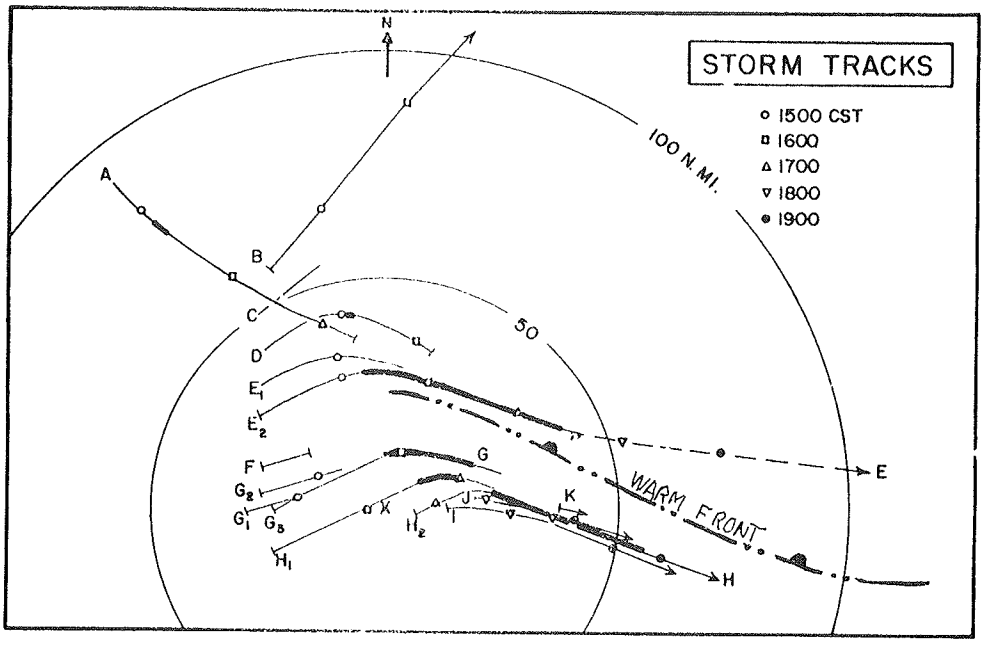

Figure 3.8a Diagram of major echo tracks on 26 May 1963. The severe stage is indicated by the heavy lines. The approximate position of the warm front (Fig. 3.8b) is shown (adapted from Browning, 1965a, p. 119).

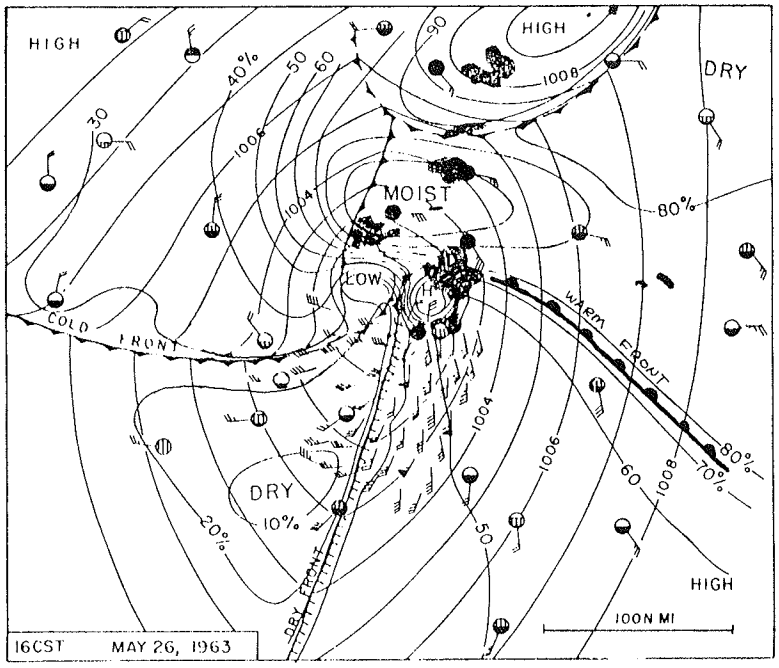

Figure 3.8b Mesoanalysis for indicated date and time. Note wind shift and moisture discontinuity along (added) warm front (adapted from Fujita and Stuhmer, 1965).

Common to these external propagation mechanisms is the role played by the convergence. Zehr and Purdom (1982), for instance, have given examples for which apparently random storm motions could be tied clearly to interacting subsynoptic scale features (including fronts, thunderstorm outflow boundaries, sea breeze fronts, and drylines) which create locally intensified low-level convergence. The implied enhancement of upward vertical motion is the suggested link between these processes and storm propagation.

Given an observed deviate thunderstorm motion which is clearly associated with some external mechanism, one of two things must be occurring: (1) the internal mechanisms are **too weak** to be effective at influencing storm motion, or (2) the internal mechanisms are **in phase** with the external processes. For situations which involve severe convection in a sheared environment (as in the Weaver and Browning cases just mentioned), the second is the most likely alternative.

By way of concluding this discussion, we should point out that whenever convective storms move, the issue of **relative flow** becomes significant in understanding the storm's behavior. If the motion is such that low-level relative inflow is enhanced, it is easy to see that the storm circulation is getting more of the latent heat energy which drives it. If we ignore the possibility that thunderstorms somehow know how to move so as to maximize their fuel intake, we have a bit of a paradox to resolve. The question is as follows: does the storm become severe because of the way it moves or does it move the way it does because it became severe? This is a classic chicken-egg (cause-effect) problem. The preponderance of evidence from a variety of sources suggests that storms develop their unique movements by the way in which they interact with their environment. Thus, the issue of their severity may well be an irrelevancy! At the risk of alienating my readers, I would say the fowl issue of the chicken-egg paradox was merely a red herring, a decidedly fishy turn of events. Once their movement is established, a

variety of other factors determine how severe the convective storms will be. Finally, once a process is established and quasi-steady, it can be argued that implications of cause and effect are entirely inappropriate -- no component of a steady process can be thought of logically in cause/effect terms.

E. The Primary Classes of Severe Storms

Having finally reached the stage where we can begin to describe the proposed classification scheme, the reader should recognize that most views of storm structure are derived from remote sensing, especially radar. What is presented here draws heavily from the work of Browning (see, e.g., Browning, 1964, 1965b; Browning and Ludlam, 1962; Browning and Foote, 1976) and Marwitz (1972a,b,c,). The primary classes described are based on a broad spectrum of observations from virtually the world over. Severe storms (or, more specifically, the physical laws governing their structure) do not recognize state, regional, national, or international boundaries. Rather, the same basic physical processes are involved in storms everywhere. Naturally, details may differ somewhat, depending on unique regional conditions, but there is no question that the storm types described are not confined to any special region. There certainly are regional differences in the relative frequencies in the various categories. These are just beginning to be explored (see e.g., Nelson, 1976; Nelson and Young, 1979), and research into geographical variations of storm type occurrence frequencies is continuing.[5]

The primary classes of severe thunderstorms are: severe multicellular, supercells, and squall lines. These three types account for the vast majority of reported severe weather. Although exact figures are not available, probably less than 10% of the total number of thunderstorms ever produce severe reports (as defined by SELS). Of these, only a small fraction produce more than minimally severe events. Therefore, most damage resulting from thunderstorms can be attributed to an extremely small proportion of the total population of convective storms. In order to do an adequate job of forecasting and analysis of these damaging storms, a substantial part of the problem is to identify those relatively rare examples of a common phenomenon which are truly dangerous. Research focuses on these relatively rare events for just this reason.

1. Multicellular Severe Thunderstorms

a. Radar Structure

This type of severe thunderstorm is probably the most common. Since most ordinary thunderstorms consist of more than a single cell, such a storm is essentially a stronger version of the common thunderstorm; i.e., a quantitative rather than qualitative difference.

So how does one recognize and identify a severe multicellular storm? Since radar is the usual storm sensor, we consider the radar structure first. Recall that precipitation usually is first detected by radar near the freezing level. Since a storm's severity generally is related to its updraft strength, it is logical to suppose that updraft strength influences the appearance of radar echoes. First of all, a strong updraft carries condensation products to higher levels before they are detected by radar. Thus, a cell

---

[5] The study of geographic variation in storm type frequencies is hindered by a lack of a generally-accepted storm classification technique. If different people have different classification schemes, it is hard to compare results. Also, the criteria used in the schemes may vary, so that even if the schemes are nominally identical, one researcher may call a given storm a supercell while another would classify it as a multicell.

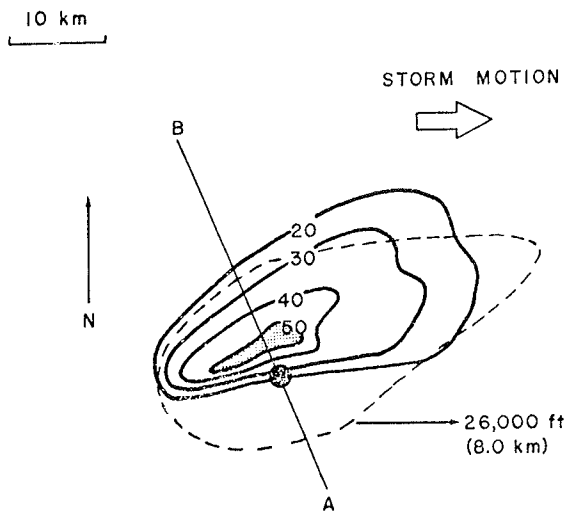

Figure 3.9a Schematic showing superposition of low, middle, and upper level radar structure for a multicell storm. The vector shows the wind at 26,000 ft, while the black dot locates the storm top (from Lemon, 1977).

which is potentially severe should have its first radar echoes at higher levels than a weaker, non-severe cell. Note that severe convection often begins with non-severe cells, so the appearance of a cell with first echo at higher levels than its predecessors may signal the transition to severe intensity.

Second, because precipitation is held aloft in and near the core of the updraft, a Weak Echo Region (WER) is developed, as in Fig. 3.9. By scanning through the storm in a sequence of tilts of the radar antenna, the WER becomes apparent as a region of "overhang". That is, middle and upper level echo can be seen to overlie regions of weak or absent low-level echo. At low levels, the primary radar indication of a strong updraft is the strong reflectivity gradient on the inflow side of the echo. Also, for a severe multicellular storm, the echo top (there usually are several!) tends to be found near or over the region of strong low-level reflectivity gradient (as shown in Fig. 3.9). Note that the absolute highest top in the complex may still be near the low-level reflectivity core, but a radar top of height comparable to the absolute maximum top is found, in a severe multicellular storm, with the reflectivity gradient. This represents a change from non-severe storms, as described by Lemon (1977), in which the echo top is typically located near or over the region of maximum low-level reflectivity, with no substantial top near the margins of the low-level echo.

This suggests that the updraft in a severe storm is more likely to be nearly vertical. If the updraft summit is more or less right over the maximum low-level echo core, substantial updraft tilt is implied, since the roots of an updraft are not likely to be where precipitation is reaching the surface. One expects the roots of severe updrafts to be somewhat upstream (relative to middle and upper tropospheric winds) from the low-level echo core.

The radar structures just described may not be **permanent** features of a multicellular severe storm. By its multicellular nature, such a storm's detailed radar structure reflects a fairly low frequency of updraft pulses, which constitute the storm complex as a whole. The time variation of features has been described by Marwitz (1972b), Chisolm and Renick (1972), and others. The severe multicellular storm consists of a **series** of strong cells, typically in various stages of formation and decay, just as in a non-severe complex of thunderstorms. The distinction between severe and non-severe multicellular storms seems to be based on updraft strength, but there may be some overall organizing process, which is absent in ordinary (non-severe) multicell

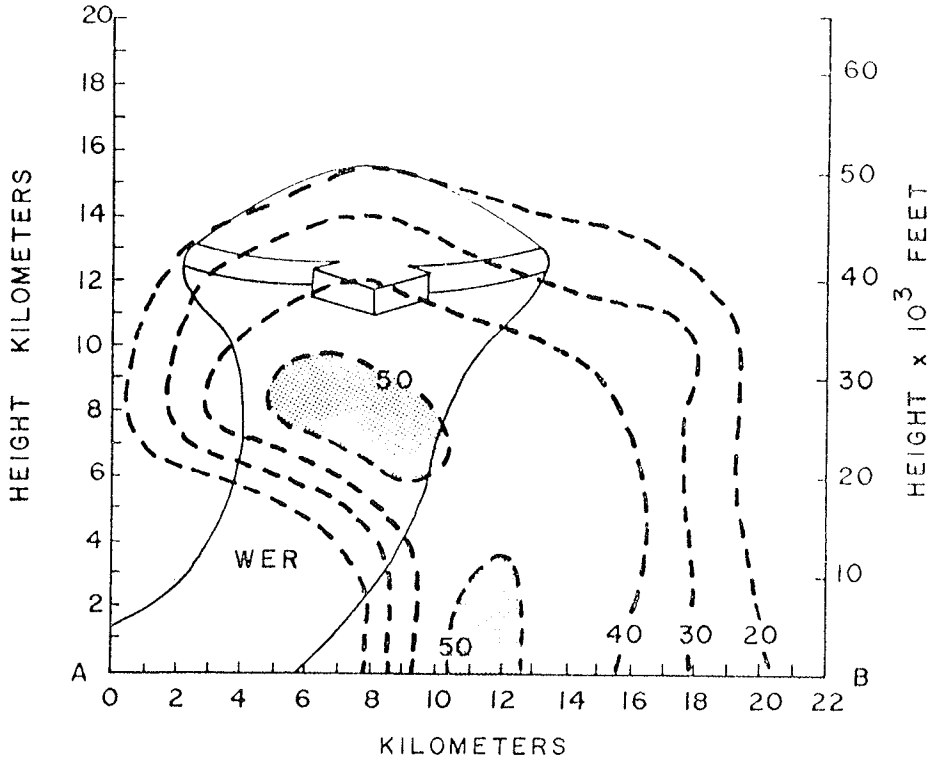

Figure 3.9b Cross section along line AB of Fig. 3.7a. Note the WER, or overhang (from Lemon, 1977).

complexes. If such a process exists, it is probably related to the way the convection interacts with its environment. It is not yet clear whether or not such an organizing process has been identified. Nor do we know if such a mechanism is **uniquely** associated with severe storms (i.e., all severe multicell storms have it and no non-severe versions do).

Part of the reason for proposing this apparent organization is associated with preferential development of new updrafts in a particular location relative to their predecessors. The typical preferred location for new cell development is on the right or right-rear storm flank. As noted above, a variety of explanations exists for this observation, but the result is a succession of strong updrafts which first develop radar echoes aloft. As this precipitation descends, a new echo begins to form on its flank. This sequence is summarized in Fig. 3.10, showing how the storm as a whole maintains a more or less steady (depending on the frequency of new cell formation) WER. It is

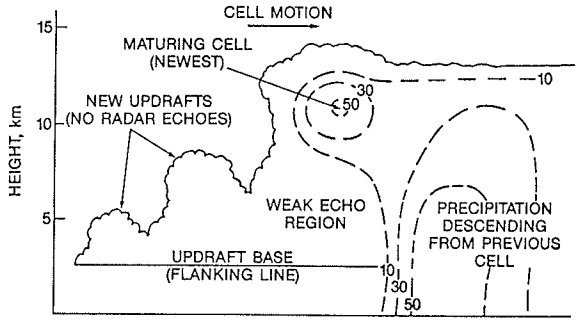

Figure 3.10 Schematic "snapshot" model of a sequence of cells, forming on the left and moving from left to right, creating a multicell thunderstorm complex. Dashed lines represent radar reflectivities (say 10, 30, and 50 dBz). Storm and cell motion vectors indicated at lower left, while cloud boundaries are indicated by irregular line.

noteworthy that each cell, in its turn, becomes the main (or dominant) one in the complex, giving way during its decay to newer cells.

The tendency for new cells to form on the right or right rear flank has an immediate impact on how the complex moves. Individual cells usually are observed to move nearly with the mean wind in the convective layer (normally from southwest to northeast). By forming new cells on the right rear flank, the complex as a whole will move slower than and somewhat to the right of the mean wind. This process is shown schematically in Fig. 3.11. The propagation effect is **discrete** -- see Marwitz (1972b), Battan (1973) or Newton and Fankhauser (1975) -- that is, it occurs in a series of separate steps, each associated with new cell formation at relatively long intervals (see Table 3.1).

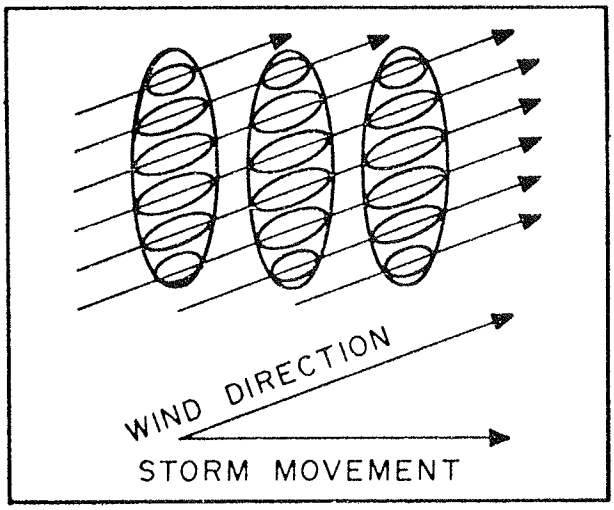

Figure 3.11 Schematic diagram showing how the development of new cells on the right flank and decay of old cells on the left flank cause the cluster as a whole to move to the right of the wind (After Browning and Ludlam, 1960).

Although multicellular events may be the most common type of severe storm, they are **not** generally the most severe. Nelson and Young (1979) have shown that their "ordinary cell" hailstorms (which includes multicellular hailstorms) have, in the mean, substantially smaller maximum hailstone sizes, smaller hailswath areas, and lower probability of producing severe weather other than hail, than do "supercell" hailstorms. The classification scheme used by Nelson and Young is somewhat different than the one used here, being based on Browning (1977). However, the basic concepts are similar and the results are consistent with the idea that multicellular severe storms are not the most severe.

b. Visual Structure

Visually, multicell severe storms have an appearance which is consistent with the radar structure. The updraft pulses which form repeatedly on the storm's flank are seen as a series of cumulus towers, each of which eventually becomes the dominant cell. Note that the youngest of these clouds have not yet formed precipitation echoes. Such a series of cumulus towers forms what is referred to as a **flanking line** (Bates, 1963; Lemon, 1976a; Doswell and Moller, 1985). Since the updrafts are discrete, each tower in the sequence is separate from its companions, reaching higher levels as it approaches its predecessor. This gives the flanking line a "stair-step" appearance, such as is revealed by Fig. 3.12. Note that the precipitation is held aloft, as suggested by radar, until the cell

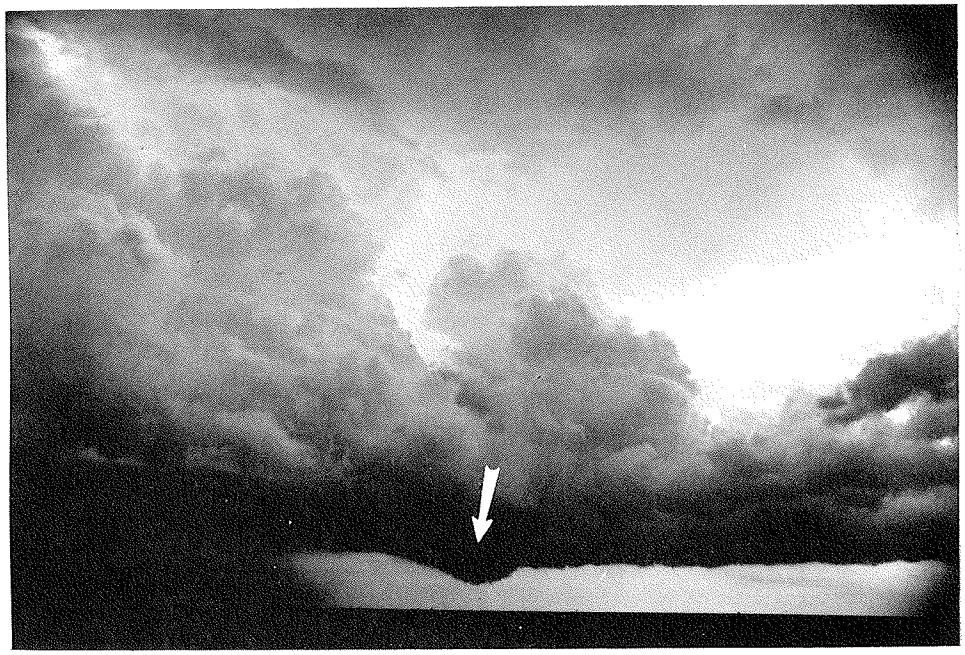

Figure 3.12 Example of a flanking line which has a stairstep appearance. Note the developing wall cloud (arrow) adjacent to the precipitation shaft on the left, with the viewing direction toward the east-northeast.

reaches its mature stage, resulting in a precipitation-free cloud base[6] beneath the flanking line towers. As seen in Fig. 3.12, a lowering of the cloud base may sometimes be observed under the flanking line of a multicell complex. This is called a **wall cloud** (see E.2.c, below).

As each updraft passes through its equilibrium level, it produces an overshooting top. The highest storm top may be seen above the edge of the precipitation shaft, depending on the viewing angle. Visually, such a structure is somewhat transient. That is, this dome persists only briefly since the updraft which supports it is not sustained. The top then subsides and a new cell takes its place. As the top collapses, the resulting divergence aloft forces an expansion of the anvil, which may take on a much "crisper" or cumuliform appearance at the time of updraft penetration and shortly thereafter (Fig. 3.13). When the cell, moving through the complex as a whole, has dissipated sufficiently, the anvil spreading slows down and the cloud edges become more fibrous. Thus, the downstream anvil is typically rather diffuse, with the last remnants of precipitation falling out under it as it moves away from the active storm region.

c. Airflow

Because the updrafts which drive the multicell severe storm are clearly separate in time and space, it is necessary to present the airflow as it evolves, rather than a

---

[6] There may well be rain or hail falling from this base (Fankhauser **et al.**, 1983) but the visual contrast with the heavy precipitation in the adjacent main precipitation cascades region suggests the basic validity of this term (Doswell, 1983). Note that there may well be heavy precipitation aloft over such a base so a radar beam which is not passing mostly below cloud base may detect high reflectivity here.

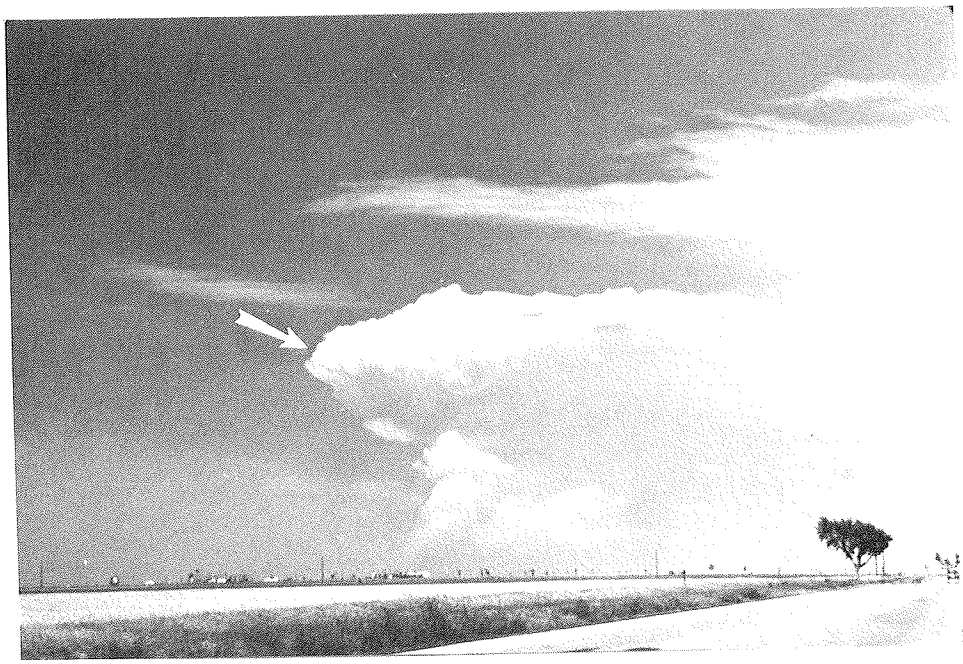

Figure 3.13 Cumuliform anvil (arrow) resulting from rapid spreading of updraft at the equilibrium level. Overshooting top has recently collapsed with this storm.

snapshot view, or one which averages out the series of impulses which characterize this storm type. This is inevitably complex to try to depict in a static, two-dimensional way. Much of our current understanding of the airflow is inferred from the behavior of radar echoes. Chisolm and Renick (1972) or Foote and Wade (1981) provide excellent examples of this evolution.

In a vertical cross section, we see a sequence something like Fig. 3.14, which tries to show how the four cells I-IV evolve. In Fig. 3.14a, Cell I is entering its dissipating stage so it is dominated by weakening downdrafts. Cell II is just reaching the stage where precipitation is beginning to form -- hence, it is dominated by updrafts. Cells III and IV are still towering cumulus forms.

Several minutes later (Fig. 3.14b), the heavy precipitation of Cell I has reached the surface and its updraft is weakening. Now the top of Cell II has passed through its equilibrium level and is decelerating, which forces it to spread out aloft. This spreading out, combined with the supporting updraft, produce a pronounced WER (as in Fig. 3.10). Cells III and IV continue to develop.

Again several minutes later (Fig. 3.14c), Cell I has all but dissipated, while Cell II has entered the mature stage. Cell II's high reflectivity core has only just begun its descent, but its precipitation has reached the surface. Cell III is on the verge of producing its first radar echo, while Cell IV is still a growing cumulus tower.

A next figure would repeat 3.14a, where Cell II replaces Cell I, Cell III replaces Cell II, and so on. Since the figure is drawn so that it follows the cells, note the propagation of the precipitation and outflow to the left, across the figure. This is the origin of the behavior depicted in a ground-relative sense by Fig. 3.11.

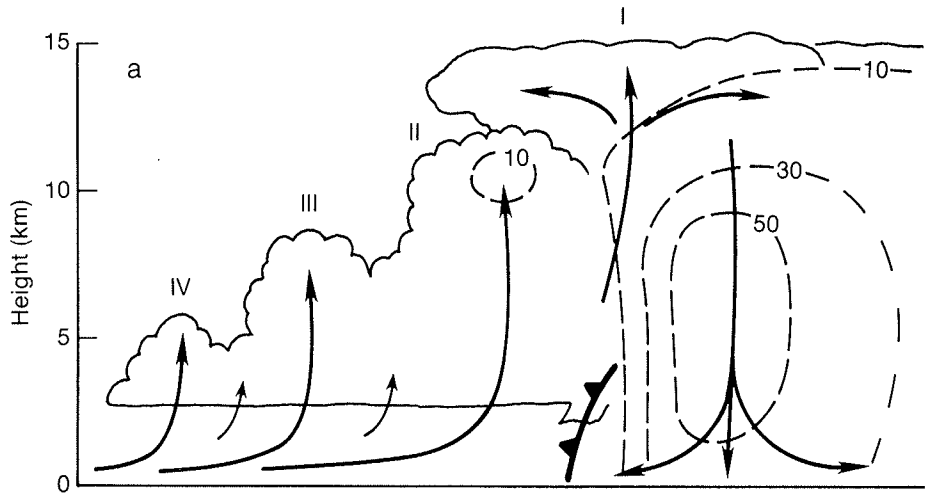

Figure 3.14a Instantaneous view of a multicellular severe thunderstorm complex, showing four cells (I–IV) in the system. Drafts are indicated by the flow lines, and radar reflectivity is depicted as in Fig. 3.10. See text for discussion.

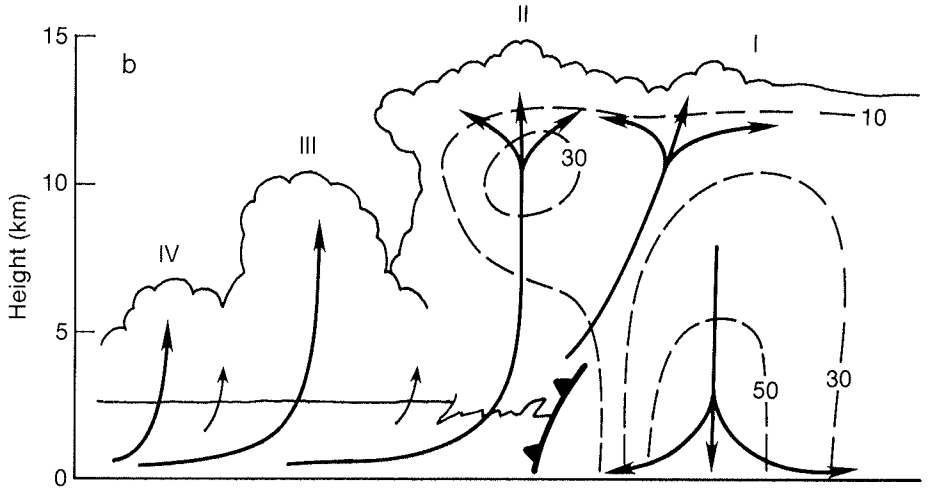

Figure 3.14b As in (a) except roughly 10 min later.

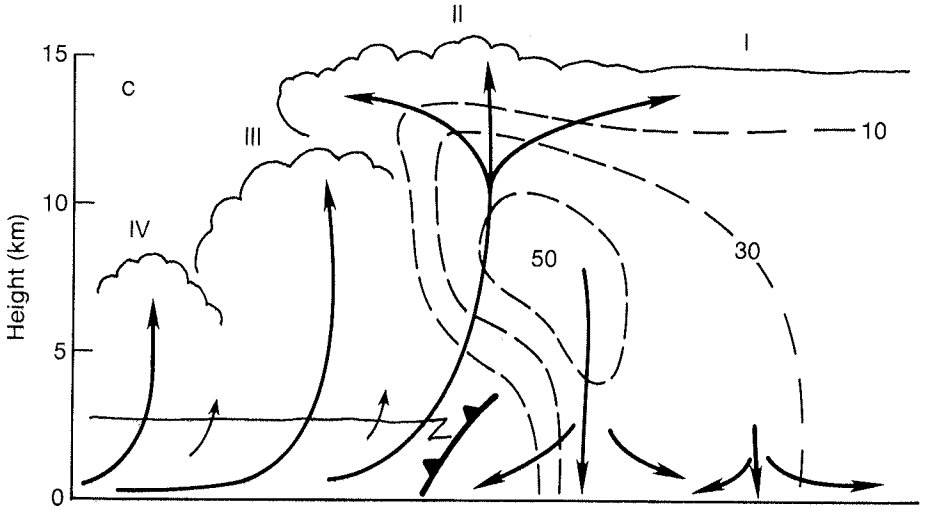

Figure 3.14c As in (a) except roughly 20 min later.

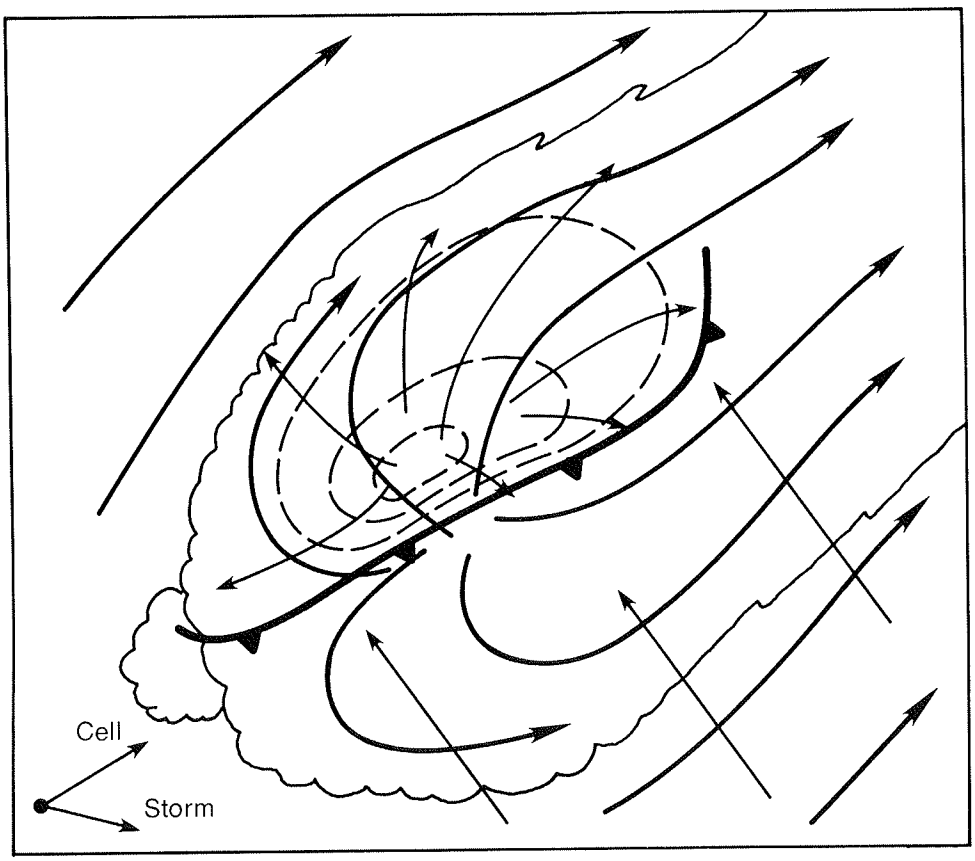

Figure 3.15 View from above of a multicell thunderstorm. Heavy flow lines are at upper levels, thin flow lines at lower levels, dashed lines suggest radar reflectivity contours (as in Fig. 3.10). Cell and storm motion vectors are indicated at lower left.

Looking down on the complex from above (say, shortly after the time of Fig. 3.14c), the horizontal flow at low and high levels is roughly as in Fig. 3.15. At middle levels (not shown in the figure), the relative environmental flow diverts around the updraft. This creates a flow pattern which resembles that of a solid object blocking the environmental flow (see Brown and Crawford, 1972). There are a variety of concepts which can be used to explain this, but they all boil down to the presence of a strong updraft core, which is essentially undiluted and stands more or less erect. Although the air in the updraft obviously is not solid, it does present a **momentum difference** to the relative winds, which must pass around it. For multicell storms, this middle-level characteristic is confused by the sequential nature of the strong updraft, and may not be present at a particular instant.

At upper levels, the updraft terminates in a region of strong divergence, which also creates the effect of a block in the flow. This upper divergence results from the rapid decrease in updraft speed forced by negative buoyancy when the ascending air crosses its equilibrium level. The upper winds are diverted around the storm as a result (see e.g., Fankhauser, 1971). Some of the air brought upward descends again in the precipitation region, mixing with environmental air in the process. Thus, the air in the downdraft is generally a mixture of low-level and mid- to upper-level environmental air. Also, much of the updraft air eventually is swept downwind in the anvil.

The characteristic WER may arise from two effects: **precipitation held aloft** in the intense updraft and **strong divergence** in the upper portions of the storm. Thus, some of the "overhang" may be visualized as precipitation "accumulating" in the updraft. However, the strong divergence arising from the rapid deceleration of the updraft above the EL is, in a storm-relative sense, likely to be nearly symmetric. This acts to move precipitation (and cloud) particles outward and across the updraft.

d. Environment

No definitive study of the environments associated with the various storm types has been done yet. This lack stems in part from the problem of identifying and classifying storm types (see Footnote No. 5). What studies that have been accomplished have not used a large enough sample to make definite statements. Thus, one should be careful in applying any general statements about environments, since exceptions will be seen.

With these cautionary thoughts in mind, some broad generalizations can be made about multicellular severe storm environments. Perhaps the most obvious is that, by virtue of being severe storms, these multicellular complexes tend to occur in relatively unstably stratified conditions -- certainly more unstable than non-severe storms. While some fairly substantial variations occur in individual cases, severe multicell storms are generally associated with 500 mb parcel buoyancies of 4 to 8°C (Lifted Index of -4 to -8°C), as shown in Marwitz (1972b).

Further, since severe storms are conceded to be associated most typically with environments showing vertical wind shear, and since the greatest number of severe storms are multicellular, it is logical to assume the presence of vertical wind shear in multicell environments. This is indeed the case. The average shear value in the cloud-bearing layer is of order 2.5×10^{-3} s^{-1} (about 5 kt [or about 2.5 m s^{-1}] per km of depth, as shown in Marwitz, 1972b or Doswell and Lemon, 1979). Marwitz suggests that multicell severe thunderstorms form in environments where the subcloud layer average wind speeds are weaker than 8 m s^{-1} ($\sim$ 15 knots), based on his limited sample. Much remains to be done to provide more substantial evidence for (or against!) such thresholds. Basically, averages do not always tell the whole story -- there can be so much variation in a parameter that its value as a forecast tool is minimal.[7]

In view of the numerical modeling results (e.g., Weisman and Klemp, 1984a) which suggest the importance of the hodograph in determining storm structure, some "typical" hodographs are presented for each of the three major storm types. As seen in Fig 3.16, there is evidence that multicell environments have rather simple, straight-line hodographs (see Chisolm and Renick, 1972; Fankhauser and Mohr, 1977). One should be cautious in too strict an application of this concept. As pointed out by Barnes and Newton (1982), the situation is further muddied when multicellular storms exist in what seems to be the same large-scale environment with other storm types.

---

[7] Physically, this suggests that the parameter may not, by itself, be relevant to the process of concern. Further, an average value may be less important than the lower and upper bounds. Forecasting severe weather is often based on parameters for which a range of values is critical, rather than some particular threshold value, beyond which "more is even better."

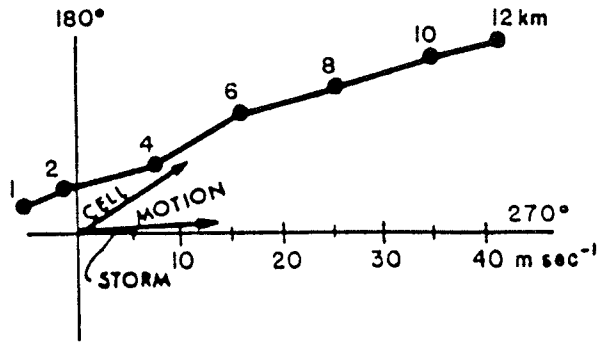

Figure 3.16 Example of a "typical" hodograph associated with multicellular storms (from Chisolm and Renick, 1972). Numbers along the line indicate the height in km.

2. Supercell Severe Thunderstorms

a. Some General Remarks

The supercell concept, first proposed by Browning and Ludlam (1962) and detailed in Browning (1964), has survived to this day with only relatively minor changes. This storm type accounts for only a small percentage of severe weather-producing storms, which are in turn only a small fraction of all thunderstorms. The percentage varies regionally, from an estimated 20% of severe storms in Oklahoma to less than 5% in the eastern U.S. (Nelson, personal communication). Nevertheless, supercells account for a much greater portion of the damage and injuries than their numbers might suggest. This is because of the extreme nature of the severe weather associated with supercells: virtually all of the violent tornadoes (see Forbes, 1981), as well as a high percentage of giant hail events (say, diameters > 2 in [5 cm]), and even some of the extreme straight-line wind (say, speeds > 65 kt [33.5 m s^{-1}]) reports.

Apart from minor modifications made to conceptual supercell models and scientific disagreements concerning the definition of a supercell, there is a continuing problem identifying a supercell in any **particular** instance. The basic conflict revolves around the idea that a supercell severe thunderstorm is qualitatively as well as quantitatively different from its multicellular cousins. Basic supercell definitions (see e.g., Lemon, 1977, or Browning, 1982) usually incorporate time continuity as a distinguishing feature (see III.C). A multicell storm can, for a few minutes, take on the supercell structure. There are no clear-cut guidelines to use, since many of the distinctions drawn in the literature are essentially arbitrary. The fact that "supercell characteristics" are commonly associated with the most intense severe storms leads one to conclude that there is value in making such distinctions, regardless of the scientific controversy which the distinctions generate. So what are supercell characteristics?

b. Radar Structure

Perhaps the most well-recognized radar feature commonly associated with the supercell is the **hook echo,** or its more general form, the **pendant echo.** This is shown in Fig. 3.17, with the pendant echo being the extension of low-level echo on the storm's rear or right-rear flank, oriented initially (when first recognizable) more or less perpendicular to the storm motion. In obvious cases, the pendant echo undergoes a "wrap-up", forming the well-recognized "Figure 6" (see Fujita, 1958a; Garrett and Rockney, 1962; Huff **et al.**, 1954). This feature clearly is associated with a small-scale circulation (called a "tornado cyclone" by Brooks, 1949) and is most typically (but not always!) accompanied by tornadoes and/or funnel clouds.

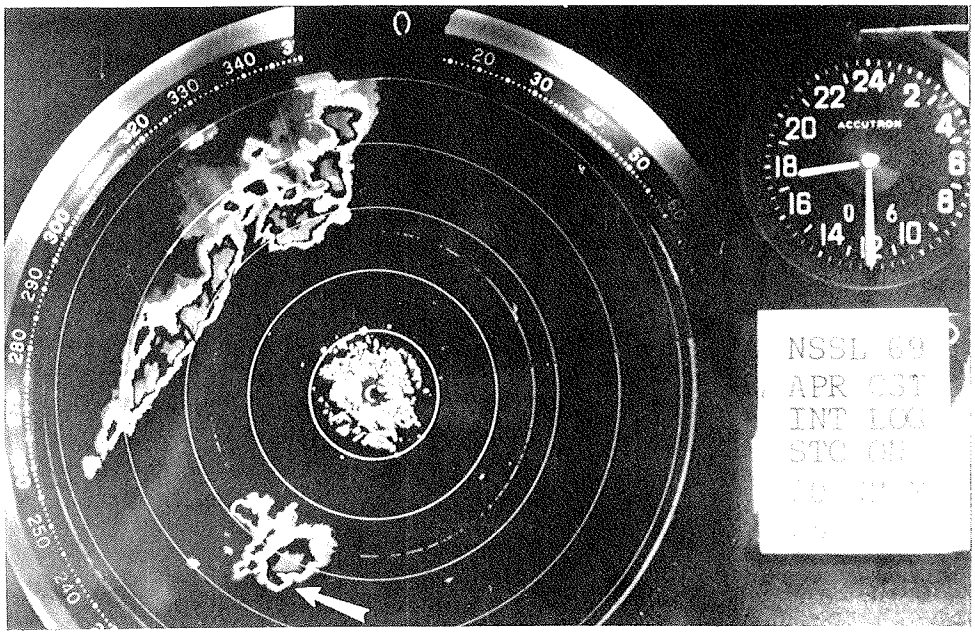

Figure 3.17 Example of a supercell with a hook echo (arrow) on a contoured radar reflectivity display. Note also the squall line approaching from the northwest (Photo courtesy of D. W. Burgess).

If hook echoes are a characteristic of supercells, does a supercell **always** contain a circulation of this sort? Results of Nelson and Young (1979) certainly support this (see their Table 5), at least in many cases. It has been proposed that supercell storms have rotating updrafts (Browning, 1982). This by itself is probably not a completely viable criterion, since circulations have been detected in a variety of convective storms, some of which are by no means supercells (e.g., Heymsfield, 1981). However, the cyclonic circulations associated with supercells are typically more intense and persistent than those with non-supercells. This seems to account for the occurrence of hook echoes, which are so demonstrative of circulations.

It is also well-known that not all supercells have hook echoes. Forbes (1975, 1981) has described "distinctive echoes" as those possessing a pendant, or other more or less empirical indications of a mesocyclonic circulation. Of these, 65% were tornadic and nearly 50% resulted in multiple tornado occurrences. Noteworthy is Forbes' finding that 60% of his sample of distinctive echoes were supercells and that only 25% were multicellular. It is important that the reader remember that the ability to detect "distinctive" features in radar echoes depends on the resolution -- all other things being equal, echoes closer to the radar (but away from ground clutter!) are more likely to have detectable features than those farther away. Beam width also affects the results -- high resolution radars are more likely to resolve small-scale features than a broad-beam radar. Thus, radar statistics may underestimate the number of echoes with distinctive features.

Forbes' data on tornadic distinctive echoes (for the single day of 3 April 1974 which included many separate tornadic storms) show that the appendage (or pendant echo) persisted for an average of over two hours! However, the first tornado occurred well over an hour after the pendant formed and the last tornado occurred about 20 minutes before

the appendage disappeared. Thus, there was about one hour of tornado occurrence, starting during the middle of the period in which the appendage was present.

Lemon (1977), Chisolm (1973), Browning (1964), and others have emphasized another radar feature which is associated with supercells. Recall that the severe multicellular storm typically develops a WER (Weak Echo Region), in which low-level echo is surmounted by a mid- to upper-level region of strong reflectivity. In supercells, this feature develops into a persistent **Bounded** Weak Echo Region (BWER), in which the weak echo region in lower levels actually extends upward into, and is surrounded by, the high reflectivities aloft. This feature, shown schematically in Fig. 3.18, has also been called the "vault" by Browning (1964, 1982). Such a structure has been postulated to represent a high speed updraft core, within the larger region of updraft. Such a strong updraft (say, of order 50 m s^{-1}) is so fast that the processes forming precipitation (see II.C) cannot operate rapidly enough to develop a radar-detectable echo until the parcels have ascended to relatively great heights. Also, there is new evidence to suggest that the BWER is associated with rotation and the origins of parcels which rise through the BWER (Weisman **et al.**, 1983b).

The reader may also think of this high-speed updraft core "punching" its way up into the echo aloft. Since supercell storms often have their beginnings as multicell complexes, a WER may already exist (Lemon, 1977). As with the change from ordinary to severe multicellular storms, the transition to supercell characteristics is one of degree, at least to some extent.

Regardless of the sensor capabilities, if the viewpoint expressed in Weisman **et al.** (1983) or Weisman and Klemp (1984b) is valid, a supercell storm can be distinguished from the multicellular variety by one important qualitative difference; **high positive correlation between vertical velocity and vorticity.** This distinction is important because it carries with it the implication that supercell dynamics are different from those operating in non-supercell storms. For instance, it suggests that supercell storms have rotating updrafts. Even given this distinction, it is conceivable that a multicell storm could, at a given instant, have these characteristics. The temporal persistence is still part of the issue and sensor resolution can still be a factor in classification.

However, when the change occurs, the development of a BWER may signal a dramatic change in the temporal behavior. Rather than a discrete series of updraft impulses, the cell can begin a new phase in which the echo remains more nearly steady for long periods. Just how long is "long"? Recall the discussion in III.C, where a "long" time compared to the convective time scale was shown to be roughly 30 min or more. During this period, the storm top remains steadier as well. Rather than ascending with each new updraft and descending as the updrafts decay, as in a multicell storm, a supercell's top only undergoes minor fluctuations. Further, there is usually only **one** major storm top, rather than the several normally observed in multicellular storms.

Since the supercell updraft remains quasi-steady (or, equivalently, the time between new updraft formation is so short that separate drafts are not detectable), the mode of movement is somewhat different in concept from that of the multicell (which involves discrete propagation). It is observed that the area of updraft (identified by strong low-level reflectivity gradients, by the BWER, and by being under the storm top) is on a supercell storm's right or right-rear flank (as in the multicellular case). However, for supercell storms, the updraft is steady (to a first approximation). This gives rise to a mode of propagation known as **continuous** propagation, to distinguish it from the discrete, multicellular type. The picture is very similar to a time-averaged view of the multicell complex and gives rise to the same sort of rightward deviation from the direction of the mean wind in the cloud layer. In fact, the rightward propagation and slowing down of the storm is often even more pronounced than in severe multicellular storms.

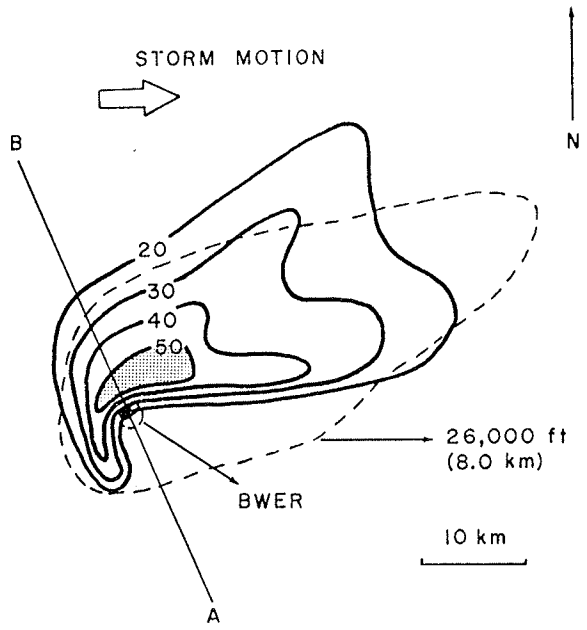

Figure 3.18a As in Fig. 3.9a, except for a supercell storm (from Lemon, 1977).

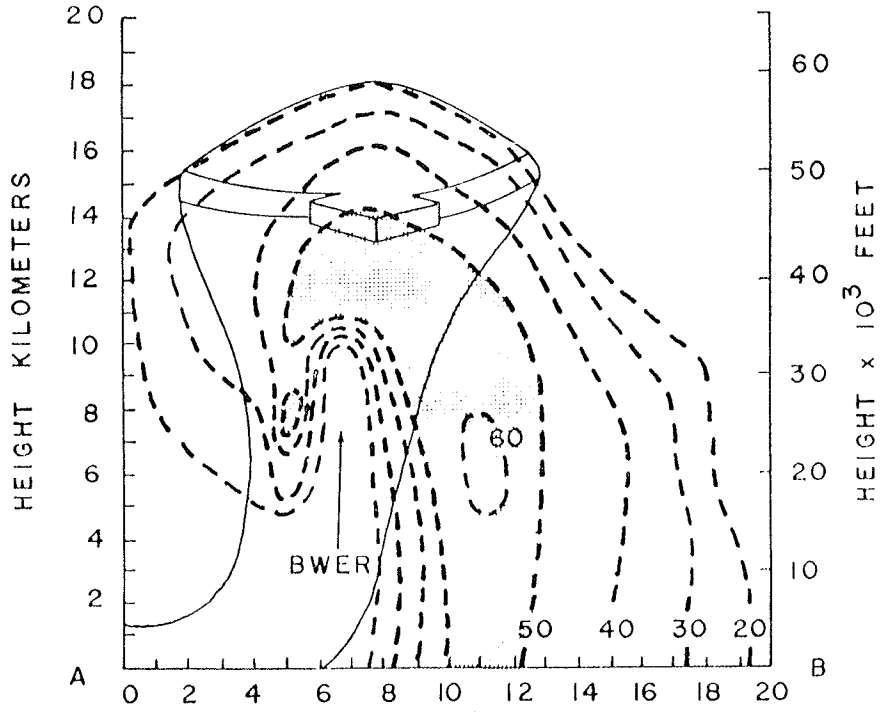

Figure 3.18b Cross section along line AB in Fig. 3.17a. Note the BWER, or vault.

This is a good point to reconsider the concept of storm splitting and deviate motion (i.e., by comparison with the mean wind), which is a fairly common characteristic of supercell storms (Achtemeier, 1969; Charba and Sasaki, 1971; Lemon **et al.**, 1978; McCann, 1983). It is observed on radar to resemble something like cell division in biology. As a storm evolves, the low-level echo may begin to lengthen in a direction more or less normal to the storm movement. Aloft, the echo may be more clearly split into separate cells even sooner in its life cycle. As the process goes on, the cell simply splits into two distinct cells which follow diverging paths. The most common development is that one cell becomes a right-mover (with respect to the mean wind), while the other develops into a left-mover (Fig. 3.19). The left-mover often resembles a mirror image of its companion, with structures (e.g., a WER, strong reflectivity gradient, etc.) to suggest the updraft is on its left, or left front flank. In fact, Burgess (1981) has suggested that the left-moving member of a split pair typically is characterized by Doppler radar-detectable mesoanticyclonic flow. It often moves more rapidly than the mean wind. In many cases, the left-mover quickly dissipates, but certainly not always. Observations show that tornadoes are rare (but not unheard of) with left-movers even though they often produce other varieties of severe events.

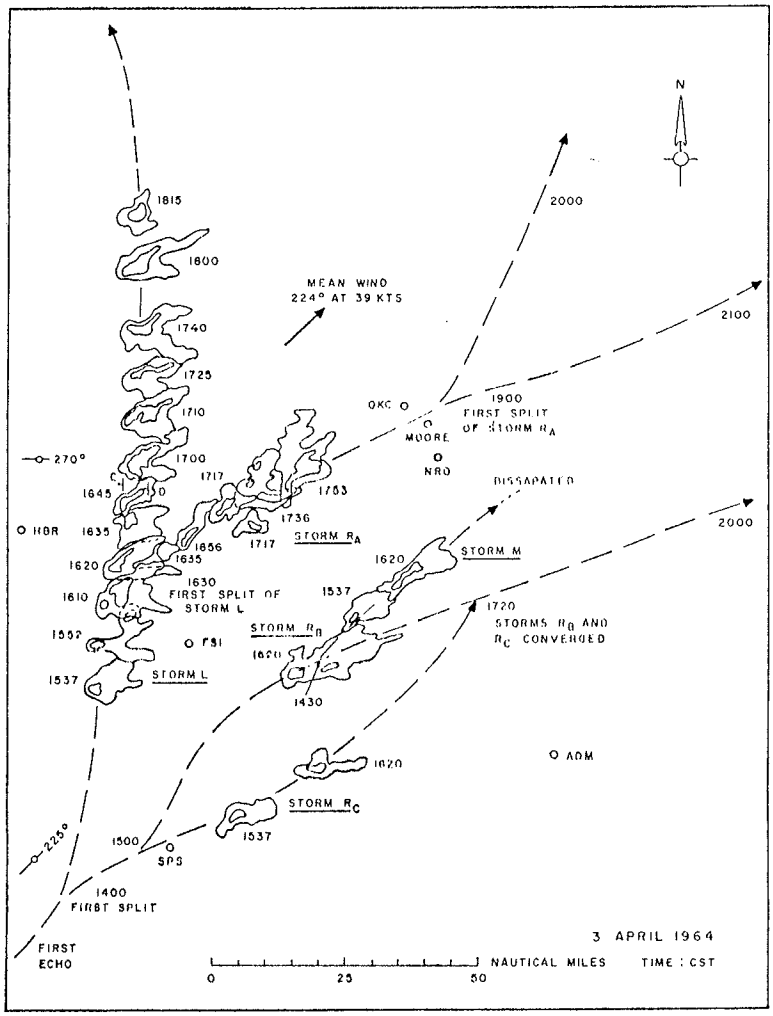

Figure 3.19 Paths of storms on 3 April 1964, showing storms splitting into both left- and right-moving (with respect to the mean tropospheric wind) systems (after Charba and Sasaki, 1971).

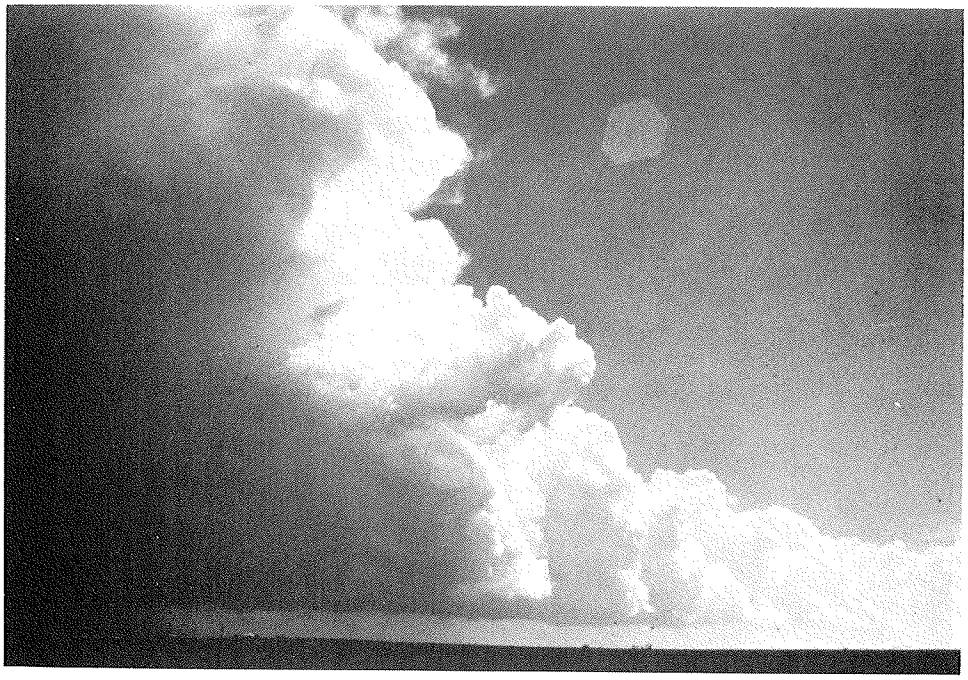

Figure 3.20 Flanking line associated with supercell thunderstorm, near Carnegie, OK on 20 April 1974, looking southeast.

c. Visual Structure

In many ways, the overall visual structure of supercells may not be distinguished easily from severe multicell complexes. On the time and space scales resolvable by an eyewitness, high frequency updraft pulses may still be distinguishable, even if a radar cannot resolve them. One basic characteristic, the flanking line, may be visually quite similar. Owing to shorter intervals between updrafts, the line may not be as clearly "stair-stepped" in appearance, instead appearing as a more nearly continuous rising band of cumulus congestus-type clouds (Fig. 3.20). The distinction seems to be that the updraft impulses seem to **merge with**, rather than to **become** the main storm tower. Many of these cloud features can only be highlighted here.

On occasion, the flanking line in a supercell develops a distinctive character. The lower portions are quite smooth and laminar, and are surmounted by rapidly boiling cumulus towers. An example is shown in Fig. 3.21. This structure can be maintained for several hours, with tornadoes forming and dissipating at intervals. Such cases have, in my experience, invariably produced multiple tornadoes when the laminar flank extends away from the main precipitation core (i.e., is **not** the tail cloud structure [see Fig. 4.32b]). A satisfactory explanation for these observations awaits further research. It can be surmised that the smooth portion of the flank is the result of forced lifting of the **negatively** buoyant air below the LFC (see I.II.C.2). When this air is forced through its LFC, then distinct cumuliform towers develop during its **positively** buoyant ascent. Note that the appearance of a persistent laminar flank can be used as an argument for quasi-steady internal storm dynamics, and against the multiple updraft concept embodied in Table 3.1. However, such a structure is not seen with every supercell event.

One commonly-observed visual characteristic of supercell storms is a substantial anvil overhang on the upwind (relative to anvil-level winds) side of the convective

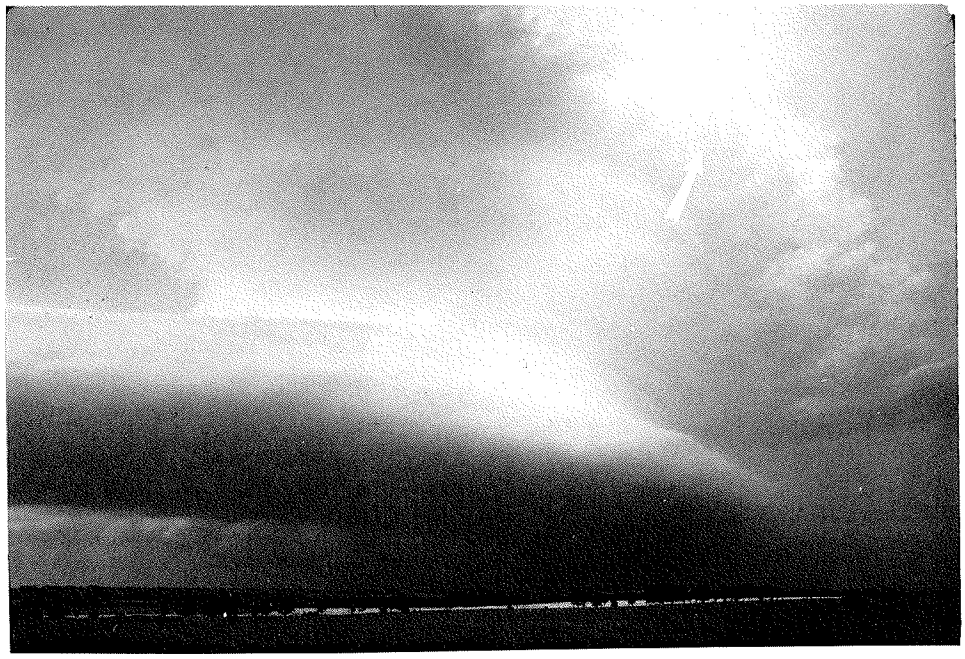

Figure 3.21 Supercell storm on 22 May 1981 in central Oklahoma, with laminar low-level flanking line (looking northeast). Cumuliform convective towers are barely visible (arrow) above the middle-level base into which the low-level flank is rising.

towers. Although Fig. 3.13 may have been a multicellular storm, it serves very well to illustrate this upwind overhang. Apparently, divergence in the upper portions of the storm is sufficiently strong to push cloud material into the impinging environmental winds (see Lemon and Burgess, 1980). Fujita and Arnold (1963) have presented an interesting example of this behavior. On some occasions, the trailing edge of the anvil can be as much as a few 10's of km behind the active convective towers during the intense phase of supercell storms.

Storm spotter training (Lemon **et al.**, 1980) currently emphasizes the wall cloud in identification of severe storms before they produce tornadoes. While the wall cloud is not **exclusively** confined to supercells, virtually all supercells possess wall clouds during their intense phase (Fig. 3.22). Wall clouds may show clear visual evidence of rotation when associated with supercells.

The discrete lowering does not appear to result from the pressure drop in a mesocyclone, but may result from the updraft tapping the near-surface air, which has higher moisture content (Schaefer, 1975). It also appears that some of the air from the outflow associated with the forward flank downdraft (within the precipitation cascade) can be pulled into the updraft core (Lemon, 1976a; Rotunno and Klemp, 1983). This has actually been observed visually. The forward downdraft air is already nearly saturated and may result in a lowering of the condensation level for the **mixture** of unprocessed and processed air which enters the updraft core, by increasing the relative humidity of the mixture. Note that evaporation of precipitation into the low-level air does **not** change its potential buoyancy, since θ_e (or θ_w) remains unchanged during such a process. However, potentially colder air from mid-levels may be mixed with forward flank downdraft air, thus reducing its buoyancy, in proportion to the amount of included mid-level air.

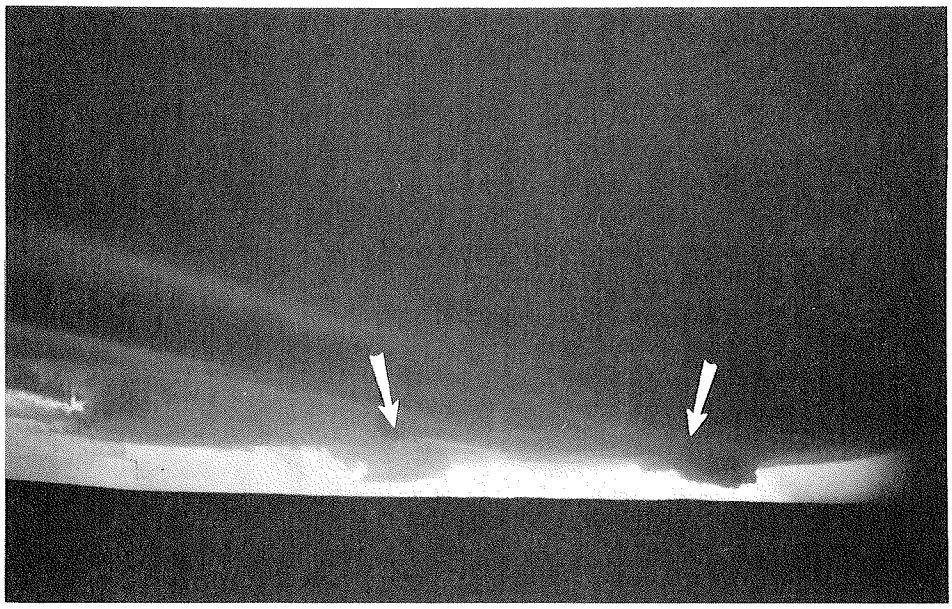

Figure 3.22 Example of wall cloud (this storm in west central Oklahoma on 18 June 1973 has two at the same time — indicated by the arrows) under an extensive updraft base. Note the precipitation cascade on the right edge (photo taken looking west) and the apparent inflow bands running from the left center edge toward the lower right into the wall cloud on the right. A tornado developed from this wall cloud about 30 min later, and a second tornado formed with the wall cloud on the left as the first tornado dissipated.

Moller **et al.** (1974), were among the first to describe a **clear slot** which often can be seen to wrap around, and partially dissipate, the wall cloud during the tornadic phase of the storm. This clear slot is associated with a feature of the supercell storm which may not occur in multicell storms; the **rear flank downdraft** (Nelson, 1977; Barnes, 1976; Lemon and Doswell, 1979). An example of this is presented in Fig. 3.23, where the clear slot can be seen to the rear and right rear of the tornado. With time, this zone of higher cloud base (or no cloud) can wrap nearly entirely around the tornado, isolating the funnel (see IV.E.1).

Supercells, by virtue of a more or less continuous updraft, may maintain an overshooting top for extended periods. Visually, this may be observed to be the result of a rapid succession of new domes replacing older ones before they can collapse entirely. However, the net result is a quasi-steady elevated dome above anvil level.

While the steadiness of the supercell (in comparison to the multicellular storm) has been emphasized, one should be aware of the evolutionary nature of supercells (Browning, 1965c). It is a rare storm, indeed, which maintains steadiness in the view of an observer. Although the radar echo may appear to be more or less unchanging, the viewer may see a series of wall clouds forming, producing tornadoes, and only dissipating after a new wall cloud has already formed (Jensen **et al.**, 1983). Note that this complex internal structure may be revealed by Doppler radar (Brown **et al.**, 1973), even though it is not obvious from reflectivity alone. Fujita (1960) has described this for the famous Fargo storm. Burgess **et al.** (1982), have proposed a model of the supercell storm evolution in terms of mesocyclone evolution (Fig. 3.24), and Storm Intercept crews (Doswell and Moller, 1985) have repeatedly observed such a sequence. Further, a supercell must eventually decay, so there is clearly an usteady character to supercells, although it is on a time scale longer than the convective time scale.

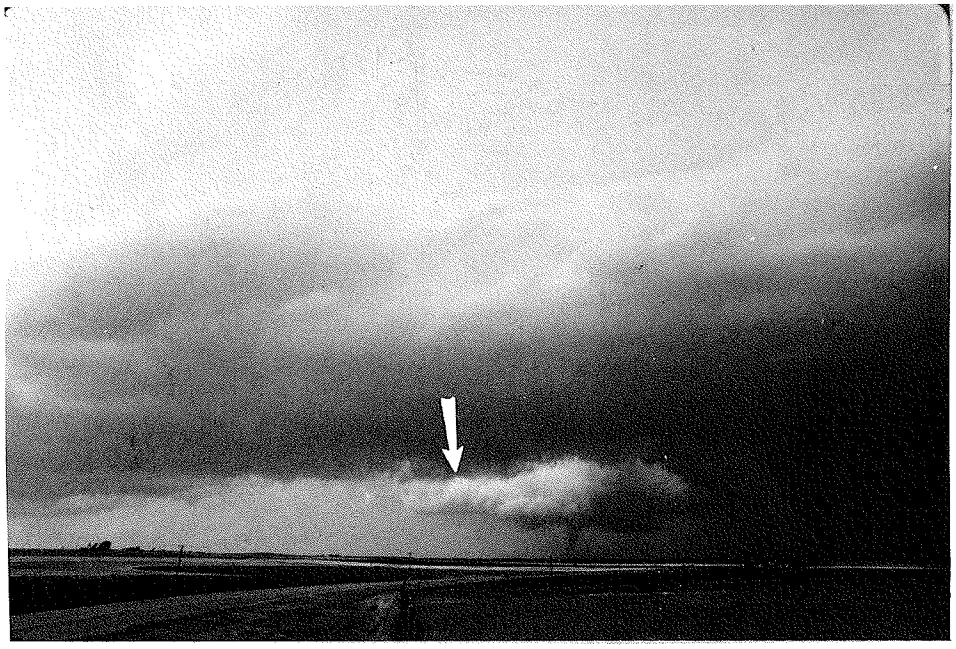

Figure 3.23 Well-defined clear slot (arrow) associated with tornadic phase of supercell thunderstorm (see text for discussion).

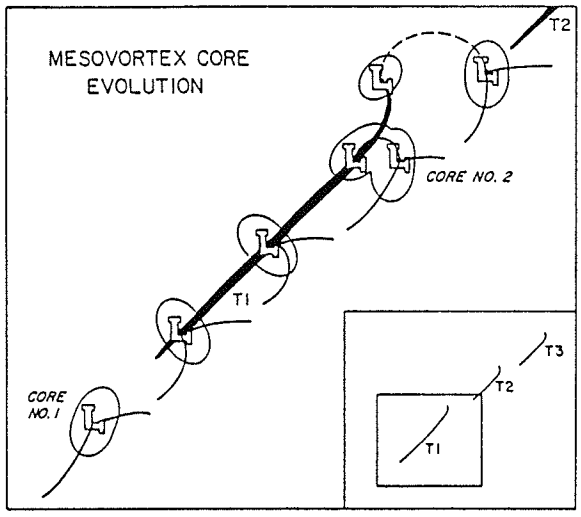

Figure 3.24 Conceptual model of mesocyclone core evolution. Thick lines are low-level wind discontinuities and tornado tracks are shaded. Inset show the tracks of the tornado family and the small square is the region expanded in the figure (from Burgess ***et al.,*** *1982)*

d. Airflow

The basic aspects of supercell airflow were first described by Browning (1964) in a classic paper. Browning deduced these features from a knowledge of the environmental winds and the trajectories of radar-observed precipitation echoes. While we have learned new subtleties with our advanced observing systems, Browning's original notions (Fig. 3.25) still provide a basis for understanding supercell airflows. Continuing support for the basic features of Browning's work abounds in the literature, both from observational (e.g., Fankhauser, 1971) and numerical modelling (e.g., Klemp **et al.**, 1981) viewpoints.

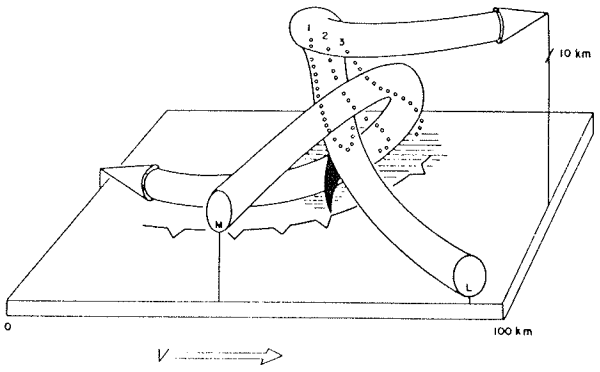

Figure 3.25 Browning's (1964) three-dimensional model of a severe right-moving thunderstorm. Low (L) and middle (M) level flow lines are depicted schematically. Also shown are some precipitation trajectories (dotted), the approximate extent of the surface precipitation, and the postions of the surface gust front and the tornado (when present).

Primary structural features are the mesocyclone, the BWER, and, perhaps, the rear flank downdraft. Some excellent presentations of various aspects of supercell airflow can be found in Browning (1977), Brandes (1978, 1981), or Foote and Fankhauser (1973), as well as other references mentioned in this section.

From a position above the storm (in analogy with Fig. 3.15), the flow looks roughly as shown in Fig. 3.26a. As with the multicell complex, upper and middle level flows are diverted around the updraft (and upper-level outflow). The main differences between supercell and multicell radar echo structure and low-level flow seem to arise through the behavior of the mesocyclone (not shown in detail in this figure -- see Fig's 4.31 and 4.43). Note that this particular figure is intended only to give a rough picture of the storm-scale drafts. In cross section (Fig. 3.26b), it is hard to portray the three-dimensional details, but an important aspect is the mid-level flow being carried around the front side of the updraft and into the precipitation cascade region (as in Browning's model).

In order to show the structure of the flow in three dimensions, Fig. 3.27 is also included, which reveals the low- to mid-tropospheric flow, in perspective view. Doppler studies have revealed that the circulation often begins more or less centered on the BWER (implying a rotating updraft). As the rear flank downdraft (RFD) develops, the circulation core comes to lie near the boundary between the updraft and the RFD. The plan view of the circulation at low levels looks remarkably like that of an extratropical cyclone (recall Fig. 3.24 and see Doswell, 1984), with gust fronts replacing the large-scale fronts. As the storm evolves, the RFD-produced gust front on the rear flank sweeps around in the circulation, inducing updrafts ahead of it. This causes the updraft region to look horseshoe-shaped (Ray **et al.**, 1981; Klemp **et al.**, 1981) and the circulation "occludes", much like the extratropical cyclone.

The entire process can take about 30 min, or it may be spread out in time for the "steadier" examples. With time, the gust front ahead of the RFD cuts off the inflow to the primary updraft and may induce new developments on the storm's right flank. This process seems to account for the rightward "continuous" propagation mode.

Note the apparent blocking effect of the storm on the environmental flow. It may be that in supercell storms, the updraft core is sufficiently protected from mixing with environment, so that the core may have vertical motions approaching those predicted by pure parcel theory (reduced by the very significant water loading and dynamic pressure effects ignored in parcel theory). In the typical supercell environment, the total buoyancy (positive area on a thermodynamic diagram) implies maximum updraft speeds (at the EL) of order 100 $m\ s^{-1}$! Doppler data analysis shows peak vertical velocities of about half this magnitude actually occur (Nelson and Brown, 1982). The reduction in

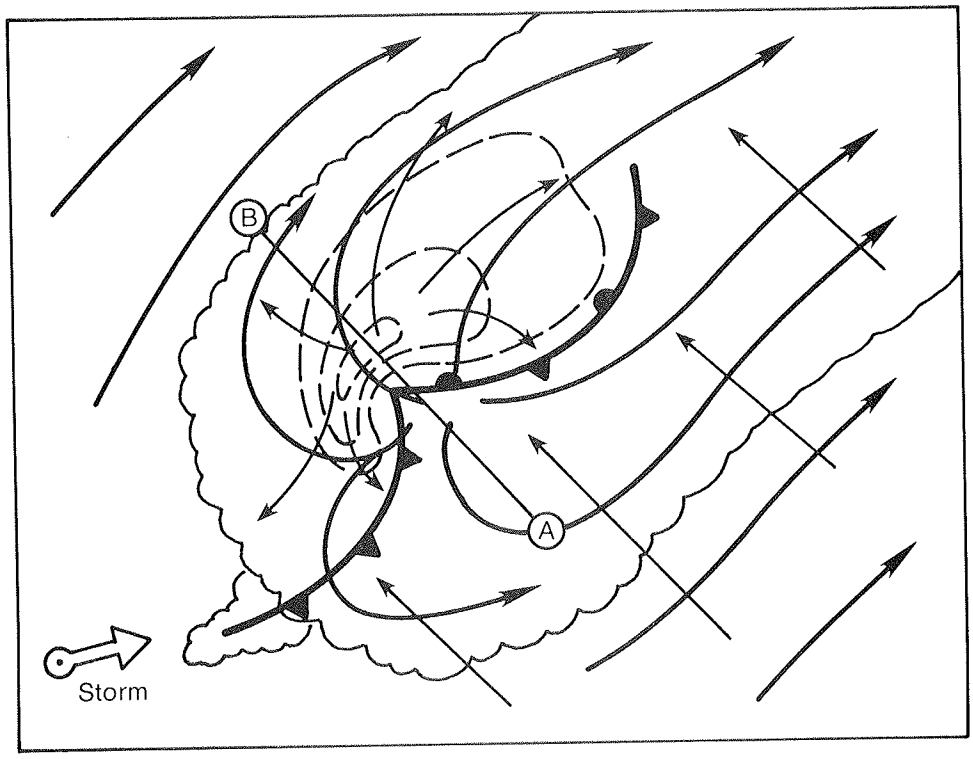

Figure 3.26a View from above of supercell storm, with lines as in Fig. 3.15. Note that storm and cell motion are the same, since the storm is basically a single long-lived cell.

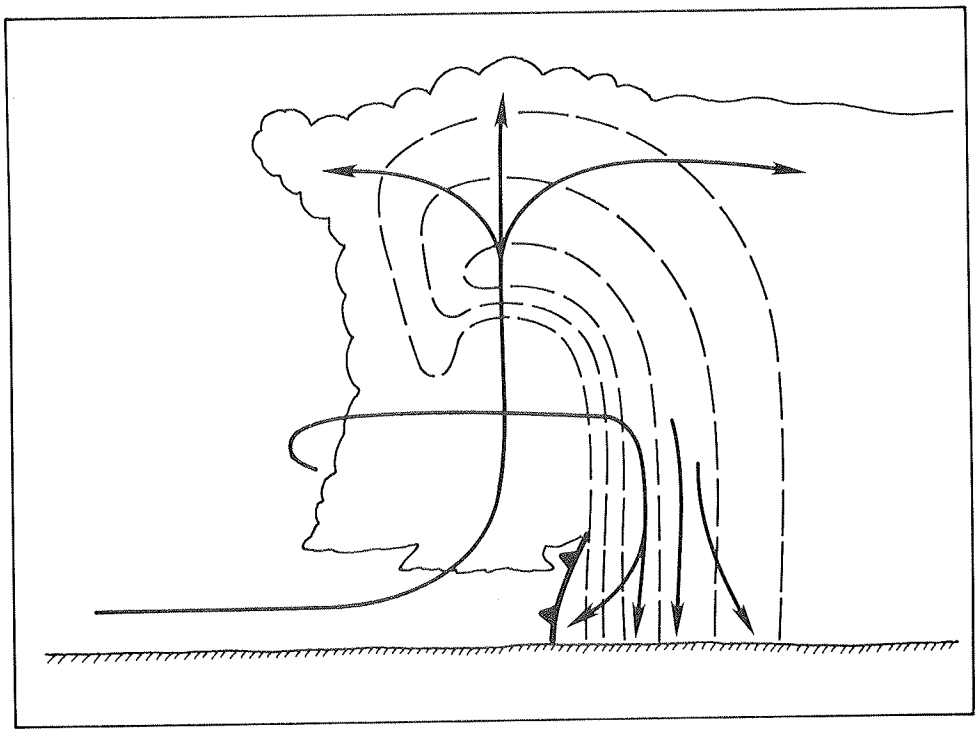

Figure 3.26b Cross section along line AB in Fig. 3.25a, as in Fig. 3.10.

peak updraft speed is most likely the result of water loading, and to a lesser extent, dynamic pressure effects. In spite of failing to attain adiabatic parcel speeds the updrafts in supercells are clearly substantial. Such strong updrafts, retaining much of their low-level momentum, could well act like obstacles to the flow. Note that Rotunno and Klemp (1982) have proposed an alternate explanation for the "obstacle flow" signatures documented in the literature, which is discussed in VI.D.

When these powerful updrafts pass through the EL, they are decelerated quickly, but can produce the rather large overshoots of the EL observed in supercell storms. Since the upper portions of the storm have such large mass flux from below, the result is extreme divergence at high levels near the storm top (Lemon and Burgess, 1980). Naturally, the implied anvil expansion rates are large for as long as the updraft is maintained. These expansion rates are consistent with satellite observations of severe storms (Purdom, 1971; Adler and Fenn, 1977; Mack and Wylie, 1982).

If updraft slope is considered in detail, it is quite obviously related to the relationship between buoyancy and shear (recall II.A.3). That is, for a given shear, the more rapidly a parcel rises, the less it will be tilted from a vertical trajectory. Since supercells are associated with environments having considerable shear and considerable instability, it is not certain how much storm tilt to anticipate. There appears to be a range of shear vs. buoyancy in which supercells are most likely (Weisman and Klemp, 1982), so there is probably a range of storm tilts associated with that range of shear vs. buoyancy. However, it is probably possible to obtain identical storm tilts in a non-supercell (or non-severe) convective storm. In short, storm tilt does not appear to be a very useful method for storm type identification. There is some evidence that supercells do not typically have slopes more than 30° from vertical, but exceptions do arise. It does appear that steeply sloping updrafts are not a **necessary** condition for supercell structure.

Finally, Fig. 3.26 does not include the circulation explicitly. As shown in Fig. 3.27 the low-level flow may be modified by the circulation as indicated. The scale of this mesocyclone is rather small. Furthermore, when the circulation is "occluding", as in extratropical cyclones, the gust frontal boundaries are stretched to ever smaller scales by the flow's deformation. This makes those boundaries hard to resolve with the detail available in our observations. The flow may appear to pass right through them and we have a problem entirely analogous to that of understanding the three-dimensional flow near the center of an extratropical cyclone.

e. Environment

Among the various storm types, supercell environments have probably been documented most extensively. An excellent general discussion of this topic can be found in Barnes and Newton (1982). Since Browning's (1964) paper, the relationship between the often-studied supercell storms and their environment is an almost mandatory issue to be addressed, so references are abundant (see e.g., Fankhauser and Mohr, 1977; Weisman and Klemp, 1984a; or Ludlam, 1980). Marwitz (1972a,b,c) suggests that the thermal instability for supercells is comparable to that of the strongest multicell environments, but tends to remain high throughout the class. In other words, supercell storms occur almost totally within strongly unstable environments (see also Hales, 1982). It is noteworthy that even in this extreme class of convection, the typical precedent sounding has a "cap" (see Fig. 3.28).

It is generally accepted that the role of this capping inversion is to restrain the release of the convective instability (Williams, 1960; Carlson and Ludlam, 1968). Rather than producing a situation with many competing updrafts, a supercell environment with a restraining inversion concentrates the energy release in a limited number of storms

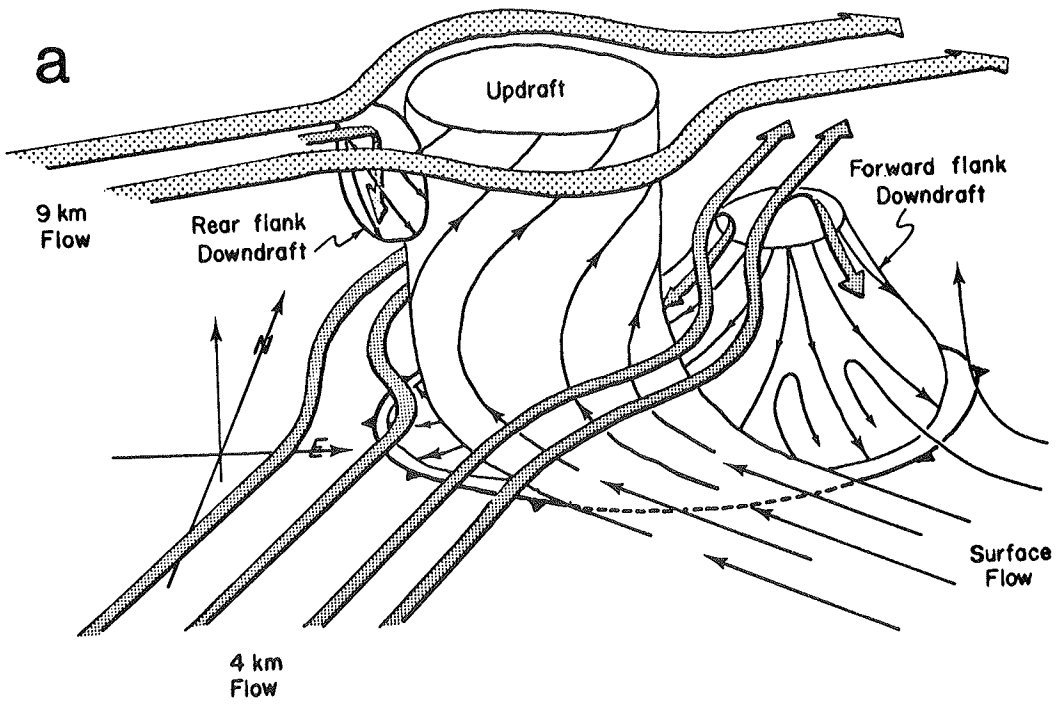

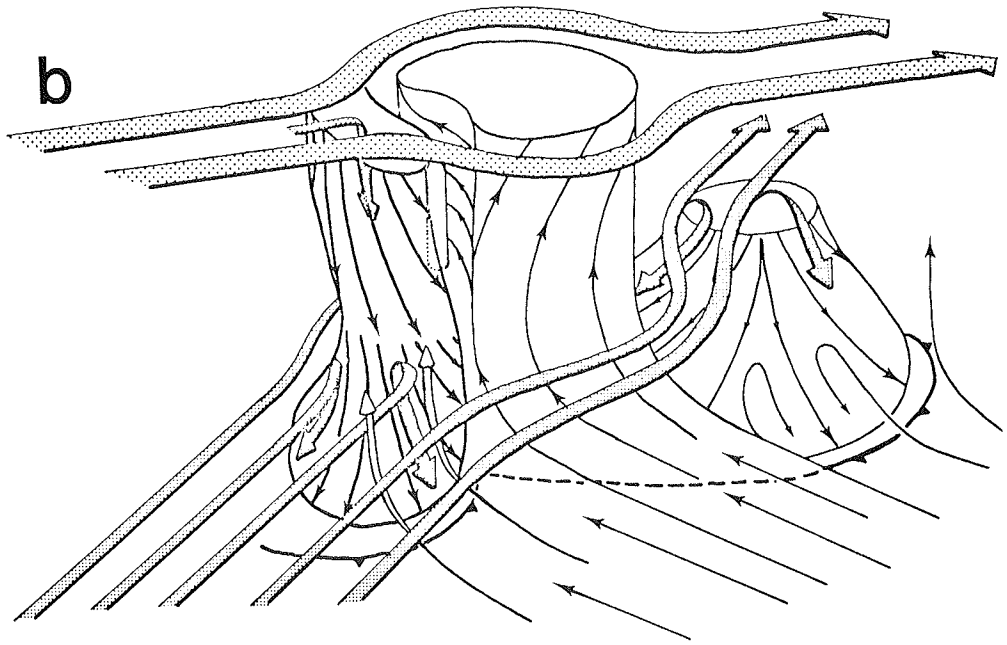

Figure 3.27 Schematic three-dimensional depiction of evolution of the drafts, tornado and mesocyclone in an evolving supercell storm. The stippled flow line suggesting descent of air from the 9 km stagnation point has been omitted from (c) and (d), for

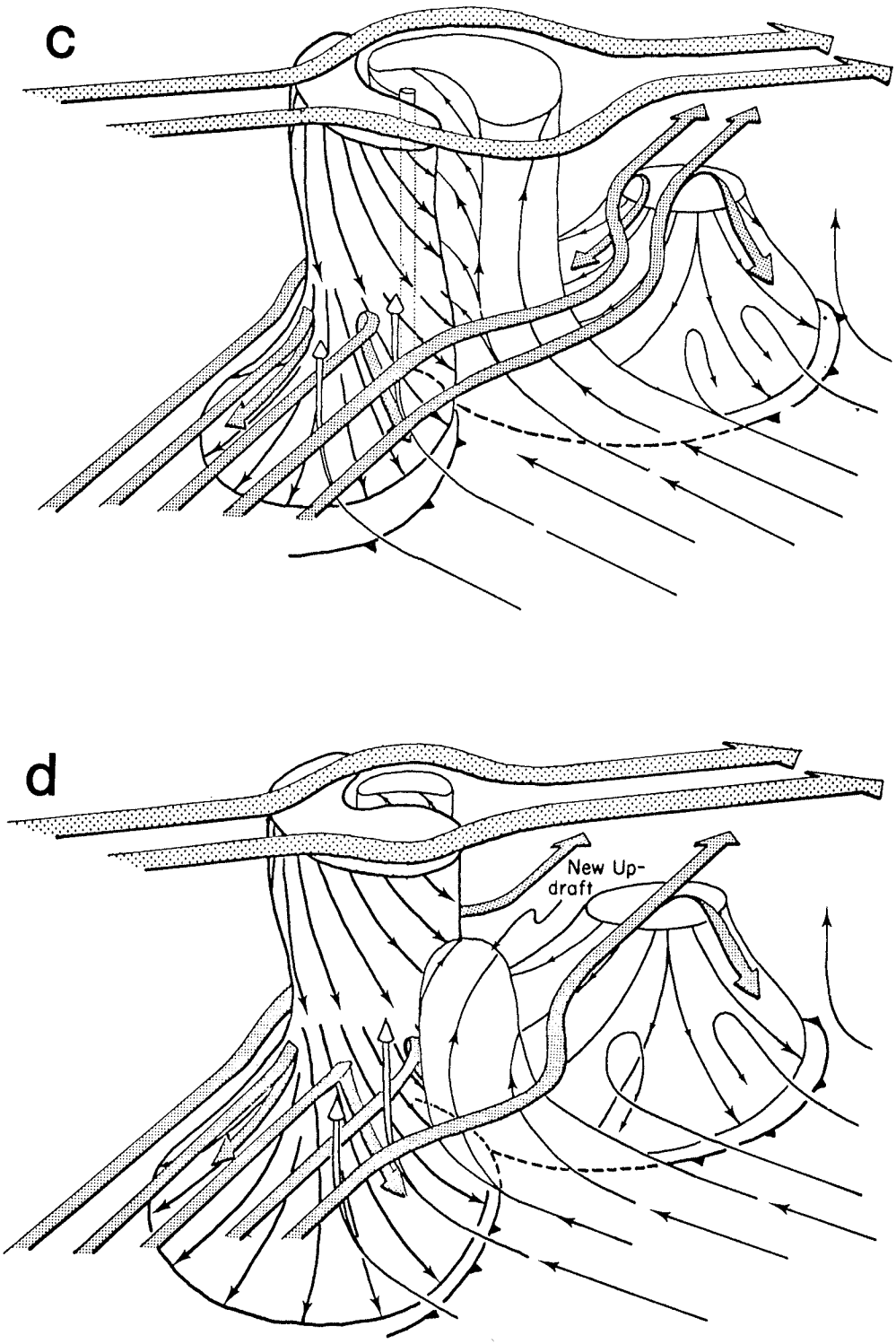

simplicity. Fine stippling denotes the TVS. Flow lines throughout the figure are storm-relative and conceptual only. Conventional frontal symbols are used to denote outflow boundaries at the surface. Salient features are labeled on the figure (from Lemon and Doswell, 1979).

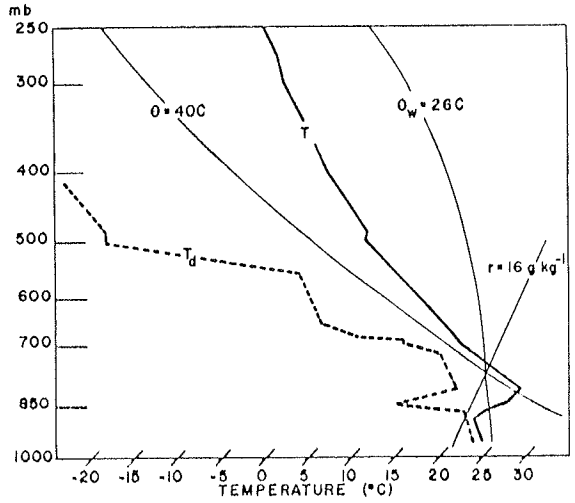

Figure 3.28 Skew T, log p plot of 1200 GMT Tinker AFB rawinsonde 18 June 1973. The temperature profile is the heavy solid line labeled T. The dew-point temperature profile is the heavy dashed line labeled T_d. The light solid lines are included for reference and show the 40°C potential temperature, the 26°C wet-bulb potential temperature, and the 16 g kg^{-1} mixing ratio curves (from Doswell, 1977).

(perhaps only one). There is also reason to believe that in the immediate vicinity of the storm, the classical sounding (typified by Fig. 3.28) is modified. As mentioned in I.II.B.2, it appears that in the **local** environment prior to the onset of convection, the inversion may be lifted and weakened, with an associated deepening of the moist layer (e.g., Beebe, 1958). It remains to be seen how general these ideas are, but the connection between supercells and some localized convergence-producing mechanism is certainly suggestive evidence for a localized erosion of the "cap".

Marwitz (1972a) has implied that a threshold value of cloud-bearing layer shear is roughly 2.5 x 10^{-3} s^{-1}. Doswell and Lemon (1979) have found a similar average value. They point out that the range is wide, although it is not clear how much of their range results from "noisy" operational data. Within the subcloud layer, Marwitz finds that the mean wind is typically in excess of 10 m s^{-1} (~ 20 kt), and the wind profile is characterized by more than 50° of veering. Doswell and Lemon find, similarly, that the subcloud layer shear is stronger, on the average, than that within the cloud layer and is better correlated to the supercell storms (i.e., has a narrower range). The suggestion that the low-level flow is a controlling factor in supercell production is supported by the numerical model results of Weisman and Klemp (1982). Note that the magnitude of the low-level flow averaged through some layer is probably less important than the vertical **shear** in that layer. However, strong low-level winds are normally associated with strong low-level shear.

The concepts resulting from the thunderstorm model sensitivity studies exemplified by Weisman and Klemp's paper can be summarized as follows. The dominant parameters are buoyancy (or, more properly, the **potential** buoyancy if a parcel is forced through its LFC) and vertical shear. Note that another expression for the potential buoyancy is **Convective Available Potential Energy** (or CAPE -- see Moncrieff and Green, 1972). The shear which is apparently of most significance is that generally below 4-6 km (see also Davies-Jones, 1984). If the hodograph has clockwise turning in that layer, the right-moving member of a split pair is enhanced; whereas for counterclockwise turning, the left-mover is favored. Note that the models show a marked tendency for storm splitting in most environments. Further, the greater the shear magnitude, the larger must be the CAPE, for supercells to be the preferred mode of convection. An example of a supercell-typical hodograph is shown in Fig. 3.29.

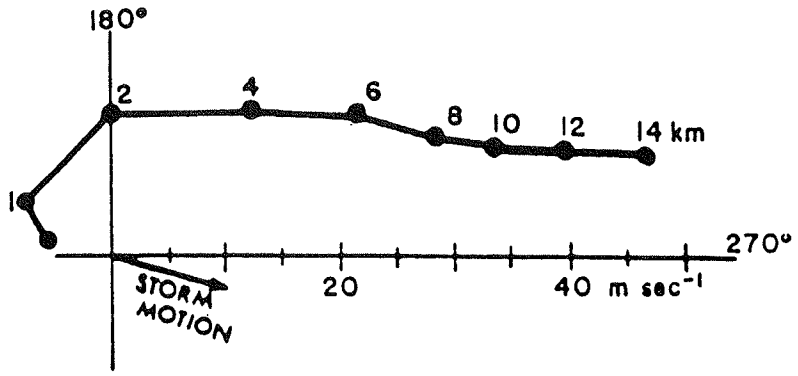

Figure 3.29 Example of a "typical" hodograph associated with supercell storms (from Chisolm and Renick, 1972). Notation as in Fig. 3.16.

These ideas have great intuitive appeal and are supported to some extent by limited observations (Rasmussen and Wilhelmson, 1983). At this point, one can and should be excited by the modelling results without having to accept them unconditionally. It is likely that the problem is more complex than a "two-parameter" one, even in some non-trivial aspects. The mesoscale variability of the storm environments has yet to be incorporated in the published model simulations. Further, the utility of the key model-derived parameters in an operational forecasting mode has yet to be determined quantitatively. Nevertheless as we shall see in Chapter VI the numerical simulations have been remarkably successful, given their relative simplicity.

3. Squall Line Severe Thunderstorms

a. Some General Remarks

We have been considering forms of severe convection which are more or less isolated in space -- single cells or groups of cells organized into a single complex. Thus far, we have ignored the well-recognized tendency for storms to occur in lines. Problems with the semantics of "squall lines" have already been mentioned (in Volume I). Exactly what is meant by a "squall line" and where are the distinctions drawn? Clearly, two points can make up a line, so it can be said that two separate storms occurring at, say Minneapolis and New Orleans form a "line". This is obviously nonsense, since the events are not connected in any meaningful way. At the opposite extreme, two separate radar echoes 10 km apart also constitute a line. In such a case, we have another meaningless "line" since it is so short. To complicate the problem further, the atmosphere is quite capable of producing **more or less** (emphasis is important) continuous lines of thunderstorms extending from, say, Minneapolis to New Orleans (e.g., Fig. 3.30). Portions of such a "line" may contain supercells, severe multicells, or ordinary thunderstorm cells (Browning, 1982). It may also include shorter lines of activity which are more nearly continuous than is the overall, large-scale line. This should be clear when seen from above (Fig. 3.31).

Historically, distinctions have been blurred. Hence, we find efforts to distinguish among line types such as Forbes' (1975) "tornado line" or references to "lines of supercells", in which supercell storms are spaced at intervals on a large-scale line of separate radar echoes. We also see considerable difference in the usage of the term

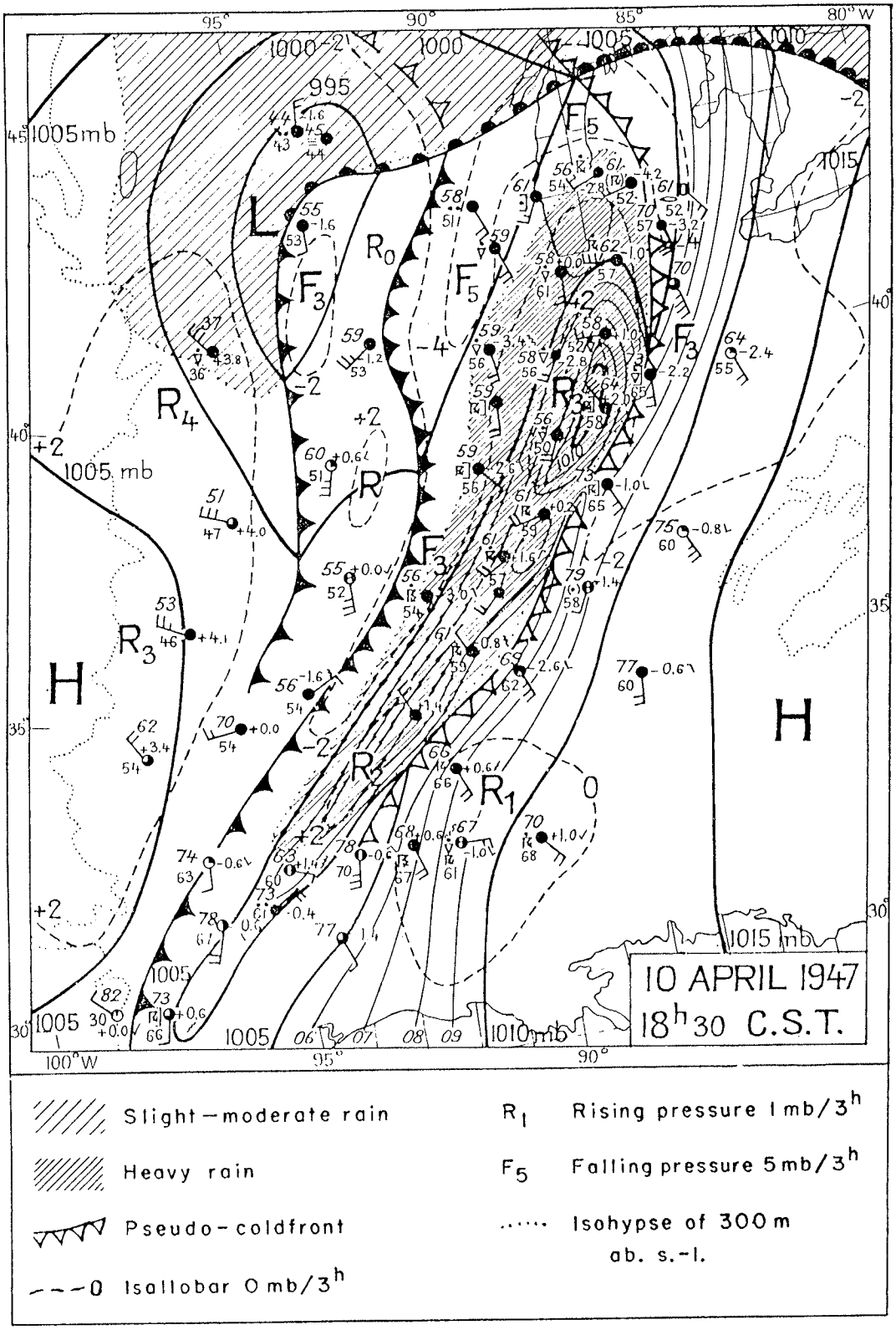

Figure 3.30 Weather map with convective system over eastern U.S., 10 April 1947, 1830 CST (from Bergeron, 1954).

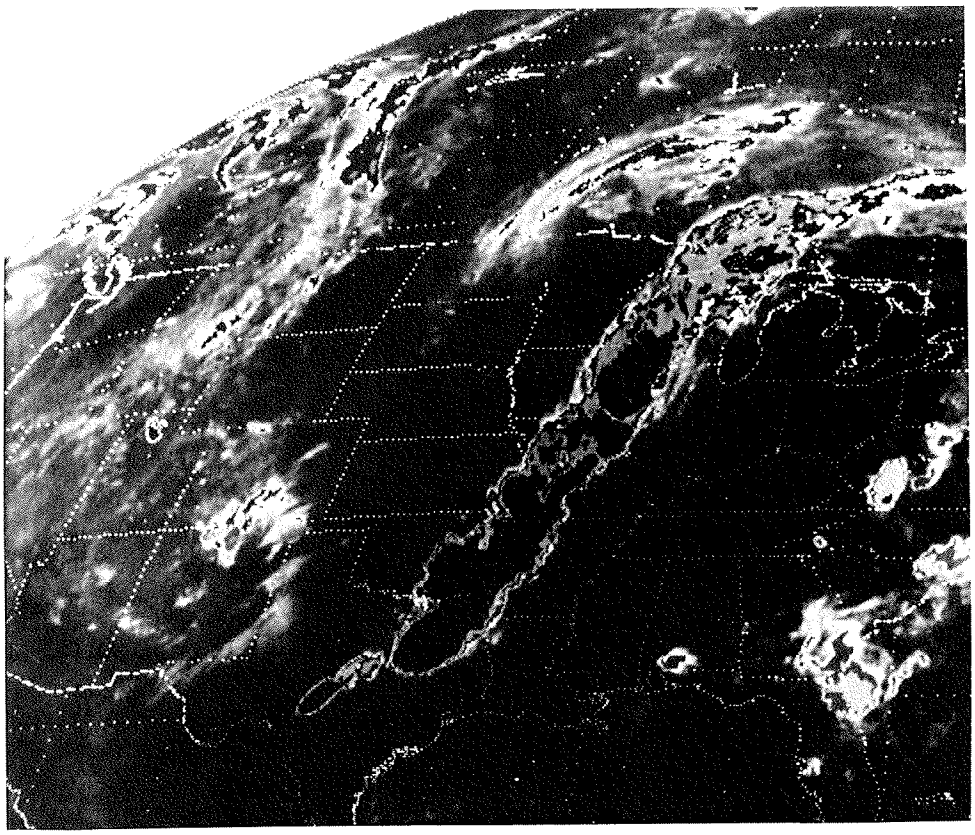

Figure 3.31 Example of long squall line event, comparable to that shown in Fig. 3.28, from a satellite viewpoint.

"squall line" (compare Marwitz, 1972c; Magor, 1959; Porter **et al.**, 1959; Palmén and Newton, 1969 [p. 401 ff.]). As indicated in **I.**III.B.7, this confusion seems to relate to the **scale** of the phenomena rather than any specific wording in the definition.[8]

In this volume, a squall line (severe) thunderstorm is one in which the individual cells are aligned laterally over a distance which is large compared to the dimensions of a single cell, and where the spacing between cells is comparable to (or less than) those single cell dimensions. Thus, in these discussions, the individual cells which make up the line become in some sense, of secondary importance in comparison to the overall line structure. While it is likely that no real system is completely describable as a two-dimensional structure, its three-dimensional aspects do appear to be relatively minor at times.

---

[8] The Glossary (Hushke, 1959) defines a squall line as "Any non-frontal line or narrow band of active thunderstorms ..." However, a "squall" is defined by the behavior of the winds -- it is a sustained gust which meets certain criteria (see Federal Meteorological Handbook No. 1 -- the manual for surface observations). If a number of stations report squalls (they almost never do!), then a "squall line" is possible.

This definition probably excludes lines of supercells and all other systems which may be referred to as squall lines, whenever the three-dimensional character of the component cells is the dominant aspect. Further, it is somewhat in contradiction to that proposed by Marwitz (1972c), since the cells are close enough to be competing for the inflow. In effect, we are trying to focus on distinct phenomena, whereas reality is always producing a blurred picture. Nevertheless, nature does seem capable of producing systems which approach this archetype.

b. Radar Structure

Perhaps the most obvious indication of the linear nature of squall lines is their depiction on radar (Fig. 3.32). As can be seen, there is a continuous line of echo at levels of VIP3 (41 dBz) or greater. Nevertheless, even the low-level echo structure normally reveals cells (high reflectivity cores) embedded within this line. A series of PPI tilt scans nearly always shows separate storm tops along the line and the distinct cells forming the line can be at various stages of formation and decay.

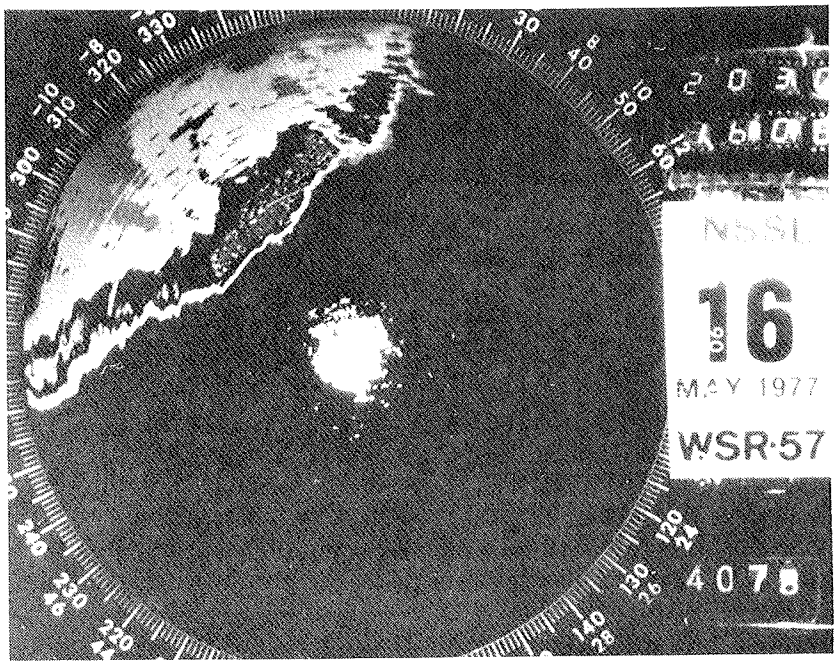

Figure 3.32 Radar photo of squall line (from Ray ***et al.****, 1977).*

Nevertheless, the essential character of the squall line is the connected nature of the cells which comprise it. In the typical case, even involving non-severe storms, the active part of the storms (located by the strongest reflectivity cores) only occupies a fraction of the area covered by detectable low-level echo. The active part is typically near the leading edge, with a large fraction of the total echo area occupied by low reflectivities. This behavior is also seen in tropical squall lines (Fig. 3.33).

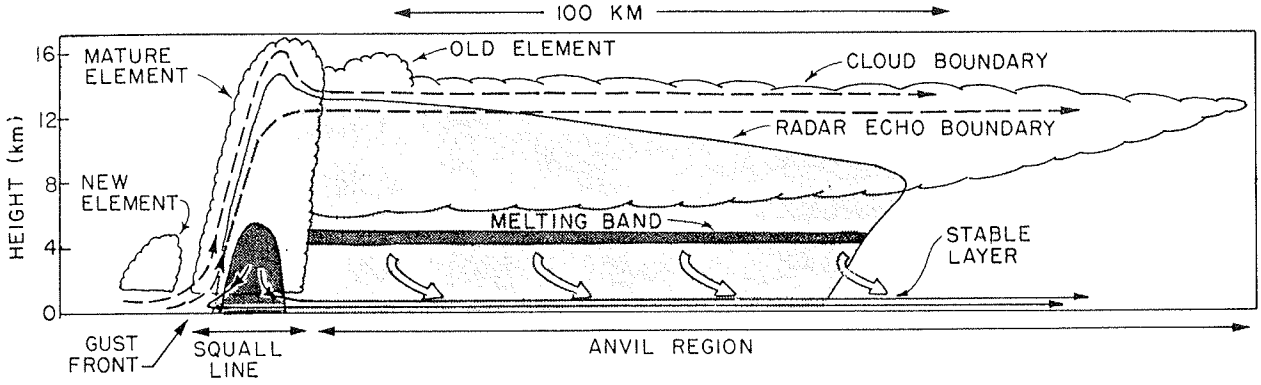

Figure 3.33 Schematic cross section through a tropical squall line system. Streamlines show relative flow, with dashed streamlines showing the convective, updraft flow, the thin solid streamlines showing the comparable downdraft, while the wide arrows depict the mesoscale downdraft below the anvil base. Shading is roughly comparable to radar reflectivity, and the scalloped line indicates the visible cloud boundaries (from Houze, 1977).

As a whole, the storm resembles the classical view of a cold front, with the leading edge being characterized by a more or less continuous sheet of updrafts. Precipitation formed in the updraft falls most heavily to the immediate rear (relative to line motion) of the updrafts. This is indicated by the strong echo gradients (recall that updraft regions often are marked by strong reflectivity gradients) on the leading edge. The vast majority of such storms are non-severe, although small hail, moderate wind gusts, and heavy rain can accompany them.

When squall line storms do produce severe weather events, they may depart from this basic structure in some fairly specific ways. A common mode of severe weather production in squall line storms is for the newest member of the line to be the event-producer. New cells often form at the southernmost end of the line. Such "tail-end" storms may have a brief period when they attain severe limits, and then settle back into the less severe behavior as they move along the line and are replaced by newer cells. This sort of storm cell will resemble the multicellular (or even supercell) model during its severe phase. On occasion, as the cell moves down the line, it can retain its distinctive character, in which case its radar structure will continue to be different from other members of the line.

In other examples of severe squall lines, some segment of the line begins to accelerate forward, producing a bend in the line and a swath of severe weather events (e.g., Charba, 1972). This is the origin of the **Line Echo Wave Pattern** or LWEP (Nolen, 1959), as shown in Fig. 3.34. Fujita (1978) has documented several examples of this behavior and attributes it to the formation of **downbursts** (see IV.C.2) at the rear of the line. This is seen by Fujita as the origin of what he calls the **bow echo.** Such events are commonly associated with severe wind gusts, as the downburst can generate very strong, diverging horizontal flow (Fig. 3.35). Note that considerable cyclonic shear is created on the northern flank of the generally west-to-east blast of wind. Such cyclonic shear may be reflected in the formation of a vortex and tornado production near the apex of the bend in the line, as shown in Fig. 3.36.

Another way in which squall lines produce severe weather may not be so dramatic. In some cases, the low-level echo can remain essentially unchanged while the nature of the storm is changing. For whatever the reason, if some segment of the line develops an

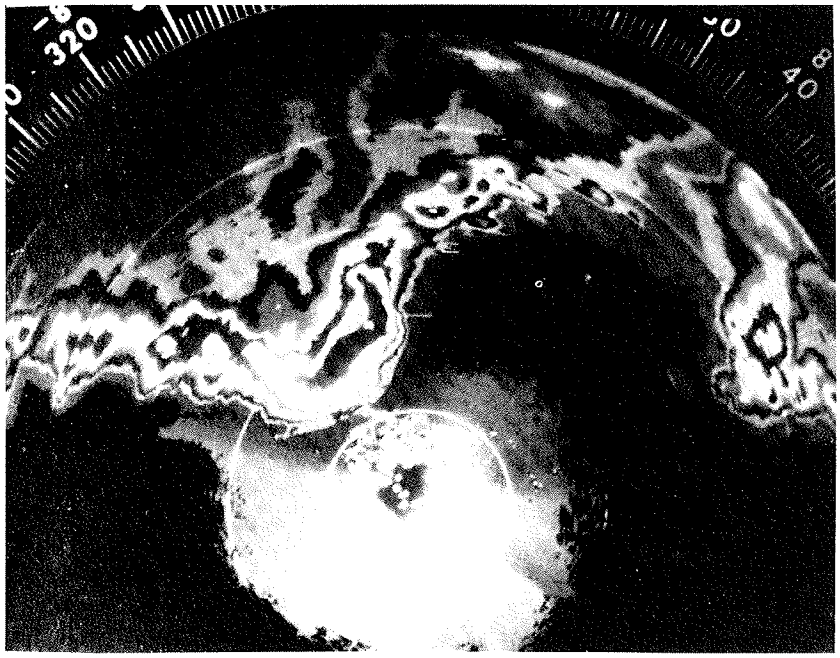

Figure 3.34 Line echo wave pattern (LEWP), embedded in a squall line (from Wilk ***et al.****, 1976).*

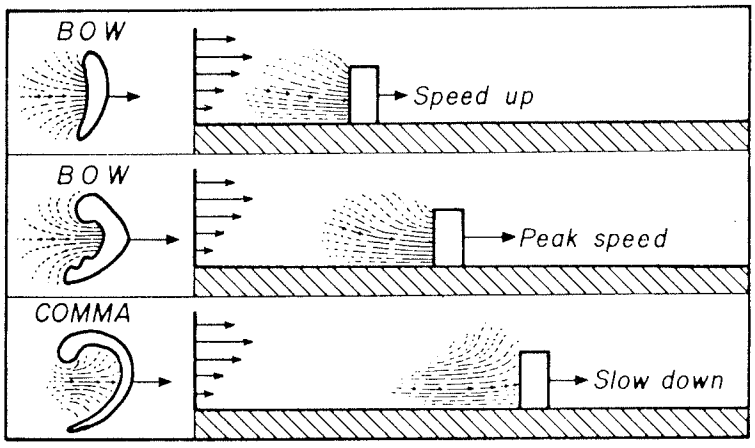

Figure 3.35a A conceptual model of wake flow behind a bow echo which turns into a comma echo (from Fujita, 1978a).

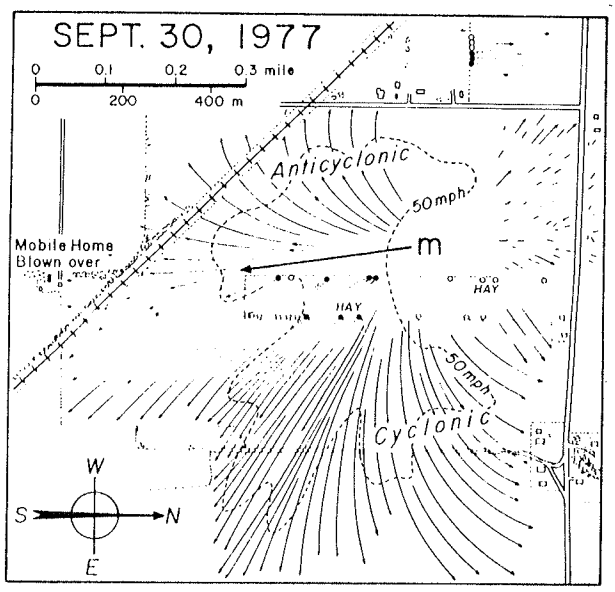

Figure 3.35b Observations of microburst event on 30 September 1977, showing cyclonic and anticyclonic curvature in outflow (after Fujita, 1978a).

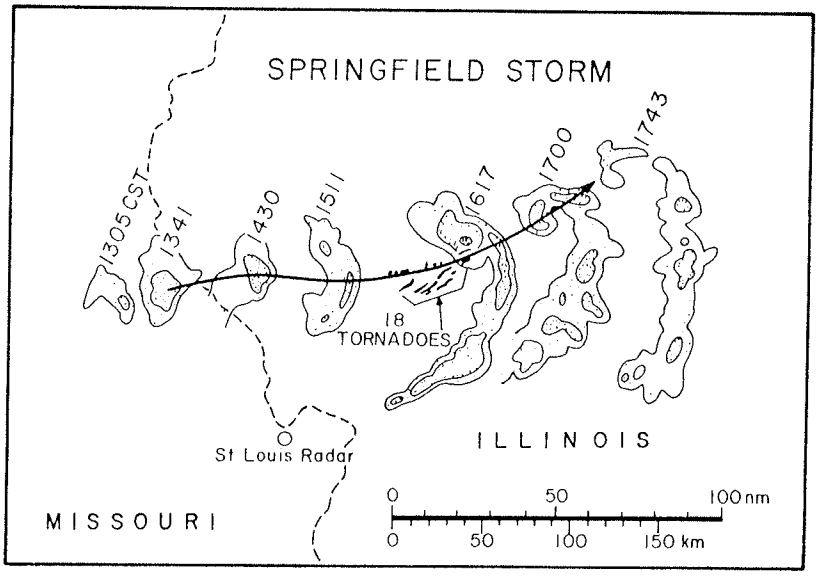

Figure 3.36 Location of tornadoes with respect to bow echo storm on 6 August 1977 (after Fujita, 1978a).

enhanced updraft (recall that a stronger than normal updraft generally signals the transition from non-severe to severe characteristics), this may not be obvious at first from the low-level echo. A tilt scan will reveal, at such times, the formation of a WER at middle and upper levels. This WER is most likely located on the line's leading edge where other, weaker updrafts exist on its flanks. With time, this should reveal itself by taller storm tops and higher reflectivities associated with the stronger cell, as well as increased reflectivity gradients in low levels. A substantial WER (Fig. 3.37) associated with a squall line is a good indicator of the development of a distinctively strong cell, which may eventually acquire supercell characteristics, within the line. Such a situation can develop into rather dramatic radar configurations, as shown in Fig. 3.38, but the WER is often the first sign of such changes.

One should be aware by now that the more intense forms of severe weather are only rarely associated with squall lines which have essentially uniform structure along the line. In by far the majority of cases, some change favoring a particular cell over the others occurs before severe events commence. The individual cells are competing for inflow as the line sweeps through the moist air, so that no particular cell is favored in such examples. This suggests that a severe squall line storm must have some mechanism operating whereby the low-level relative inflow is **concentrated,** rather than being spread out more or less uniformly along the advancing gust front. Breaks in the line are one mechanism for reducing the competition between cells -- in effect, the first cell north of a break in the line can behave much like the "tail-end" cell.

It is in this fashion that "intersecting squall lines" may play an important role. It is relatively rare that radar echo lines converge in this manner -- of course, if such an event is observed, the potential for an episode (probably brief) of severe weather is certainly enhanced. However, the most common case is where a squall line (as we have defined it) approaches some low-level boundary, perhaps created by earlier storms. That is, the active squall line is encountering a boundary which does not have intense convection along it at the time of intersection.

c. Visual Structure

During its formative stages, a squall line which forms by building along its southern end can resemble a multicell complex. A series of convective towers develops along a line, each rising to maturity at the end of the line (Fig. 3.39). These rapidly merge with the earlier cells, just as in a multicellular storm. This repetitive process may continue through the life of the squall line, but a different series of events soon begins to predominate. Rather than simply dissipating, as in the multicell storm, the cells along the line produce a series of gust fronts which move out ahead of the complex and trigger new convective towers on their leading edge. Thus, while the southern end of the line may continue to develop new cells on its right or right rear flank (resulting in a generally southward propagation of the end of the convective line), the squall line now begins to produce new convection on its forward flank.

Squall lines can begin in ways other than this "back-building" process (Bluestein and Jain, 1985). Equally common, according to Bluestein and Jain, are squall lines forming when convection develops a many places along a line more or less simultaneously. Less frequently, squall lines can evolve from within a broken area of convection or within a region of weak, stratiform precipitation. In any case, once the line is formed, the interaction among cells produces a quasi-continuous line of outflow.

Such a process can become self-sustaining, as older convection dissipates, moving along the line and also being left behind by the advancing gust front, which is generating new updrafts. Since downdrafts produced by the decaying cells contribute their cold air

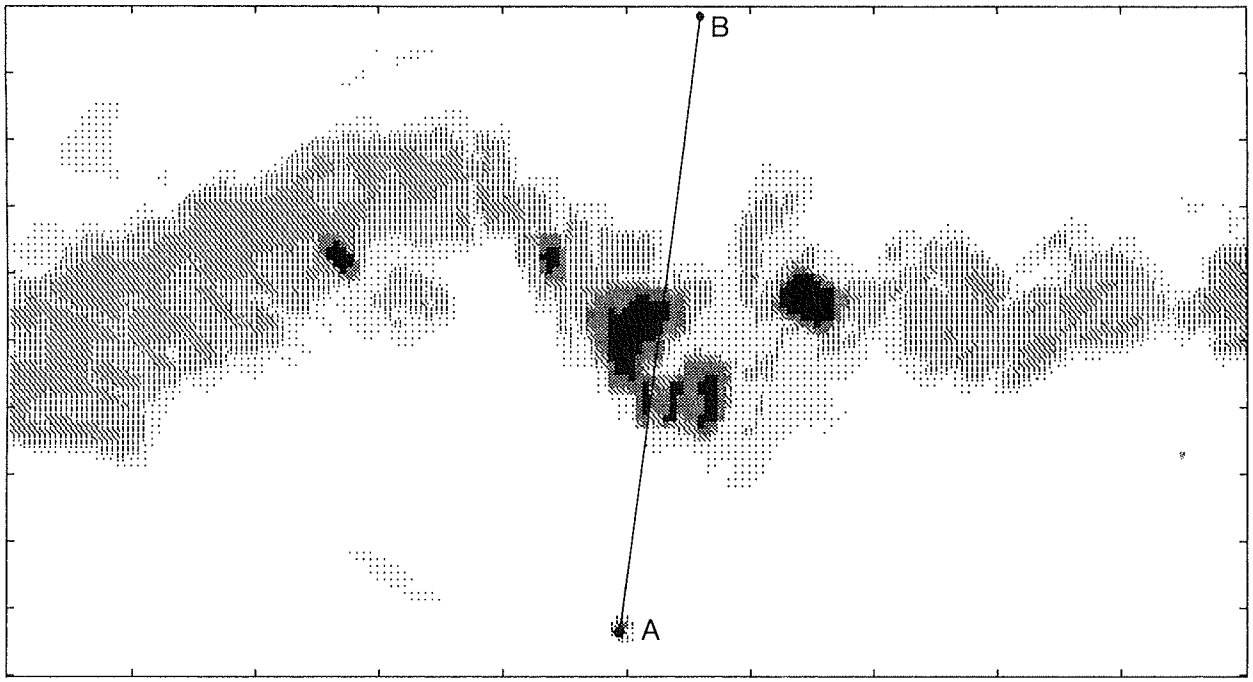

Figure 3.37a Low-level radar depiction of squall line on 4 July 1984 in south central Nebraska at about 0450 GMT. Shading is proportional to reflectivity as seen by airborne radar, with the peak values roughly 45 dBz (courtesy of D. Jorgensen). Position of the aircraft is at point A, and the tick marks along the bottom and top margins are at 12 km intervals.

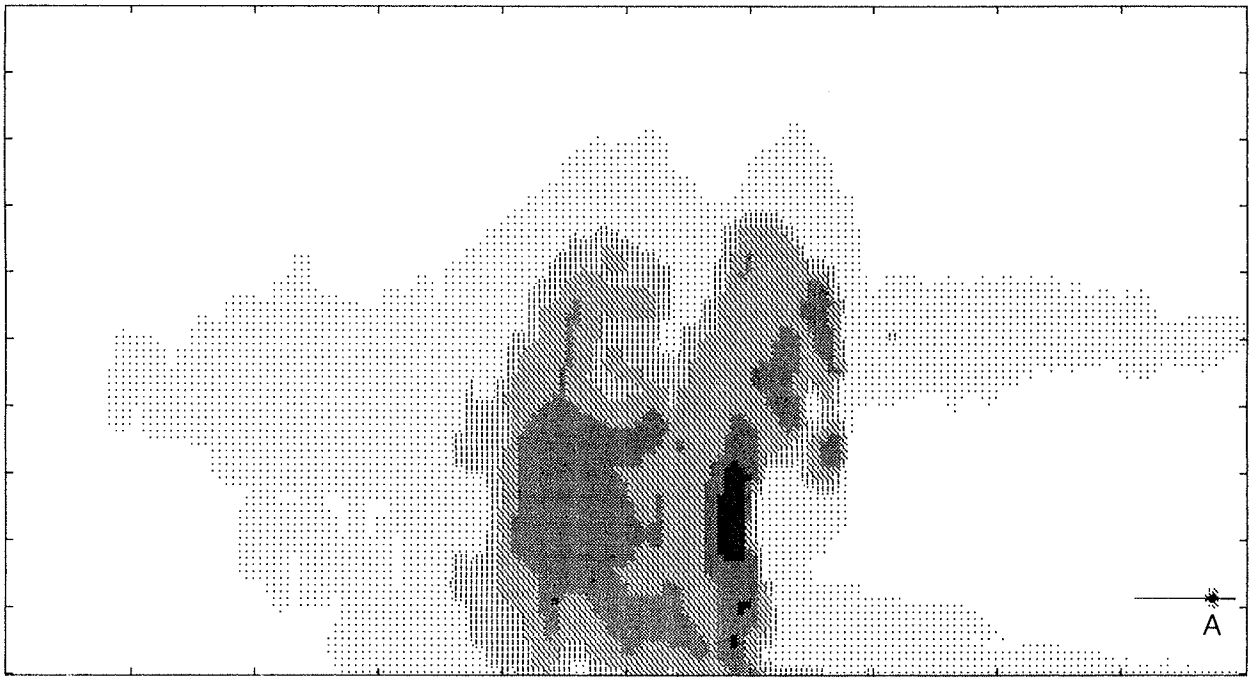

Figure 3.37b Cross section along line AB of Fig. 3.35a, showing a WER along the leading edge of the squall line. The level and location of the aircraft is shown by point A on the far right side of the figure. Horizontal tick marks are at about 6 km intervals, and the vertical tick marks are at 2 km spacing. Note the evidence of an older, dissipating cell behind the vigorous new cell on the leading edge. This storm produced considerable wind damage and large hail.

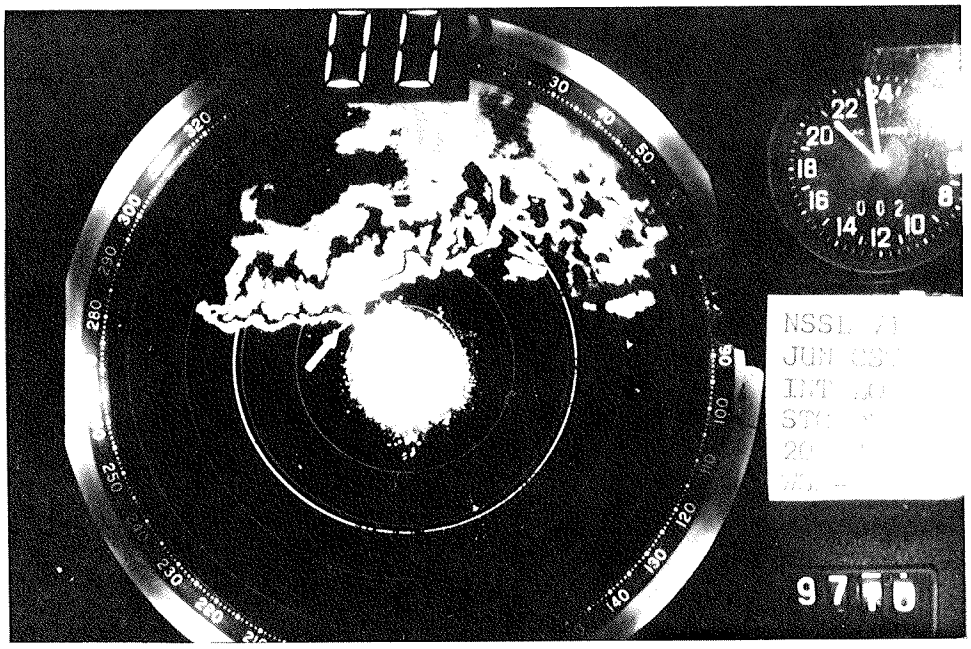

Figure 3.38 Radar photograph showing low-level reflectivity display with pronounced hook echo (arrow) embedded in a squall line (Photo courtesy of D. W. Burgess).

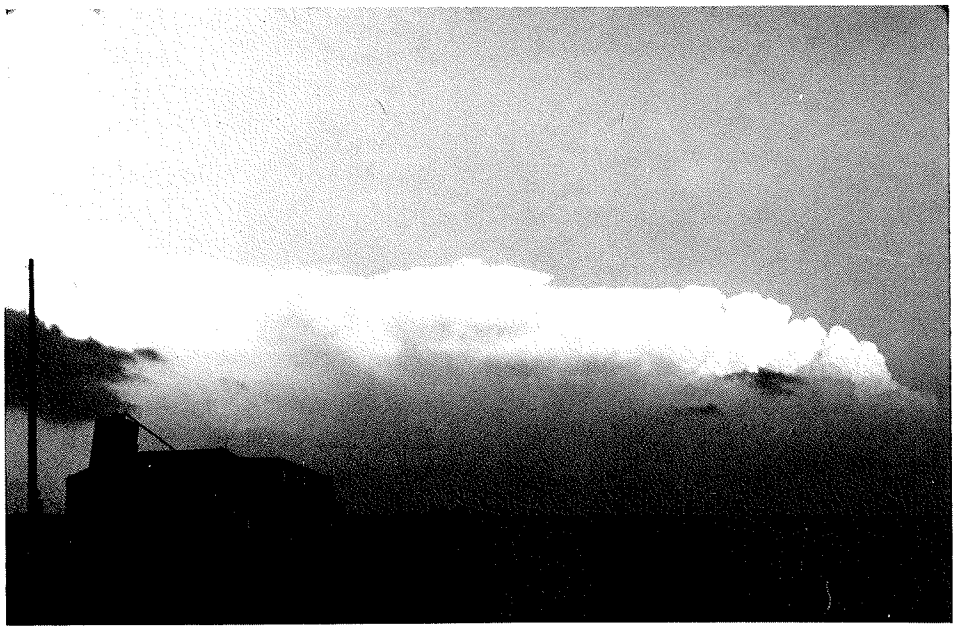

Figure 3.39a View of squall line from the northwest, showing developing cells at the southwest end of the line (far right in photo) with more mature, older activity within the line (from right to left in photo).

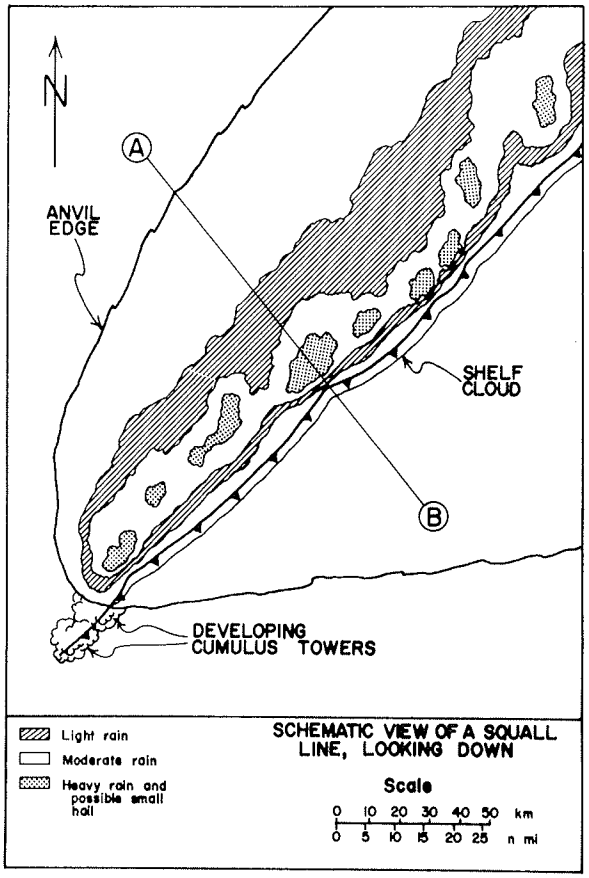

Figure 3.39b Schematic structure of squall line. Note that the view in Fig. 3.37a is as if the observer were seeing this squall line from location A in this schematic.

outflow to the line's gust front, the process can continue in this leapfrog fashion as long as the air being lifted by the gust front is capable of supporting convection (i.e., is unstably stratified and has sufficient moisture content). By the way, this is a simplified description, and it does appear that even in a truly two-dimensional convective system, the behavior is strongly dependent on the shear (Thorpe **et al.**, 1982).

This process results in the development of cumuliform towers along the front flank of the line. These repeatedly form, merge with more mature elements in the line, and give way in turn to newer towers. Often, low- and mid-level cloud decks develop out ahead of the more active portions of the line. These leading cloud decks frequently obscure the more convective portions of the line from view, so that from ahead of the storm, the approaching squall line appears as a more or less amorphous mass of gradually lowering clouds. In such cases, the first real visual clue to the nature of the storm comes when the leading edge of the low-level gust front approaches. This gust front is typically marked by a shelf, or roll cloud (more officially, forms of "arcus" cloud).[9] The advancing gust front "scoops up" the near-surface air, which usually has the highest moisture content (Fig. 3.40). Further, some of the high relative humidity air in the outflow may be recycled into the updraft along the gust front. Thus, a lowered cloud base results, just as in the wall cloud situation discussed earlier. Since the lifting is along a line rather than being concentrated into a small area, the resulting lowered base is more or less

[9] Under the right conditions, a cold front which is particularly sharp can produce a shelf (or, more properly, an arcus) cloud on its leading edge -- with or without any higher clouds above it (Livingston, 1971).

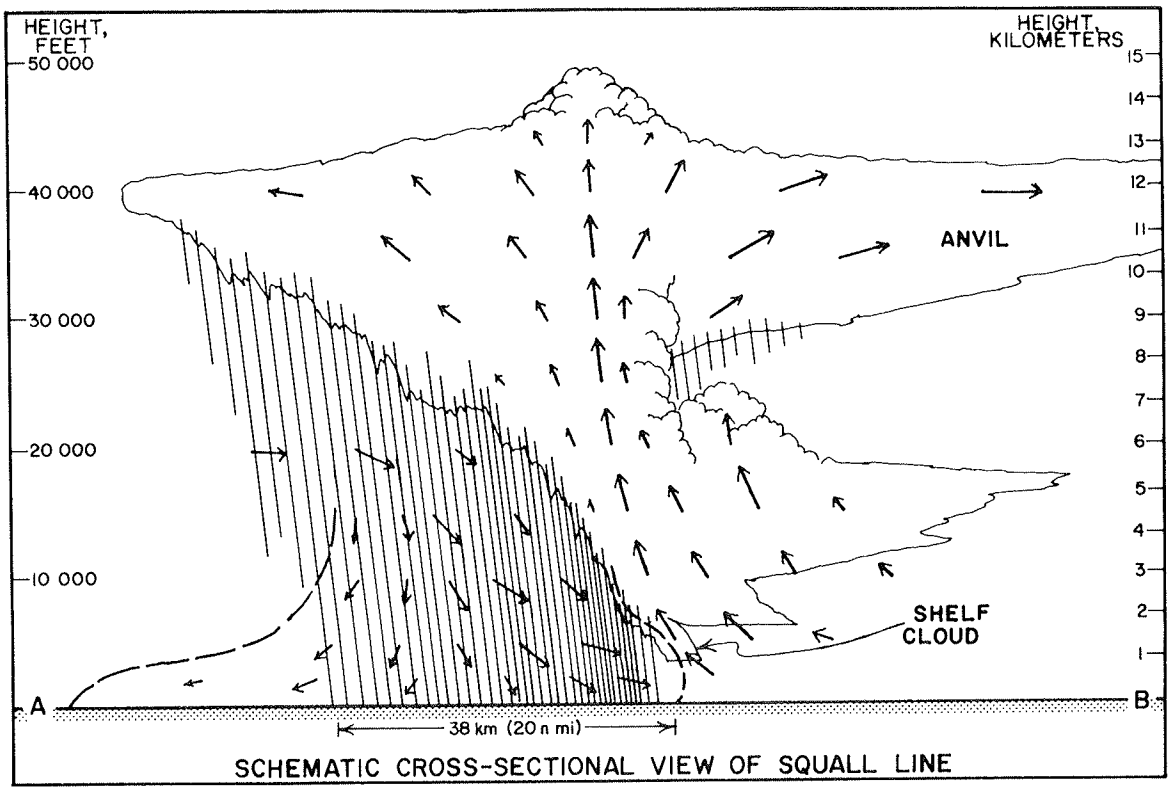

Figure 3.40 Cross section along line AB of Fig. 3.37b.

linear (see Fig's 3.21 and 3.22 in Vol. I). A shelf cloud is a lowered base which is **attached** to the cloud base above. It may be smooth and wedge-shaped, or it may have a terraced appearance, with several layers of cloud involved. It can also be quite turbulent and ragged. A roll cloud may be similar, but is **not attached** to the cloud base above it and often assumes the appearance of a long, horizontal tube. In some cases, the roll cloud appears to have a slow rotation about a horizontal axis associated with it. This rotation may be created by the shear between inflow (updraft) and outflow (downdraft). Another viewpoint about the creation of the rotation is described by Wakimoto (1982), in which the leading edge of the outflow rolls up, as revealed by precipitation (see his Figs. 3 and 9). Such an origin may be related to soenoidal generation of vorticity about a horizontal axis by the intense frontal temperature gradient (see Goff, 1976 or Mitchell and Hovermale, 1977). The rotation is not related **directly** to tornadic rotation.

As the gust front passes a fixed location, the precipitation may begin immediately or, in mature or decaying squall lines, may be delayed considerably (or never occur at all at the fixed point). Behind a shelf cloud, the appearance of the clouds is usually quite ragged and turbulent. Cloud base rises rapidly, giving a vaulted appearance (Fig. 3.41). Descent may be evident visually in the sloping clouds immediately behind the gust front. In the boiling, turbulent clouds, eddies may form and dissipate rapidly, perhaps even forming brief funnel clouds (Hexter, 1962). Generally speaking, such eddies rarely, if ever, touch down as tornadoes. These are distinct from "gustnadoes" which may develop along the gust front's leading edge (see Forbes and Wakimoto, 1983; as well as B.2 and F.5 [Fig. 3.53] in this chapter).

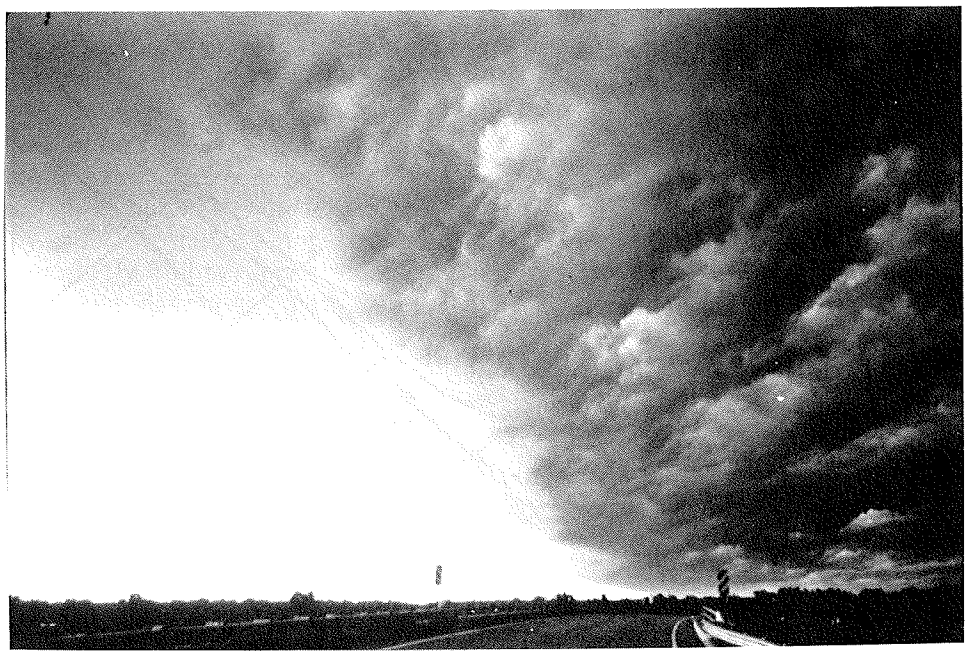

Figure 3.41 Example of "vaulted" appearance behind an outflow shelf cloud, resulting from subsiding air (see Fig. 3.38).

Viewed from the rear, a squall line of the sort we have been describing generally has no distinct cloud structures. Since the air is descending to the rear of the line, clouds tend to dissipate and all that can be seen is the falling precipitation beneath the storm anvil. Since the heaviest precipitation is usually close to the leading edge of the storm, skies gradually lighten after the storm passes, often giving way to clear skies in the wake of the anvil. This period of diminishing cloudiness and precipitation can be brief or protracted. In slow-moving systems with substantial "stratiform" precipitation areas (low reflectivity), this period may account for the majority of the storm-total precipitation. Perhaps far off to the south, cumuliform towers can be seen at the tail end of the line (recall Fig. 3.32). Mammatus formations may also be present in the anvil far behind the active part of the squall line.

d. Airflow

Since the squall line, as we have defined it, is basically the same all along its length (except, perhaps, at the southern end), the airflow patterns can be visualized in essence by a vertical cross section through the line (Fig. 3.40). Naturally, such a simplification is not without its limitations and may omit significant fine detail, especially in the more severe cases. Nevertheless, the basic flow patterns are generally much less complex than multicell or supercell storms. Since the squall line as a whole may move with a large component **across** the upper level flow, the relative flow at upper levels can have a large component in the plane perpendicular to the plane of the cross-section. Individual cells, moving with the vertically-averaged upper flow, pass **through** the cross section. The divergence at upper levels, common to all convective storms, spreads the anvil out (Fig. 3.42). Ahead of the line, the spreading is in the same direction as the line motion so the anvil may not extend very far out in front of the storm. To the line's rear, this spreading is opposed to line movement, so the anvil in mature squall lines will be quite extensive on the rear side. That is, the back anvil edge advances slower than the convective line which produces it. This is consistent with the region of anvil

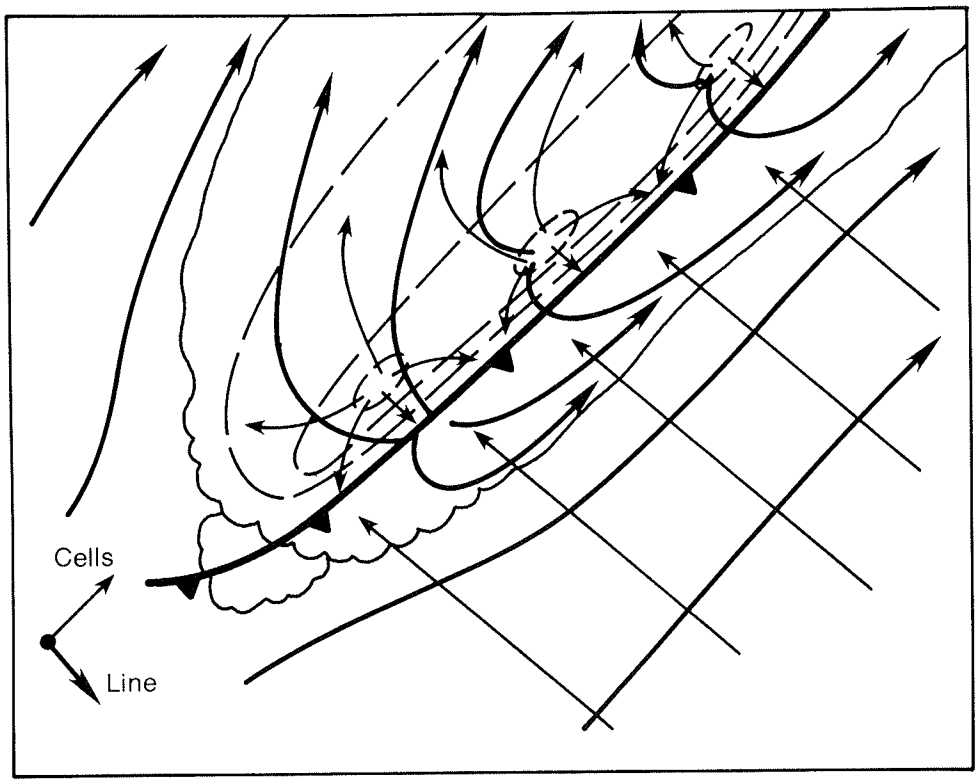

Figure 3.42 View from above a squall line storm, with lines as in Fig. 3.15. Note that the cell at the southern end of the line often is stronger than older cells to the northeast (north is to the top of the figure).

precipitation which may persist long after the active convective precipitation has passed. Tropical squall lines described by Zipser (1977), Houze (1977), Gamache and Houze (1982) and others have a similar structure.

However, since tropical squall lines occur in an environment which generally has weaker shear, the relationship of the anvil boundaries to the line of active convection can be more subtle than in mid-latitude systems. The issue is, in some sense, determined by the relative flow. This, in turn, is related to the line movement. Tropical squall lines seem to have two modes of line propagation: a **fast** (about 11 m s^{-1}) mode and a **slow** (about 2 m s^{-1}) mode (LeMone **et al.**, 1984; Barnes and Seickman, 1984). Interestingly, the upper-level relative flow in both modes ends up being about the same (10-15 m s^{-1} -- see Fig. 2 in LeMone **et al.**,1984), so the rate of anvil spreading in both modes should be roughly comparable.

Thus, when the convective line moves more slowly than the flow aloft, the anvil may well extend much farther downstream than upstream (relative to the upper flow). In such a case, anvil precipitation may be falling ahead of the active convection. Also, it may well happen that the anvil level flow is **along** the line of active cells. Such situations often are associated with quite slow line movement. Thus, the anvil spreads roughly equally ahead and behind, forced in those directions only by the divergence of storm cell tops.

Within the active portion of the storm, there is a very obvious updraft/downdraft interface. The basic flow is, as noted before, similar to the classical view of a "cold

front wedge" only on a smaller scale. Naturally, the cells embedded within the line contain the strongest vertical circulations, while the spaces between strong cells probably exhibit similar, but weaker, vertical flow.

In the regions **between** the strong cells, it is also probable that the updrafts, by being weaker, have greater slopes. Thus, in a relative sense, there is enhanced flow **through** the line between cells (Fig. 3.43), where air rises over the cold air dome produced by outflow but is not lifted to great heights. Such air should pass into the region of generally lighter precipitation falling from the anvil to the rear of the line's active towers and descend. This mixes with the air descending from mid-levels in the wake of the storms.

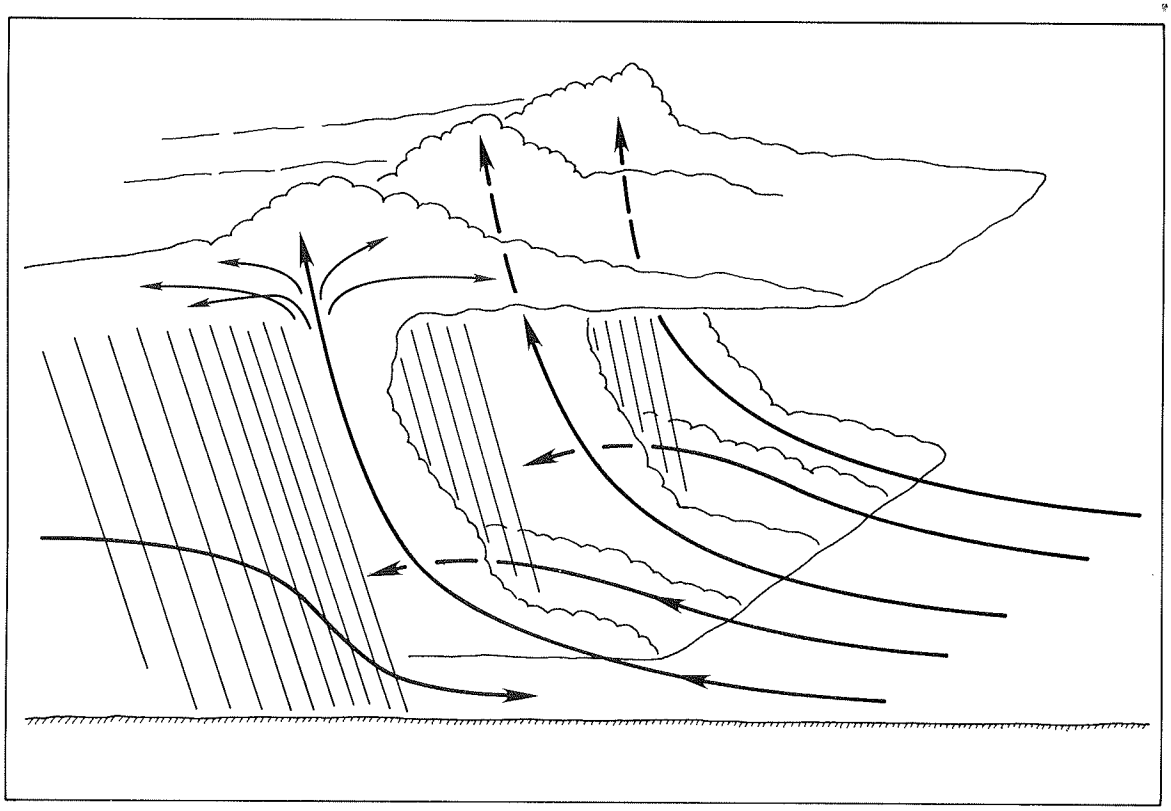

Figure 3.43 Schematic depiction of low-level flow, relative to squall line motion, when line contains distinctly separate cells. Note that the distinct updraft towers may not be visible owing to intervening cloudiness.

In cases involving strong cells embedded within a large squall line, the flow structure is complicated by these more three-dimensional features. While not documented, it is likely that such distinctive cells have relative flows resembling that of their more isolated counterparts. In the case of the Bow Echo (or LEWP), the most obvious feature of the flow is the "jet" of stronger horizontal winds created by the downburst.

Note also the weaker, higher-based updrafts ahead of the strongly convective portion of the line. This creates the often-observed lower and middle cloud decks ahead of the storm. Since the flow in a squall line is basically self-generating, it can persist for

many hours without substantial change. In some senses, this type of storm may represent the closest approximation to a true "steady-state" storm complex. Further, it is quite clear that such storms are remarkably efficient at overturning large amounts of moist, unstably stratified air and at converting moisture into precipitation. Thus, squall lines are a common form of organized convection.

e. Environment

To date, Bluestein and Jain (1985) have provided the only effort to document observations of the differences between squall line environments and those of other storm types. For comparison purposes, their composite squall line hodograph is presented (Fig. 3.44). It resembles a straight-line hodograph above about one km, but shows most of its curvature beneath that level. It should be pointed out that squall lines often exist in the same (to within the limitations of our sensors) environments with other, more isolated storms. This suggests that some very small scale aspects, perhaps on the scale of the storms themselves, may force the linear structure. It is noteworthy that in most situations involving coexisting isolated storms and squall lines, the isolated storms develop **in advance** of the squall line. This can be interpreted in at least two ways: the isolated storms modify the environment "seen" by the line, or the isolated storms are associated with localized forcing whereas the line is forced in a line-like fashion (e.g., by a front).

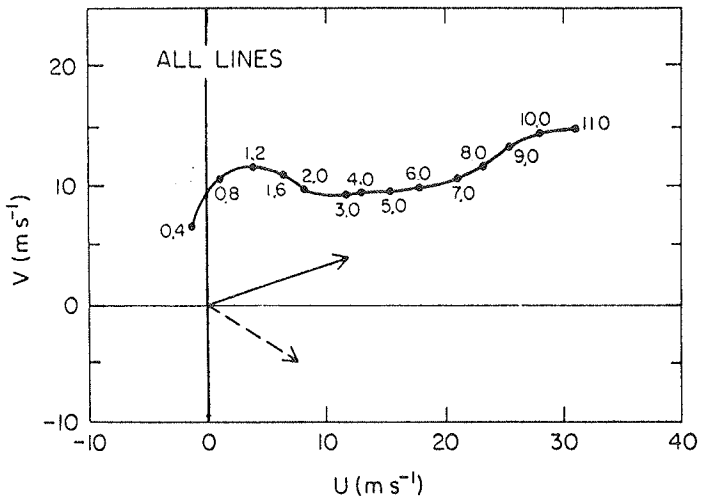

Figure 3.44 Composite hodograph from 40 Oklahoma squall line cases (from Bluestein and Jain, 1985). Notation as in Fig. 3.16 except that the cell motion (solid vector) and line motion (dashed vector) are shown.

We have generally looked to the environment to provide clues as to why convection is organized the way it is. This is, I believe, a consequence of our success in relating the **supercell** form of convection to environmental factors. One annoying problem in trying to understand squall lines is their propensity for being tilted upshear. In their most simple (linear) form, the momentum transport arguments to which we have already referred cannot produce an updraft tilted upshear. An interesting hypothesis to explain the observed upshear tilt has been advanced by Seitter and Kuo (1983). The Seitter-Kuo mechanism is based on the fact that the precipitation drag effect is not directly coupled to the thermodynamics of parcels. This means that the effective buoyancy of the parcels is not necessarily determined by pure parcel theory.

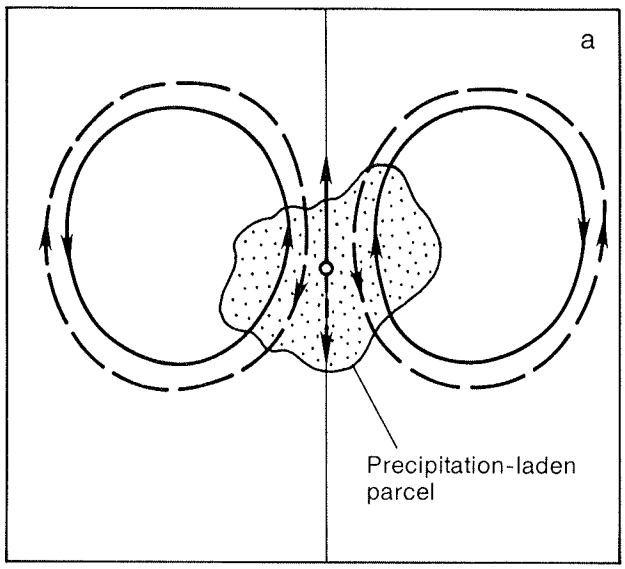

Figure 3.45a Model showing the separate contributions to parcel motion from thermodynamic buoyancy (solid) and water loading (dashed). In this case, the updraft is vertical and the effect of water loading is in phase with the buoyancy acceleration. The net motion is determined by the relative strength of the two effects. In such a model, the precipitation is falling back down through the updraft.

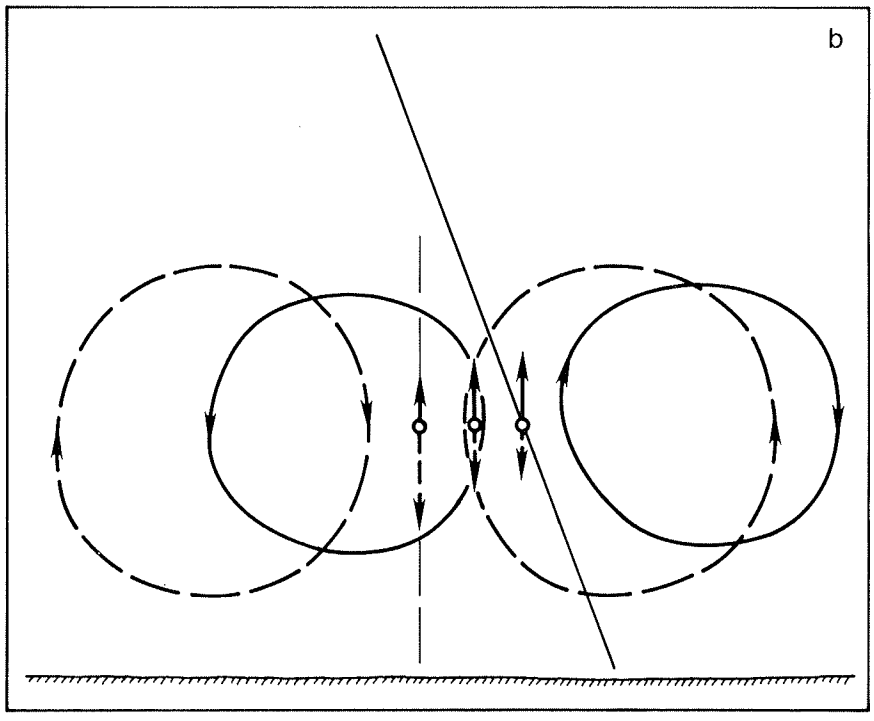

Figure 3.45b Model of a tilted updraft in which falling precipitation can fall out of the updraft. The separate contributions from water loading and buoyancy are depicted schematically for three different parcels, showing that even in the absence of shear and evaporative effects, the interface between updraft and downdraft in such a system tends to increase its tilt. In the presence of shear, this process and the tilting effect of the shear can be roughly in balance and the system propagates downstream while maintaining an upshear tilt.

Thus, in this model, the characteristic upshear tilt in squall lines is dependent on the existence of precipitation within the storm. As Seitter and Kuo describe it:

> ...the weight of the precipitation causes an erosion of the upshear side of the updraft. The erosion process is more severe on the upshear side of the updraft, so a more upshear slope is produced as the mechanism proceeds. The evaporative cooling of downdraft air by precipitation, which maintains the downdraft, plays an important role in establishing the upshear slope. In the mature storm, a balance is established between the water loading mechanism and the environmental shear which is stable to small changes in the slope.

As explained by Emanuel (personal communication), the precipitation drag effect produces a circulation which is somewhat out of phase with that produced by buoyancy, whenever the updraft is tilted, even in the complete absence of shear (see Fig. 3.45). In Emanuel's greatly simplified model of this process, it results in a propagating, tilted convective circulation, even in an unsheared environment. When evaporation and shear are included, some fairly realistic results are obtained which suggest that the presence of upshear tilt in squall lines results from an instability uniquely associated with **precipitating convection.** This turns out to be related to Kessler's (1969) condensation oscillations (recall the discussion of this in II.C.4).

A suggestion from Emanuel's model is that a balance can develop between the propagating disturbance and the shear, in accordance with Seitter and Kuo's more complicated numerical simulation. More research is needed to establish these results more conclusively, but this mechanism appears to be a promising means of explaining how quasi-steady propagating squall lines arise with upshear tilt.

It appears that the nature of the interaction between a squall line and its environment is quite subtle. Clearly, this is a potentially fruitful avenue for research, since the squall line normally is a substantially less severe form of convection. To be able to distinguish squall line from supercell cases using the larger-scale data would be quite valuable. There are other recent modelling results which are encouraging in this regard (e.g., Wilhelmson and Klemp, 1983).

F. Secondary Classes of Severe Storms

1. Some General Remarks

Although the primary severe storm classes are well-documented and account for the preponderance of significant events, there exist severe weather-producing storms which do not quite fit these primary groups. Because the secondary severe storm types are responsible for fewer noteworthy events than the primary storm classes, they are correspondingly less thoroughly studied. This should not be considered as justification for ignoring them. Such storms may not be as clearly associated with organized synoptic and subsynoptic weather systems, as considered in Volume **I.** Their occurrence often seems to be associated with "small mesoscale" or storm-scale phenomena which are inherently undetectable by conventional weather data. However, enough information exists about them to describe their structure (to a limited extent). Further, these storms occur often enough to be able to generalize about members of the class. Because of their limited documentation, it is not possible to describe their environments very confidently.

2. Pulse Storms

Perhaps the most common severe weather producer among the secondary classes is the so-called **pulse** storm. Such a storm, described by Wilk **et al.,** (1979), Wilk and Dooley

(1980), Lemon (1977), and Chisolm and Renick (1972)[10], closely resembles an ordinary non-severe thunderstorm cell in many respects, although it does have radar-detectable signatures. In essence, it is a cell which, for some reason, possesses **briefly** an intense updraft. This strong updraft lasts only a short time, during and immediately after which the storm produces a short episode of severe weather and then dissipates (hence, its name). Owing to its short life cycle, the analyst/forecaster has relatively little time to react to detection of its presence before the severe phase is over.

Early in its life, the first clue to the pulse storm's existence is the development of its first radar-detectable echo at higher levels than non-severe storms. Wilk **et al.** (1979) suggest that first echoes for pulse storms develop at 7 to 9 km AGL (compared with 3 to 6 km AGL for ordinary thunderstorms). They go on to state:

> The height of the 50 dBZ echo is also much higher, persistent, and maintains continuity with descent to the ground. In fact, if the height of the 50 dBZ echo reaches or exceeds 9 km, the storm can be interpreted as severe with considerable certainty. The occurrence of large hail at the surface, some times in excess of 5 cm, has been found to be within the 50 dBZ area.

Such storms generally are not tornado producers, but can develop hail and wind gusts exceeding severe limits. Their radar depiction, summarized in Fig. 3.46b, should be contrasted with Fig. 3.46a which corresponds to an ordinary storm cell. The pulse storm, then, generally can be distinguished from coexisting non-severe storms, but perhaps only with difficulty. There is insufficient documentation for these storms to try to characterize how their larger-scale environments differ, if at all, from those in which no such storms occur. In general terms, one might expect that pulse storms are associated with weakly sheared, moderately unstable environments -- i.e., those typifying "air mass" storm conditions. There is no information suggesting how pulse storms receive the impetus for their short-lived strong updraft pulse. Presumably, their visual appearance would differ only in minor aspects, if any, from ordinary thunderstorms. Of course, heavy rain and intense lightning may also accompany these storms.

3. Dryline Storms

This class of potentially severe storms represents an enigma. Only recognized recently as a separate class of storms (Burgess and Davies-Jones, 1979; Davies-Jones **et al.**, 1976; Bluestein and Parks, 1983), these storms have been observed most commonly to have formed near drylines -- hence, their name.[11] Bluestein and Parks have used the term "low-precipitation" ("LP") to refer to such storms. As described by Burgess and Davies-Jones, they can have a deceptively weak appearance on radar. Visual observations have suggested that precipitation from dryline storms can be quite scanty, which is consistent with their modest radar reflectivity, even at close range. However, a somewhat conflicting observation is that whatever precipitation does reach the ground often includes large hail (observations of 2 3/4 in [7 cm] hail have been recorded), even though radar echoes are not particularly strong.

The suggestion from these observations is that dryline storms, perhaps by virtue of their association with a source of dry air, have very low precipitation efficiency (see V.A

---

[10] Chisolm and Renick refer to this as a "single cell hailstorm."

[11] This name is not entirely satisfactory, for reasons which should become clear -- in the absence of a better suggestion, the name is used here, but with some misgivings.

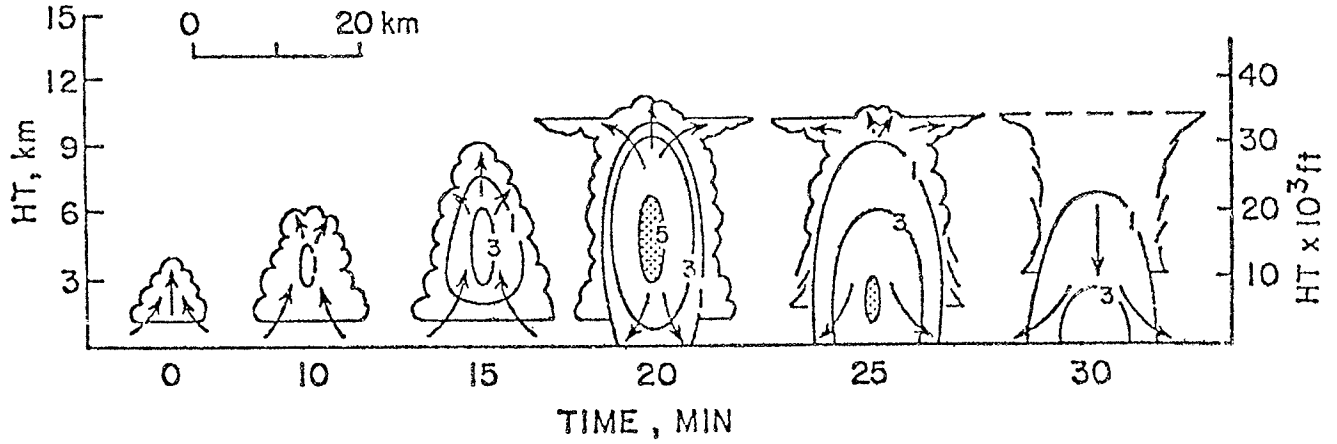

Figure 3.46a Radar depiction of an ordinary thunderstorm, showing life cycle of radar cross section. Cloud features are schematic, while contours are at VIP levels.

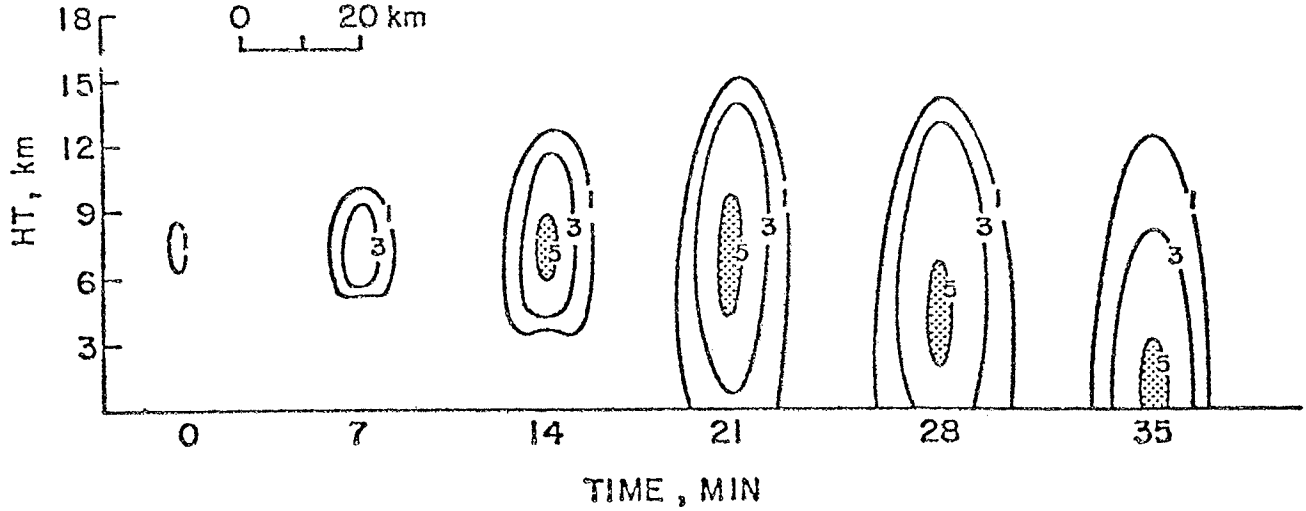

Figure 3.46b Radar depiction of a "Pulse"-type severe thunderstorm to be compared with Fig. 3.46a. Note the appearance of echo at a greater height and the maintenance of a strong reflectivity core in the descent of precipitation to the surface. Contours are as in Fig. 3.46a.

for details on this term). What precipitation that occurs seems to be falling from the anvil, well ahead of the main updraft. The modest precipitation cores may not be sufficient to produce an important downdraft (Davies-Jones **et al.**, 1976) and storm-relative flow may be weak at mid-levels, where other severe storms usually ingest dry air for downdraft production. It is quite possible that these storms are a low-precipitation version of supercells (see Bluestein and Parks, 1983).

In spite of all these apparently negative factors, dryline storms seem to have a tendency to develop strong, rotating updrafts, a characteristic of supercell storms. Further, they can produce damaging tornadoes. The absence of a strong downdraft (a) precludes the likelihood of damaging straight line winds (unless the mesocyclone in such a storm attains damaging wind levels at the surface), and (b) suggests a different mechanism for tornadogenesis, since supercell tornadoes generally are located near an updraft/ downdraft interface (Lemon and Doswell, 1979). It is not yet understood why

dryline storms show such a strong proclivity for rotation. Anticyclonic rotation has been observed, but cyclonic circulation is most common.

Note that dryline storms are often non-severe, and may only develop funnel clouds, occasionally at mid-levels (rather than from the updraft base). In contrast to pulse storms, their visual structure is the most characteristic feature, while their radar depiction seems to hold few clues (they may have a strong reflectivity gradient on their rear flank). An example of this visual structure is shown in Fig. 3.47. Note the rather small size of the updraft and the limited precipitation shaft, well removed from the updraft. Also, observe the striations in the cumuliform updraft tower which suggest a spiral nature to the apparently rotating updraft. Not all "dryline" storms have these obvious striations, whose origin is not known. Also, this case seems to have a rear flank/occlusion downdraft to the immediate left of the tornado. This storm produced two documented tornadoes and giant hail, so it is a "classical" example of a non-classical severe storm. Figure 3.48 shows a smaller, apparently weaker example -- even such small storms may produce large hail.

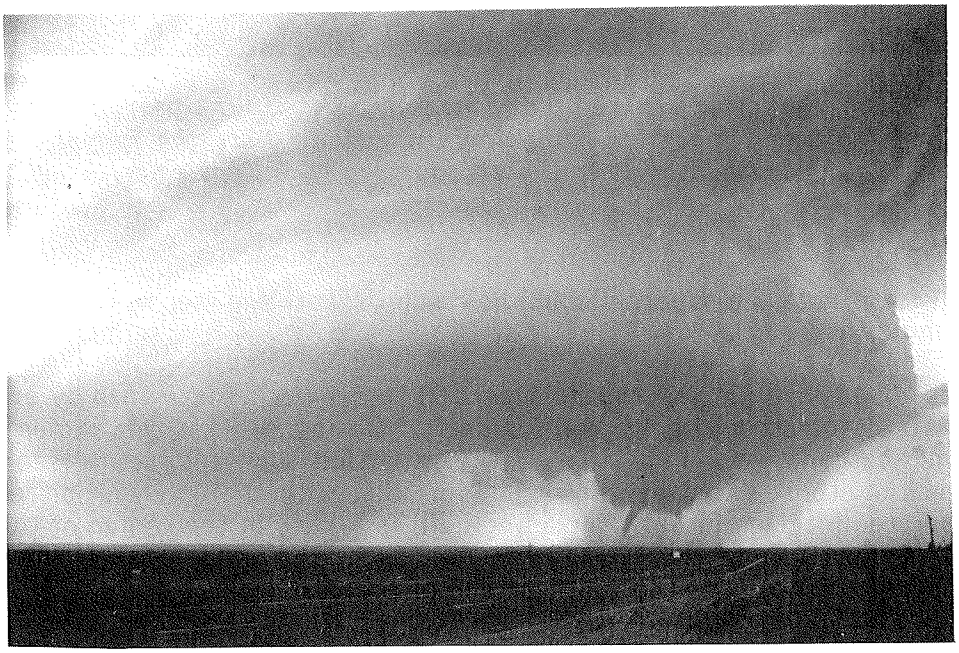

Figure 3.47 Dramatic example of a tornadic dryline storm, showing cloud structures suggestive of strong rotation (Photo courtesy of A. Moller)

While dryline storms seem to be closely identified with the dryline as a synoptic feature, not all thunderstorms which form near the dryline are of this type, nor do all such storms occur in the vicinity of a dryline. The dryline can produce the entire spectrum of thunderstorm activity, up to and including classical supercell storms.

4. "Modified" Supercells

At this time, it is not obvious whether this is a separate storm type or is simply another variation on the supercell theme (as dryline storms may well be). Recognition of this particular storm structure is even more recent than that for dryline storms (Moller and Doswell, 1985). What makes this storm interesting is that it may at times be a

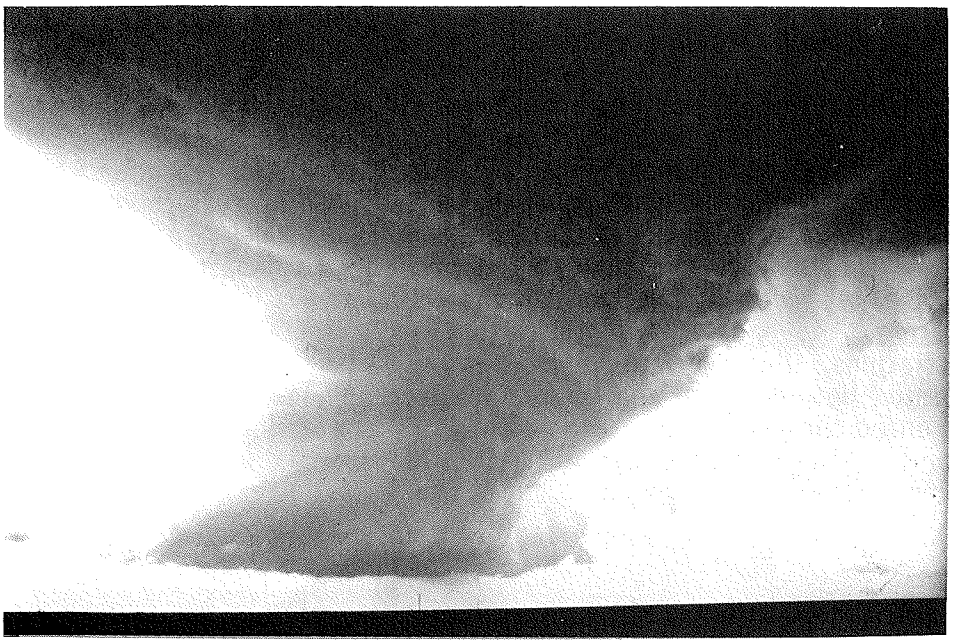

Figure 3.48 Much weaker example of a dryline storm than in the previous figure, but still showing cloud features suggestive of cyclonic rotation. Note the funnel cloud (arrow), which apparently never touched down (Photo courtesy of S. Tegtmeier).

transitional form between supercells and bow echo/squall line storms (with the transition perhaps going either way).

As discussed in E.2.c the classic supercell storm is characterized by an essentially rain-free base associated with its main updraft. Downstream of this region is the main precipitation cascade (see Fig. 3.26). The **modified** supercell storm seems to be a variation on the storm structure shown in Fig. 3.26, with the essential difference being that intense precipitation (usually including hail) is falling in the region of the rear flank downdraft. An example of this is shown in Fig. 3.49. The updraft takes on an arc shape, with new updrafts forming at the southern end of the gust front.

Because of the heavy precipitation behind the outflow, such a storm is a prime candidate for rapid acceleration of the gust front associated with the rear flank downdraft. The hook echo in these storms may be exceptionally large relative to the rest of the echo -- resulting in a more or less crescent-shaped echo configuration at low levels (Fig. 3.50a). In effect, relative to the radar echo, this storm has its updraft on its **front** side, whereas the updraft on a regular supercell is on its **rear** side. The second storm described by Weaver and Nelson (1982) appears to be such an event. Curiously,in many cases these storms do not seem to be about to dissipate, which supercells often do when the rear flank downdraft accelerates rapidly (cutting off the inflow to the updraft).

The **tail cloud** (see Fujita, 1960 and Fig. 4.32b for this accessory cloud feature) in modified supercell storms is often quite pronounced (as in Fig. 3.49) and seems to be associated with a **pre-existing** boundary. The boundary is usually one laid down by an earlier storm's outflow (as in the example shown by Weaver and Nelson; also see Bartels and Rockwood, 1983). The steadiness of this storm type may be related to the fact that they propagate along this pre-existing boundary. Tornadoes may occur at the leading edge of the gust front (which occurred in the Weaver and Nelson example) or they may

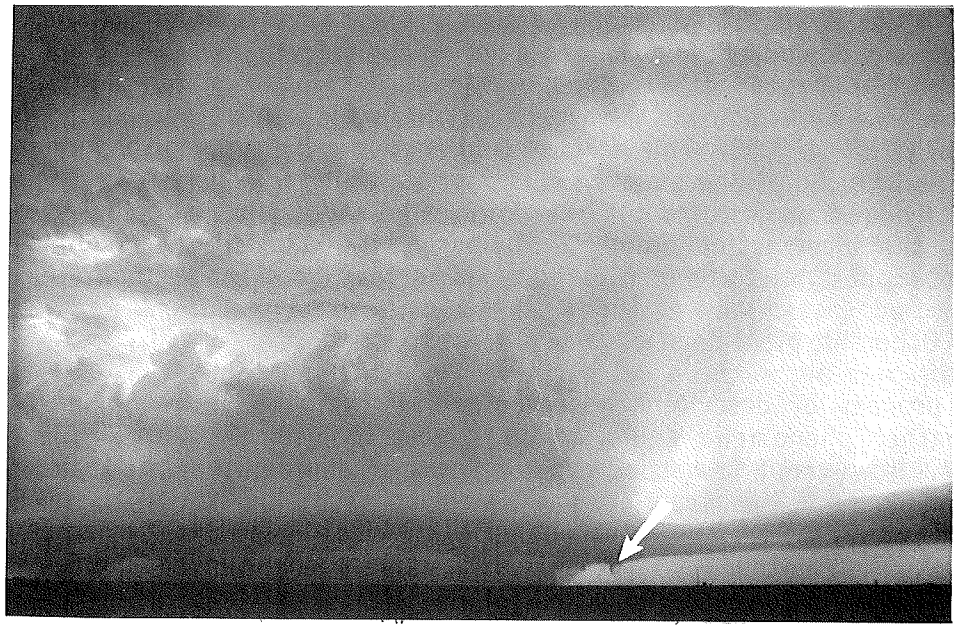

Figure 3.49 Example of a "modified supercell" — note the heavy precipitation shaft in lower left center, with cumulus towers rising ahead of the precipitation. Anvil precipitation (much lighter) is to the right. The cloud band feeding in from the lower right marks an outflow boundary from another, distant storm. The arrow points out a small funnel cloud.

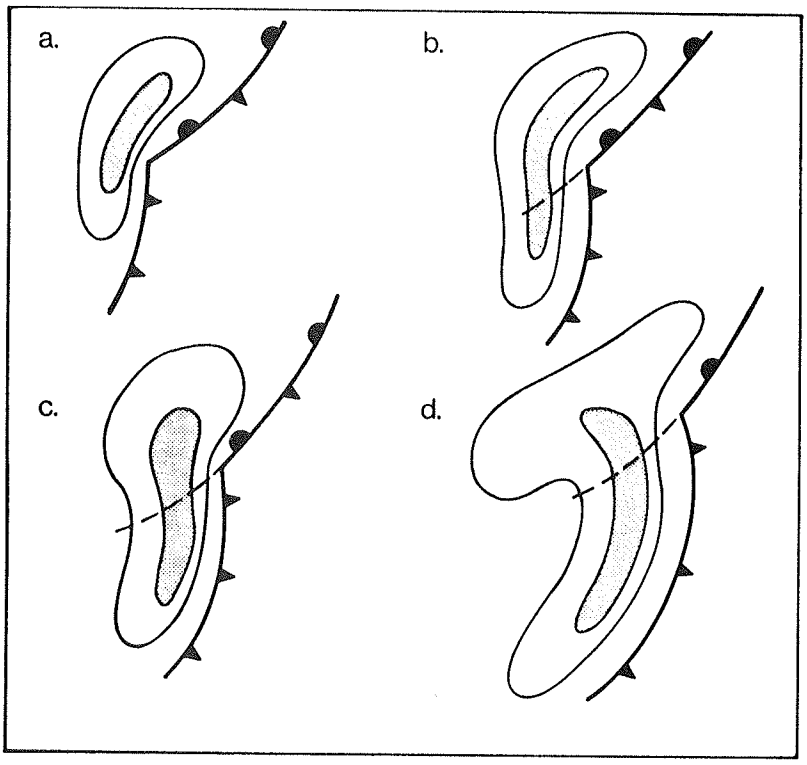

Figure 3.50 Schematic evolution (a-d) of "modified supercell" storm, showing development of bow echo structure. Contours are schematic reflectivity, with the stippling showing higher reflectivity region, while dashed line indicates location of original quasistationary boundary as storm propagates along it.

develop with the mesocyclone (which persists at the intersection of the outflow produced by the rear flank downdraft and the pre-existing boundary).

A scenario by which such a storm might evolve into a bow echo is illustrated schematically in Fig. 3.50. This process may also be applicable to the common evolution of supercells into squall line events. It is possible that the reverse evolution could occur if the rapidly-moving gust front slows down, allowing a more classical supercell to redevelop at the intersection point. Obviously, many details remain unexplained and undocumented, possibly to be elucidated by numerical storm modelling in the future.

5. Other Atypical Severe Storms

The process of describing observed storms which have been known to produce severe weather phenomena could go on almost indefinitely. One must call a halt somewhere. However, a few storm types deserve an abbreviated description.

Brown **et al.** (1982) and Caracena **et al.** (1983a) have described strong wind gust-producing storms on the High Plains. Such storms occur in environments similar to Newton's Type A sounding (see **I.II.C.1**), and the cloud base is high. In fact, the convection may appear rather ragged and weak to the observer (see Fig. 3.51) and still produce strong wind gusts. The gust potential exists because of the evaporation capacity and a nearly dry adiabatic lapse rate in the dry low-level air -- precipitation formed aloft rapidly evaporates as it descends, chilling the air and forcing further descent. If the air can continue to descend by evaporative cooling to counteract the compressional heating, strong downdrafts result. In turn, these produce the strong outflow winds.

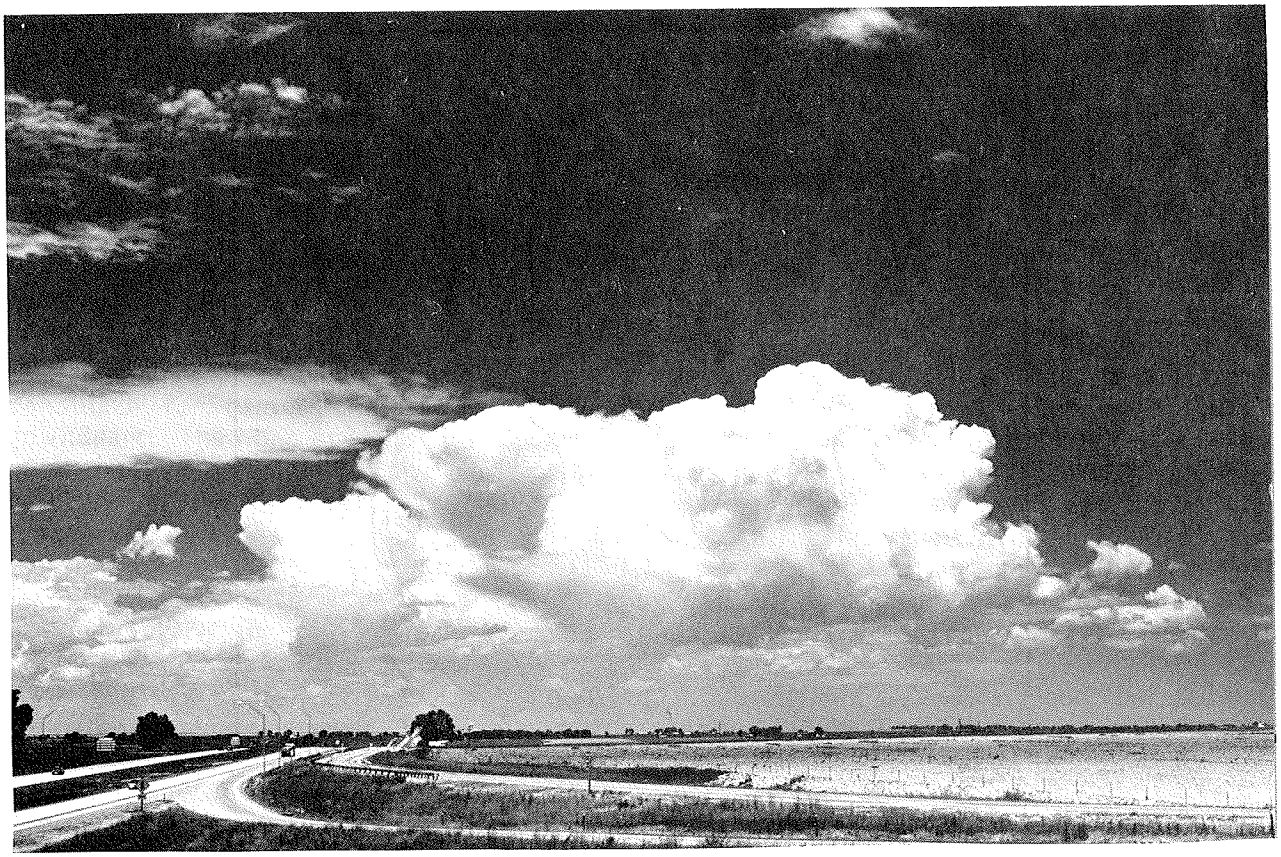

Figure 3.51 Example of weak, high-based convection which can produce microburst events in the High Plains. Note the virga falling from the nearest cloud base.

A quite poorly documented event is the production of funnels aloft and, rarely, tornado touchdowns from cumulus clouds in varying stages of development short of a cumulonimbus. Strong-to-violent tornadoes occurring with supercells typically occur only after the thunderstorm has been in existence for at least 30 min to one h. However, the towering cumulus stage of early thunderstorm development may be associated with funnel and tornado occurrence (Burgess and Donaldson, 1979). Such tornadoes are generally of lesser intensity than those associated with a mature severe storm.

Occasionally, vortex-producing cumulus clouds never go on to become thunderstorms and may not even produce a radar echo. In such cases, the tornadoes and funnels are very much akin to waterspouts, as described by Golden (1974). Other examples may occur under conditions of very cold air aloft -- the so-called "cold air funnels" described by Cooley (1978).

Besides these phenomena, there are valid observations of funnels from the weakest of fair weather cumulus (Fig. 3.52). It certainly appears that the atmosphere can create intense vortices in a variety of ways, not all of which require a severe thunderstorm. A small fraction of these non-storm-related vortices may touch the surface briefly and, hence, fit the definition of a tornado, without being very significant (except, of course, to those who might be unlucky enough to suffer damage).

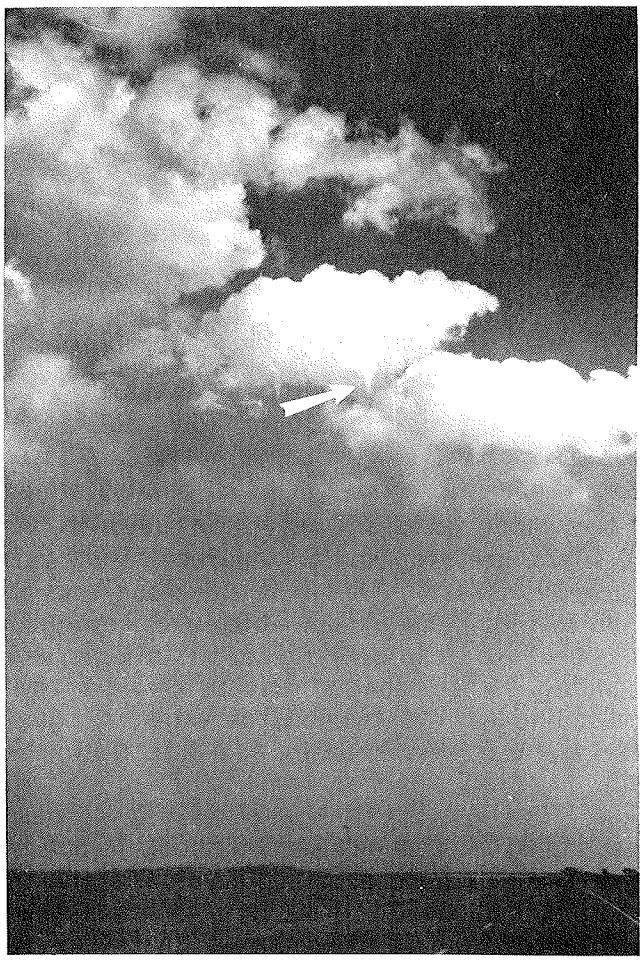

Figure 3.52 Funnel (arrow) associated with fair-weather cumulus. This event persisted for nearly 10 min.

Apart from the dust whirls beneath the flanking line of a severe thunderstorm (Lemon and Doswell, 1979; Bates, 1963), many of these "secondary" vortices occur under conditions when the analyst/forecaster is not likely to expect severe weather. One final example of a secondary type of vortex does create a problem because it occurs in association with gust fronts. Rather than being tied to a strong, distinctive cell in the line, such "gustnadoes" (Fig. 3.53) are brief, relatively weak, and not usually accompanied by a funnel cloud. Since they are so small and brief, they have not received much attention, although they might create local intensifications of damage in a basically uniform straight-line wind situation.

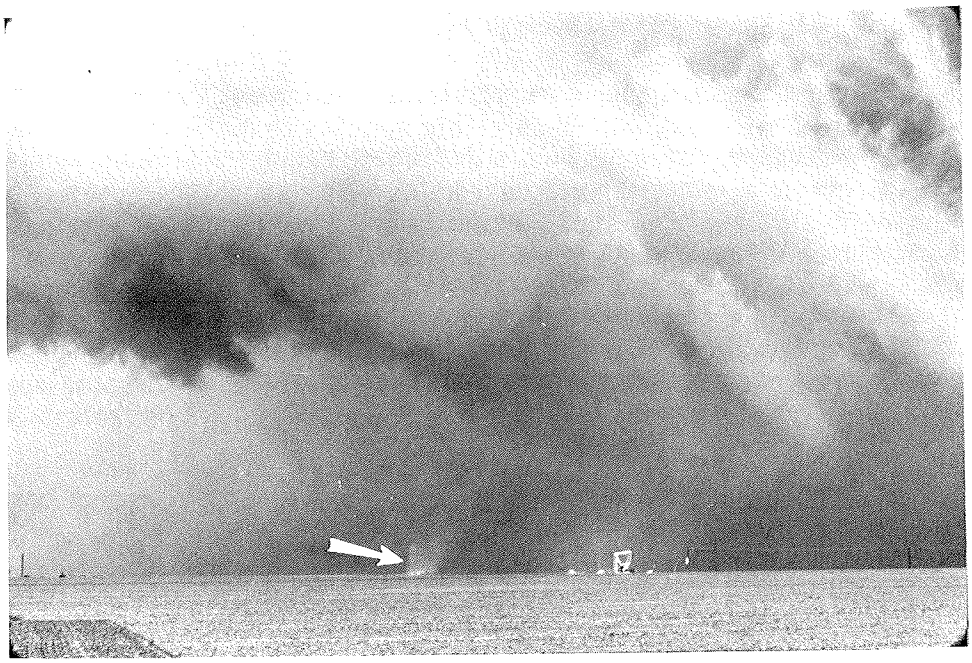

Figure 3.53 Gustnado (arrow), made visible by dust from plowed fields, associated with outflow gust front. Note the absence of a funnel and/or circulation at cloud base above the debris whirl.

It is not within the scope of this work to argue with the essentially arbitrary dividing line (or lines!) which are proposed to separate "true" tornadoes from a host of non-qualifying convective vortices. Nor is it necessary to do so. In essence, by restricting the discussion to those phenomena which are most clearly and unambiguously tornadoes, most of these problems can be avoided. As always, a void is thereby created in the reader's understanding. This probably reflects a void in the science, since there is relatively little understanding (or observations of scientific quality) available for this broader class of convective vortices. Forbes and Wakimoto (1983) have an excellent discussion on this topic.

Most of these "secondary" tornadoes are difficult, if not impossible, to forecast. However, being aware of the existence of these atypical storm types may help enhance the credibility of spotters and public observers in situations where their reports otherwise seem utterly fantastic. The probability that they will produce significant damage is extremely low, but the analyst/forecaster should recognize their known characteristics.

IV. Evolution and Character of Severe Events

> The sky had been cloudy all day, and at this time the clouds were coming from the south...and at 4 p.m. the first flash of lightning was perceptible....From this time the lightning was a continued glimmer and the thunder a constant roll....At 4:30 p.m. the rain fell in torrents, the wind blew in all directions....and showers of driving hail, of which some stones measured eight inches in circumference...While the tornado was raging here, so little inconvenience was experienced five miles to the north, from either wind or rain, that persons were able to continue ploughing during the whole passage of the storm.
>
> -- Prof. John Chappelsmith, Smithsonian Institution, "Miscellaneous Contributions for 1855"

A. General Remarks on Severe Event Climatology

In this chapter, there are three sections (IV.C.3.a, D.2.a, and E.5.a) on severe event climatology, each based on data collected at NSSFC, Kansas City. These present the data on convective wind gusts, hail, and tornadoes (respectively), using the threshold criteria of III.B.1. In order to get a perspective on these climatological results, some discussion is needed.

Many serious problems make the interpretation of the severe weather occurrence data a dangerous process. Some of these are discussed in Galway (1977, 1983), Kelly **et al.** (1978), Doswell (1980), Schaefer and Galway (1982), Grazulis and Abbey (1983), Doswell **et al.** (1983), and elsewhere. In essence, the problems boil down to this: in order to take its proper place in the climatological record, a severe event must be **observed, properly perceived** as a severe event, and stimulate the observer (or observing system) such that it is **reported** for the record.

Clearly, variations in population density have an important effect on whether or not the event is observed. It is tempting to use population data to weight the climatological records. This is not entirely satisfactory (as we shall see) for a variety of reasons. Some interesting arguments concerning the effects of population on reporting of tornadoes can be found in Elsom and Meaden (1982). Over and above the population distribution factor, events may be difficult to observe because of the time of day of occurrence, or because of the lack of appropriate measuring devices, or because of intervening clouds and/or topographic features. The presence or absence of spotter networks, as well as their training (both in recognition and in reporting procedures) can have a serious impact on whether events are observed.

The issue of proper perception of the event is a critical one. For many reasons, a truly severe event may not be viewed as significant and, obviously, a non-severe event can be improperly classified as a severe one. Virga might be reported as a tornado, a tornado may be improperly classified as a downburst, or hail size may be estimated incorrectly. Since much of our data has its origin in the observations of essentially untrained people, there is a considerable potential for errors of perception.

Beyond these problems, a properly-classified severe event observation may simply never be reported. A farmer seeing a tornado in his open field might not feel it is his duty to report it to anyone. A hail event witnessed by a law enforcement officer might never be passed on because a tornado was occurring nearby. There are a lot of things which have to be done right in order that events get reported and it is easy to envision the process working consistently better in some places (and at some times) than others.

As with perceptions about events, the lack of training (in this case with respect to procedures) which characterizes many observers can have a serious impact on the climatological record.

What is most disturbing is the lack of uniformity with regard to these factors. If everyone had the same training, and followed the same procedures, it might be possible to apply some simple correction factors to the data and have a reasonable expectation that the results would be representative of the true distribution of severe weather events. This is not the case.

These issues are compounded further by the fact that some events are more clearly **noticeable** than others. The combination of a relatively marginal meteorological event with a vulnerable human situation -- e.g. a weak tornado and a mobile home -- can make the event itself significant far beyond its **meteorological** intensity. Galway (1983) has suggested that we know far more about **killer** tornadoes, regardless of their intensity, than those which do not cause casualties. Events which produce casualties may be characterized by distorted intensity statistics, merely by the accidental coincidence of the event with a populated area. Historically, it is clear that killer tornadoes once formed a much larger percentage of the total reported, even though the population has increased steadily.

One might legitimately question the meteorological significance of a weak microburst which, by pure chance, results in a large death toll (Caracena **et al.**, 1983b). Perhaps tens of thousands of such weak microbursts occur annually over the nation. All but a very small fraction of these minimal events have very low noticeability, in keeping with their meteorological importance. Naturally, events of minimal meteorological importance can still be of great significance to individuals, on rare occasions.

For reasons obviously rooted in practicality, we end up knowing the details of only a select few, highly noticeable meteorological events. This would not be the serious problem it is if the errors made as a result were **random**. Operationally, this has serious implications. How does one evaluate forecasting methods, warning decisions, and so forth if one has, at best, a dim picture of what actually occurred? The answer seems to be: not very well. Clearly, if one's goal in operations is to improve the quality of the forecasts/warnings, then any errors in perception of the meteorological events are seriously detrimental to achieving that goal.

One also has to remember that there has been little consistency over the years in the attitudes of those collecting the data. Galway (1977) has an excellent short summary of the history of tornado occurrence statistics. Asp (1963) provides a more detailed history of tornado reporting up to 1963. The early 1950's represent a change of some importance in the collection of severe weather (especially tornado) reports. This is undoubtedly a result of the then-new Severe Local Storms Forecasting Unit (SELS). With the establishment of SELS, it became an issue of national scope to collect data for verification purposes. Also, the issuance of severe weather forecasts heightened public awareness.

Beginning in the mid-1950's, the primary responsibility for these data rested with the state climatologists (of the federal government -- see Changnon, 1981). These federal positions were abolished in 1973, with the responsibility for collecting the data passing to the staff members of the forecast offices. Because this responsibility has been **added** to their regular duties, it is difficult for them to pay as much attention to the task as it deserves.

Storm Data has provided some continuity in the record of severe weather events since 1959, although it can only be as good as the data it receives from its sources. Further, there have been episodic changes in the procedures for reporting events, which introduces some distortions in the record. Since 1981, Dr. T.T. Fujita of the University of Chicago has assumed responsibility for **Storm Data,** owing to federal budget pressures.

The reason for dwelling at such length on the quality of the severe weather climatology is that both meteorological and non-meteorological decisions are made at times, based upon that record. With all the problems, these data are all we have. If one is aware of the problems in the data, then the temptation to use it for purposes beyond its capability can be resisted. As suggested by Changnon (1982), "Let the user beware!"

Finally, all the severe weather event data used in this volume have been keyed to the **Normalized Solar Time** (NST) first proposed by Kelly **et al.** (1978). This method of accounting for the diurnal variation converts all event occurrence times to a day with 12 equal-length "hours" between sunrise (0600 NST) and sunset (1800 NST). At night, there are another 12 equal-length "hours", with a nighttime "hour" lasting (in general) a different amount of real time than a daytime "hour". This is most easily understood by examining Fig. 4.1.

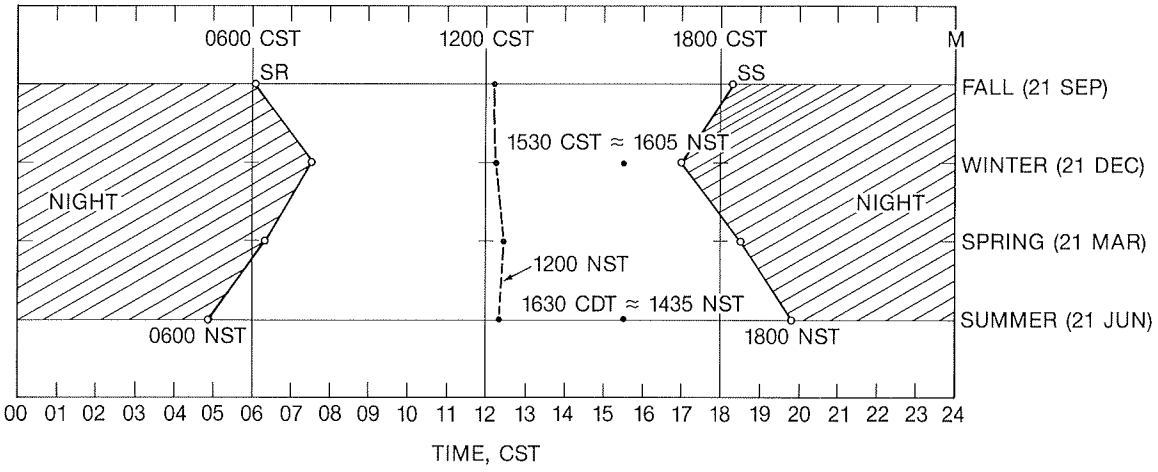

Figure 4.1 Application of NST concept to Kansas City, MO. Hatching shows nighttime hours, SR denotes sunrise and SS stands for sunset. See text for discussion.

In the example, at Kansas City, MO on the day of the summer solstice, the daylight period is 14h, 56 min long. If this is divided into 12 equal "NST hours," then each such is 74.667 ordinary minutes long. On the other hand, each nighttime "NST hour" is only 45.333 ordinary minutes. A Kansas City severe weather event on that date which occurs at 1630 CDT (or 1530 CST) converts to about 1435 NST. If it happened at 1530 CST on the date of the winter solstice (an unlikely but not impossible event!), the NST time is about 1615.

The whole point of NST is to understand the severe weather in relation to the solar heating cycle. An event at 1530 CST on the date of the winter solstice is much later in the solar day than one at 1530 CST in summer. All times shown in this volume's climatological summaries are in NST.

This chapter considers the three main classes of severe events -- winds, hail, and tornadoes. We wish to understand how these events are initiated, attain severe limits, and decay. Further, what is known about their distribution in space and time is presented, both on a climatological basis and on the scale of the storm itself. Inevitably, some historical perspective is needed in places in order to understand where current efforts are going and how the science got to where it is now.

B. Damage Assessment

1. Hailfalls

A major problem in determining the distribution of storm events lies in the area of after-the-event damage assessment. Most severe thunderstorm events of the types described in the previous sections are either unobserved at the time of occurrence, or are observed only by distraught "participants". Therefore, establishing the true pattern of events after the fact is difficult, if not impossible. Since hailstones often melt within a short time after the hailfall, the only ways to know the size of the hailstones after the fact are: have the observers place them in their freezers,[1] or accept whatever limited eyewitness reports may exist. Remember that hail damage is not always well-correlated with hailstone size. This is because most events involving giant hail (say, diameters >2 in) are characterized by relatively low numbers of the giant stones. Of course, such large stones can do spectacular damage -- penetrate roofs, perforate vehicular sheet metal, break windows, etc. Also, there are examples with relatively high numbers of giant stones, and these can be truly devastating. However, the most damaging hailstorms produce large numbers of small to moderate-sized hailstones (say, diameters up to 1 3/4 in), sometimes driven by strong winds. Crops can be completely stripped and flattened, large numbers of windows broken, trees denuded of their leaves, and so forth. Should the same storm occur over thinly populated areas, it may never be recorded. As Changnon **et al.** (1977) have noted, hail insurance claims can be quite valuable in helping understand (after the fact) the distribution of hail events, although the size distribution may not be available from such data.

2. The F-Scale System

In order to characterize the strength of tornadoes, Fujita (1971) has developed a system of damage classification which is used widely to assess, qualitatively, the speed of winds in storms. This scale has also been applied to non-tornadic damaging winds (e.g., Fujita and Wakimoto, 1981). Basically, the F-scale estimates are based on the observed effects produced by the storm. Examples used for this scheme are shown in Fig. 4.2.

This scale has been applied to most tornado events since 1916 (Fujita, 1976; Kelly **et al.**, 1978) and continues to be the standard for rating tornado intensity. Using the F-scale, one can also categorize tornadoes as **weak** (F0, F1), **strong** (F2, F3), or **violent** (F4, F5).[2]

---

[1] Hailstones to be preserved should be put into airtight containers before placing in the freezer, since ice can sublimate -- i.e., pass directly from solid to vapor without melting first -- in the freezer.

[2] No one has ever rated (or observed) a tornado of intensity greater than F5. In fact, F5 tornadoes are extremely rare events, averaging about two per year (Schaefer **et al.**, 1980a).

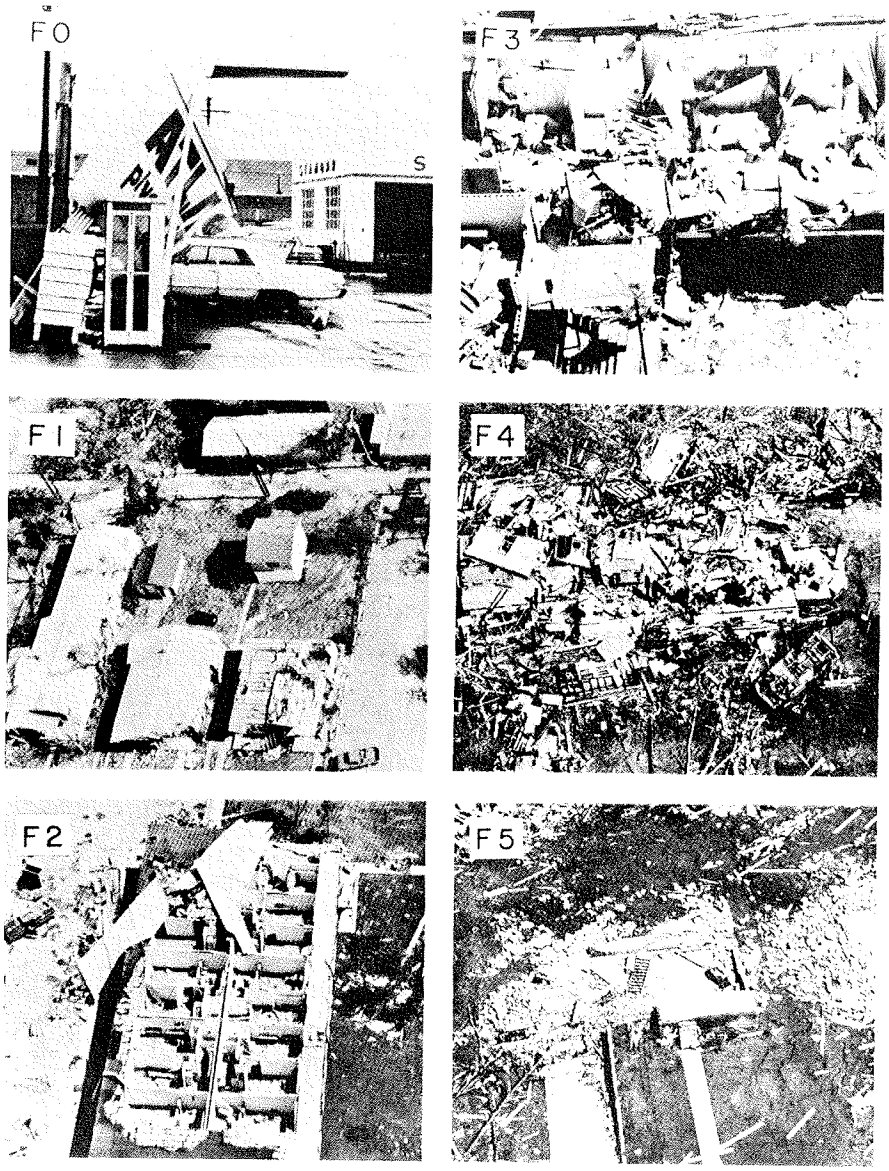

Figure 4.2 Damage intensity examples used for F-scale determination (from Fujita, 1978a).

One should also be aware of several defects inherent in this scheme. As seen in Fig. 4.2, the F-scales are based on the wind effects on **man-made structures.** This poses a problem for estimating storm strength when structures are not present, as in storms occurring over open country. In fact, F-scale data generally show that the strongest rated storms are almost totally confined to populated areas. If we reject the notion that violent tornadoes are so malevolent as to seek out cities to destroy, the logical conclusion is that F-scale statistics are heavily dependent on having structures available for the storm to damage.

Further, there is a certain amount of subjectivity and room for interpretation of the observed effects. People with nominally similar backgrounds may find it easy to differ about the F-scale of an event by as much as two F-scale numbers! Certainly, a

major factor in assessing the wind strength needed to produce a given effect is the engineering data appropriate to the structure involved (see, e.g., Marshall and McDonald, 1983). For example, a cheaply-constructed tract home may have quite different response to a 150 mph wind than one carefully engineered to be resistant to wind-loading. Many of these points are discussed in Minor **et al.** (1977) and Marshall **et al.** (1983). These factors are not always known after the storm.

Finally, it is not at all clear that the wind speed estimates attached to the F-scale numbers should be taken literally. They represent a useful relative scale but should be used with caution, especially on the high end (Minor **et al.**, 1977).

3. Tornado vs. Straight-Line Winds

Perhaps one of the most challenging tasks confronting an investigator is to decide whether the observed damage resulted from a tornado, a "straight-line" wind, or both. This is complicated by the fact that "downburst" storms (e.g., Fujita, 1978a) can produce tornado-like damage, and vice-versa.

There are several pitfalls to be avoided in making such assessments. First, one should not rule out the possibility of a tornado when there is "no evidence of twisting" in the damage patterns. A tornado's destructive power is both enhanced and diminished as a result of its forward motion. That is, the forward motion adds to the overall wind speed on the right side of the path, and subtracts from it on the left (for a cyclonic tornado in the northern hemisphere). When the rotary wind speeds are marginal for damage, this effect can restrict the damage to one side of the storm path, the right side. In such a situation, all the destruction would be the result of winds from roughly the same direction, even though the event was truly tornadic. Incidentally, the scale of tornadic rotation is well beyond that required to twist objects like trees -- one should not assume that an absence of twisted trees is an indication that only straight winds are involved.

Another error arises with a funnel cloud not in contact with the ground. In such cases, the damage can be attributed falsely to straight winds. The statement is often made that the tornado was "at treetop level" or "at rooftop level", and so could not have caused the destruction. **A tornado cloud need not reach all the way to the ground for the storm to be an actual tornado; the tornado is the rotary wind, not the cloud.** Wind damage associated with a funnel cloud is most likely a tornado, unless the events are widely separated in space and/or time.

Yet another mistake is for damage accompanied by a roaring sound to be attributed to a tornado. While not yet completely understood, the roaring sounds often associated with tornadoes are not unique to them. There are credible accounts by qualified observers that non-tornadic wind storms can also be accompanied by loud roaring sounds. While this in no way diminishes the potential threat posed by a storm which produces such sounds, it is not necessarily a tornado. This is especially pertinent for storms after dark.

When possible (as is only rarely the case), it is desirable to conduct **both** aerial and ground surveys. Patterns which are not obvious from the ground, such as the broadly diverging flows associated with downbursts, are often readily distinguished from the air. When roads are sparse, continuous damage events widely separated by open terrain are not connected easily and properly when viewed at ground level. However, details of the damage patterns which might be invisible or could escape attention from an airborne platform could be crucial in a damage assessment. For example, a house may be moved off its foundation because of inadequate attachment between frame and foundation. This might not be obvious to an airborne observer. Since a detailed survey is usually reserved

for "significant" storms being investigated for research purposes, ordinary damage assessment must limit itself to less expensive tools. This makes uneven-handed treatment of events an inevitability.

One should not be too quick to discount bizarre or unusual reports by eyewitnesses. Legitimate tornadoes can develop from ordinary towering cumulus clouds, with no radar echoes present. Also, one should be aware of "gustnadoes" -- the short-lived eddies which can occur along an otherwise straight-line wind-producing gust front. In rural areas, the populace is often a source of keen and interested weather observers, especially in places where severe thunderstorms are relatively common.

Methods for soliciting reliable reports of severe weather have been discussed by Lemon (1979). In any situation where a judgment must be made, those making it should keep in mind the nature of tornadoes (already discussed) in deciding whether or not a given event was indeed a tornado. Long, narrow paths of damage with convergent (or at least non-divergent) patterns are likely to be tornadoes (Davies-Jones **et al.**, 1978). Short, relatively wide paths with diverging patterns in the debris are likely to be downburst-type "straight-line" winds. Be alert for concentrations of intense damage within broad damage zones. These may indicate: (a) tornadoes embedded in regions of straight-line winds, (b) suction vortices embedded in a single, large tornado, (c) microburst events embedded in a larger-scale downburst situation, or (d) gustnadoes along a damaging outflow. Further, tornadoes and microbursts can occur in close proximity, with overlapping damage (Forbes and Wakimoto, 1983). Careful study may be required to decide which variation on the themes above is most appropriate.

Finally, some mention should be made of some tornado path characteristics. Since tornadoes can occur in families, it may appear that the event was a single tornado with a "skipping" tendency. It is sometimes difficult to separate true long-path tornadoes from those events with a series of short-path tornadoes produced by a single long-lived supercell. Gaps in the damage can arise from passage over open country or complexities in a multi-vortex tornado during a single continuous tornado event. What we have learned about tornado life cycles suggests that **tornadoes seldom skip.** Most times, the gaps in a long damage swath are the result of the interval between **separate tornadoes** in a cyclic tornado-producing storm (see III.E.2.c). This interval can be short enough in time and space to give the appearance of a "skip" even though it actually represents a gap between distinct tornadoes.

Unless eyewitnesses are knowledgeable, even their reports may not be helpful in resolving this issue. Apart from research-mode surveys and events witnessed by trained observers, it is probably safe to assert that errors in either direction (i.e., calling a single tornado a multiple event and vice-versa) permeate the record, contaminating the statistics (e.g., those compiled by Schaefer **et al.**, 1980b). Although the authors of statistical summaries may recognize their limitations, users of those statistics may not, so as we have said, "let the user beware".

C. Straight-Line Winds

> When I opened my eyes it was so dark I could not see the length of the deck....I now remember to have heard a strange rushing noise to windward....a flash of lightning almost blinded me. The thunder came at the next instant, and with it a rushing of winds that fairly smothered the clap. The instant I was aware there was a squall...I knew the schooner must go over....The flashes of lightning were incessant, and nearly blinded me...the schooner was filled with the shrieks and cries of the men....
> -- James Fenimore Cooper, "Ned Myers; or A Life Before the Mast"

1. Gust Fronts and Downdrafts

Strong straight-line winds associated with severe thunderstorms are nearly always generated by the outflow which occurs at the base of a downdraft. On some occasions, the inflow to the updraft may approach severe limits and produce spotty damage. However, these situations are rather uncommon and probably are limited to only a small fraction of extremely intense supercell storms.

Therefore, the mechanics of downdrafts are the primary key to the existence of strong straight-line winds. So what creates and maintains a downdraft? Since a downdraft is a form of vertical motion, buoyancy (specifically, negative buoyancy) must have a major role to play. The vertical equation of motion states that the acceleration of parcels downward (or upward) is basically equal to the negative (or positive) buoyancy -- neglecting the effects of friction. Several aspects of buoyancy have already been mentioned (in II.A.). If the parcel is not accelerated significantly[3] it is said to be in a state of **hydrostatic balance.** In such a state, the pressure gradient force upward is cancelled by the downward force owing to gravity. Changes in "buoyancy" result from changes in the pressure gradient force, since gravity is not subject to meteorologically significant change. The pressure gradient force can be altered by changing (a) the pressure gradient, or, (b) the density.

Most demonstrations of buoyancy emphasize **density** changes -- e.g., hot air or helium balloons. These two examples are the main ways to change atmospheric density: change the **temperature** (at a given pressure) or change the **parcel constituents.** Atmospheric parcel temperature changes are created by diabatic effects, and adiabatic compression/expansion.[4] In the case of downdrafts, the main diabatic temperature change mechanism is evaporational cooling. The details of this process are described by Kamburova and Ludlam (1966). They conclude that the most favorable conditions for downdraft enhancement by evaporative cooling are (a) small drop sizes, (b) large liquid water content, and (c) an environmental lapse rate close to dry adiabatic. Air descending under these conditions (neglecting entrainment) is being heated adiabatically by descent, but the majority of the heat produced is being used to evaporate droplets, so the parcel remains negatively buoyant and its descent continues to accelerate.

In analogy with updrafts (recall II.A.1.), downdraft air can continue to sink after negative buoyancy is lost. The acceleration is then upward, but the motion stays downward until the positive buoyancy can cancel all the inertia of the descent built up while the parcel was cooler than its environment. Presumably, under certain conditions, positively buoyant parcels can reach the surface before all their downward momentum is used up. This probably explains the occasional observations of "heat bursts" (Williams, 1963; Lowe, 1963; Burgess **et al.**, 1977; Johnson, 1983), in which warm outflows occur at the surface.

As already noted, a change in the water vapor content can also alter the density by changing the air's mixture of constituent gases. However, increasing the water vapor

---

[3] Remember that this does not mean there is no vertical motion. Rather, the vertical motion is not changing. For large scale motions, the vertical acceleration typically is very small in comparison to that owing to gravity. Thus, it can be neglected for many purposes, but is not truly zero.

[4] For a parcel at a given pressure, only diabatic influences can change its temperature.

content makes the air more positively buoyant.[5] Evaporation of liquid water does contribute in this way, but the effect is substantially less than the influence of the evaporative chilling. Thus, the net result is to increase negative buoyancy as long as there is a supply of small droplets to evaporate.

These are the basic principles of downdraft generation. However, as mentioned earlier, the **drag effect** of the liquid water also serves to enhance parcel descent. Since this effect is not included in the frictionless equation of motion, it is **physically** distinct from buoyancy. Even so, it may be convenient to treat precipitation drag as part of the buoyancy term (e.g., Kessler, 1969, p. 72 ff.). Physically, the motion of drops relative to the air tends to impart some of the drops' velocity to the surrounding air, since air is not an ideal fluid (i.e., without viscosity). The greater the quantity of liquid water, the greater is the precipitation drag. To the extent that the drops are small relative to a parcel, the drop size spectrum has no effect on the precipitation drag -- i.e., only the total liquid water content matters. Therefore, large liquid water contents not only contribute to the evaporative effects, but also to precipitation drag.[6]

Finally, it is possible that downdrafts (or updrafts, for that matter) can be initiated and maintained by changes to the pressure gradient. The total pressure is dominated by the hydrostatically balanced portion. By subtracting that part out, the pressure which is contributing to vertical acceleration is obtained, by definition. How do non-hydrostatic pressures arise and how large are they? The non-hydrostatic pressure gradient force is determined by specifying the change in vertical velocity, but buoyancy has a major role in determining that force. Since it is often noted that parcels in the updraft accelerate through regions of negative parcel buoyancy, there is reason to believe that significant non-hydrostatic pressure gradients can exist.

When considering non-hydrostatic pressures, it is worth observing that the term "non-hydrostatic" is somewhat misleading. That is, the condition of hydrostatic balance is most clearly associated with the environment (large-scale), while within the immediate vicinity of (and within) convection, one has **perturbations** from this hydrostatic environment. These perturbations can be broken down into **buoyant** and **dynamic** components (see Wilhelmson and Ogura, 1972 or Weisman and Klemp, 1984a). In some sense, the buoyant component can be thought of as "incorporating" the hydrostatic part of the perturbations.

The dynamic part of the perturbation pressure is complex in the atmosphere, and arises from velocity gradients in the flow. A greatly simplified form of this dynamic pressure effect is the so-called **Bernoulli effect.** The type of flow involved is steady, inviscid, incompressible, and through a tube[7] of varying cross section (Fig. 4.3). In such a limited situation, there is pressure within the fluid even when it is at rest (the so-called static pressure) and a contribution when the velocity is non-zero (a dynamic pressure)

---

[5] Water vapor molecules are lighter than oxygen or nitrogen molecules, the major constituents of dry air.

[6] Lest one doubt that precipitation drag is a real phenomenon, consider the observation of what happens if one throws a bucket of sand into the air. As the mass of sand hits the surface, one can easily observe dust being driven outward. Therefore, the falling sand particles have dragged air downward, creating a downdraft which, in turn, forces outflow at the surface.

[7] This tube need not be confined by **physical** walls. It may be a "stream tube" whose boundaries are defined by streamlines of the flow. Since such lines are everywhere tangent to the flow, the fluid does not cross them.

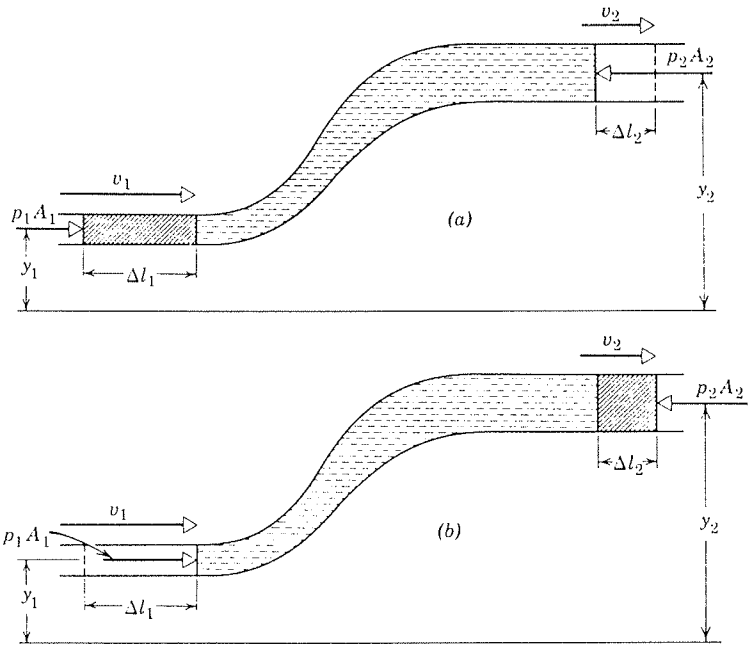

Figure 4.3 A portion of fliud (hatching and horizontal shading) moves through a tube from the position in (a) to that shown in (b) — from Resnick and Halliday (1966, Ch. 18).

which is equal to one-half the product of the fluid's density times the square of the flow speed. This effect is the physical basis for the venturis used in carburetors, but the atmosphere's flow field is more difficult to deal with.

Several authors (e.g., Newton and Newton, 1959; Alberty, 1969; Rotunno and Klemp, 1982) have considered dynamic pressures in conceptual and numerical thunderstorm models. Some of this has been mentioned earlier (III.D). Given the fact that substantial velocity gradients can arise in intense convective storms, it is not out of the question that the downdrafts in such storms may be driven (at least in part) by dynamic pressure forces.

Having developed a downdraft somewhere aloft and provided some means for it to be sustained (e.g., evaporation of rain into dry environmental air), consider what happens when it strikes the earth. Obviously, it must spread laterally. The leading edge, called the gust front, has been discussed before (see I.III.B.7 as well as II.B.3 and III.E.3.c). The stronger the downdraft, the greater the horizontal wind speeds in the outflow. As suggested by the work of Charba (1974) and Goff (1976), the outflow is not steady, but seems to pulsate with a periodicity roughly equivalent to the life cycle of a single cell. Thus, the outflow gusts may attain severe limits for only brief periods during the storm outflow. Strongest winds are likely to occur fairly early in the life cycle of the outflow, with the intensity of the outflow decreasing as it moves away from the core of the downdraft.

Note that high pressure (the "mesohigh") is typically located at the foot of the downdraft. This provides an appropriate pressure field for a diverging outflow from the downdraft base. It arises from both thermodynamic and dynamic causes. Since the downdraft generally is negatively buoyant, its greater density implies higher (hydrostatic) surface pressure. Further, since the downdraft literally reaches a "stagnation point" at the surface, there is a dynamically induced (non-hydrostatic) origin to the mesohigh as well (Wakimoto, 1982).

Available evidence suggests that a storm brings air from mid-levels (say 700 mb) down to the surface in the core of the downdraft, so the downdraft must be experiencing relative inflow from those levels. Further, the inflowing mid-level air should be potentially cold and dry, to enhance the effectiveness of evaporative chilling. Should a storm occur which has little or no mid-level relative inflow, or in environments with warm, wet air (relatively) at mid-levels, the potential for severe surface wind gusts is correspondingly diminished (although not to zero -- see Caracena **et al.**, 1983b). Further, if a severe wind gust-producing storm moves into such an environment, even when other factors remain favorable for the storm to continue, its downdraft potential decreases -- which, in turn, reduces its total potential for severity. The role of the downdraft is receiving considerable attention, and it appears that in most severe storms (putting aside some of the non-typical severe storms described in III.B.2.), a strong downdraft is associated frequently with the production of severe weather. This also suggests that strong straight-line winds are common to many severe storms, even if the wind speeds only approach, but do not exceed severe limits as defined in III.B.1.

2. Downbursts

Recently, Fujita and others (see Fujita and Byers, 1977; Fujita and Caracena, 1977; Fujita, 1978a) have called attention to what Fujita has termed a "downburst". His definition of a downburst is "...a strong **downdraft** [emphasis added] inducing an outward burst of damaging winds on or near the ground." On this basis, any damaging straight-line wind produced by a thunderstorm is a downburst. However, a downburst is not a newly-discovered phenomenon which is essentially different from the downdraft/gust front already considered. Downbursts are simply concentrated downdrafts -- "microbursts" are, in turn, concentrated (smaller-scale) downbursts (Caracena **et al.**, 1983a). Further, a definition which requires "damage" is not entirely satisfactory -- a downburst in open country over plowed fields may not produce damage, but is the same event (meteorologically) as one in a populated area.

At least some fraction of the severe storm events reported as tornadoes are, in fact, downbursts. In many cases, Fujita's recommended technique of aerial surveying can help to resolve the issue of tornado vs. down- (or micro-) burst.[8] The issue of inferring the storm type from damage patterns is considered in more detail in IV.B.3.

The reader is urged to consult the references in order to get a feeling for the observations of damaging downdraft-induced surface winds. Be cautious, however, in accepting Fujita's original hypothesis that the air which reaches the surface has its origins near the storm top. There is no evidence that the air at such high levels actually reaches the surface, even if one can draw streamlines showing descent from that level to the surface. The issue is whether the parecel **trajectories** can be traced from storm top to the surface -- and this has not been convincingly demonstrated. Rather, all available evidence suggests that the downdraft air which reaches the surface has its origins in mid-levels (see Charba and Sasaki, 1971; Browning, 1964; and Byers and Braham, 1949).

3. Distribution of Wind Gust Events

a. Climatological

When considering the climatological distribution of convective wind gust events, all the caveats of IV.A. apply. Based on the NSSFC data, the distribution of all reported

---

[8] This is complicated by the occurrence of "gustnadoes" as described in, e.g., Forbes and Wakimoto (1983).

wind events from 1955 to 1982 (inclusive) is shown in Fig. 4.4. A casual glance at this might suggest that population centers bias the data heavily: note, for example, Kansas City, MO; Oklahoma City, OK; St. Louis, MO. However, one might observe there are no such maxima at Little Rock, AR; Chicago, IL; Omaha, NE; etc. Does the absence of peaks in occurrence statistics at specific points represent some sort of meteorological reality?

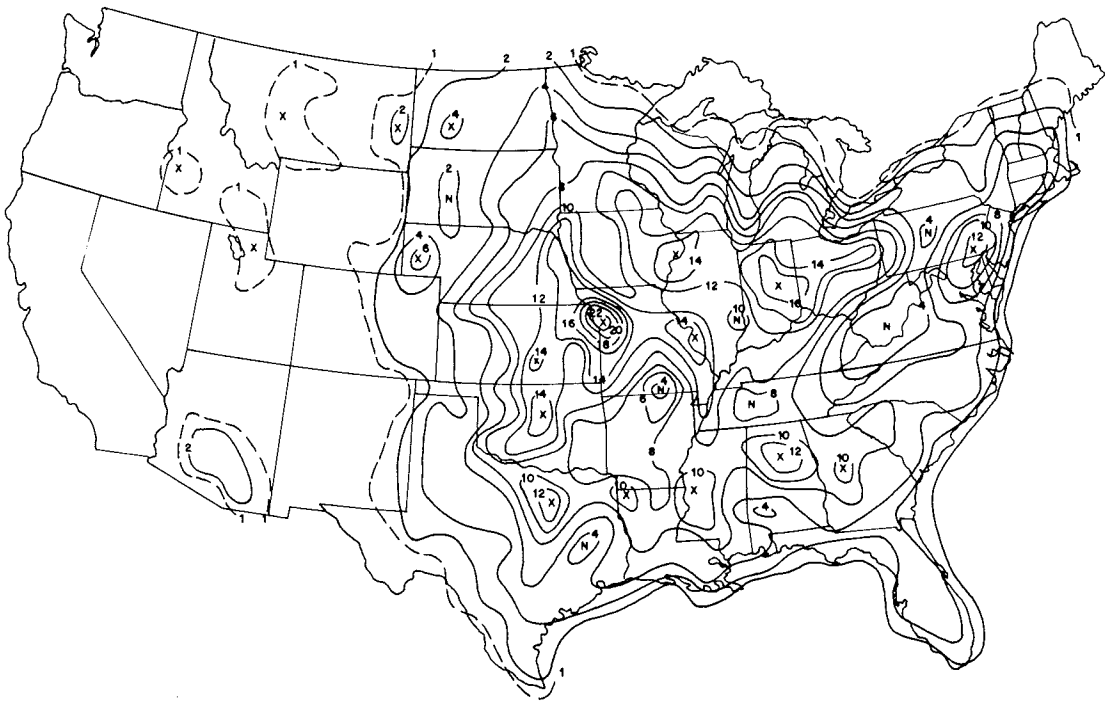

Figure 4.4 Distribution of all reports involving convective wind gusts, for the period 1955-1982 (inclusive). Contours are reports per 2° latitude-longitude overlapping square (normalized to 10,000 n mi^2), per year. Thus, a contour value of 10 means 10 reports per 10,000 n mi^2 per year within a 2° latitude-longitude square.

It should be obvious by now that it is difficult, if not impossible, to be certain. Some general features do seem worthy of mention, however. There appear to be several axes of high frequency: one running roughly north-south from central Texas to the eastern Dakotas; another trending northwest to southeast from Minnesota through Ohio (see Johns, 1982); a third which seems to pass through the northern parts of states surrounding the Gulf of Mexico; and finally, one passing along the East Coast with a prominent maximum in extreme southeastern Pennsylvania. Minima appear in Appalachia, the Ozarks, and west of the Continental Divide.

Curiously, the Red River separating Texas and Oklahoma is a relative minimum, while the Mississippi River shows as a relative maximum along much of its length. The isolated minimum in eastern Texas, as well as the one in southeastern Illinois are equally confusing, but the data do not really permit much speculation. For the eastern Texas minimum, the area is well removed from any weather office and hence, preparedness efforts are hard to accomplish. This leads to a situation with relatively few trained spotters in the area. Further compounding the problem is that the counties involved have been the responsibility of different weather offices at different times (Moller, personal

communication), owing to changes in the organization plans over the past 10-15 years. One could easily apply this sort of discussion to many of the anomalies we see in Fig. 4.4.

If we examine only those wind events which consist of measured (or estimated) wind gusts >65 kt (Fig. 4.5), the pattern is not markedly different from that of all wind events. Population centers appear prominently again, but are not identical to those of

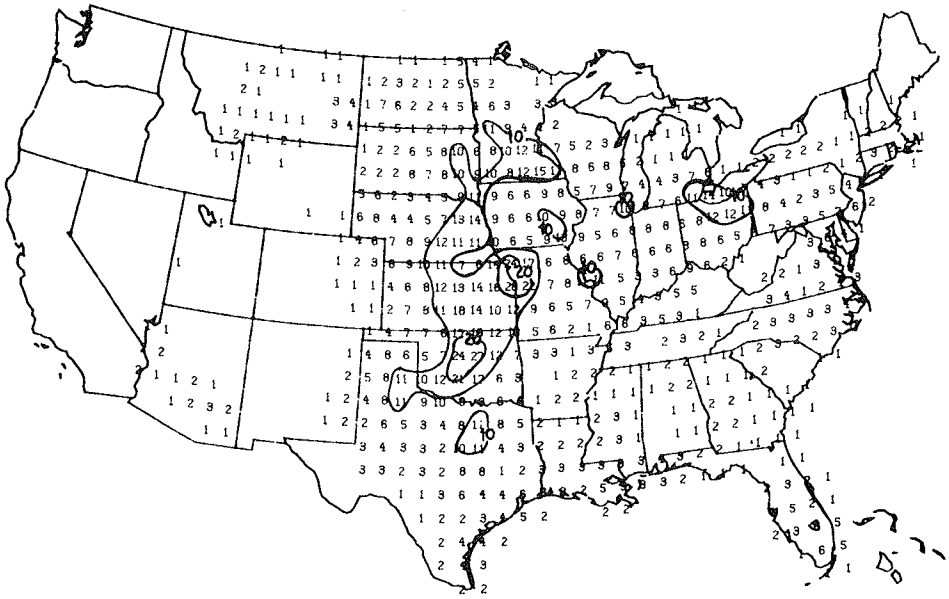

Figure 4.5 Geographic distribution of measured wind gust reports >65 kt, expressed as an annual frequency, per 2° latitude-longitude overlapping square, normalized to 10,000 mi², times ten. This should be compared with Fig. 4.4, as described in text.

Fig. 4.4. For example, Chicago, IL now appears as a maximum. One factor about the climatology shows more clearly in Fig. 4.5 than in Fig. 4.4: The axes described by Johns (1982) for frequency of northwest flow (NWF) outbreaks. One (referred to by Johns as the "A1" axis) runs from the eastern Dakotas across the Upper Mississippi Valley into southwestern Pennsylvania. The other (Johns' "A2" axis) coincides roughly with classical "Tornado Alley", running nearly north-south from eastern Nebraska to northwestern Texas. The A1 axis we see here clearly reflects the contribution of NWF events, which have a marked preference for strong convective wind reports. In contrast to NWF climatology, the A2 axis dominates Fig. 4.5, reflecting the greater overall severe weather frequency in that region. Observe that wind reports exceeding 65 kt are about 23% of wind events involving a speed measurement, but only a bit more than 7% of all convective wind gusts. If one had to make an estimate of the true percentage of wind gusts exceeding 65 kt, it is likely that it falls somewhere between these two figures.

Almost 70% of all convective wind gust reports are the non-specific "wind damage" variety. Reasons for this are clear -- only when the wind occurs at a station with wind measuring equipment can a quantitative value can be given for the wind speed.

Alternately, observers can **estimate** the peak wind speed. For trained observers, this is not too bad, but many events are reported by untrained observers who generally tend to overestimate the wind speed. The extent to which this contaminates the wind speed values given in the climatological record is not known. As shown in the Appendix, NSSFC has some fairly strict criteria for judging whether or not to log a "wind damage" report.

The diurnal distribution of wind events (with respect to NST, recall) is shown in Figs. 4.6 and 4.7. There is a broad peak in the late afternoon with a sharp drop-off after sunset. It should be noted that the percentage of reports in the "wind damage" category is slightly higher from midnight to noon, than it is after noon, but it is not known whether this is statistically significant. Figure 4.8 shows that for those reports with a speed given ("measured" means both actually measured and estimated speeds), there is some trend for the percentage exceeding 65 kt to be higher from midnight to noon. Of course Figs. 4.6 and 4.7 shows the **number** of such events to be much lower during that time. After noon, the percentage of winds >65 kt fluctuates but stays near the average for the entire day (23.2%).

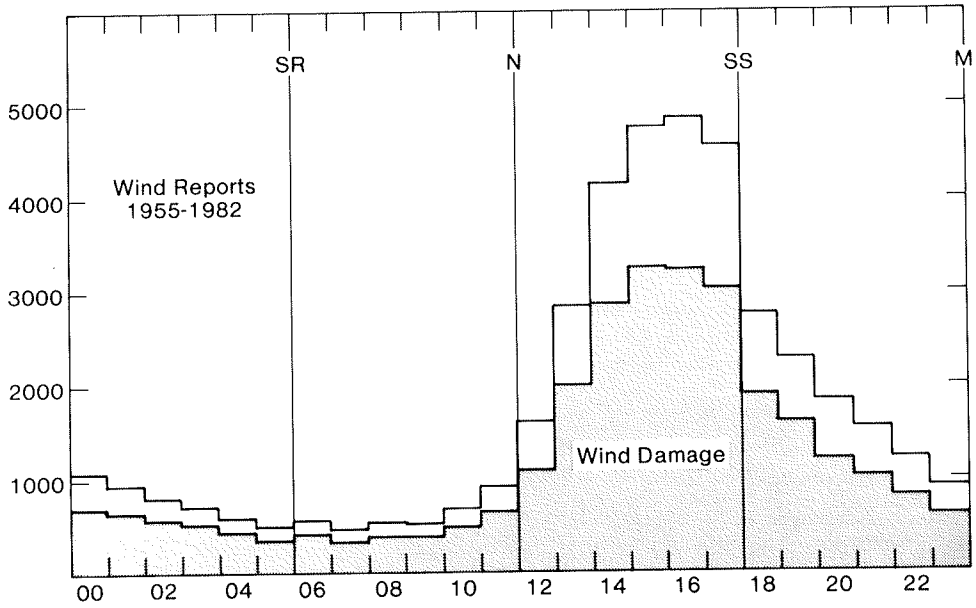

Figure 4.6 Diurnal variation of all wind reports, in NST. Letters SR, SS, M and N are as defined in Fig. 4.1.

Seasonally, convective windstorms have a broad mid-year maximum, peaking in June, but remaining high until September as seen in Figs. 4.9 and 4.10. Whereas these and Fig. 4.11 show that there is little systematic seasonal variation in the percentage of reports which are measured gusts >65 kt, there is a slightly higher percentage of "wind damage" reports in the off-season (say, October through March) than in the warm season (76.3 vs. 67.2%). Reasons for this are not apparent.

Note that the diurnal and seasonal distributions shown in these figures are for the entire conterminous United States. There are regional variations in the diurnal and seasonal distributions (see e.g., Kelly **et al.**, 1985).

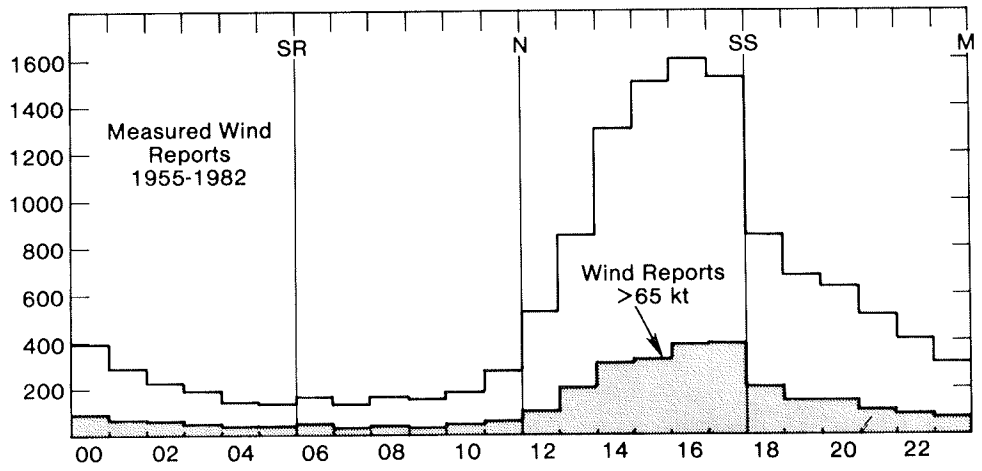

Figure 4.7 Diurnal variation in "measured wind" reports (see text) in NST. Notation as in Fig. 4.6.

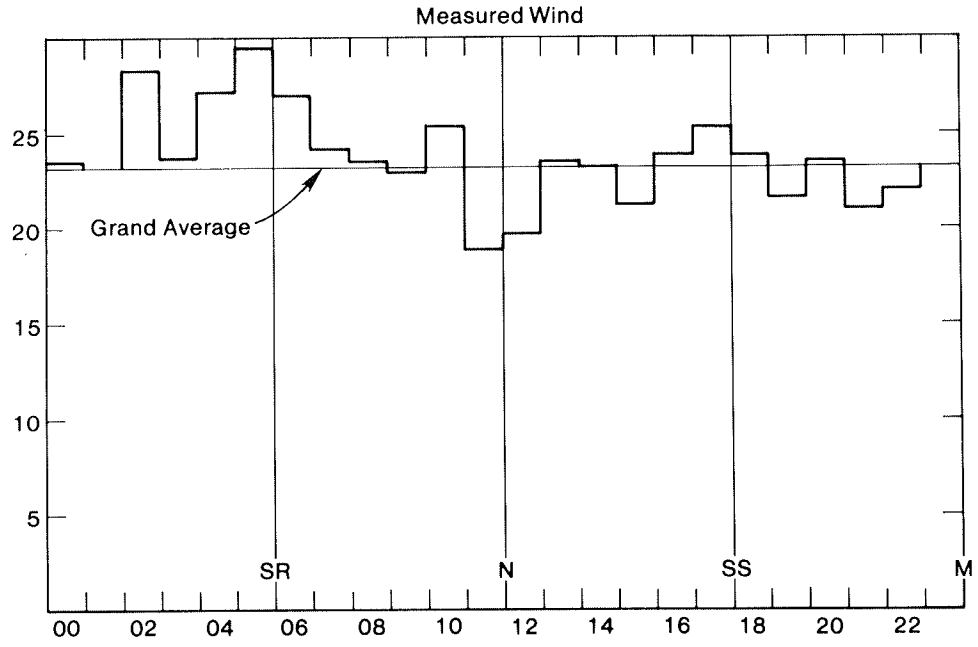

Figure 4.8 Diurnal variaton in the percentage of measured winds >65 kt. Notation as in Fig. 4.6.

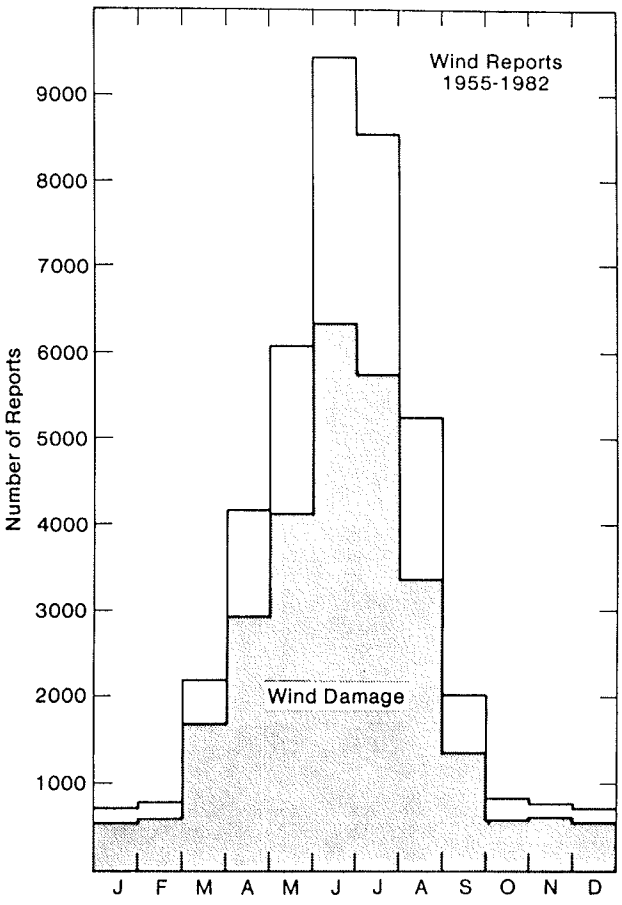

Figure 4.9 Monthly variation of all wind reports. Letters along bottom denote months.

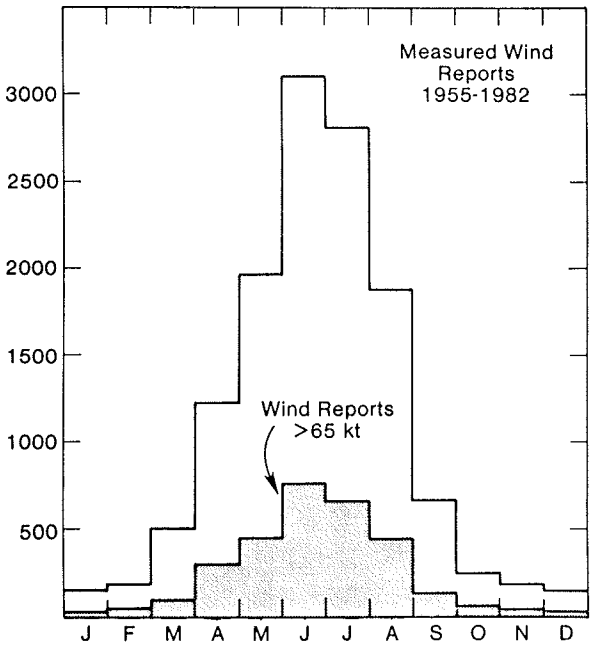

Figure 4.10 Monthly variation of measured wind reports. Notation as in Fig. 4.9.

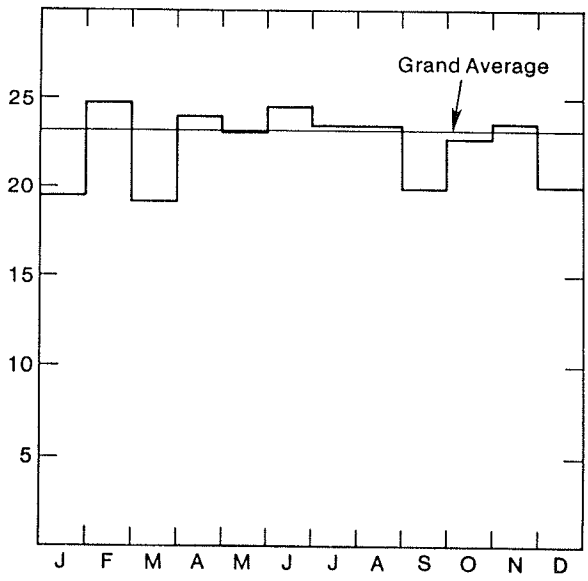

Figure 4.11 Monthly variation in percentage of measured wind reports >65 kt. Notation as in Fig. 4.9.

b. Storm-Relative

The distribution of severe wind gusts with respect to the storm has been touched on numerous times already. However, some clarification and summary is valuable here. When considering the location of events with respect to "the storm", recall that the whole storm is composed of localized up- and downdrafts -- not all of this structure is depicted in a radar display. Further, the organization of drafts is strongly dependent on the storm type. Since the most likely region of strong surface wind gusts is associated with outflow (produced by downdrafts), some review of the structures associated with different storm types is appropriate.

In general, the strongest straight-line winds are not located at the foot of the downdraft. This rather obvious fact suggests that the strongest horizontal flows are found on the **margins** of the downdraft regions, where horizontal pressure gradients are large (see e.g., Lemon, 1976a). This suggestion is also rather obvious, since pressure gradient forces are the dominant mechanism for producing flow accelerations. One should recall that the perturbation pressure maxima associated with downdrafts have both buoyant and dynamic components.

An often-used argument in explaining the outflow intensity is the combination of two processes, which add to the outflow. The argument begins with the downdraft producing some given amount of outflow. To this, so the argument goes, must be added the storm motion and any momentum transported from upper levels. These ideas are illustrated schematically in Fig's 4.12 and 4.13.

While this argument has great intuitive appeal, it is a misleading representation. It is important once again to distinguish between storm motion and air (or parcel) motion. Recall that "the storm" is most properly considered as a system, with its constituent parcels constantly changing as air flows through it. The motion of the storm is influenced substantially by accelerations imposed on those parcels by internal storm processes. Perhaps as important is the recognition that the parcel momentum contributes to, but does not totally account for, the storm motion which also includes propagation. The observed wind at the surface cannot be found in this manner.

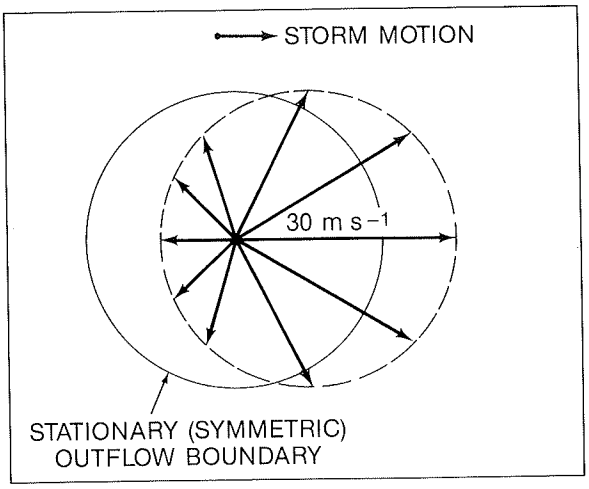

Figure 4.12 Schematic showing enhancement of outflow in the forward direction as a result of storm motion. A 20 m s^{-1} symmetric outflow for a stationary storm reaches 30 m s^{-1} on the forward edge when the storm moves at 10 m s^{-1} (see text).

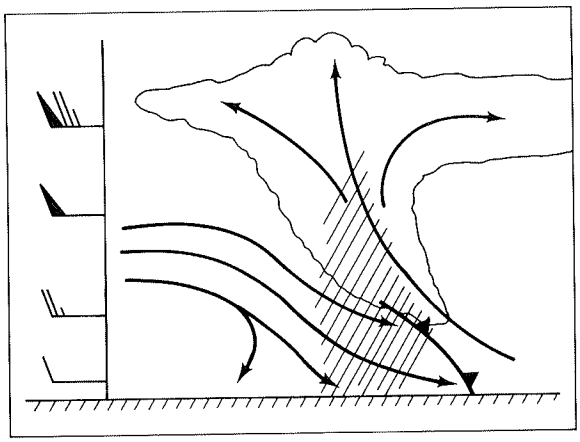

Figure 4.13 Schematic showing transport of horizontal momentum downward in the downdraft area of the storm. Wind profile is on the left, and precipitation is suggested by the hatching. The storm is moving from left to right.

If a parcel with some initial horizontal momentum is brought down to the surface in the storm, its velocity (i.e., speed and direction) past some point (which defines the wind at that point) is the result of the accelerations imposed on it during its descent in the storm. Those accelerations include dynamic pressure effects, the assorted vertical accelerations which cause the parcel to descend, and the interactions with the surface. It is not at all clear that one should have to add storm motion to parcel motion to give the parcel motion! If and when propagation effects arise, it is equally unclear that they somehow can be added to parcel velocity.

Given this situation, it should be clear that different storm types can have different distributions of intense surface wind flow. Recall that with supercell storms there are two areas associated with downdrafts. The first, located near the reflectivity core, is the forward flank, or rainy downdraft. As described by Lemon and Doswell (1979), this downdraft usually involves a mixture of mid-level and low-level air. Such a mixture reduces the overall negative buoyancy, since low-level air is generally both potentially warmer and more moist than that at mid-levels. On the other hand, the high liquid water content suggests a large contribution from precipitation drag. Most typically, the forward flank downdraft is not the region of the strongest outflow winds in supercell storms. In examples which attain severe limits, the strongest winds are usually northerly or northwesterly -- hence, arising on the southern margins of the outflow.

The rear flank downdraft generally descends with a smaller fraction of low-level air and so has a greater thermodynamic potential for negative buoyancy. This tendency is somewhat modified by the requirement for enough liquid water to provide evaporative cooling during descent. In supercell storms, the greatest potential for strong straight line winds with the rear flank downdraft is typically close to the updraft region (which is in the high reflectivity gradient region on the right flank of the low-level echo). Strongest rear flank outflows are generally westerly or northwesterly, as shown in the example of Fig. 4.14. For this example, the wind vectors have been objectively analyzed from 5 min averages at the mesonetwork sites. The unsmoothed original wind data show peak gusts in the range of 60 kt within the isotach maximum of the figure. Note also that the ouflow associated with the precipitation core is considerably weaker, along the confluence line ahead of the mesocyclone circulation.

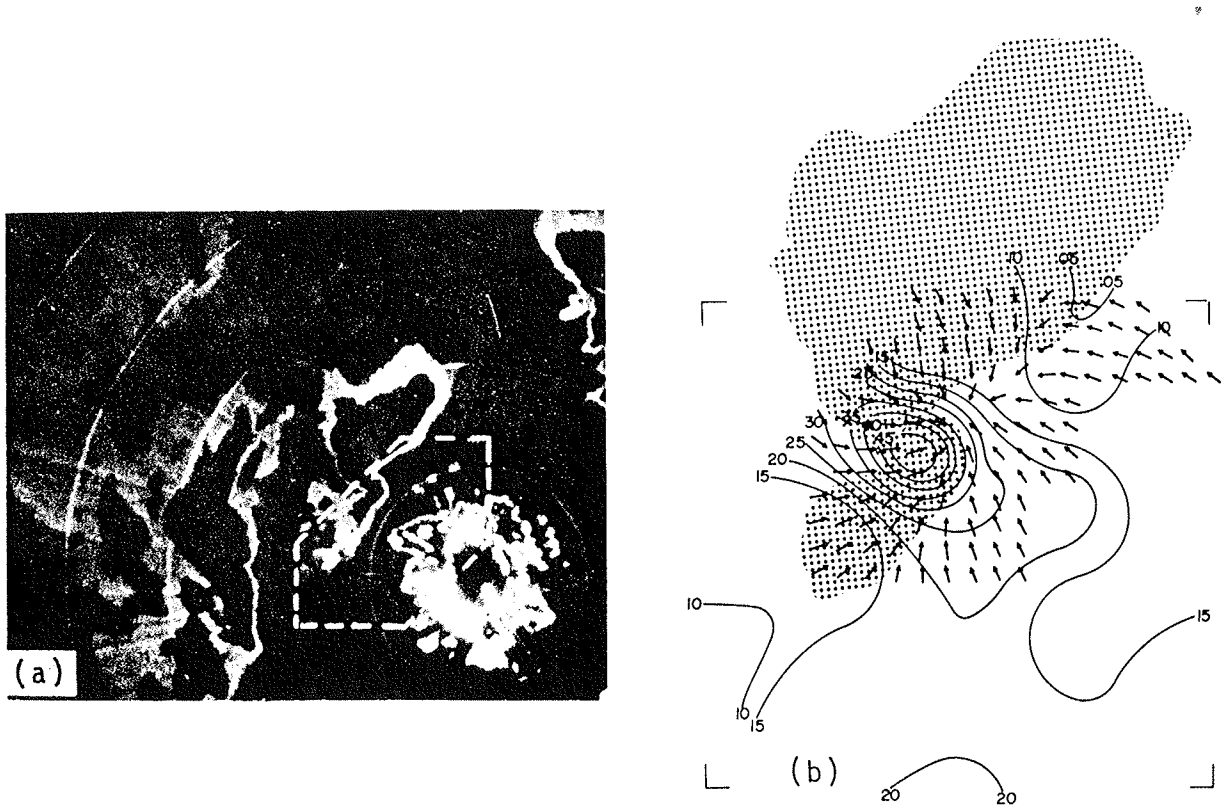

Figure 4.14 An example of supercell outflow with the rear flank downdraft showing the radar display (a) and the objectively-analyzed surface wind field (isotachs labeled in kt) for 0043 CST 30 April 1970 (from Wilk and Barnes, 1982).

At times, the mesocyclone of a supercell storm becomes extremely intense at low levels. Such a situation produces a potential for strong surface winds with both outflow and inflow. Since low-level mesocyclones are typically found on outflow boundaries, some of the air involved in the circulation has origins in the outflow -- the mesocyclone is a **mixer** of distinct air masses, similar to the extratropical cyclone. Within this class of events, a common situation is for the strongest winds produced (often northerly or northwesterly) to be on the outflow side of the mesocylone (the RFD outflow). This seems related to Fujita's (1973) "twisting downdraft". Intense surface mesoscyclones may be both philosophically and observationally difficult to distinguish from a tornado,

because the wall cloud associated with the mesocyclone can be at or very near the ground. This gives the storm the appearance of a large, turbulent tornado.

For multicellular storms, the picture is not quite so complex. There is a suggestion (e.g., Nelson, 1977) to the effect that development of a rear flank downdraft may signal the transformation from a multicellular storm to a supercell. Thus, a multicellular storm may not have a rear downdraft. However, even if a rear downdraft does exist in multicellular storms, its role does not seem so crucial as in supercells. Further, on occasions the RFD seems to overwhelm the storm, thus resulting in storm dissipation, rather than intensification. This distinction remains somewhat speculative at this writing and no completely convincing evidence is available.

Regardless, strong surface winds in a multicellular storm appear to be more common with the forward, rainy downdraft. The multicell complex tends to be less intense than a supercell and the likelihood of any weather phenomenon exceeding severe limits is correspondingly less. This is not inconsistent with the idea that multicell severe storms produce most severe weather reports, since supercells are much less common, but more likely to produce severe weather than multicell storms. Since mesocyclones reaching the surface are relatively rare for the multicell complex, the complications involved with surface circulations are generally absent.

The strongest downdrafts (and, hence, the strongest outflows) occur after the most intense updraft "pulses" have passed through the storm complex. The collapse of these strong individual cells is followed by the greatest potential for damaging surface winds. Since the updraft periodicity is on the order of 15-30 min, the accompanying severe wind gust episodes should build and wane with about the same periodicity. However, the actual surface occurrence lags the radar indications of peak updraft by perhaps 10 min. Needless to say, the temporal variations are quite rapid and may not be of significance to the analyst/forecaster as long as the complex as a whole remains strong.

The squall line type of severe storm has a dramatically different structure from supercell and multicellular storms, so the occurrence of strong surface winds is somewhat different. Since the squall line has, for many purposes, a two-dimensional character, with downdrafts behind the updrafts, the surface wind gusts are associated much more closely with the onset of precipitation.[9] Since the winds generally decrease as the outflow moves away from the precipitation area (in which the downdraft core is typically located), severe surface winds are rarely encountered when the gust front is separated from the precipitation by a significant amount. The immediate vicinity of the gust front is where most severe phenomena occur. Note, in Fig. 4.15, the general sequence of events associated with the passage of a gust front (refer also to I.III.B.7). As detailed by Charba (1974), a **windshift** is the first event. This is followed by the **gust surge,** during which wind speeds increase rapidly. Note that the initial rapid pressure rise is along the windshift, not the gust surge axis. Following the gust surge is the **density surge** which is associated with the passage of cool air. Onset of precipitation in most severe wind gust examples is within a few minutes of these events, and there may be substantial complexity to the wind structure behind the initial gust front. That is, there may be several wind speed maxima behind the leading edge of the outflow. Absolute maximum severe wind speeds are probably most frequent close to the heavy precipitation, but considerable variation from case to case can be expected. The occurrence of small-scale detail (downbursts and microbursts) can make the picture even more complicated.

---

[9] In supercell and multicell storms, precipitation from the downstream anvil may begin quite some time before any important weather events commence at those downstream points.

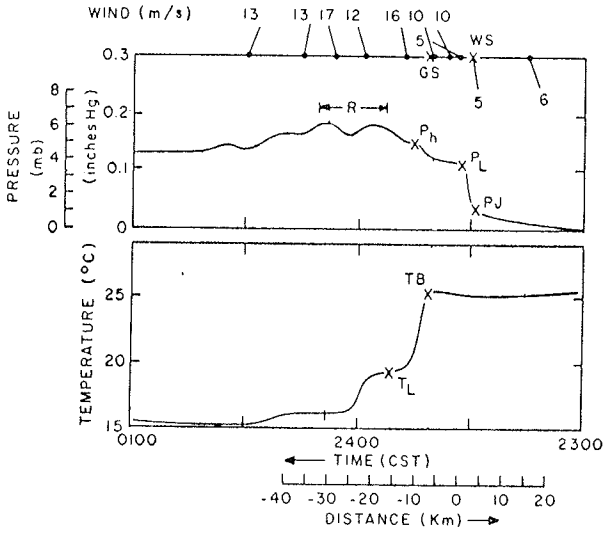

Figure 4.15 Sequence of events associated with gust front passage. The events marked have the following meanings: PJ is the pressure jump, P_L is a temporary leveling pressure, P_h is the mean pressure level following the gust front, TB is the temperature break, T_L is a temporary leveling temperature, WS is the wind shift, R denotes the period of precipitation, and GS is the gust surge (adapted from Charba, 1974).

The occurrence of severe wind gusts in "classical" squall line cases (wherein the line's two-dimensionality is high) is usually rather spotty.[10] Maximum wind speeds in such cases are not likely to attain very high values -- the severity of such storms is rather marginal. However, if the structure of the radar echoes indicates any obvious departure from a two-dimensional structure, the potential for really damaging weather is greatly increased (recall III.E.3.b). The formation of a single, dominant cell embedded in the line (or ahead of it) means that the situation has changed from essentially a squall line to a multicellular or supercell case. Formation of various radar echo structures (LEWP's, WER's, etc.) which retain the linear nature but suggest a new character are especially significant. Fujita's model of the bow echo storm (Fig. 4.16), although not fully documented in its details, seems to represent a fairly common evolution. The LEWP may represent the development of a bow echo storm within a larger scale squall line (Fig. 4.17).

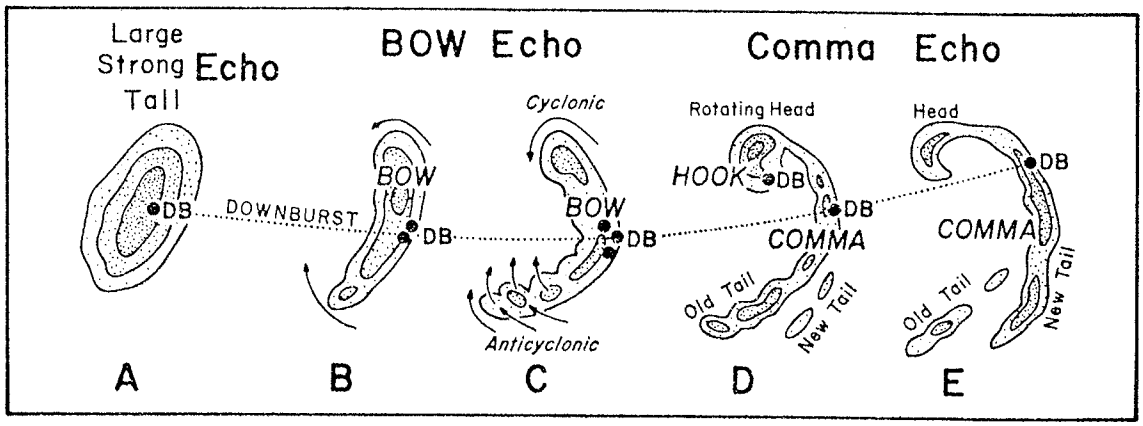

Figure 4.16 A typical morphology of radar echoes associated with strong and extensive downbursts. Some bow echoes disintegrate before turning into comma echoes. During the period of strongest downbursts, the echo often takes the shape of a spearhead or a kink pointing toward the direction of motion (from Fujita, 1978a).

[10] The damage might solely be the result of embedded "gustnadoes" on some occasions.

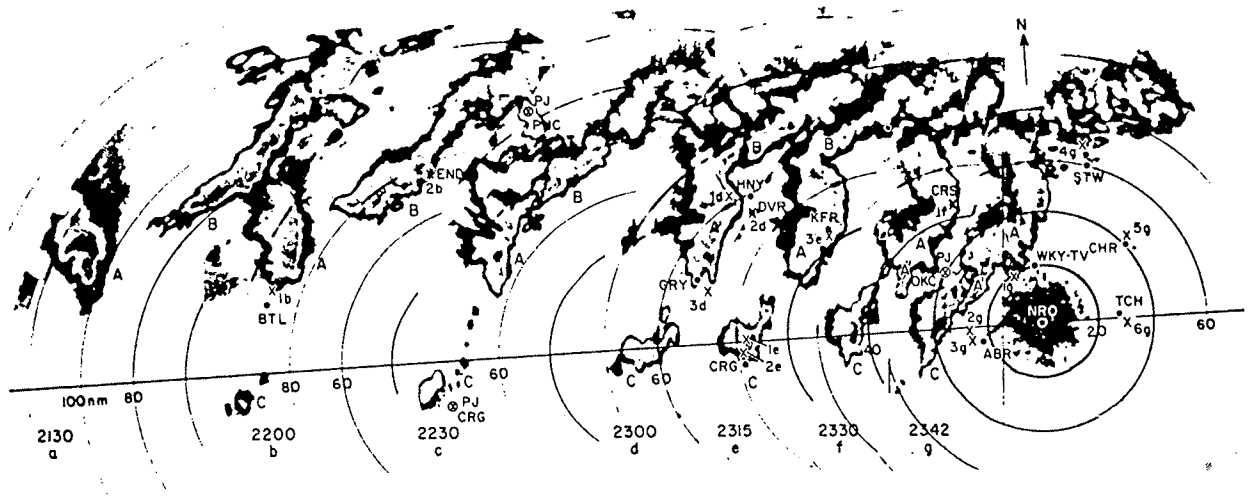

Figure 4.17 Example showing time sequence (CST) of radar echoes as a squall line on 31 May 1969 in central Oklahoma develops a bow echo/LEWP configuration (from Charba, 1972).

Finally, some mention of the strong wind gust-producing storms characteristic of the high plains in the summer is of value. These certainly contribute to the totality of severe convective wind gust reports. As pointed out by numerous authors (e.g., Braham, 1952; Krumm, 1975; MacDonald, 1976; Brown **et al.**, 1982), these are most likely under conditions of a deep, dry mixed layer and mid-level moisture (Fig. 4.18). Under these conditions, high-based (relatively weak) convection (recall Fig. 3.46) can develop and precipitate into the very unstable dry air below. This is ideal for producing intense downdrafts, as the evaporating precipitation causes the sinking parcels to be negatively buoyant for most, if not all, of the descent. What one often sees is virga, with blowing dust beneath it (Fig. 4.19) and little or no surface precipitation.

Such storms are of concern not only for their contribution to the overall severe weather threat but also because of their simplicity. In effect, the so-called "dry microburst" event is close to an idealized model of the downdraft mechanisms which operate in other, more complex storm types (e.g., supercells).

D. Hail

> Hail is ice, and water freezes in winter; yet hailstorms occur chiefly in spring and autumn and less often in the late summer, but rarely in winter and then only when the cold is less intense....Some think that...the cloud is thrust up into the upper atmosphere...and upon its arrival there the water freezes....But the fact is that hail does not occur at all at a great height...they froze close to the earth, for those that fall far are worn away by the length of their fall and become round and smaller in size.
>
> -- Aristotle, **Meteorology**

1. Physics of Hail Formation

Just as the downdraft is the central element in development of severe surface wind gusts, the updraft is at the heart of understanding hail formation. Further, just as we had to consider the microphysics involving condensed water to determine how downdrafts attain severe limits, we must examine the microphysics again to see how hail events occur. However, since hail is a condensate product, microphysics become even more

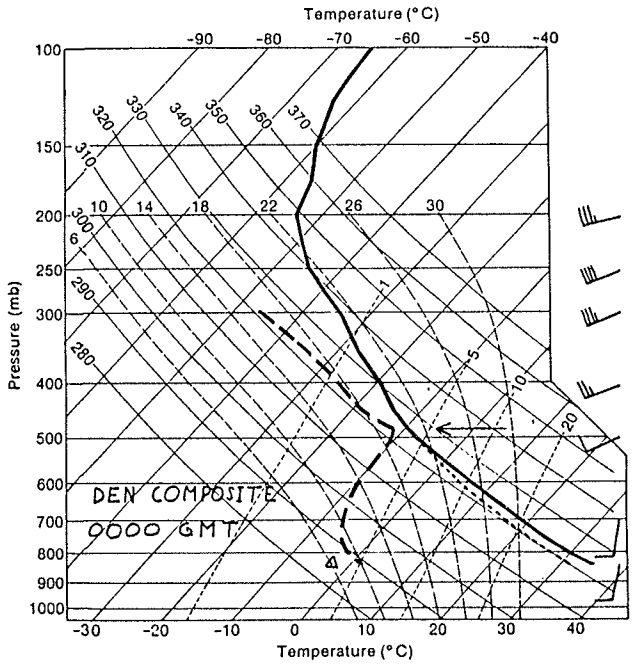

Figure 4.18 Composite sounding for Denver, CO associated with "dry microburst" events (from Brown ***et al.****, 1982).*

Figure 4.19 Virga descending from high cloud base and blowing dust beneath associated with a microburst event (photo courtesy of E. Szoke).

important. The production of hail illustrates most vividly how the dynamics and kinematics of the storm structure interact with the microphysics. Details of that interaction are not understood fully, of course. A central question concerns the necessity for the particles which become hailstones to be **recycled** -- i.e., to be raised and lowered several times within the storm. Such a concept comes reailly to mind when one examines cross sections of hailstones (Fig. 4.20). The recycling hypothesis is a natural idea for explaining the different growth modes implied by the "growth rings".

Clearly, the size and weight of observed hailstones imply a large terminal fall velocity. In order for a hailstone to grow to a given size, an updraft speed roughly equal to (or greater than) the stone's terminal fallspeed must be present. Otherwise, the stone would fall through the storm before it could grow to its observed size. Of course, a stone can grow as it falls but this is limited by the height of the freezing level. It is difficult to see how much additional growth could occur as the stone finally descends. Using Nelson's (1980) formula for the terminal fallspeed over a range of hailstone diameters from 5 mm to 10 cm results in the graph of Fig. 4.21. Note that there is some evidence that for very large stones, say 4 cm or larger, there is an abrupt reduction in drag (Young and Browning, 1967). This results in higher fallspeed estimates, as shown. It is likely that the physics of falling hailstones is much more complex than suggested by this simple graph. For instance, most hailstones are not perfectly spherical. However, these values are likely to be at least representative for most stones.

Peak values for a 10 cm (~ 4 in) diameter stone range from 40 to 60 m s^{-1}. These correspond to a rough lower bound for the speed of the updrafts involved. As we have

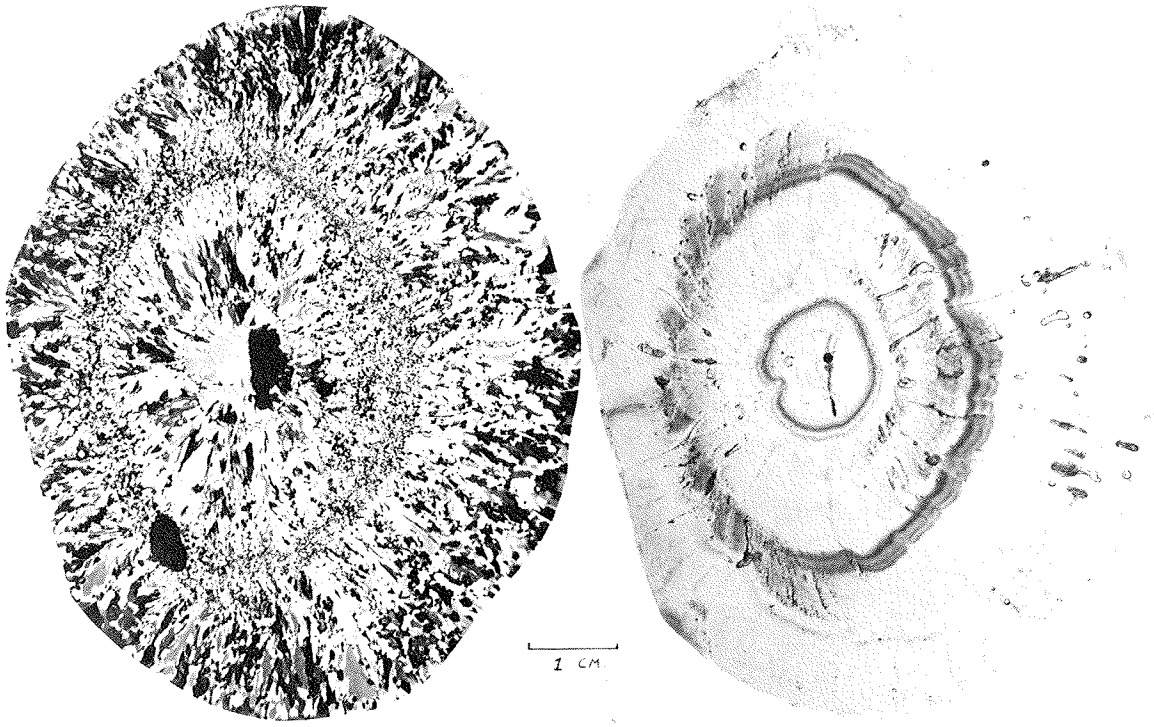

Figure 4.20 Cross sections of hailstones in polarized (left) and ordinary (right) light. Crystalline structure shows clearly in section viewed through crossed polaroids — note relationship of crystal size to visible layer structure. Stones fell at Iraan, Texas on 6 May 1968 (photo courtesy of N. Knight).

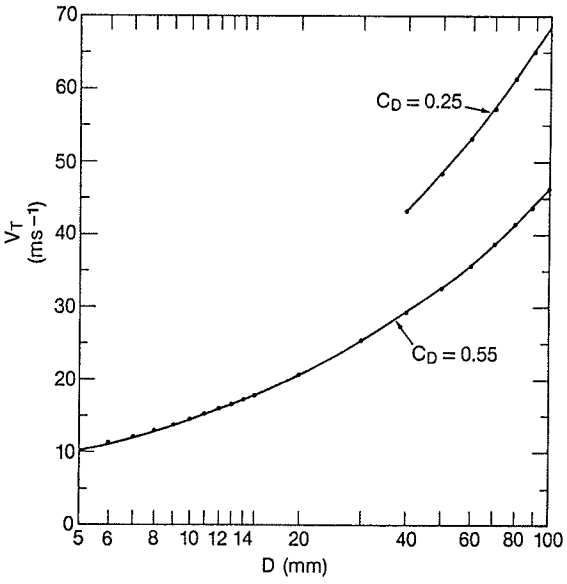

Figure 4.21 Graph of terminal velocity (V_T) as given by equation in Nelson (1980). Note difference in V_T for different drag coefficient, C_D (see text).

seen, such strong updrafts may exist during the storm. Note that 40-60 m s^{-1} updrafts are within the limits described by Davies-Jones and Henderson (1975), using rawinsonde ascent rate data.

An excellent summary of hail growth studies is found in Nelson (1980), and in the literature he cites. Certain key concepts which Nelson discusses are valuable in understanding how hailstones grow. Knight and Knight (1970) have indicated that a hailstone's origin is with an embryo: either a "frozen drop" or a graupel particle[11] with a diameter of roughly 5 mm. While the origins of these embryos are still not entirely clear, it should be noted that the "frozen drop" is somewhat larger than the largest raindrops (typically 1 to 3 mm in diameter), so it is not clear that its production is as simple as the freezing of a raindrop.

Concentric rings observed in hailstones are generally considered to result from changes in the mode of stone growth -- i.e., whether that growth is "wet" or "dry". As Nelson (1980) describes it:

> The concepts of wet and dry growths are associated with one of the most critical hailstone growth factors -- the heat budget. Hailstones grow mainly by accreting supercooled water. Heat release associated with freezing this water is quite substantial. If the hailstone can dissipate all this released heat, then dry growth occurs. Any net heat gain merely raises the temperature of the hailstone's surface. If, however, all the heat cannot be dissipated, the hailstone surface temperature remains at 0°C and some accreted water remains unfrozen. This unfrozen water may either be shed or remain with the hailstone in cavities.

It might be natural to assert that this alternation in growth mode is the result of numerous recycling passes -- up within the updraft, falling outside the updraft core to much lower levels, and being re-entrained into the updraft to rise again. This idea has held sway for a long time [see, e.g., Ludlam's (1963) Fig. 11, showing the trajectory of a hailstone].

---

[11] Graupel is a snow pellet (Huschke, 1959).

Recently, the recycling hypothesis has come under scrutiny. Nelson's (1980, 1983) results suggest quite clearly that the growth mode can alternate without calling upon recycling. In essence, the major environmental (i.e., within the storm) factors which determine the growth mode are the temperature and liquid water content. It appears that minor variations in position of the stone (while remaining in the updraft), combined with the local changes of the environmental factors superimposed on the basic updraft, are sufficient to produce alternating growth modes. Showing that it is possible to dispense with the recycling hypothesis is not by itself sufficient evidence to reject it entirely, but it is certainly a substantial result.

In any case, recycling continues to be a candidate for explaining the origin of embryos, although Miller and Fankhauser (1983) have even suggested that embryo origins need not incvolve recycling. As noted by Ludlam (1963), a small droplet (i.e., a cloud particle) is carried upward through the growth zone (where updraft water is mostly supercooled -- say, from -5°C to -25°C) too rapidly to reach observed embryo size. Such a growth zone is likely to be only a few km deep, through which a small drop might be carried in about a minute or two. Apparently, it is not possible to produce a large enough droplet in one pass through the updraft, starting at cloud base.

Nelson (1983), Browning and Foote (1976), Heymsfield **et al.** (1980), and Browning (1977) have suggested that embryos may fall into the growth zones from above by being ejected at higher levels and falling into the updraft (forming an "embryo curtain" -- see Fig. 4.22) -- this is a modified recycling concept. Nelson also speculates that flanking line updrafts may produce embryos which can be injected into the main updraft. According to Nelson, the main embryo type from either of these injection mechanisms should be graupel. However, the observations suggest that many, or perhaps the

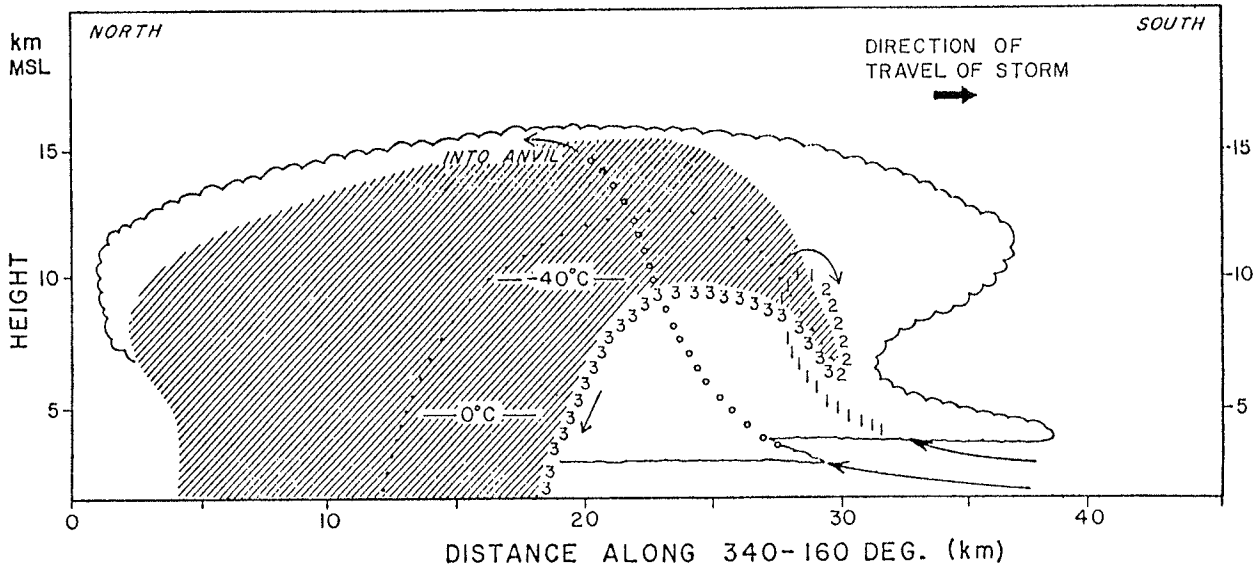

Figure 4.22 Schematic model of hailstone trajectories within a supercell storm. Trajectory with numbers 1, 2, and 3 along it shows the three stages in the growth of large hailstones, with 1 and 2 corresponding to the embryo stage. The "embryo curtain" is the finger of echo (hatching) where hailstone embryos reside and may be recycled before beginning their rapid growth into large stones (from Browning and Foote, 1976).

majority, of giant hail embryos are "frozen drops" (Knight and Knight, 1974). It may well be that some graupel particles fall far enough to melt before being refrozen on their way back up. The details are still not yet clear and this area -- embryo origins -- remains an active topic of research (Knight, 1981).

Small scale variations of updrafts can have an important effect on the distribution of liquid water and, hence, on the stones within the overall updraft region (see II.C). Strong updraft cores, associated with weak echo regions on radar, have low liquid water contents (for reasons already discussed). Above these regions, rather large reflectivities (and liquid water contents) are found -- when the weak echo regions are bounded, higher liquid water contents surround the updraft cores. Observations (e.g., Wilson and Fujita, 1979) with vertically-pointing radars suggest that details of microphysical and dynamical importance exist in the draft structure of storms on scales below the resolution of horizontally-scanning radars (also see Battan, 1980). Analysis of this fine structure awaits higher resolution sensing methods. However, the indication is that knowledge of these details might help explain the observed characteristics of hailstones.

Hailstone size provides a rough indication of the storm's updraft strength. However, hail production is sufficiently complex that the mere possession of a strong updraft is not adequate to ensure that a given storm will produce hail. In fact, Nelson (1983) has suggested that the violent updraft in some supercells actually **inhibits** giant hail formation. Further, there is not sufficient information in conventional or research data to predict whether or not a given storm will produce hail. Operationally available data certainly do not allow the accurate prediction of the size or the quantity of hail produced (see I.II.C.2, esp. Tables 2 and 3). In other words, there is a loose association between updraft strength and hail size. If one accepts the idea that storm type is related to the environmental wind shear, one must infer that hail is related to wind shear, because hail seems quite definitely related to storm type. Beyond these notions, current understanding simply does not have much to add.

Numerous efforts are underway (Eccles and Atlas, 1973; Srivastava and Jameson, 1977; and Barge and Humphries, 1980) to develop methods for hail detection via radar. Reflectivity, per se, is not sufficient, as suggested by the occurrence of large hail in dryline storms which have modest peak reflectivity. Further, the existence of high reflectivity does not guarantee hail occurrence. Note that large hail should not melt significantly during its descent, since large hailstones have such high fallspeeds. Smaller hailstones may depend on an appropriate local temperature environment during their descent in order to reach the surface before melting. It seems plausible to use storm structure as seen on radar, especially those features associated with supercell and multicell severe storms to identify potential hailstorms (Lemon, 1978). It also appears that research into remote sensing methods is going to provide some useful approaches for operational hail detection (e.g. Jameson and Heymsfield, 1980).

2. Distribution of Hailfall Events

a. Climatological

Broadly speaking, the annual hailfall distribution (Fig. 4.23) is similar to that of convective wind gusts (Fig. 4.4). However, there are some clear differences which one should note. For one thing, the overall frequency is lower for hail than for wind (26,838 vs. 41,455 total reports). Another noteworthy change is that hail is much more clearly confined to the Central and High Plains, west of the Mississippi River. All the axes described in the section on wind events (IV.C.3.a) are present, but the dominant one is that running north-south. Further, there is a clear high plains maximum (along the Front

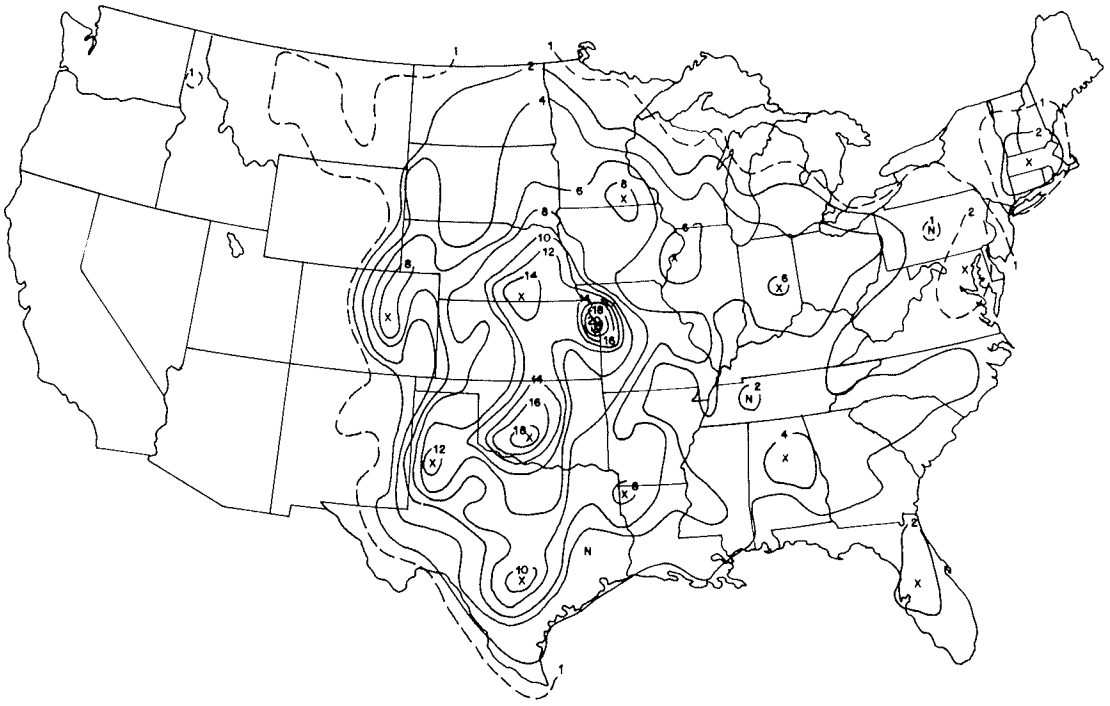

Figure 4.23 As in Fig. 4.4, except for all reports involving hail.

Range in Colorado) which is only marginally present in the wind climatology. As with wind, the population centers are obvious, especially Kansas City, MO (again!).[12]

If one restricts attention only to hail reports >2 in (Fig. 4.24), perhaps the most obvious contrast in pattern with Fig. 4.23 is that the Kansas City maximum has disappeared. Note also that the prominent peaks in eastern Colorado and southern Texas have also diminished. Of all the hail reports >3/4 in, only 4895 (~ 18%) have diameters >2 in. Further, while Fig. 4.23 has some suggestion of Johns' A1 high frequency axis (Johns, 1982), there is little or no indication of it when considering hail >2 in. Thus, NWF outbreaks seem to have relatively little likelihood of producing giant hailstones.

In the area of diurnal variation (Fig. 4.25), hail shows the typical late afternoon peak and steep decline after sunset. Recall that there are regional variations in the diurnal (and seasonal) distributions. Interestingly, the percentage of reports >2 in, as shown in Fig. 4.26, reveals that giant hail is predominantly a late afternoon event, on a percentage basis, as well as in absolute numbers. Recall that for wind reports, there was some tendency for early morning measured wind gusts to show a higher percentage of speeds in excess of 65 kt. Very little of what hail falls in the "off-hours" is >2 in. Note that NSSFC logs almost no non-quantitative hail reports (see The Appendix). In contrast with winds, it is comparatively easy to estimate hail size, even for an untrained observer. However, untrained observers do often report hailstone circumference rather than diameter, which can create some confusion and errors in the record.

---

[12] It is readily apparent to me that Kansas City, MO is **not** the non-tornadic severe weather capital of the country! While the data suggest it, and it is not obvious how to disprove it, my experience rebels at this conclusion, and one should not take these data literally. Rather, they serve to illustrate the problems.

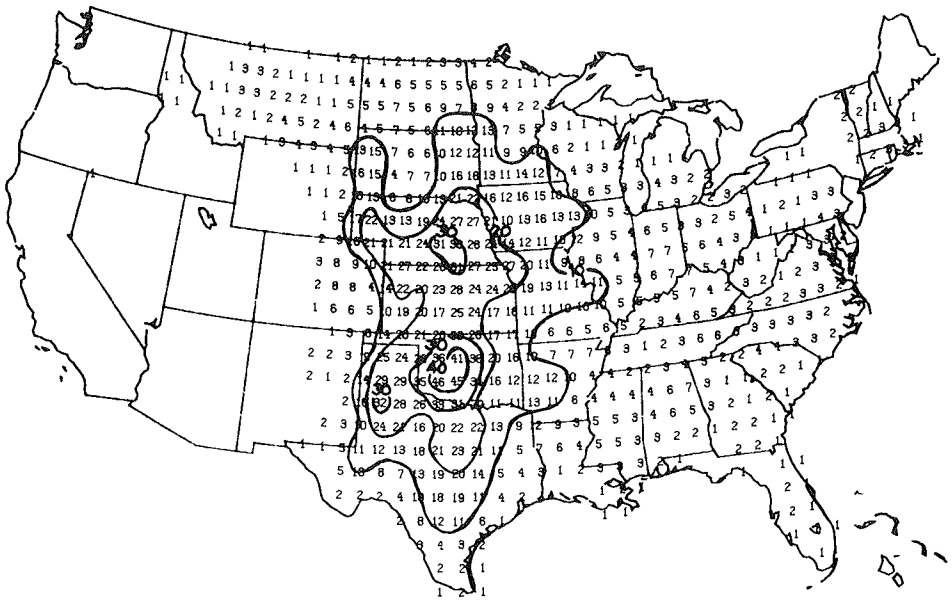

Figure 4.24 As in Fig. 4.5, except for hail events >2 in.

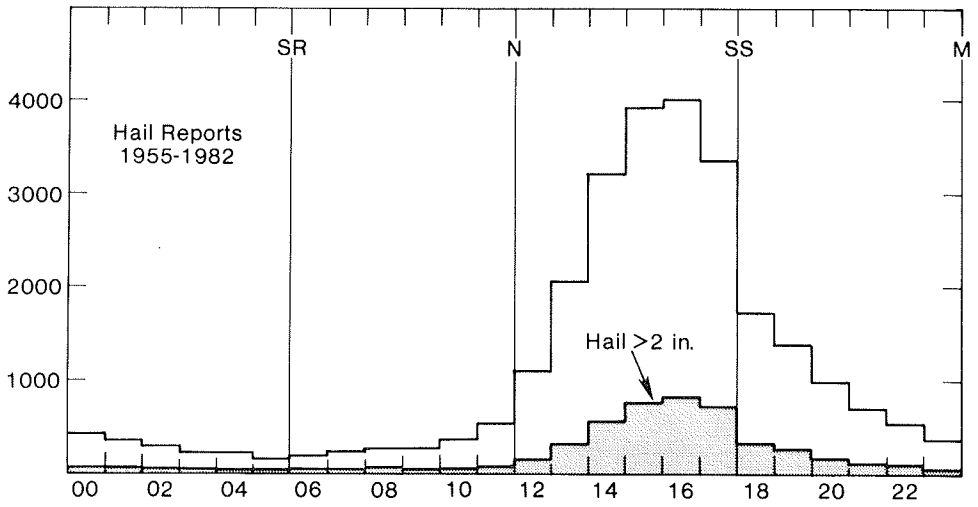

Figure 4.25 Diurnal variation of hailfall reports, in NST. Notation as in Fig. 4.1.

The seasonal peak in hailfall events, shown in Fig. 4.27, occurs earlier than for wind events, with May representing the absolute peak, and June not far behind. The amount of summer hail (July through September) is declining markedly through the season. As with the diurnal variation, the really large hail is confined to the seasonal peak period, with relatively little of the "off-season" hail getting to large size (Fig. 4.28).

b. Storm-Relative

The basic physical processes governing hail formation suggest that hailfalls reaching the surface do so in the precipitation cascade region of the storm complex. This area is generally **ahead** (with respect to storm motion) of the updraft core for

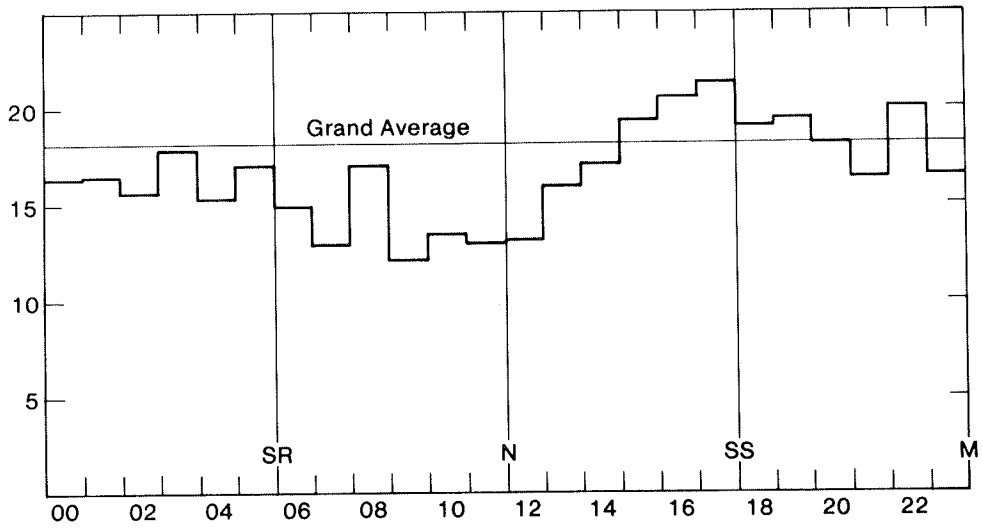

Figure 4.26 Diurnal variation in the percentage of hailfalls with diameters >2 in. Notation as in Fig. 4.1.

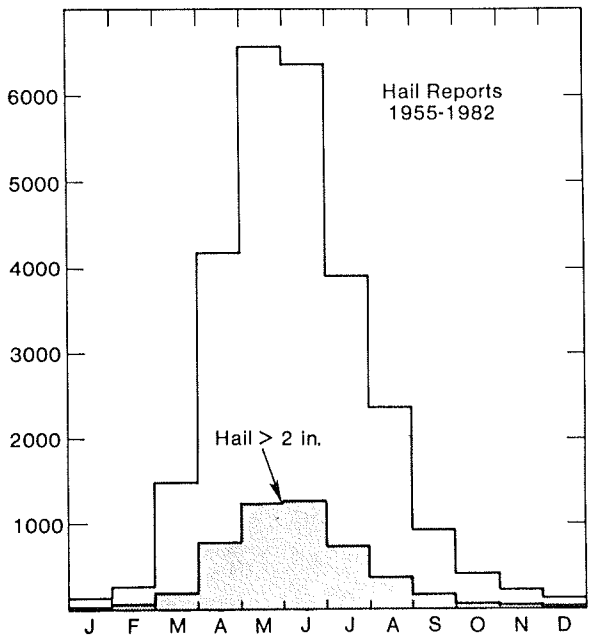

Figure 4.27 Monthly variation of hailfall reports. Notation as in Fig. 4.9.

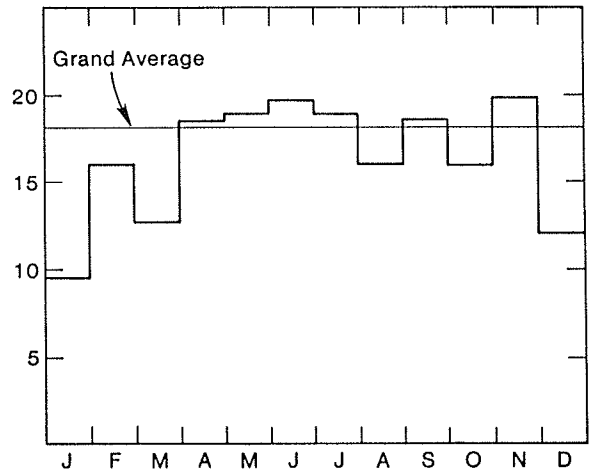

Figure 4.28 Monthly variation in the percentage of hailfalls with diameters >2 in. Notation as in Fig. 4.11.

supercell and multicell severe storms. With squall lines, the precipitation cascade is typically **behind** the updraft zone. In general terms, hail forming in the updraft is "pushed" across it by relative flow and upper-level divergence, eventually finding itself falling through weak updraft (or downdraft) so that it can descend to the surface. One should recall the fountain analogy used in II.C.4.

In Nelson's (1980) supercell model results, the largest hailstones fall in the low-level reflectivity core region. In nature, the very largest stones fall through the updraft periphery and reach the surface near the reflectivity gradient zone. An excellent example of this can be found in Burgess **et al.** (1979), in which a severe hailstorm produced hailstones up to 4 in (10 cm) within areas of low-level reflectivity less than 20 dBz. Small stones have an opportunity to migrate to weak updraft regions or into downdrafts before they descend. The very largest stones may actually fall in regions where the updraft can support all other forms of precipitation -- thus, the giant hailstones may be the only precipitation reaching the surface in that part of the storm. This implies a **size-sorting** process which is consistent with observations (e.g., Browning and Donaldson, 1965). Since large stones fall faster than their smaller companions, it is reasonable that some sorting should occur.

Such a distribution of hail (and rain) is generally observed in supercell and multicell storms. Browning and Donaldson (1965) present the following observations for an Oklahoma supercell episode on 26 May 1963:

> 1) There is a tendency for the righthand edge of the hail associated with each storm to extend to the right (south) a few miles further than the heavy rain. According to Newton (1963) this is fairly typical behavior.
>
> 2) There is a tendency for the onset of the heavy rain to be delayed with respect to the onset of the hail. This is very striking in the case of Storm G, which during a 90-min period produced hail over a distance of 30 mi before producing any rainfall totals exceeding 1/2 in. It is clear from the small separation from one another of the isohyets for 1/2 and 1 in., however, that when heavy rain did at last reach the surface, it became intense within a matter of minutes.
>
> 3) In all storms, tornadoes touched down on the downwind (east) side of the regions of largest hail. A similar poststorm survey revealed

identical behavior in a tornado near Charlton City, Mass. (Atlas **et al.**, 1963). In all storms the first tornado remained in contact with the ground for less than 8 mi. In the cases of Storms E and H, however, other tornadoes later occurred within the same swaths of minor wind damage.

4) The tornadoes occurred toward the right flank of the swaths of hail and heavy rain, as was the case in the Horsham storm studied by Ludlam and Macklin (1959) and in the 1913 South Wales storm discussed in Geophysical Memoir No. 11 of the Meteorological Office, London, and quoted by Browning and Ludlam (1960: Fig. 45).

The distribution of rain, hail, and tornadoes with these storms is summarized in Fig. 4.29, taken from Browning and Donaldson's paper. These findings are consistent with a wide range of supercell experience.

It often happens that exceptions exist, however. One source of difficulty is hailfall reporting statistics. It is commonly observed in SELS that once tornadic activity begins, hailfall reports show a dramatic drop-off (Doswell **et al.**, 1983). This should not be construed as a suggestion that large hailfalls do not occur during tornadic phases of the storm. Rather, at least some contribution to this phenomenon is the attention-getting

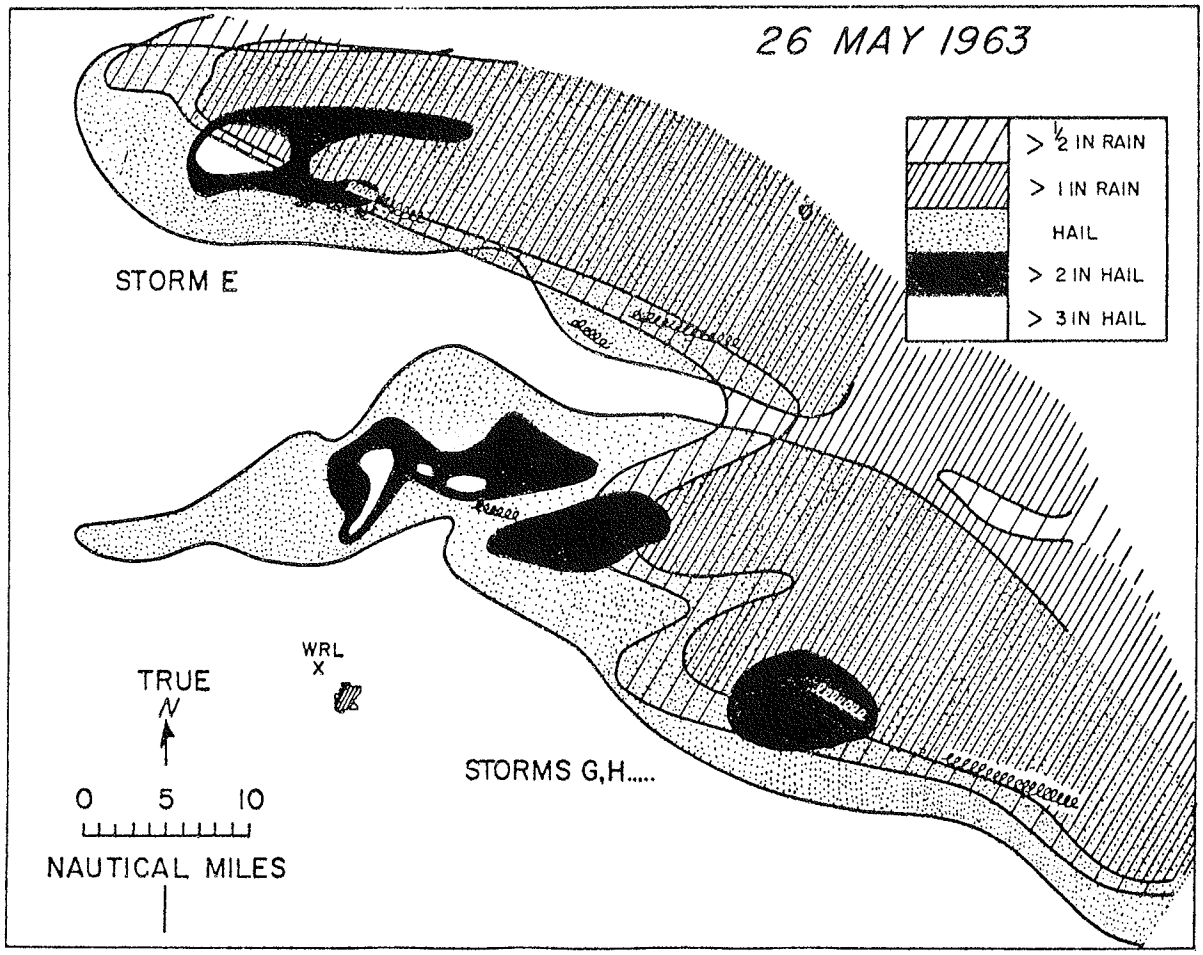

Figure 4.29 Comparison of the distributions of maximum hail size, rainfall, and tornadoes associated with Storms E, G, and H (from Browning and Donaldson, 1965).

nature of tornadoes. While research results suggest that peak stone sizes occur before tornado touchdown, large hail (perhaps not the largest) may continue to fall even beyond the tornadic phase. Detailed poststorm surveys (most often done only by researchers) reveal this is usually the case.

A more interesting apparent exception is the occurrence of tornadic storms which produce no reported hail. While such events are not thoroughly documented, SELS experience seems to point to such events being most common in the Gulf Coast states during late winter or early spring. Without careful follow-up investigation, one cannot be sure that hail did not, in fact, occur. If such storms are a reality, the implication is that some factor (or combination of factors) in the environment is acting to suppress hail formation (see Nelson, 1983) without being detrimental to tornadogenesis. It is not obvious what that factor (or factors) might be.

Previously, the distinction has been made (see III.E.1.) between multicell and supercell hailstorms. Multicell storms do not usually produce the giant hailstones (say, >6 cm) seen with supercells. Such an observation is consistent with the picture that supercells have stronger and steadier updrafts. On the other hand, multicellular hailstorms should not, therefore, be taken lightly. The most damaging stones with regard to crop damage can be those produced in great numbers and particularly when driven by strong winds. When giant stones occur, they are often relatively far apart and may be mixed with mostly small stones. The multicellular storms which occur on the high plains result in a climatological maximum in hailfall events (Chagnon **et al.**, 1977) and account for extensive crop losses, even if peak hailstone size is smaller (on the average) than in supercells. As always, the classification problem is important. Nelson and Knight (1982) describe a hailstorm type that is rather ambiguous. It is characterized by large BWER's, but they are relatively transient, with many severe events occurring in succession during the hail-producing phase of the storm. Such storms can produce copious hailfall, large stones, and extensive hailswaths.

Since the processes which result in tornadogenesis are, to some extent, associated with supercell collapse (see III.E.4), it is not surprising that, typically, hailfall commences before tornado touchdown and peak sizes are attained shortly before the tornadic phase in supercell evolution. With multicellular storms, the time-varying behavior of the complex should, and does, result in a complex hailfall behavior. For supercells characterized by cyclic building and collapse, a multicell-like series of events is likely. The peak sizes of surface-observed stones generally occur shortly after peaks in updraft intensity, but considerable spatial and temporal variation in hail occurrence is observed. Hailfalls at the surface may reflect the passage of several size-sorted hailshafts, so giant stones can be mixed with many smaller ones. This complicates the process of determining the actual events after the fact.

Squall line storms, as defined here, do not concentrate their energy in a single updraft, so this type of storm should not, in general, be as intense. This is indeed the case. Hailfalls are typically brief and the size and number of stones involved are smaller than in other storm types. Since the heavy precipitation is typically confined to a narrow zone behind the surface gust front, hailfall may be accompanied by strong winds, implying some potential for damage beyond that expected on the basis of hailstone size alone. However, significant hailfalls are not characteristic of squall line storms, unless there is some special cell or region (see III.E.3) within the line.

Within the secondary storm classes described earlier, dryline storms and "modified" supercells can produce significant hail. The occasional occurrence of giant hail (perhaps with little or no accompanying rainfall) is somewhat of a puzzle with dryline storms: weak radar reflectivities are not consistent with giant hailstones. If one remembers that

particle size is more important to a radar than the number of particles, this observation is disturbing enough. When one remembers that high liquid water contents are considered vital to hailstone growth physics, the situation is further confused. While dryline storms have been observed to rotate and seem to develop strong updrafts, the radar top of the 4 June 1973 Storm A described by Davies-Jones **et al.** (1976) was substantially lower than Storm B (not a dryline-type storm) in its immediate vicinity. This suggests that the updraft was correspondingly weaker. Yet, Storm A did produce large hail.

One possible explanation lies in the small overall size of dryline storms. Thus, the region of hail production and fallout is small compared to the volume scanned by the radar beam. This smooths out and reduces the amplitude of the observed reflectivity. Verification of this (and detailed explanation of dryline storm dynamics) awaits further study. Available information suggests that the dryline storm is a very low precipitation efficiency type of supercell, which is also characterized by small size, but such a generalization must be very tentative. Little more can be said currently about dryline storm hailfall patterns.

E. Tornadoes

> It often happens in such cases that the first part of the moving body is deflected because of the resistance due either to the narrowness or to a contrary current, and so the wind forms a circle and oddly....the exhalation, failing to break away from the cloud because of its density, first moves in a circle for the reason given and then descends because clouds are always densest on the side where heat escapes. This phenomenon is called a whirlwind when it is colorless; and it is a sort of undigested hurricane...So the whirlwind originates in the failure of an incipient hurricane to escape from its cloud: it is due to the resistance which generates the eddy, and it consists in the spiral which descends to the earth and drags with it the cloud, which it cannot shake off. It moves things by the wind in the direction in which it is blowing...and forcibly snatches up whatever it meets.
>
> -- Aristotle, **Meteorology**

As discussed in the process of describing storm types, a variety of events meeting the definition of a tornado can occur. In what follows, the emphasis is on those tornadoes which are associated with supercell (and, perhaps, the very strongest multicellular) storms. Such tornadoes account for a proportion of damage, injuries, and deaths far beyond their contribution to the "tornado" totals. Further, such tornadoes are understood better than the other events, since supercell storms are most well-understood of all storm types.

1. Tornado Life Cycle

While it easily can be argued that tornadoes are as unique as fingerprints, sufficient observations exist to propose a sequence of events (i.e., a life cycle) characteristic of tornadoes. As always, exceptions exist, and some of these are discussed where it is appropriate.[13] Broadly speaking, this life cycle is most appropriate for "strong"

---

[13] Superimposed on the life cycle to be described here are moment-to-moment fluctuations which can be visually dramatic, but may not be dynamically important. These fluctuations include variations in the amount of condensation associated with the tornado (which can change repeatedly during the life cycle) and the detailed behavior of "suction vortices" (to be considered in IV.E.2).

tornadoes (see III.B.2). Nevertheless, weak tornadoes also fit within this description, since they follow the early stages but never progress into the stages characteristic of more intense tornadoes. This distinction is expanded upon in what follows where it is appropriate to do so.

As described above, tornadoes in supercell storms are most commonly associated with a wall cloud. The wall cloud is a characteristic feature of the **organizing stage** (Golden and Purcell, 1978a)[14] of the tornado life cycle. This cloud feature, when observed to be rotating and persists for more than a few minutes, is a very reliable tornado precursor sign (Lemon **et al.**, 1980).[15] An example which happens to have been rotating but not persistently is shown in Fig. 4.30. To review the nature of the wall cloud briefly, it is characteristically located on the right rear flank of the storm (with respect to storm movement), attached to the rain-free cloud base under the flanking line, where the flanking line merges with the main storm tower. This locates the wall cloud upshear

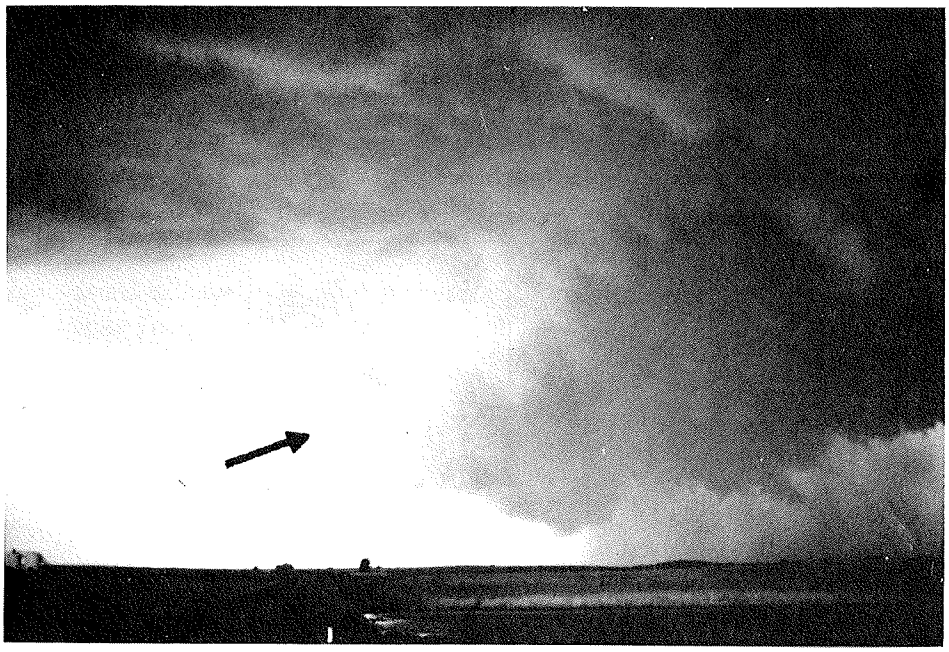

Figure 4.30 Transitory wall cloud (arrow) associated with strong multicell storm on 30 May 1982, near Binger, OK. Such features were seen to form and dissipate repeatedly with this storm. Note adjacent precipitation shaft (looking almost due north).

---

[14] The Golden and Purcell terminology is used in these notes. It should be noted that the life cycle described by Golden and Purcell was recognized independently some years before, as seen in Carrier and Beebe (1960).

[15] When wall clouds are seen to persist only briefly before dissipation, tornado occurrence is unlikely. In some multicellular storms, wall clouds form and dissipate repeatedly on a time scale roughly equal to that associated with successive updraft (cell) formation (i.e., about 20 min). If a multicell storm succeeds in making the transition to supercell status, the wall cloud becomes much more persistent. Transitory wall clouds in a multicell storm even may be seen to rotate but their brief life cycle usually precludes the occurrence of strong tornadoes.

from the main precipitation cascade region, as illustrated schematically in Fig's 4.31 and 4.32. Prior to tornado development at cloud base, the wall cloud is often quite turbulent and changes its appearance rapidly. Accessory cloud features like the collar cloud and the tail cloud may be present (as shown in Fig. 4.32b). During the organizing stage, occasional tornadic dust whirls may be observed under the rain-free base, with no apparent visual connection to that cloud base (Bates, 1963). Such events fit the definition of a tornado, but are most often a mere prelude to more significant events.

Even this early, the primary tornado may already have developed (invisibly) and debris may be seen beneath or closely adjacent to the wall cloud. In many cases, the condensation funnel is first visible as a short, smooth "spike" descending from, or adjacent to the wall cloud (Fig. 4.33). Although the condensation funnel may not have reached the surface, a debris whirl beneath it is evidence that the tornado has, in fact, already touched down. Tornadoes occur which never become more intense than this stage. Such tornadoes may be most common on the high plains where low moisture content and relatively weak tornado intensity might combine to preclude a condensation funnel reaching the surface in most cases. Despite fluctuations in funnel length and

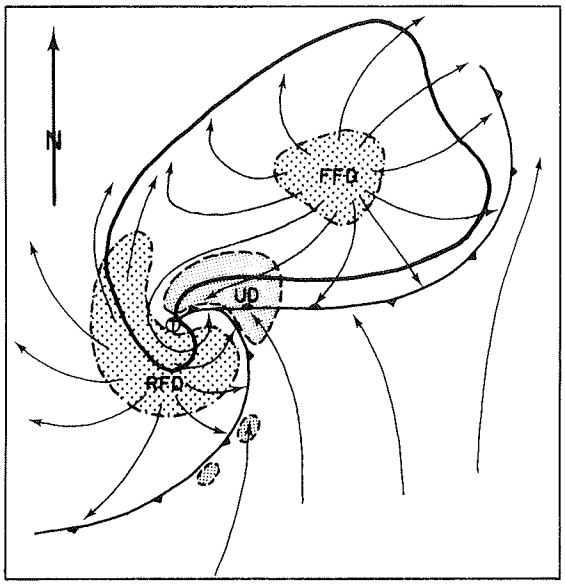

Figure 4.31 Schematic flow associated with supercell thunderstorm, showing forward flank downdraft (FFD), updraft (UD), and rear flank downdraft (RFD) — from Lemon and Doswell, 1979).

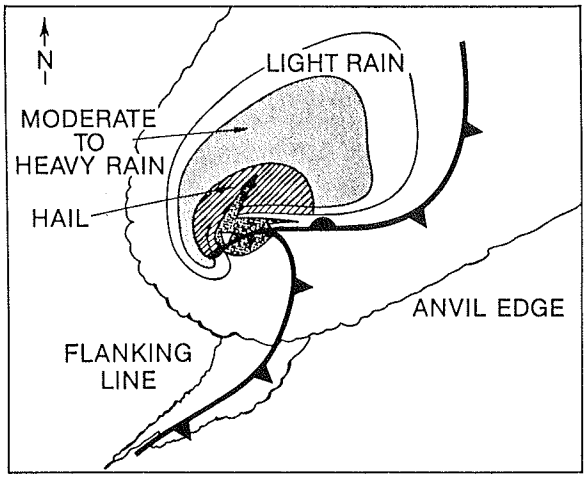

Figure 4.32a Supercell storm schematic, showing horizontal distribution of surface weather. Tornado may be at "▽" symbol or on leading edge of cold outflow.

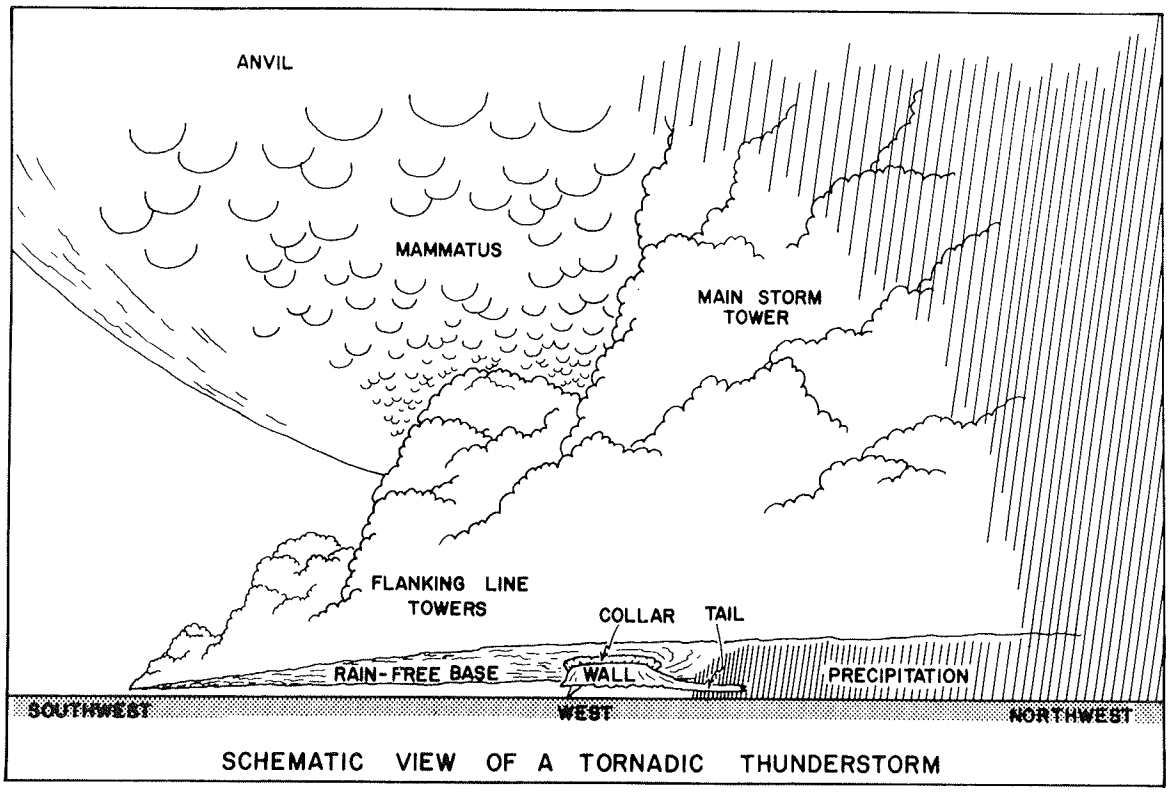

Figure 4.32b Visual schematic of a tornadic thunderstorm showing wall cloud and its relationship to other features of the storm.

width, the continuity of the debris (and/or damage) path is evidence that a single event is occurring.

Late in the organizing stage, the funnel may suddenly exhibit a thin, needle-like extension which finally comes in contact with (or close proximity to) the ground. This joins with the debris whirl and is unmistakable evidence of touchdown.[16]

Many tornadoes occur which never proceed beyond this stage of development (i.e., go directly into the decay phase). For those that do continue to intensify, the funnel expands in width rapidly and the tornado enters the **mature stage** in its life cycle (Fig. 4.34). At this time, a **clear slot** is usually seen to be wrapping around the wall cloud/tornado in a cyclonic sense from the right rear side (Lemon and Doswell, 1979). In the mature stage, the tornado attains its maximum width and the funnel cloud may become enveloped entirely with dust and debris (Fig. 4.35). Presumably, this is the time when the circulation is most intense and the surface damage most extensive.

Some tornadoes may remain in the mature stage for a considerable time, with minor fluctuations in intensity. Most commonly, after attaining maturity, the tornado enters the **shrinking stage.** As the name suggests, the funnel cloud begins to decrease in diameter, may appear to "lift", although continuing surface debris production indicates that the tornado itself is still in progress (Hoecker, 1960; Fujita, 1960), and may begin

16 Poor visibility, a lack of suitable tracer material, or obscuring foreground features may prevent observation of a pre-existing debris whirl.

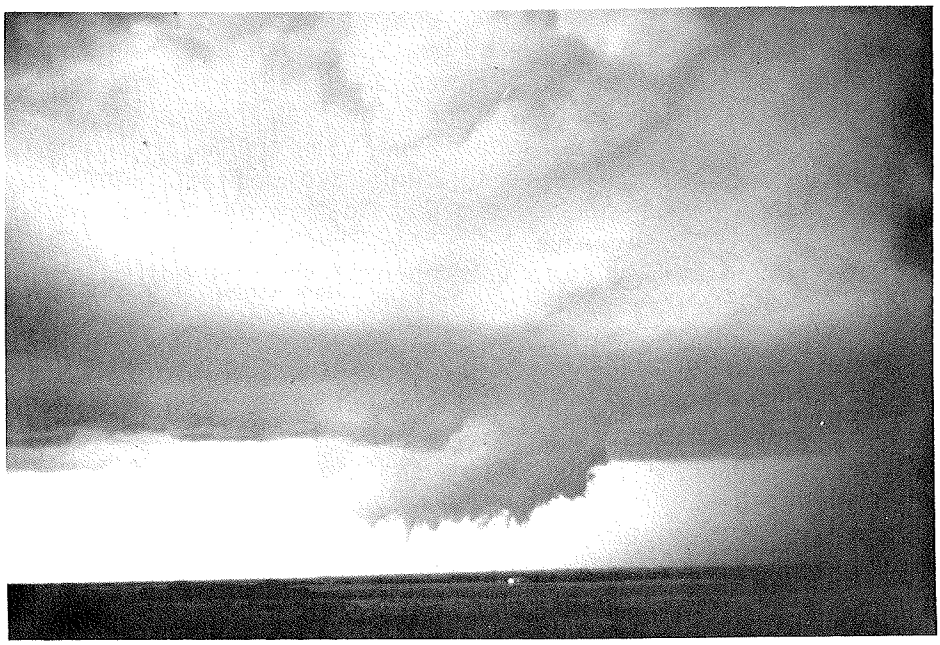

Figure 4.33 Organizing stage in tornado life cycle. Note that while visible funnel is not touching the ground, damage may already be underway (Photo from NOAA spotter training slide series — Lemon ***et al.,*** *1980 — taken by S. Tegtmeier).*

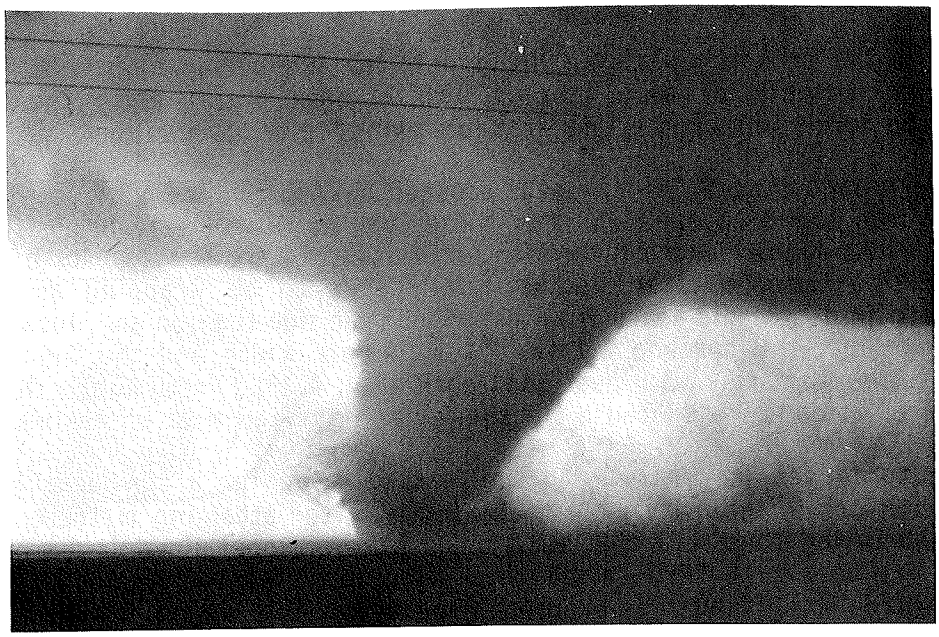

Figure 4.34 Mature stage in the tornado life cycle (Photo from Lemon ***et al.,*** *1980 — taken by G. Moore).*

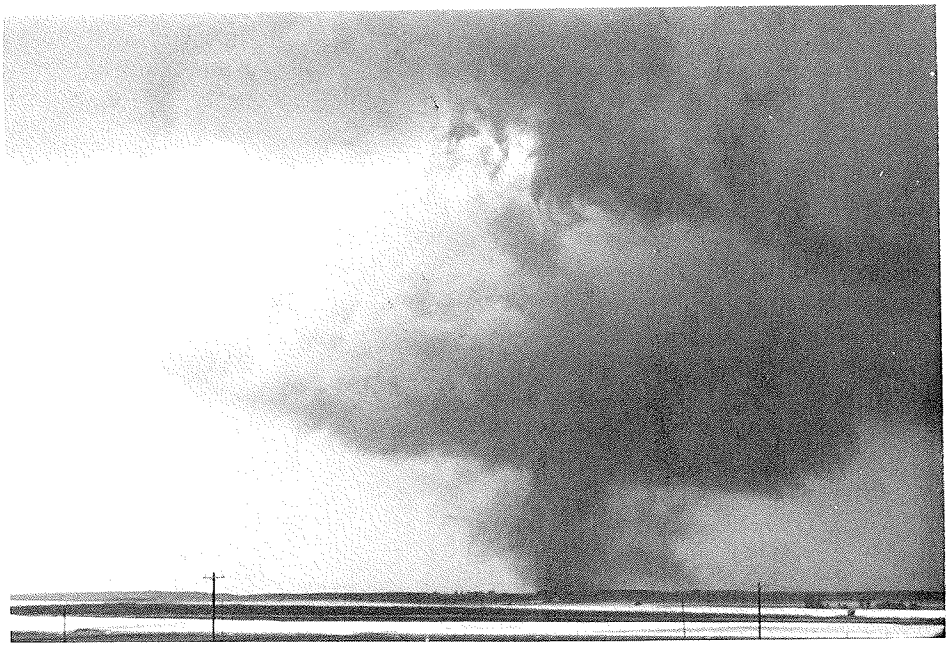

Figure 4.35 Example of a tornado nearly totally obscured by the dust and debris it has raised.

tilting away from the vertical (Fig. 4.36). By this time the clear slot may have wrapped around to the tornado's front side. This development is usually marked by an erosion of the wall cloud, revealing more and more of the tornado's vertical extent and leaving the tornado close to (or perhaps extending beyond) the cloud edge associated with the cumulonimbus. As Golden and Purcell note, this stage is **not** necessarily associated with a decrease in the destructive power of the tornado, but usually the damage path width decreases as the funnel cloud shrinks.

At some point in the shrinking process, the tornado enters the **decaying stage.** By this time, the wall cloud often is completely dissipated, leaving the funnel exposed as a rope-like tube (Fig. 4.37). As this occurs, the funnel may become quite contorted, perhaps with sections of it lying parallel to the surface. The condensation tube may become segmented, with gaps appearing between cloud base and the surface debris whirl. At times, it may give the appearance of having been "stretched beyond its limits". At least in the early stages of the decaying phase, the tornado may still be capable of severe damage, so it should not be treated lightly despite its appearance of weakness. As the tornado dies, the rope funnel disintegrates and surface debris is no longer generated.

If the condensation funnel has lifted during the shrinking stage, a rope-like funnel characteristic of the tornado's decay stage may once again establish visible contact with the surface shortly before the tornado ceases. Alternatively, the decaying stage may be associated with the cessation of surface damage, while a cone-shaped funnel aloft persists for some time. This latter case is not as common as the evolution into a rope funnel. Occasionally, the surface circulation (and debris whirl) may continue for a time after the rope funnel disappears.

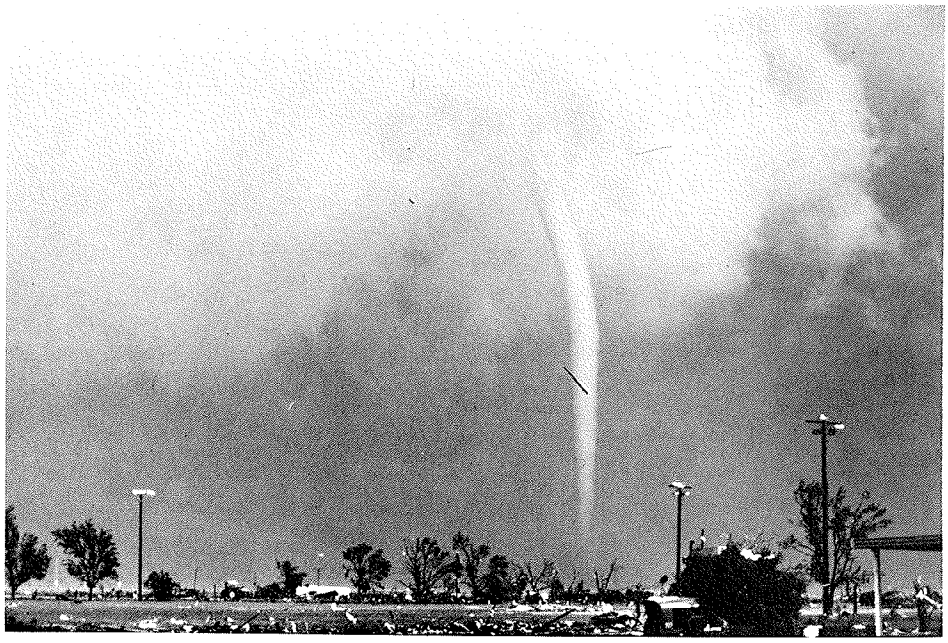

Figure 4.36 Shrinking stage in tornado life cycle.

Figure 4.37 Rope stage in tornado life cycle (Photo from Lemon ***et al.,*** *1980 — taken by J. McGinley).*

In storms like the Fargo, ND storm of 20 June 1957 (Fujita, 1960), a sequence of several tornadoes form, reach varying stages of maturity, and decay during the life of a single supercell storm. This is a process clearly related to the cyclic evolution of the parent storm (recall Fig. 3.23). The development of a new wall cloud often begins at the time an existing tornado is still in progress. Shortly after (say, 5-10 min) one tornado has dissipated, another one forms in association with the new wall cloud (Jensen **et al.**, 1983). Also, it has been observed that one wall cloud can be associated with two or more tornadoes -- in such cases, the first tornado may develop close to, but not directly from the wall cloud base. With the demise of that tornado, the wall cloud is not dissipated by the passage of the clear slot and another clear slot intrusion may be associated with subsequent tornado development from the wall cloud base. Such variations on the overall theme have not yet been extensively documented, but have been repeatedly observed. Storms which maintain their vigor through multiple episodes of tornado production must represent some sort of "super multicell" structure which is not yet fully understood (Jensen **et al.**, 1983). It is such events which make a dynamical definition of a supercell (such as proposed by Weisman **et al.**, 1983a) more desirable.

Important variations of the life cycle just described are associated with some of the few "violent" tornadoes subjected to detailed visual observation (e.g., the Xenia, OH tornado of 3 April 1974, the Wichita Falls, TX tornado of 10 April 1979 or the Binger, OK tornado of 22 May 1981). In such cases, the tornado does not descend as a needle-like tube. Rather, a broad, truncated cone funnel is observed during the organizing and mature stages (Fig. 4.38). The touchdown is marked by an extensive debris cloud, often including multiple vortices within the debris. Actual condensation funnel touchdown may be obscured by debris, usually coming well after violent damage is underway. Apparently, the Xenia, OH storm of 3 April 1974 never did establish funnel cloud contact with the surface, save during brief suction vortex touchdowns early in its lifetime.

Figure 4.38 Violent tornado, showing secondary vortices in surface debris beneath a truncated, broad cone-shaped funnel cloud (Photo courtesy of E. Rasmussen).

Dissipation of these violent tornadoes also may depart from the typical pattern described. Instead of an evolution into a rope-like funnel, the broad column of clouds and debris seems suddenly to lose its vigorous circulation and quickly disintegrates. Residual debris may stay in the air for awhile, but the tornadic circulation has ceased. The shrinking and decaying stages appear to be by-passed. This is yet another area where observations are not sufficient to generalize very far, although the sequence of events has occurred often enough to speculate on the commonality of those events with such storms. Note that not all violent tornadoes produce these variations.

2. Structure

Recalling that we are considering only a restricted class of atmospheric vortices (those associated with supercells), what are the known characteristics of such tornadoes? In order to answer this, recall the means by which our current understanding has been obtained. Prior to the advent of Doppler radar, conceptions of the tornado's structure had been derived almost wholly from damage surveys, visual observations (qualitative and, occasionally, quantitative) and simulations of tornadoes (laboratory and mathematical models). This presents an interesting dilemma. If one proposes a model of the vortex, one is free to experiment with and study the model in great detail. This means that, **for the model,** one can infer the distribution of wind, pressure, and whatever other variables are described in the model. Unfortunately, there were few measurements from nature by which the model's validity could be checked. Thus, scientists could argue ad infinitum about the virtues (or vices) of their models without ever knowing which model (or what parts of the model) did the best job of simulating reality. No one knew for a fact whether the air in the core of the vortex was rising, sinking, or neither. No one knew how high the vortex extended into the cumulonimbus. No one knew how low the pressures could go, where the winds were strongest, how the winds varied with distance from the axis, etc. The field was wide open for speculation, but little existed to guide the choices among the various theories.

What few quantitative measurements existed were of dubious value in settling these questions. Photogrammetric measurements (e.g., Hoecker, 1960) have considerable uncertainty and require several assumptions. The use of photography taken by untrained eyewitnesses usually involves cameras of unknown optical quality, used in only roughly known locations at roughly known times to derive the motions of tracers, whose relationship to air motions is also uncertain (Rasmussen, 1982). Further, photogrammetry can make little contribution to understanding behavior **inside** the cloud. The rare pressure and wind measurements are always troubled by questions of calibration, sensitivity, and location in space and time with respect to the tornado. One can use the scanty measurements to "prove" almost any model. Using damage to infer the winds is almost always plagued with the lack of engineering data for structures hit, and by uncertainties about how a particular element of damage was actually done by the storm. When damage to structures is total, one can use the engineering estimates only to determine a lower bound for the windspeed (if 50 m s^{-1} destroys a structure, so will 100 m s^{-1}!).

Lest this discussion lead to an excessively negative view of photogrammetric and engineering measurements, it should be noted that considerable insight has been gained from them. In spite of the limitations which restrict the quantitative details of photogrammetry, the very important qualitative picture derived from the technique has been valuable. In using engineering studies for cases where the destruction is not total, some quite important upper bounds on the wind speeds in tornadoes have been developed, including the spatial and temporal variations along the tornado's path. See Davies-Jones **et al.** (1978) for a discussion of damage variations in space and time with a particular tornado.

Once Doppler radar came into use for storm research, it became possible to map the wind field within the storm at frequent intervals. Naturally, there are sources of error and uncertainty associated with the winds so produced (e.g., see Brown **et al.**, 1981). However, it has become increasingly evident that Doppler radar has provided us with tremendous new insights into severe storms. Of particular interest is the identification of the TVS, or **Tornado Vortex Signature** (Burgess **et al.**, 1975a,b; Brown and Lemon, 1976; Brown **et al.**, 1978). Comparison with visual observations and damage survey data reveals that the Doppler radar signature can, with high certainty, be directly associated with the tornado. Thus, the vortex can be identified before a visible funnel appears, or damage begins. Also, one can map the location and intensity of the vortex within the heretofore hidden parts of the storm.

Because Doppler radars can obtain winds, one might expect to measure the wind structure directly and answer many of the questions mentioned. Unfortunately, it is not that easy. In fact, the tornadic circulation itself is, in general, below the resolution of Doppler data. However, there are some indirect ways (see, e.g., Brown **et al.**, 1978; Zrnic' and Doviak, 1975, for details) of inferring the answers to some of these issues. Doppler radar measurements finally can begin to fill some of the gaps in our knowledge. The possible application of Doppler **lidar** (using light waves instead of radio waves) offers a chance to obtain data of high enough resolution to yield direct answers (see Schwiesow **et al.**, 1977). Perhaps most important is the opportunity to use the Doppler data in concert with the photogrammetry and modelling efforts to help corroborate the findings of all three. This beneficial interaction among the various sources of information is becoming increasingly important (see Lee **et al.**, 1981). Doppler data and photogrammetry are complementary -- single Dopplers only "see" the wind component **along** the line of sight, photogrammetry (single camera) only measures the wind component **across** the line of sight. This makes the two data sources together more than twice as valuable as either one alone.

All of this is well and good but one is perhaps still inclined to ask, "So what do we know about tornado structure?" Perhaps the best answer at this moment is that we have learned a lot, but a great deal is still unknown. The reader may wish to consult some recent reviews of the subject (e.g., Davies-Jones and Kessler, 1974; Fujita, 1978b; Lewellen, 1976; Lee **et al.**, 1981; Davies-Jones, 1982a; Snow, 1982,1984).

A natural and long-accepted assumption about the tornado vortex is that the distribution of tangential wind speeds is similar to that of a so-called **Rankine Combined Vortex**, as illustrated in Fig. 4.39.[17] Such a vortex has a core in solid rotation (the tangential wind speed is directly proportional to the radius), and is irrotational outside the core (the tangential wind speed is inversely proportional to the radius). There is an implicit assumption that the wind is distributed symmetrically, so the variation along any radius (at a fixed height!) is identical to that at any other radius. In some ways, the Doppler data tend to confirm this distribution, insofar as resolution allows -- see e.g., Brown **et al.** (1978, their Fig. 11). However, the detailed data in time and space needed to provide better confirmation of this simple model have not been obtained. Further, visual observations and photogrammetric data (e.g., Golden and Purcell, 1977) suggest that pronounced asymmetries exist and departures from the model variation of speed with radius (and height) are present.

---

[17] More sophisticated theoretical vortex models exist. It does not serve the purposes of these notes to detail them, but the interested reader should refer to Lewellen (1976) or Rotunno (1979) for further information on them.

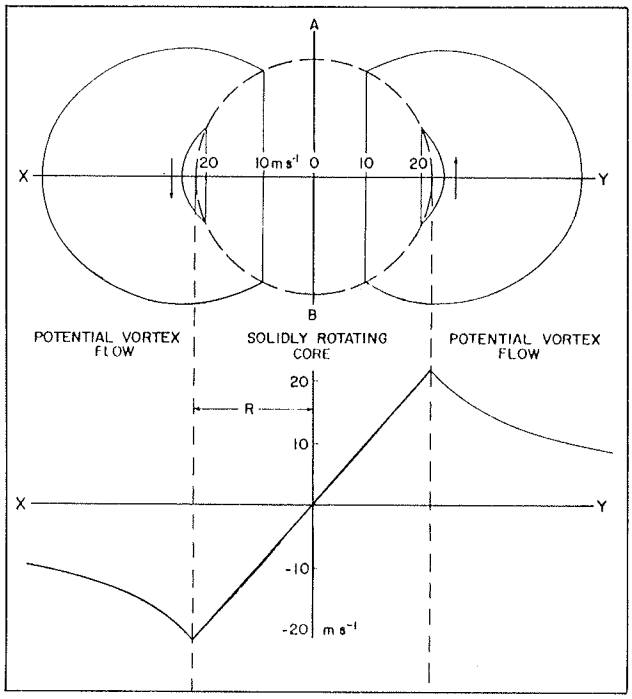

Figure 4.39 Single-Doppler radar horizontal mesocyclone signature of a stationary, nondivergent Rankine combined vortex (top) and a velocity profile along axis X-Y (bottom — both from Lemon ***et al.****, 1977).*

Further evidence for asymmetry is found in the existence of multiple vortices embedded within the overall circulation (see Peterson, 1976; Fujita, 1970; Agee **et al.**, 1976). Although the existence of multiple vortices was recognized long ago (as noted by Peterson, 1976), Fujita's (1970) work has stimulated examination of the phenomenon with modern methods. Laboratory models (Ward, 1972; Agee **et al.**, 1977; Davies-Jones, 1976) and theoretical analysis (Jischke and Parang, 1974; Davies-Jones, 1973; Snow, 1978; Rotunno, 1982; Gall, 1983) have combined with photogrammetry and damage pattern analysis (Fujita, 1970; Forbes, 1978) in an attempt to analyze the multiple vortex tornado. The subject remains one of active research but no definitive picture has emerged. Snow (1978) has implied that the strong horizontal shear associated with the area near the radius of maximum tangential wind results in the formation of smaller scale vortices, but admits that his model makes no unequivocal statement. Gall's (1983) linear model supports this notion. Everyone seems to agree that flows with high **swirl ratio** (ratio of tangential to radial velocity; or rotation to inflow) are most likely to develop multiple vortices. Thus, the existence of multiple vortices is possible with tornadoes of a variety of tangential winds (i.e., strengths) -- it is **not** restricted to violent tornadoes. Further, a tornado can posses multiple vortices at various stages in its life cycle and can switch back and forth between single and multiple vortex structures.

Regarding the flow along the axis of the circulation, the laboratory and mathematical models seem to suggest that it may be upward in some cases, downward in some, and may have both in other situations (see Fig. 4.40). Leslie's (1977) laboratory measurements reveal a downward flow in multiple-vortex circulations (down the core inside the radius about which the sub-vortices rotate -- see his Fig. 4). This is substantiated by Rotunno's (1982) numerical model. For single vortex tornadoes, the direction of the axial flow appears to vary considerably as a function of the swirl ratio. Interested readers should consult Davies-Jones (1976; 1982a,b), Lewellen (1976), Morton (1966) and others for more details. Leverson **et al.** (1977) have made aircraft penetrations of waterspouts, but the single-level measurements are not able to provide the complete picture we seek. Further, it is hard to know how to apply waterspout measurements to tornadoes.

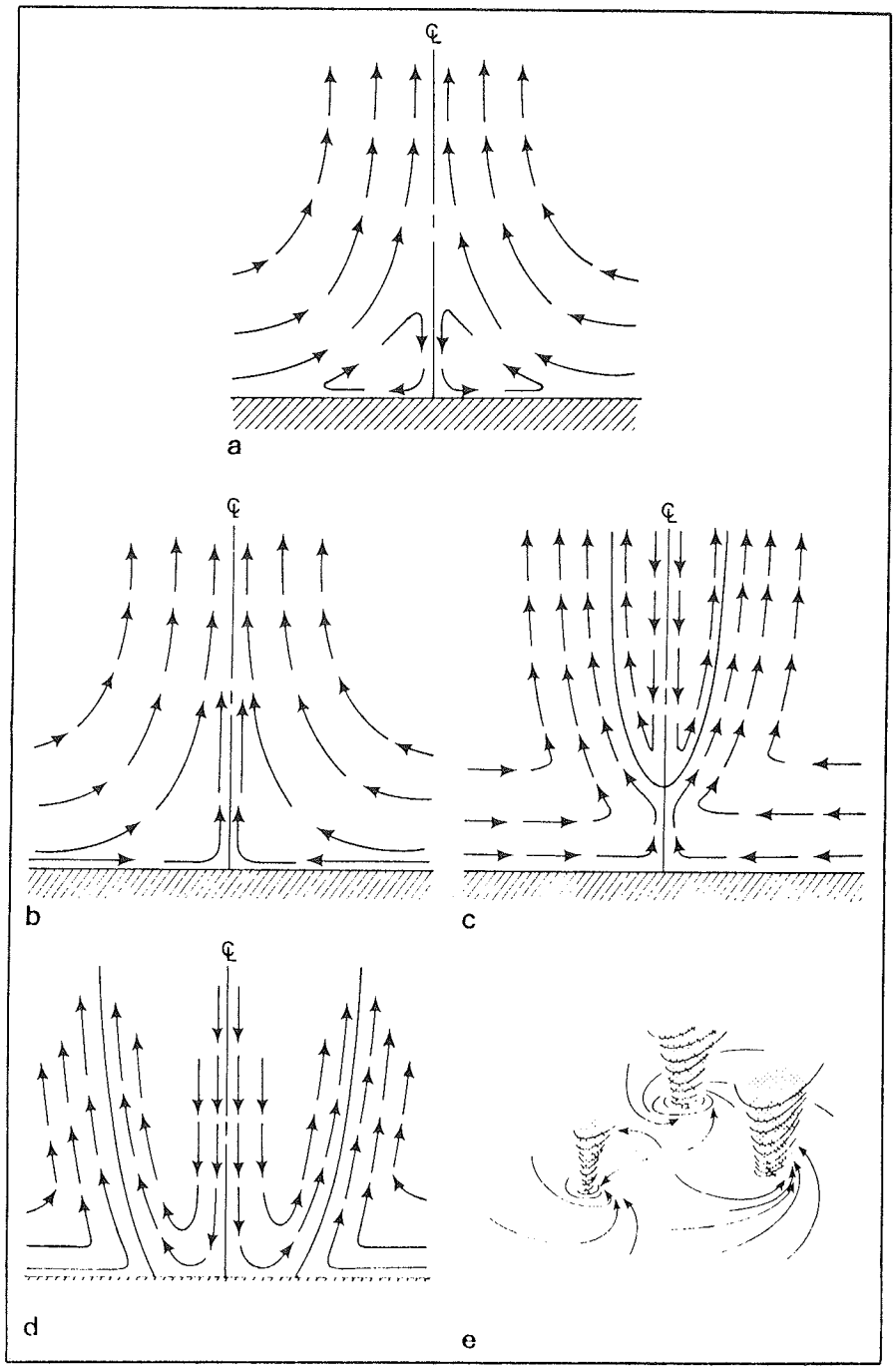

Figure 4.40 Effect of increasing swirl ratio on vortex flow: (a) Weak swirl — flow in boundary layer separates and passes around corner region; (b) one-cell vortex; (c) vortex breakdown; (d) two-cell vortex with downdraft impinging on ground (core radius increases rapidly with increasing swirl ratio); and (e) multiple vortices (from Davies-Jones, 1982a).

The importance of the swirl ratio in vortex dynamics cannot be ignored. In real tornadoes, as opposed to laboratory and theoretical model tornadoes, it is difficult to know the value of the swirl ratio or how it changes. To some extent, it is possible to infer the magnitude of this parameter from the vortex structure observed. However, it is difficult to make general statements about the detailed nature of tornado flow fields, since many of the details remain in doubt. Hence, the swirl ratio in real tornadoes is difficult to specify.

Vertical variations of tornado winds also remain in doubt. Tangential and vertical wind components have largely been derived from photogrammetry (e.g., Hoecker, 1960; Golden and Purcell, 1978b; Forbes, 1978; Rasmussen, 1982). This method, as discussed before, leaves some doubt about the details. However, the results cited (and others) indicate that tangential wind speeds increase rapidly with height above the surface, attaining a peak within a few hundred meters and then (apparently) decreasing rather slowly with height. Wilson and Rotunno's (1982) work supports this, in the sense that the pressure and wind distributions of their model are consistent with the motion of an elevated speed maximum (and pressure minimum).

The vertical motions near the vortex also increase rapidly with height near the surface -- vertical accelerations of a few g (where g is the acceleration owing to gravity -- about 10 m s^{-2}) have been inferred from the photogrammetry.[18] Radial flow is widely accepted to be confined to the lowest few hundred meters, where surface friction (boundary layer) effects predominate (see Rotunno, 1979). In one case (Davies-Jones **et al.**, 1978), the debris pattern in wheat gave the impression of a translating "sink" with no clear evidence of rotation (see their Fig. 4 -- this has clear implications for damage assessment -- see IV.B.3). This is reasonable, in light of the theoretical models (e.g., Kuo, 1966), which suggest that radial inflow dominates the flow near the surface.[19]

One important question which has been answered is the tornado's vertical extent. Once the TVS had been linked to the actual tornado, Doppler data could provide a clear picture of where the tornado exist within the cloud. As described in Burgess **et al.** (1975a,b) or Lemon and Doswell (1979), the tornado often is first detected aloft (say, roughly 4-9 km) and develops both downward and upward. At the time the vortex is on the ground (usually several tens of minutes after first detection aloft), it may extend much (if not all) of the way through the echo (Lemon **et al.**, 1982). In summary, as this is being written, quantitative data to answer some key questions about the structure of the tornado vortex are just now being obtained. Dramatic new increases in our knowledge are anticipated over the next several years.

3. Wind Speed Estimates

The maximum wind speed within the tornado circulation is given a separate treatment because it is of great importance to the storm's damage potential. The same observation tools used to deduce the overall structure of a tornado are applied to this issue, so the discussion can be equally controversial. Once again, some brief historical perspective is useful.

---

[18] A parcel starting at the surface and rising under an acceleration of one g reaches a height of 1 km in less than 15 s!

[19] Naturally, the debris patterns associated with multi-vortex tornadoes are more complex (Fujita, 1970, 1974, 1978b; Prosser, 1964).

At times, the damage produced by a tornado seems to require some extraordinary winds in order to explain the events. These include perforation of metal objects by flying debris (see Pearson and Miller, 1971), blades of straw driven into wood, fowl stripped of their feathers (see Galway and Schaefer, 1979), and so forth. Such events have led to some estimates of maximum tornado winds into the range of supersonic speeds. Further, because ordinary meteorological processes cannot give rise to supersonic speeds, some researchers have suggested an electrical origin for tornadic winds (e.g., Vonnegut, 1960; Colgate, 1967).

Recently, careful analysis of tornado damage by professional engineers virtually has eliminated the notion of extraordinary wind speeds (see Minor **et al.**, 1977). Since generally accepted extreme wind speed estimates no longer approach or exceed sonic values, there is no longer any necessity to call upon mechanisms outside ordinary meteorological processes. Electrical phenomena are likely to represent only a negligible contribution to tornadic circulations (Watkins **et al.**, 1978; Davies-Jones and Golden, 1975), if they contribute at all. More likely, electrical effects are created by the storm (see VII.C.2) and are essentially results, rather than causes.

Naturally, the maximum wind speed in any given storm is dependent on the strength of the storm (or, perhaps, the two are equivalent). It is clear that there are variations in strength from tornado to tornado, as well as from point to point during the life cycle of any given event (see Fig. 4.41). It also is clear from damage surveys that the most intense winds in tornadoes are confined to a relatively small fraction of the overall damage area. There must be some absolute maximum wind speed at low levels, at some point in space and time during any given storm's life cycle. This should produce some absolute maximum surface damage, provided there is something to damage. Although we cannot rely on this latter condition being satisfied in any particular tornado, there certainly have been enough tornado damage surveys to get a feeling for the order of magnitude of the extreme winds in tornadoes.

It should be noted that Doppler radar also offers some clues regarding this estimate of extreme wind speeds. This technique is discussed by Zrnic' and Istok (1980), Hennington **et al.** (1982), and others. Briefly, although the most commonly presented

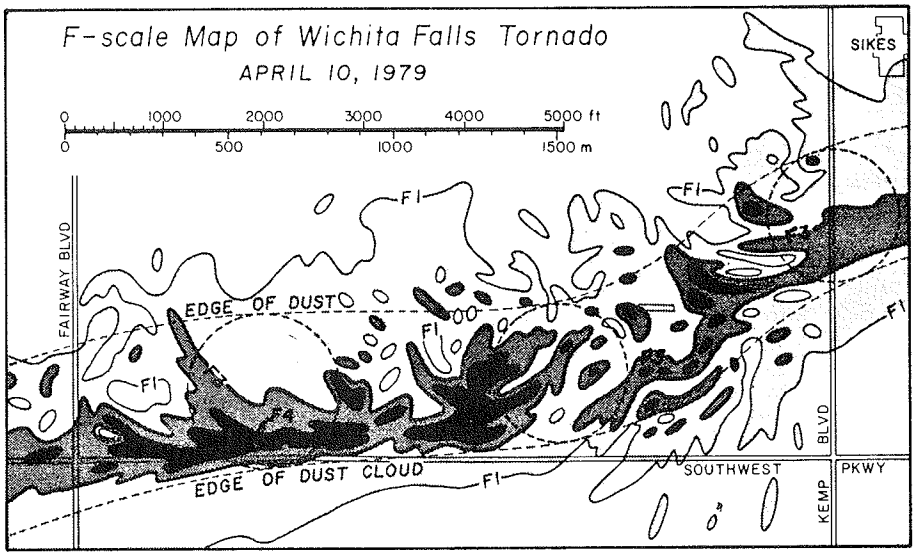

Figure 4.41 Contour map of F-scale values (from Fujita, 1981)

output of Doppler data is the average velocity in a volume, the Doppler also gives an estimate of the range of velocities in that volume. The actual volume in which measurements are taken depends on the range from the radar, the pulse repetition frequency, and other radar characteristics -- however, the radial depth is typically a few hundred meters and the azimuthal separation (which depends on range, of course) is of the order of a km. If only the average velocity is considered, this is clearly too large to resolve the peak velocities in a tornado (see Fig. 4.41). However, the estimates of the velocity spectrum (roughly related to the range of velocities) enable one to give a pretty good guess at the extreme values observed. Measured this way, Doppler radars have "seen" peak speeds in the vicinity of 100 m s^{-1}.

If only the extreme events are considered, some convergence of opinion has recently occurred. That is, research findings based on damage surveys, photogrammetry, models, and remote sensing techniques are now in basic agreement (Lee **et al.**, 1981). The agreed upon, absolute maximum wind speed (Golden, 1976) is about 300 mph (or 260 kt, or 135 m s^{-1}). Most tornadoes are quite a bit below this in their peak winds. In fact, most tornado damage can be explained with values of 100-150 mph. Since the energy of a 100 mph wind has four times the energy of a 50 mph wind, it doesn't take very strong winds to account for most of the damage. Recall that the strongest winds in a tornado are found above the surface, perhaps by several hundred meters. Surface damage is probably the result of winds that are weaker than the peaks produced aloft. Thus, while the surface effects for a particular tornado may point to a peak wind speed of, for example, 150 mph, the absolute peak winds anywhere in the tornado may be around 200 mph.

A maximum wind speed estimate can be translated into an estimate of the pressure drop, by using the assumption that winds are in cyclostrophic balance. Davies-Jones and Kessler (1974) detail the derivation which shows that the total pressure drop is roughly equal to the square of the maximum wind speed times the density. Using this for a 300 mph maximum gives a total pressure fall of about 185 mb. This is well in excess (by about an order of magnitude) of most observations cited by Davies-Jones and Kessler. A variety of explanations can be used to rationalize this discrepancy: only weak tornadoes were sampled, the tornadoes passed too far from the instruments to measure the extreme pressure drop, the instruments couldn't respond fast enough, etc. As stated in Lee **et al.** (1981), "More dependable estimates of the maximum pressure deficit in tornadoes await direct measurements with fast response instruments...." Recently, serious efforts to obtain such measurements have begun (Bluestein and Bedard, 1982; Colgate, 1982).

4. Theories of Tornadogenesis

If speculation that tornadoes arise through electrical forces is discarded, then the field of candidate theories is considerably reduced. Up to the advent of Doppler radar observations, a credible theory could not be subjected to a careful comparison with reality. Another problem which has plagued tornadogenesis theories is that one really needs to specify what kind of tornado is being considered. As before, attention here is restricted to those tornadoes which are associated, most generally, with supercell storms possessing well organized mesocyclones.

Producing a tornado is, in its simplest terms, a matter of concentrating enough vorticity about a quasi-vertical axis. When tornadogenesis is examined in this way, the problem is reduced to an examination of the terms in the vorticity equation (e.g., Hess, 1959, Ch. 16). With only a few exceptions, most theories of tornadogenesis in the past have relied exclusively on the so-called **divergence** term in the vorticity equation. In essence, this term can be understood to increase rotation (vorticity) by means of conservation of angular momentum. That is, in terms of the often-used analogy with an

ice skater: by drawing the arms inward, a slowly turning ice skater can speed up the rotation dramatically. In other words, by bringing the mass of a spinning object closer to the axis of rotation, the speed of that rotation must increase to maintain constant angular momentum. If any doubt as to this point persists, the reader should consult a physics textbook (e.g., Resnick and Halliday, 1966, Ch. 13).

As stated by Davies-Jones and Kessler (1974), a value for convergence of 10^{-3} s^{-1} over a circle with a radius of 10 km (typical thunderstorm values) can result in an increase of vorticity from a "background" value of 10^{-4} s^{-1} (roughly a midlatitude value for the Coriolis parameter) to tornadic values ($\sim 10^{0}$ s^{-1}) in about three h. Since small-scale convergence in a severe storm may be even larger, and since the background (subsynoptic scale) vorticity can be much larger than the Coriolis parameter to start with, it has long been felt that tornadogenesis occurs through convergence, with no need to call upon other mechanisms. Different investigators had subtly different scenarios about how the real process evolved, but there was no substantial disagreement that convergence of ambient vorticity was the mechanism for creating tornadic vorticity.

Occasionally, dissident voices could be heard. In an interesting model, Browning and Landry (1963) proposed that streamwise vorticity (i.e., vorticity about a horizontal axis, oriented along the flow) at low levels would be tilted into the vertical as the low-level air ascended in the updraft. Barnes (1968, 1970) suggested that the vorticity associated with the mesocyclone could be produced by the tilting term in the vorticity equation (see Hess, 1959, p. 248 ff.). Although he does not explicitly state it, one assumes that Barnes attributed the tornadic vorticity to concentration of the vorticity already present in the mesocyclone. Earlier, Ludlam (1963) went even further:

> It is tempting to look for the spin of the tornado in the vorticity present in the general air stream as shear and tilted appropriately in the vicinity of the interface between the [up- and down-] drafts...

Ludlam noted that the position of the tornado (see his Fig. 11) was near the interface between up- and down-drafts.

Doppler radar data, storm intercept observations, and numerical model simulations of tornadic storms have produced considerable new insights into tornadogenesis. The arguments which depart from more traditional convergence mechanisms have been summarized by Lemon and Doswell (1979). Calling upon a variety of data sources and references, they propose that **tilting** may be the primary initiation mechanism for tornadoes. Principal observations in support of this, as presented in their paper, are twofold. First, the tornado often is detected initially aloft, where convergence and vertical stretching (owing to change of vertical velocity with height) are at a relative minimum. Second, as Ludlam noted, tornadoes are located near the interface separating the updraft from the recently-documented rear flank downdraft. Tornado occurrences which are consistent with these observations are generally confined to supercell storms with mesocyclones. While other types of tornadoes occur (even with supercell storms), tornadoes associated with strong, persistent mesocyclones are apparently the most intense and long-lived events, which produce the majority of damage and casualties.

These observations are inconsistent with tornadogenesis solely via convergence. If convergence is the dominant process, the tornado should be located on or near the updraft axis, not near its periphery. Also, since convergence is predominantly a low-level phenomenon, tornadoes should first appear at low levels (some, in fact, do so). Rather than adjusting the theory to fit the observations, one is inclined to look for new theories.

Note that current laboratory tornado models are not capable of simulating tornadogenesis on an elevated updraft-downdraft interface. To that extent, laboratory vortex models have only limited value in simulation of real tornado vortices. Numerical model simulations (see below) have not yet succeeded in reproducing all these features of the observations, although it is anticipated that success is not likely to be long in coming (see e.g., Klemp and Rotunno, 1983).

Thus, in seeking revised notions of tornadogenesis, we have a host of theory, models, and observations to guide the process. The new Doppler radar observations and numerical simulations have been especially valuable in refining our concept of tornadogenesis beyond the simple arguments using conservation of angular momentum. One can obtain a feeling for how our concepts have evolved by reading Brandes (1984), Klemp and Rotunno (1983), Davies-Jones (1982b), or Lemon and Doswell (1979). Quite clearly, tilting of vorticity originally about a horizontal axis has become much more important in these theories. A more subtle point has been emphasized by Davies-Jones (1982b) -- the tilting and stretching terms are really different aspects of the same process, if we consider the **three-dimensional** vorticity equation. While Lemon and Doswell (1979) suggested that the **solenoid** term in the vorticity equation could possibly be of importance, many authors have chosen to omit it via order-of-magnitude arguments, as embodied in a scale analysis. Curiously, Klemp and Rotunno (1983) have produced model results which indicate that solenoidal vorticity generation may be quite important, but the vorticity produced is about a **horizontal** axis. This contribution to the total horizontal vorticity is then subsequently tilted to result in strong vertical vorticity.

Another important element in our revised tornadogenesis theories has been the recognition of the rear flank downdraft. As described by Lemon and Doswell, this feature of the supercell storm has been poorly recognized and certainly not well-understood, in spite of clear visual evidence in many tornado photographs. Since the Lemon-Doswell model was first presented, the rear flank downdraft's structure and mechanism (as well as its possible role in tornadogenesis) has been clarified. The process of **vortex breakdown,** described by Brandes (1978) and others is capable of creating downward motion in the core of the mesocyclone (clearly, an issue related to the mesocyclone's swirl ratio!). The numerical simulations of Klemp and Rotunno have further elucidated this process, in which a high-vorticity ring develops (Fig. 4.42), with a downdraft inside that ring. That downdraft, dynamically forced via something like vortex breakdown, they refer to as the **occlusion downdraft.** This small-scale downdraft is distinct from the region of descent on the storm's rear flank (Fig. 4.43). Thus, rather than being a process which, in some sense, "causes" tornadogenesis, the occlusion downdraft (and its associated clear slot) may be a result of the processes amplifying low-level vorticity within the mesocyclone.[20]

Progress in developing an understanding of supercell circulation (e.g., Weisman and Klemp, 1984a; Klemp and Rotunno, 1983) has had an enormous impact on tornadogenesis theories. Although the numerical models do not resolve the tornado circulation explicitly, they can offer insight about mechanisms operating on scales just above the tornado itself -- i.e., the tornado cyclone. The production of a mesocyclonic circulation is most likely the result of vorticity tilting (see Fig. 4.44). The cyclonic member of the cyclonic/anticyclonic couplet produced by tilting is favored dynamically (Weisman and Klemp, 1984b) whenever the wind shear vector turns clockwise in the low levels (say, below 6 km).

---

[20] I can safely say that the Lemon-Doswell model did not intend to imply that the RFD **caused** tornadoes. Rather, we intended to show that there was an association, which has certainly proven to be the case (e.g., see Marshall and Rasmussen, 1982).

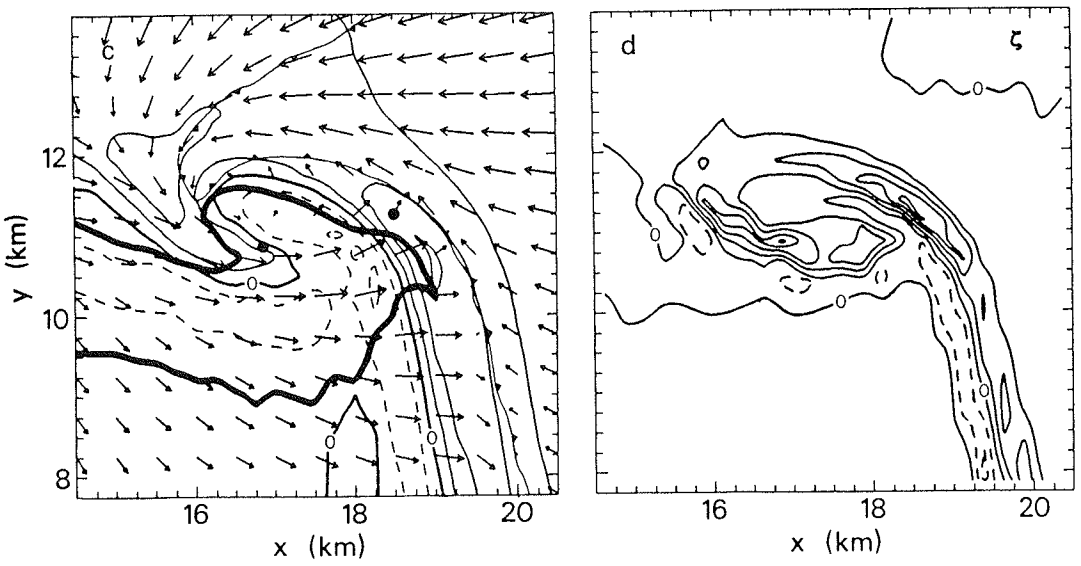

Figure 4.42 Output at height of 250 m from detailed numerical simulation of supercell storm, showing (left) outline of "radar echo", horizontal wind flow, and vertical motion; and (right) relative vorticity. The simulated radar echo is the 0.5 g kg^{-1} rainwater contour, the wind vectors are scaled to have a speed of 20 m s^{-1} when their length is one grid interval, the vertical motion is at 2 m s^{-1} contour intervals (negative values dashed), and vorticity is at 2 x 10^{-2} s^{-1} intervals (negative values dashed) — from Klemp and Rotunno (1983).

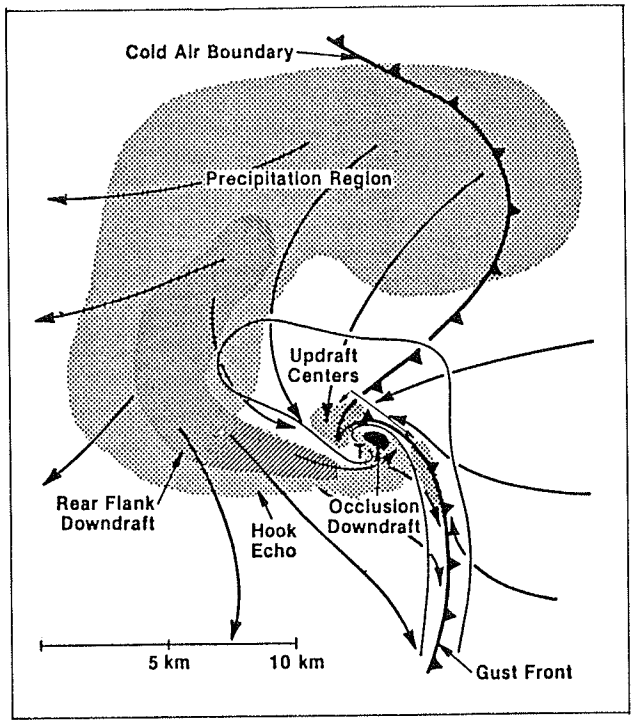

Figure 4.43 Schematic low-level flow field based on numerical simulations of supercell storms (from Weisman and Klemp, 1984b).

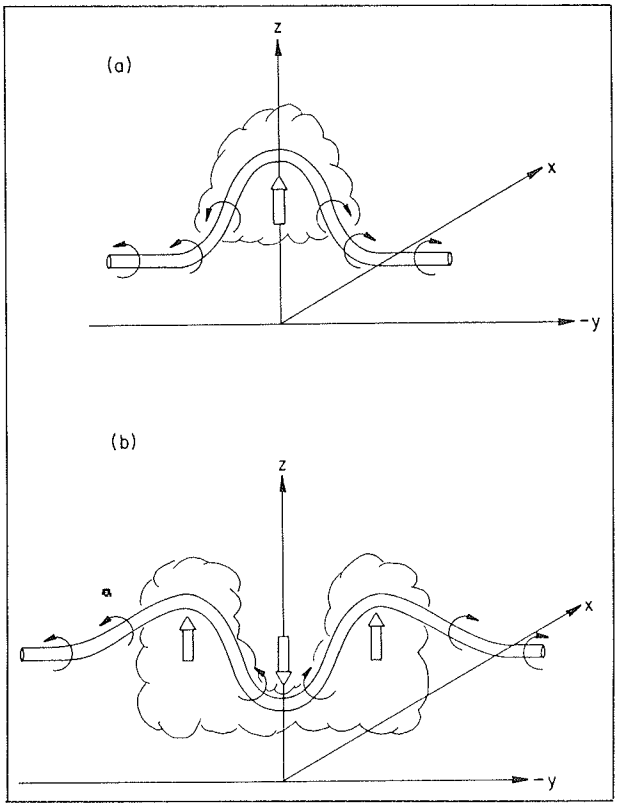

Figure 4.44 Schematic showing how a vortex tube associated with the environmental shear changes its orientation by interacting with a convective element. In (a) the convection is dominated by updraft while (b) shows the effect of a storm split, with two updrafts separated by a downdraft (from Rotunno, 1981)

Given a cyclonically rotating updraft, some new things are possible. Rotunno (1984) has argued that the mid-level rotation wraps potentially cold air around the forward side of the updraft, where it descends in the precipitation cascade region on the left front flank of the updraft (see Fig. 4.43). This produces, in Rotunno's argument, a favorable situation for generation (via solenoids) of horizontal vorticity. Since the low-level air ahead of the updraft (near the storm-scale "warm front") is drawn into the developing circulation, this produces tilting of the appropriate sense (to give increasing cyclonic vorticity at low levels). The fact that, in supercells, tornadogenesis follows precipitation reaching the surface lends credence to the notion that this solenoidal production and subsequent tilting is a major factor in the process.

This increase in low-level vorticity seems to yield an increasing swirl ratio, inducing the occlusion downdraft. The updraft is distorted into an arc-shaped (or "horseshoe"-shaped, as in Klemp **et al.**, 1981) region, with high vorticity at low levels associated with strong updraft. Vorticity maxima along the updraft arc are apparently associated with tornado cyclones (recall Fig. 4.42), in which the final spin-up to tornadic vorticity occurs.

This final increase of vorticity is not yet understood. It may well be a simple matter (relatively), involving only conservation of the tornado cyclone's angular momentum. From time to time, it is noted that a thin "sheet" of high vorticity (as in the case along a gust front) is dynamically unstable. For frictionless flow involving an infinitely thin vorticity sheet, theory predicts it will "roll-up" into a series of vortices (Fig. 4.45). Thus, it is tempting to speculate (see e.g., Brandes, 1981) that tornadic vorticity arises through this roll-up process along the gust front, perhaps augmented by convergent amplification. The fact that we do not usually see quasi-simultaneous roll-up of several vortices along the gust front/outflow boundary presents a challenge to this

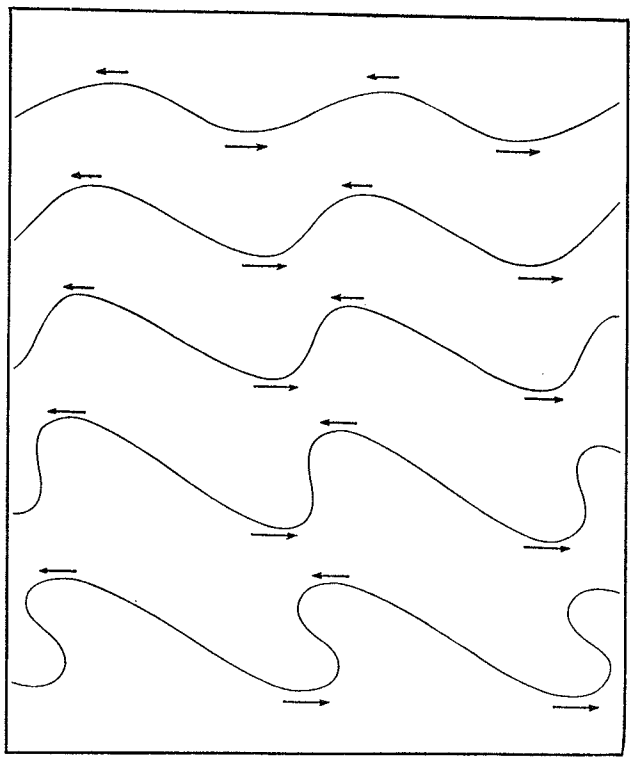

Figure 4.45 Successive stages in the "rolling-up" of an infinitely thin sheet of vorticity (from Godske ***et al.****, 1957 — p. 311).*

theory. There are some situations (e.g., Carbone, 1982, 1983) where such a hydrodynamic instability may be important for tornadogenesis, but it does not appear to be so in supercell tornado events.[21]

Clearly, some things remain to be resolved/explained in tornadogenesis. A really satisfactory explanation for the final spin-up remains to be found. The rare anticyclonic tornado may well result from tilting which produces the anticyclonic vorticity seen in certain parts of the storm, but the details remain unclear. It does not appear that anticyclonic tornadoes are the result of the left-moving (presumably anticyclonic) storm-scale rotation of a splitting storm pair. The rear flank downdraft's role (as opposed to the occlusion downdraft) remains confusing, with respect to tornadogenesis. Truly confirming evidence about the various aspects of the numerical simulations awaits better observations, despite the compelling similarities between simulations and real storms (see Ch. VI).

5. Distribution of Tornado Events

a. Climatological

As with the climatological distributions of other types of severe weather, it is obvious that what we do know about tornado distribution is a very imperfect picture of the actual occurrences. Clearly, tornadoes occur in the midwestern United States with the greatest frequency known anywhere on the earth. This is related to the unique features of the region's physical geography (see I.III.F).

---

[21] It also may have an important role for "gustnado" events (see III.B.2) along the outflow boundary. This theory was also applied, unsuccessfully, to the extratropical cyclogenesis problem (Godske **et al.**, 1957; Ch. 10).

Keeping these thoughts in mind, consider Fig. 4.46, showing the distribution of all reported tornadoes during the period 1950-1976, as presented by Kelly **et al.** (1978). Note the broad axis, oriented roughly north-south from Texas into the eastern Dakotas. Broadly speaking, this corresponds to "Tornado Alley". Superimposed on this is a secondary axis running northeastward from west Texas across central Oklahoma and into Indiana and Ohio. Finally, the presence of a "Dixie Alley" can be seen across the Gulf Coast states from southern Texas eastward and then along the Florida peninsula. These are clearly related to the axes discussed with respect to other types of severe weather.

When one considers only those tornadoes classified as violent (see below), quite a different picture emerges. Figure 4.47 shows the equivalent distribution to Fig. 4.46, but for violent tornadoes only. The frequency values are only a few one-hundredths as high as for all tornadoes. That is, violent tornadoes only account for a few percent (say 2-3%) of the total number of tornadoes. Further, their distribution is dramatically different. The violent tornadoes during the period of record are not concentrated in the tornado "alleys". As described by Kelly **et al.** (1978), the length of the record is simply too short to make any reliable statement about the actual distribution -- two of the four maxima

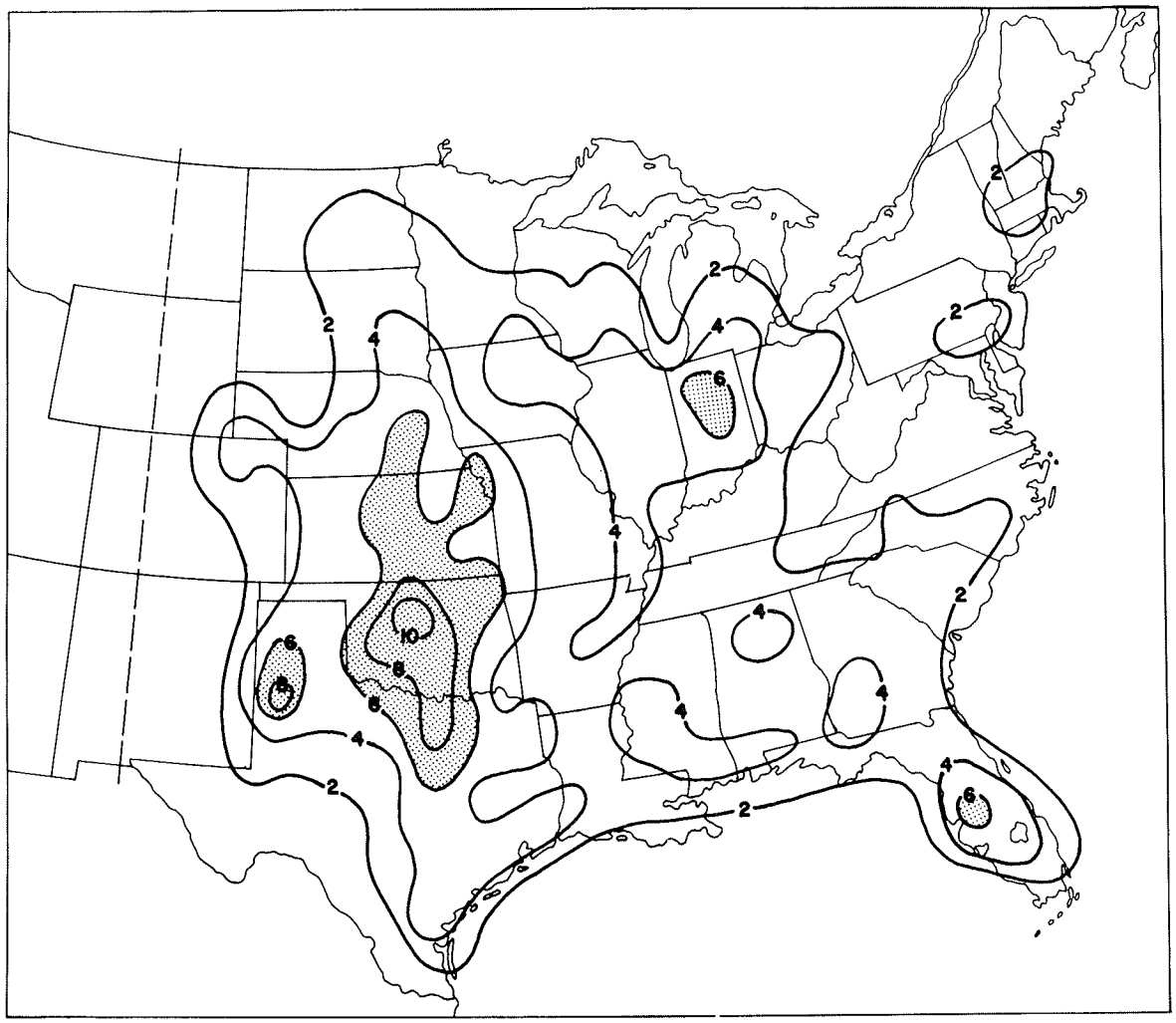

Figure 4.46 Map showing frequency distribution for all tornadoes 1950-1976 (inclusive), in units of tornadoes per 2° latitude-longitude overlapping square, normalized to 10,000 n mi² area, per year (adapted from Kelly ***et al.****, 1978).*

in Fig. 4.47 are the results of one or two tornado outbreaks. Essentially, not enough violent tornado events have occurred during the 27-year period to develop a statistically reliable data base.

Another climatological aspect of tornadoes is their diurnal distribution. Kelly **et al.** (1978) use NST to describe this, as mentioned before in these notes. Their Fig. 1 is reproduced here in Fig. 4.48. To no one's surprise, the occurrence of tornadoes peaks in the middle to late afternoon. However, when considering tornadoes by intensity category (see below), as in Fig. 4.49, there are some dramatic differences. During the period of peak frequency during the day, the percentage of tornadoes classified as weak is decreasing (from a midday peak) while the percentage of strong tornadoes is increasing

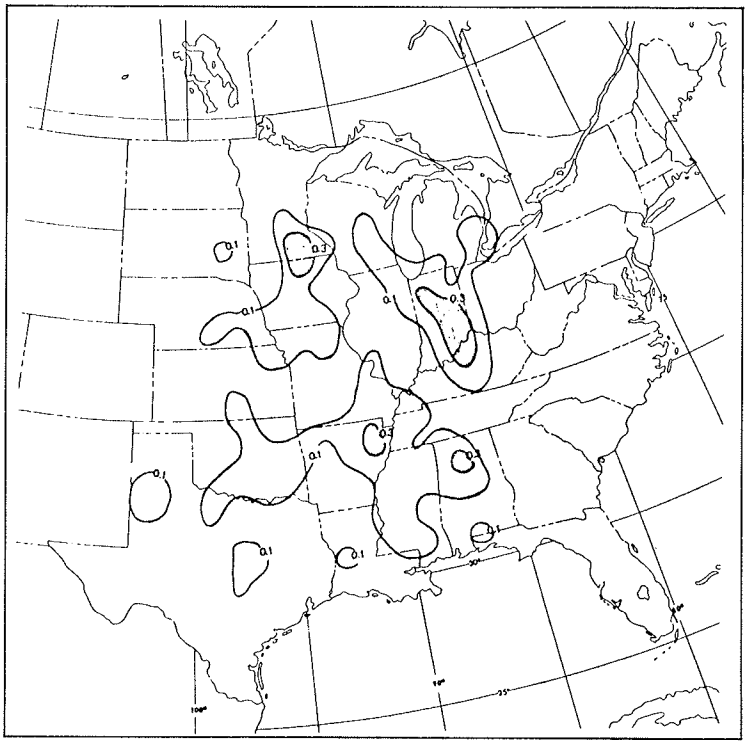

Figure 4.47 As in Fig. 4.46, but for violent tornadoes only (from Kelly ***et al.****, 1978).*

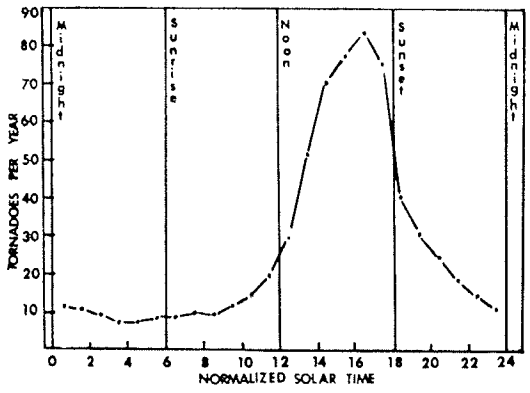

Figure 4.48 Average annual diurnal (NST) distribution of tornadoes (1950-76) (from Kelly ***et al.****, 1978).*

(from a midday minimum). The percentage of tornadoes classified as violent (bottom line of Fig. 4.49) shows almost no diurnal variation.

If the seasonal variations are considered (Fig. 4.50), the general perception of tornadoes as a springtime phenomenon is confirmed. However, once again breaking this down into three intensity categories by percentages, Fig. 4.51 shows some significant features. Concentrating as before on the spring period of peak frequency, it can be seen that the percentage of weak tornadoes is increasing (from a winter minimum), while that for strong tornadoes is decreasing (from a winter maximum). Although the percentage of violent tornadoes shows only small changes during the year (the absolute number of such storms changes little), there is some preference for them to occur in the early spring (Mar-Apr).

Those wishing to know more about tornado climatology should examine the references (Kelly **et al.**, 1978; Schaefer **et al.**, 1980a,b; McNulty **et al.**, 1979; and references mentioned in those papers). However, one topic deserves further mention. There is a definite propensity for tornadoes to occur in groups, or **outbreaks.** Galway (1977) has considered this subject in considerable detail. He has defined tornado outbreak categories in two ways: by the number of tornadoes (Galway, 1975) and by outbreak type (Galway, 1977).

Galway's number categories include 6-9, 10-19, and >20 tornadoes. As he points out, the tornadoes in a true outbreak are connected geographically and temporally,

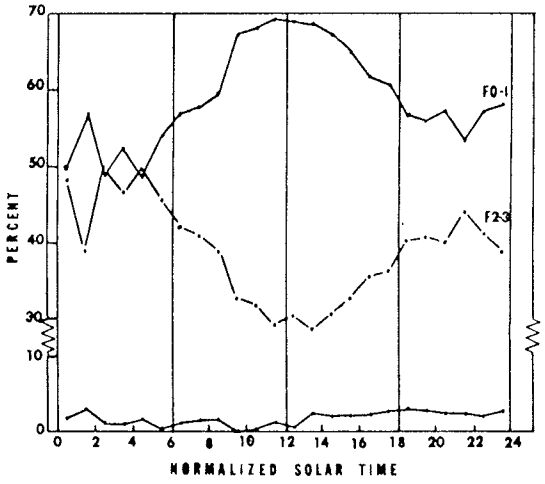

Figure 4.49 Percentage of hourly distribution of tornadoes attributable to each F-scale category (from Kelly ***et al.****, 1978).*

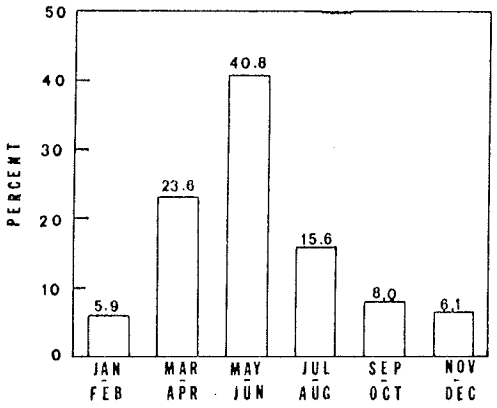

Figure 4.50 Bimonthly tornado distribution (from Kelly ***et al.****, 1978).*

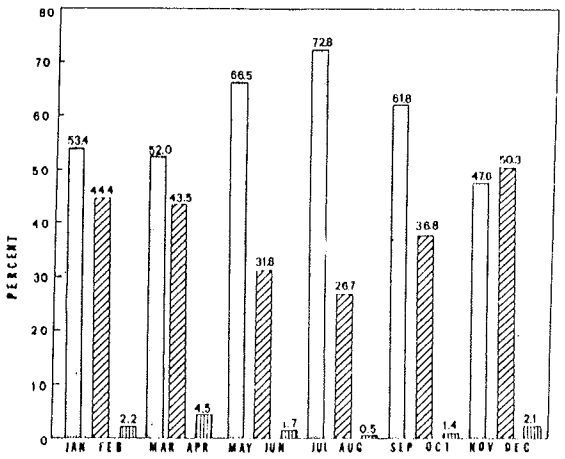

Figure 4.51 F-category breakdown within each bimonthly period (expressed as a percentage of corresponding bimonthly period): weak, stippled; strong, cross hatching; violent, vertical hatching (from Kelly et al., 1978).

rather than being scattered about in space and time. In his two papers on tornado outbreaks, Galway (1975, 1977) has documented the importance of outbreaks to the overall tornado problem. During the period from 1950 to 1975, outbreaks of 10 or more tornadoes only accounted for 22% of the total reported tornado occurrences, but these tornadoes were responsible for more than 55% of the total tornado-related death toll!

The outbreak types described in Galway (1977) are: **Local, Progressive,** and **Line.** In the period from 1950 to 1975, there were 209 outbreaks of 10 or more tornadoes, of which 13% were the Local type, 57% were Progressive, and 30% were classified as Line outbreaks. The definitions of the types are as follows:

> LOCAL -- An outbreak in which activity is confined to a roughly circular envelope of $\sim 1.0 \times 10^4$ n mi^2, with a duration rarely exceeding 7 h. The 34 cases classed as local averaged 5 1/2 h.
>
> PROGRESSIVE -- An outbreak that progresses (advances) generally from west to east with time. The distance between the first and last tornado report is normally greater than 350 n mi. The 152 progressive outbreaks averaged 394 n mi in length, with the mean envelope of activity encompassing $\sim 5.4 \times 10^4$ n mi^2 and lasts an average of 9 1/2 h.
>
> LINE -- An outbreak with limited eastward progression that forms on an axis, generally oriented north-south. The tornadoes tend to occur at widely separated locations along the line at approximately the same time. The average line outbreak has a duration of about 8 h, and covers $\sim 5.9 \times 10^4$ n mi^2.

Examples of these are given in Galway's (1977) paper. It is noteworthy that Moller (1979) has developed a similar outbreak classification scheme independently, based solely on tornado events in the southern plains region.

b. Storm-Relative

Prior to the establishment of truly mesoscale data collection for research and the development of advanced weather radar, relatively little was known about where tornadoes occurred with respect to the thunderstorm and at what point tornadoes were most likely to develop in the parent thunderstorm's life cycle. In this regard, the studies by Browning (1964, 1965b,c,d) and Lemon (1977) have been key contributions. Some

aspects of this have been considered above (e.g., see III.E.2). Once again, recall that for these notes, the primary concern is with tornadoes associated with supercell storms. Other types of tornadic events are less well-understood and are the subject of current research (e.g., Holle and Maier, 1980, Forbes and Wakimoto, 1983).

If we consider a "classical" tornadic storm (a northeastward-moving supercell), the picture at the surface (or levels near the surface) is generally like Fig. 4.32a. Note that location of the tornado is generally within the southwestern quadrant of the radar echo, at the "shank" of the hook. Thus, it is toward the trailing edge of the precipitation echo. An observer (fixed) watching the storm approach first sees something much like Fig. 4.52, which shows only an indistinct area of precipitation approaching. Thus, the observer first encounters the gust front associated with the forward flank downdraft (which is usually not very distinct). Then, light rain commences, gradually becoming more intense. In many cases, small hail then falls (mixed with the rain), and the hail becomes larger as the storm continues to pass. Then a brief period of giant hail (say, diameters >2 in) with little or no rain might occur, just prior to the cessation of any precipitation. Close on the heels of this abrupt termination of rain and/or hail comes the tornado. Although the tornado is near the rear flank of the storm, it may be followed by a brief burst of rain and/or hail, before the storm moves by.

Many variations of this scenario are possible since the storm may have somewhat different directions of movement, as well as different orientations with respect to its movement. If a storm moves more nearly eastward and retains the same orientation as in Fig. 4.32a, it is possible that points over which the tornado travels may not experience any precipitation prior to the tornado. However, the above description is probably most common. Since locations north and south of the tornado track pass through quite different parts of the storm, observers only a few miles apart may see quite different event sequences (see the quote at the beginning of this chapter)!

Further, fixed observers can encounter a supercell at different stages in its evolution. Since the storm generally exists for periods of an hour or so before tornado production (perhaps the first in a series), observers during the early stages may encounter only precipitation of one sort or another, including giant hailfalls. Since tornadogenesis is apparently associated with the rear flank/occlusion downdraft, the strongest "straight" wind gusts begin near tornado touchdown time and may continue to be maintained for a time after the tornado dissipates.

Storms which produce tornadoes cyclically, one after another, maintain their basic radar structure while the portion of the storm containing the hook echo usually undergoes repeated hook formation and "wrap-up" with each tornado event. Further, it is not uncommon for tornadoes to form along the leading edge of the gust front ahead of the hook or down along the flanking line (to the right of the hook's path). While such tornadoes are normally weak and brief, it is important to note that they can be very near to the edge of the radar echo, or even outside it!

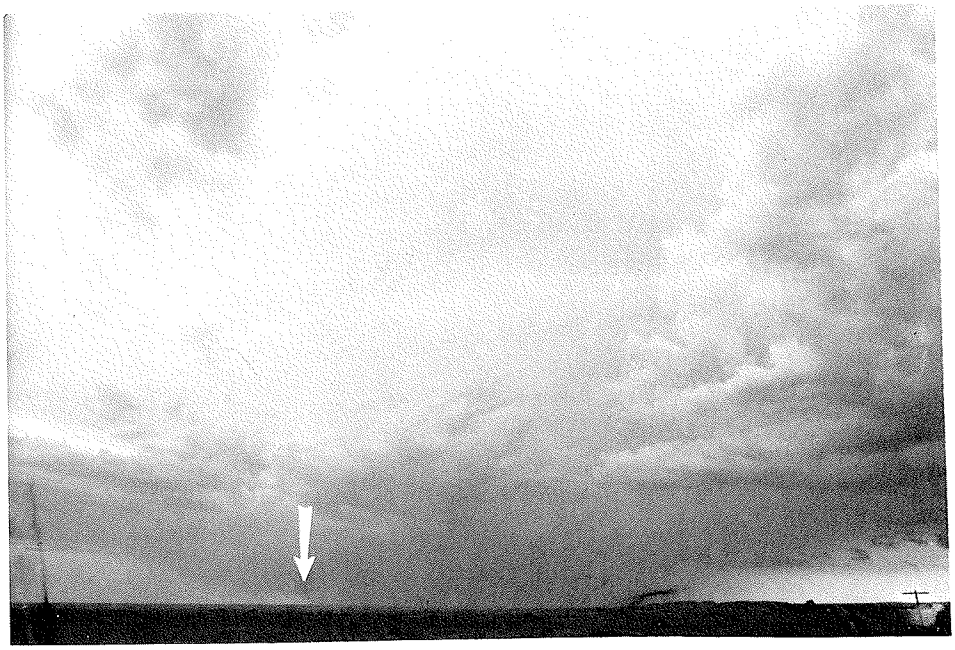

Figure 4.52 View to the west of an approaching severe thunderstorm. The part of the storm where severe weather events occur is usually on the southwest flank (arrow), and from this viewing angle and distance, it is impossible to evaluate the severe weather threat with any certainty.

V. Flash Flood-Producing Convective Storms

> But the greatest changes in these relations of fall, pool, and dams are caused, not by the ordinary spring floods, but by extraordinary ones that occur at irregular intervals. The testimony of trees growing on flood boulder deposits shows that a century or more has passed since the last master flood came to awaken everything movable....These floods may occur during the summer, when heavy thundershowers, called "cloudbursts", fall on wide, steeply inclined stream basins furrowed by converging channels, which suddenly gather the waters together in the main trunk in booming torrents....[An] ancient flood boulder stands firm in the middle of the stream channel....It is a nearly cubical mass of granite about eight feet high, plushed with mosses over the top and down the sides to ordinary high-water mark.
>
> -- John Muir, **My First Summer in the Sierra**

A. The Concept of Precipitation Efficiency

1. Introduction

Flash floods have assumed a leading position on the nation's list of fatality-causing weather phenomena. In recent years, deaths from flash floods have exceeded tornado fatalities regularly. In some years flash flood deaths may even move ahead of the lightning-related toll, thus earning for a time the dubious distinction as top killer phenomenon (Mooney, 1983). A primary reason for this is the increasing population dispersion in the United States, combined with more recreational use of areas prone to flash flooding.

Most flash flood events are predominantly convective in nature. Rare exceptions to this result from tropical cyclones (which certainly have convective aspects!), ice jams, and occasional large-scale events (which may have convective storms embedded within a region of heavy stable rain). The study of Maddox **et al.** (1979), mentioned in I.III.G, details the synoptic scale aspects of flash flood-producing convection.

However, there is an important concept not yet discussed which helps to distinguish convection with flash flood potential from those events which pose relatively little threat of flooding. This concept is **precipitation efficiency**, and it is keyed to the structure and evolution of the convection. Since the synoptic scale setting is generally believed to have some control over storm structure and evolution, it ought to be possible to anticipate Precipitation efficiency, at least in principle.

So what is meant by precipitation efficiency? In its most simple terms, this is the ratio of the **total precipitation reaching the surface** to the **total input of water vapor** to the storm. Consider the ordinary thunderstorm cell described in II.B. As the cell develops in its initial cumulus stage, virtually all the condensed water vapor is forming **cloud** particles, so the cell's instantaneous efficiency is zero -- no precipitation is reaching the surface. The mechanisms described in II.C begin to act as the storm approaches maturity, and the precipitation descends rapidly to the surface. Since the mature phase in an ordinary thunderstorm is relatively brief, the input of water vapor to the storm begins to drop off as the surface precipitation totals are rising. This means that the instantaneous efficiency may become quite large, perhaps approaching or exceeding 100%. Then, as the storm dissipates, the precipitation ceases, leaving a certain amount of high- and mid-level cloud, which is evaporated and carried downwind in the flow aloft.

Thus, if the precipitation efficiency is defined as the **instantaneous** ratio of input (water vapor) to output (surface precipitation), it varies over a cell's life cycle as shown schematically in Fig. 5.1. In the early stages, there is no precipitation, so it remains at zero efficiency until precipitation commences. During the dissipation phase, the input is small, diminishing to zero while precipitation continues, giving infinite efficiency! The instantaneous efficiency clearly is not a very useful variable. What really matters is the ratio of the areas under the input and output curves, which is about 0.4 (40%) for the example shown.

In order to estimate quantitatively a typical cell's efficiency, assume it is 10 km in diameter and 10 km deep, with a lifetime of about 25 min. If the storm movement is at 15 knots ($\sim$ 7 m s^{-1}), it moves about 10.5 km during its existence (see Fig. 5.2), giving a total area of 183.5 km^2. If the average rainfall over the entire area is 0.1 in (0.254 cm)[1] the total volume of rain produced is about 4.7 x 10^5 m^3. Previously (in II.B.4), it was shown that such a storm just about replaces its entire volume during its lifetime. Further, if the storm averages about 1.0 g of condensed water for each m^3 of volume, then the total volume of condensed water (assume that all water vapor input condenses in some form) during its lifecycle is about 1.6 x 10^6 m^3. Therefore, the ratio of precipitated water to input water vapor is about 0.3 or 30%, a reasonable figure. Leichter and Dennis (1974); Caracena **et al.** (1979); or Foote and Fankhauser (1973), have calculated precipitation efficiencies ranging from near zero to more than 100%, for real storms.

One brake on a given storm's efficiency arises if it has a relatively brief lifetime. However, having a long precipitation-producing life is not sufficient to produce high precipitation efficiency. For example, the supercell certainly can have a long lifetime

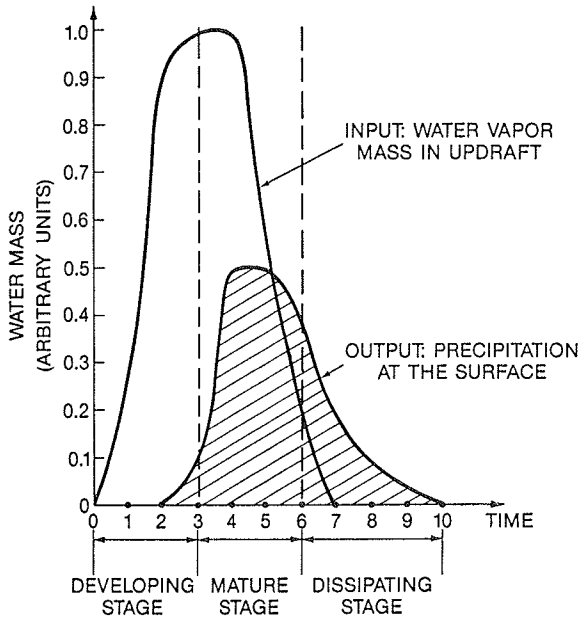

Figure 5.1 Schematic showing evolution of input and output during life cycle of thunderstorm cell. Time scale is in arbitrary units, but divided into stages referred to in text for cell life cycle. Note that instantaneous precipitation efficiency varies from zero (at t = 1,2) to infinity (from t = 7 onward).

[1] Note that a considerable amount of the total area receives no precipitation, since the storm does not precipitate until it reaches an advanced stage. Further, some areas are under the updraft and receive little or no precipitation. Finally, most of the area actually precipitated upon receives only a fraction of the peak value. Hence, 0.1 in over the whole area is probably a reasonable estimate for an ordinary thunderstorm.

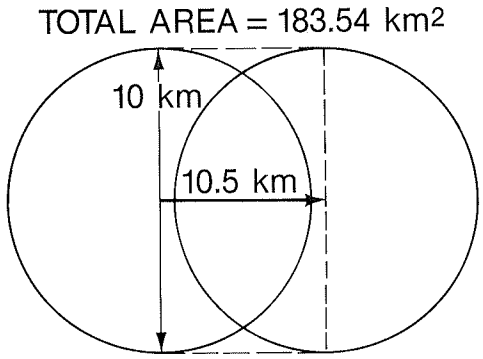

Figure 5.2 Area swept out by storm of 10 km diameter, which moves 10.5 km during its lifetime.

and remain in the precipitating phase for the vast majority of its life. A strong downdraft driven by evaporation is an essential element in supercell structure and evolution, so the supercell's precipitation efficiency can be rather low, perhaps no more than that of an ordinary thunderstorm (Newton, 1963).

The supercell structure is closely related to the environmental wind shear profile (recall III.E.2.e). In fact, it is tempting to generalize about the effect of shear on precipitation efficiency. This is hardly a new concept, apparently originating with Marwitz (1972d) and reappearing from time to time as new data are collected (e.g., Foote and Fankhauser, 1973; Fritsch and Chappell, 1980). As seen in Fig. 5.3, numerous data sets have been used to provide some notion of the shear-precipitation efficiency relationship. Although an "eyeball" fit of the data to the line looks reasonable, there is considerable scatter below shear values of about 3.0 x 10^{-3} s^{-1} and the nearly vertical nature of the fitted curve below this value makes it rather questionable. Also, there are

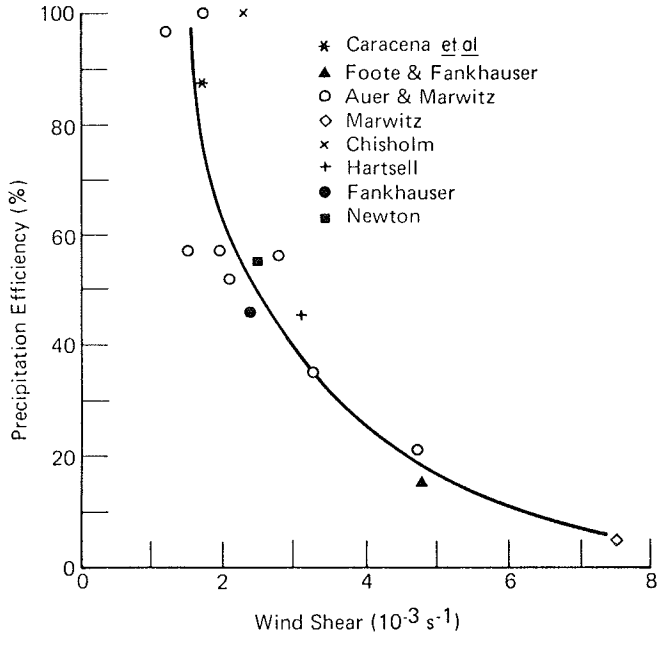

Figure 5.3 Precipitation efficiency as a function of wind shear in the storm-bearing layer (from Fritsch and Chappell, 1980). Symbols noted on the figure refer to the following data sources: Caracena et al. (1979), Foote and Fankhauser (1973), Auer and Marwitz (1968), Marwitz (1972d), Chisolm (1973), Hartsell (1970), Fankhauser (1971), and Newton (1966).

some gaps in this picture, with few observations above 3.0×10^{-3} s^{-1}, so one should be cautious in using this relationship -- it seems physically reasonable, but the quantitative aspects probably should not be pushed too far.

Evaporation of rainfall during its descent can also be a major factor in precipitation efficiency. For storms on the high plains, it is not uncommon for the low-level relative humidity to be quite low. The precipitation falling from high cloud bases (common on the high plains) may evaporate entirely before reaching the surface, yielding zero precipitation efficiency! In general, storms which exist in environments having large mean relative humidity over substantial depths are likely to have higher precipitation efficiency (all other things being equal) than storms in environments with low mean relative humidity.

2. Storm Types Involved

If ordinary thunderstorms and supercells are not likely to have high precipitation efficiency, then what types are likely to be prolific rain producers? Perhaps the best way to answer this is to examine flash flood cases and see what storm types are involved. Drawing on numerous case studies from the literature, both recently and in the past (Hoxit **et al.**, 1978; Maddox **et al.**, 1978; Hales, 1978; Merritt **et al.**, 1974; Staff, RFC, Tulsa, and DMO, Kansas City, 1964; Lott, 1954; etc.), it is found that there are two basic structures which result in flash flood events: slow-moving multicellular storm complexes (which can vary in size over a fairly broad range of scales) and slow-moving squall lines. The scale associated with the multicellular complexes can range from little larger than the individual convective cells to large mesoscale systems 100's of km in diameter. A similar statement could be made about the overall length of flash flood-producing squall lines.

The two major storm types involved develop long lifetimes for their overall structure, without much change in **individual cell** lifetimes. As described in III.E.1 and III.E.3, multicellular and squall line storm types have long lifetimes by virtue of repetitive new cell generation. This is not a random process. Rather, it occurs in preferred areas where large moisture flux convergence is created -- by the synoptic scale weather pattern, by mesoscale features which may have been generated by the cells themselves, or by storm interaction with the environment. As older cells move away from the generation zone, they take with them their convection-inhibiting outflow and low-level divergence, allowing the new cells a chance to reach maturity unhampered by dissipating older cells. Thus, a long-lived complex can process moisture into precipitation quite efficiently, especially when storms exist in an environment wherein evaporative effects are minimized.

Note that **storm complex** movement is emphasized here. It is often assumed that "storms" move slowly in flash flood situations. This is usually true with respect to the complex, or squall line, as a whole. However, the individual cell movement can be rather rapid. In fact, it often is the succession of moving cells, passing over the same area at about the same heavily-precipitating stage in their life cycle (the so-called "train effect"), that creates the enormous local rainfalls seen in flash floods.

Chappell (1984) has emphasized the important role played by storm propagation in producing what he terms "quasi-stationary convective events." As he puts it:

> Meteorological processes on several scales must work together synergistically to bring a storm complex to a quasi-stationary condition for a few hours. Physical processes occurring on synoptic and mesoscales, on down to the minute scale of cloud droplets are involved in a delicate interplay to create this quasi-stationary storm system.

This creates a problem in trying to characterize the flash flood-producing storm's environment, because this "delicate interplay" can arise in a wide variety of ways.

It should be self-evident that storm systems which move quickly are unlikely to produce serious flash flooding, regardless of their precipitation efficiency and instantaneous rainfall rate (both of which may be quite high). Perhaps the most obvious place to look for slow-moving storm systems is environments which have relatively weak environmental winds. Indeed, this is the potential spawning ground for the classical, quasi-circular mesoscale convective complex (MCC), to be dealt with below. However, this is **not** the only way to produce a quasi-stationary convective event.

For events to be convective, there must be an unstable thermodynamic stratification, or convective available potential energy (CAPE -- recall III.E.2). For heavy precipitation to occur, there must be an abundance of available moisture. Beyond these two simple (and rather obvious) requirements, the synoptic/mesoscale environmental processes must operate to:

(a) force new convection in ways such that the propagation of the system as a whole has a component which is opposed to the movement of the convective elements,

(b) provide a steady supply of CAPE and moisture to the system, and

(c) prevent the "exhaust products" of convection (outflow with little or no CAPE) from choking off the system.

These requirements can arise in environments with relatively weak flow, relatively strong flow and, presumably, almost anywhere in between. One has to remember that when large convective rainfall rates (say, in the range of a few inches of rain per hour) are present, it doesn't require more than a few hours of such precipitation to have flash floods!

If the potential for quasi stationary convective events exists through virtually the whole range of environmental wind speeds, it is somewhat hard to restrict the class of storm types involved.

3. Heavy Rain and Severe Weather

It is worth pointing out once again that severe weather and flash floods are hardly mutually exclusive (see I.III.G). With the typical supercell, one fact becomes abundantly clear: supercells process an enormous amount of mass and moisture during their extended lifetime. Foote and Fankhauser (1973) found, for a strong, persistent multicellular storm, net water vapor inflows of 8.5×10^6 kg s^{-1}, a value consistent with Dennis **et al.** (1970) or Auer and Marwitz (1968). Supercell values generally should equal, or perhaps exceed, this amount. By virtue of such large moisture influx, a supercell storm can produce prodigous precipitation amounts even if its efficiency is not high. Further, supercells often move rather slowly (e.g., the Grand Island, Nebraska storm of 3-4 June 1980), so the rainfall may be confined to a small region. Thus, supercell storms, in addition to their high threat of severe weather, also carry an implicit threat of flash flooding when storm movement is slow.

Another combined threat situation can arise in certain cases of flash flood potential (see e.g., Belville **et al.**, 1980; Maddox and Dietrich, 1981; Howard and Doswell, 1983). In essence, there are circumstances when storms which have high rainfall potential are also capable of episodes of severe weather. Severe events are most

frequent early in the development of a multicellular complex or squall line, before the cells have had much chance to interact. As the squall line or complex "fills in", the severe weather threat diminishes and heavy rainfall is the common feature. Some potential for severe weather remains, even well into the life cycle of these extended thunderstorm structures, whenever a particular cell is observed to be favored (see, e.g., III.E.3.b). Obviously, the forecast problem is seriously magnified when the potential for both severe weather and flash flooding is present.

B. The Mesoscale Convective Complex

Perhaps the most common heavy rain-producing situation in the central U.S. occurs in association with what Maddox (1980) has called the Mesoscale Convective Complex (MCC). These are, classically, a warm-season phenomenon. It was not until geostationary satellites provided continuous, enhanced-infrared images over a period of years that the MCC occurrence frequency became apparent. This phenomenon is described in detail by Maddox (1980), Fritsch and Maddox (1981), Maddox **et al.** (1981) and Maddox (1983).

In essence, it has been found that much of the late-spring through fall thunderstorm activity in the central U.S. is associated with MCC's. The MCC arises through the combined effects of many individual storms, often producing a system large enough (meso-alpha scale) to be detected by conventional rawinsonde data.

Early in its development, the MCC's component thunderstorms are relatively isolated and the severe weather threat is at its highest. At this time, the developing storms are indistinguishable from multicell or supercell complexes or squall lines. Under favorable synoptic conditions, described by Maddox (1983), the net effect of the convection is to produce a persistent circulation, **organized on a much larger scale than the individual elements.** In its mature phase, this circulation is characterized by a large mass of rain-cooled air and a "bubble" high at low levels, a meso-alpha scale region of rising warm air at mid-tropospheric levels, and a strongly divergent, cold air pool at the highest levels (Fig. 5.4).

MCC circulations are both large and persistent. As long as the MCC has a source of inflowing moist, unstably stratified air, it continues in its mature phase. Dissipation usually occurs when the complex moves away from its source of such air. Synoptic-scale forcing in MCC cases is often rather weak in middle and upper tropospheric levels. Instead, the dominant synoptic scale feature is **strong, low-level warm advection** (Maddox and Doswell, 1982), often associated with a low-level jet stream. This setting provides the system with the needed continuing influx of CAPE and moisture, as well as the lift needed to generate new convection.

Because of the typically weak upper flow structure, MCCs may move rather slowly. Further, the environment typically is consistent with that described in Maddox **et al.** (1979); i.e., a deep layer of high relative humidity and weak vertical wind shear. This combination of circumstances makes the flash flood threat quite high in MCC cases, as discussed previously. The effect of the meso-alpha scale circulations is to enhance and/or maintain the flash flood potential for the duration of the episode.

It should be noted that under stagnant synoptic conditions (common during the warm season), MCCs (or other heavy rain-producing storms) can occur over the same region on more than one day in succession. The soaking of the region by previous heavy rainfalls often plays a crucial role in determining the flash flood potential of a given event (e.g., Hales, 1978). This factor can turn an already serious situation into one of high disaster potential.

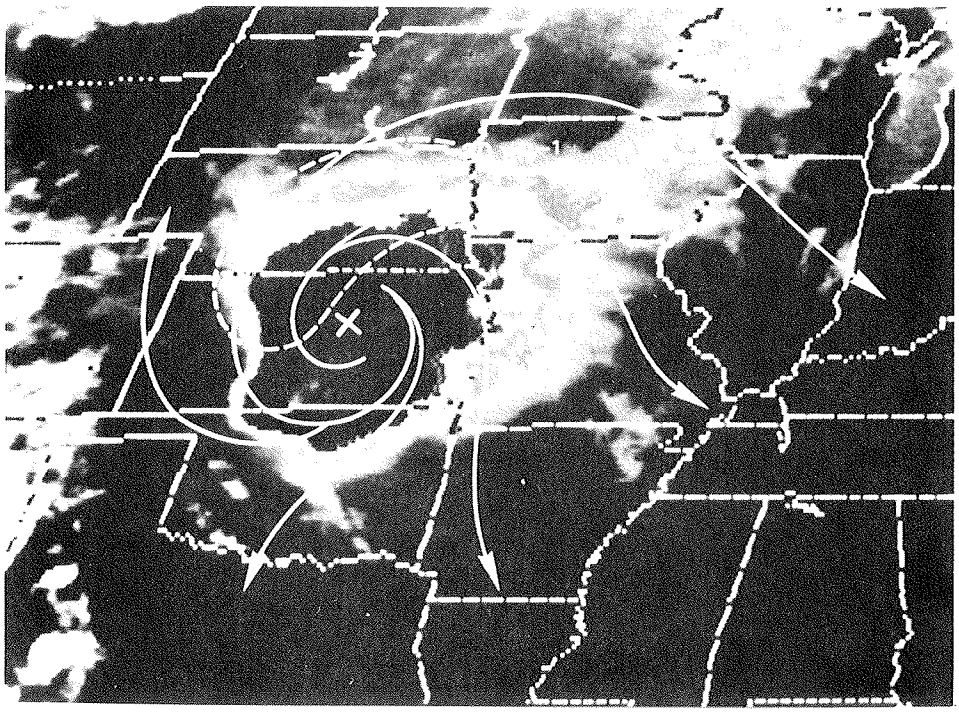

Figure 5.4 Example of influence of MCC on upper level flow, superimposed on satellite image. Dashed line corresponds to isotach value of 20 m s^{-1}.

C. Convective Systems in Strong Environmental Flow

In stark contrast to the rather benign settings for meso-alpha scale, cold-topped, quasicircular MCC's, the spring or fall situations involving one or more rather fast-moving Mesoscale Convective Systems (MCSs) can be characterized by all the features of strong baroclinic weather systems. The MCSs involved may be MCCs, squall lines, supercells, meso-beta scale complexes, and so forth. In effect, the "overall system" is composed of a series of MCSs (perhaps of several different types). The individual MCS plays a role roughly analogous to the individual convective cell in an individual MCS. These situations are rather common in the spring and fall along the Gulf of Mexico coastal states, but certainly occur at other times and places.

The primary difference between these and the warm-season systems is the strength of the environmental flow. Rather than mid-tropospheric winds in the range of 20 kt (10 m s^{-1}) or less, speeds of 100 kt (50 m s^{-1}) are not uncommon. The common factors with warm-season events are substantial CAPE and moisture. A sequence of satellite images during one of these events is seen in Fig. 5.5, covering a period of 54 h! It is not difficult to infer the synoptic pattern from this sequence of images. One sees the evidence of a strong subtropical jet stream across Mexico and south Texas, with a series of substantial

Figure 5.5 Series of satellite images showing the evolution of a "super MCS" event, involving a sequence of convective systems passing repeatedly over a confined area during April 1983: (a) 0100 GMT 05 April, (b) 0900 GMT 05 April, (c) 1500 GMT 05 April, (d) 2100 GMT 05 April, (e) 0100 GMT 06 April, (f) 0630 GMT 06 April, (g) 1500 GMT 06 April, (h) 2100 GMT 06 April, (i) 0000 GMT 07 April, and (j) 0700 GMT 07 April.

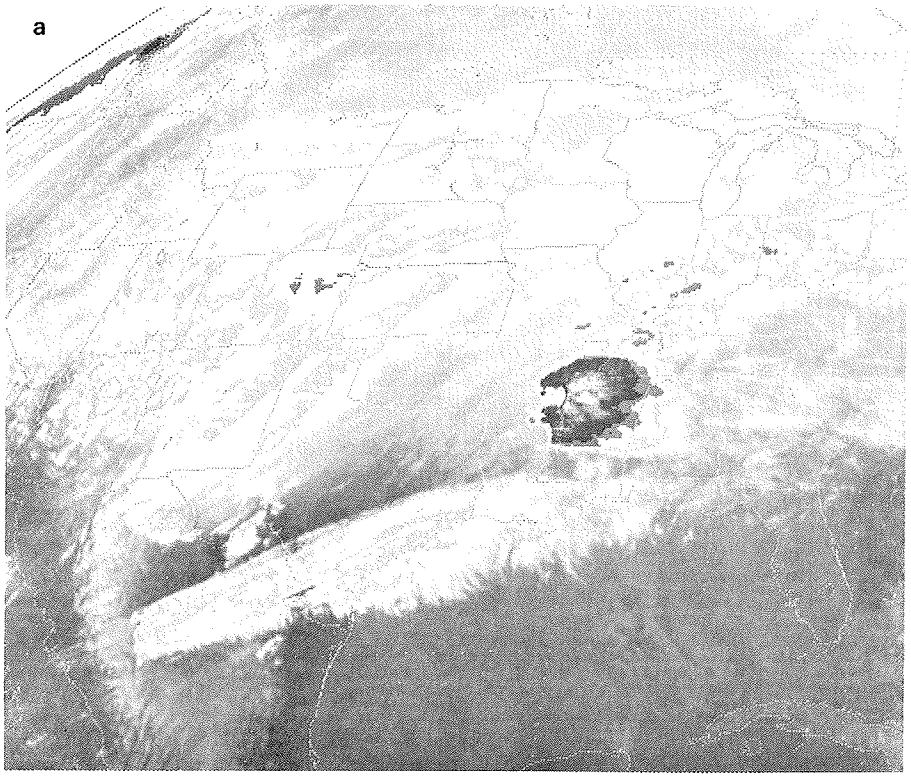
a

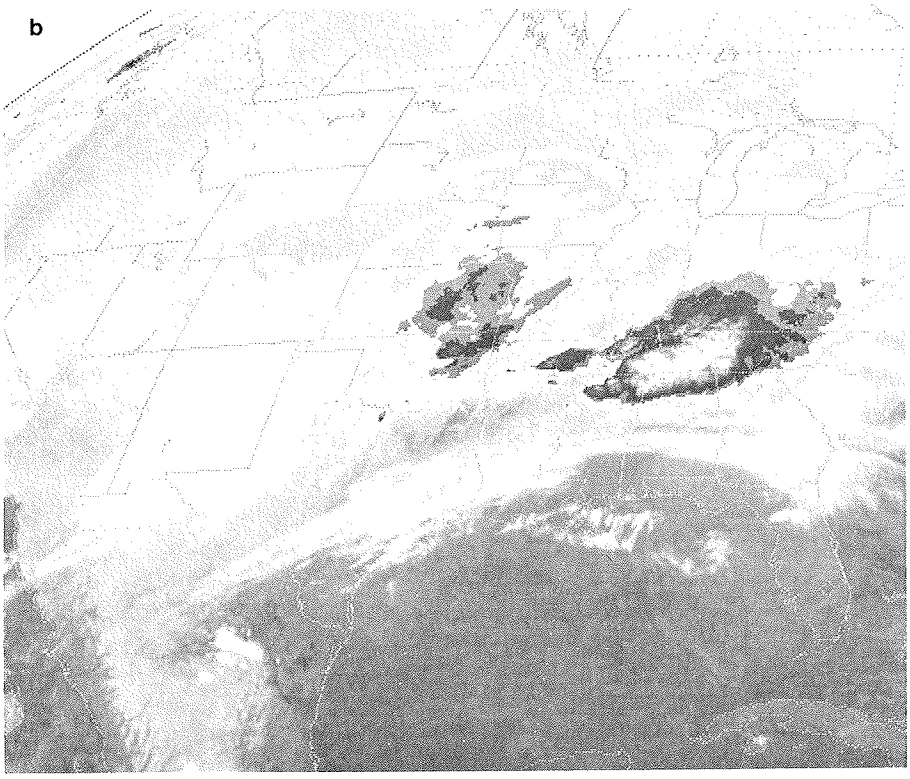
b

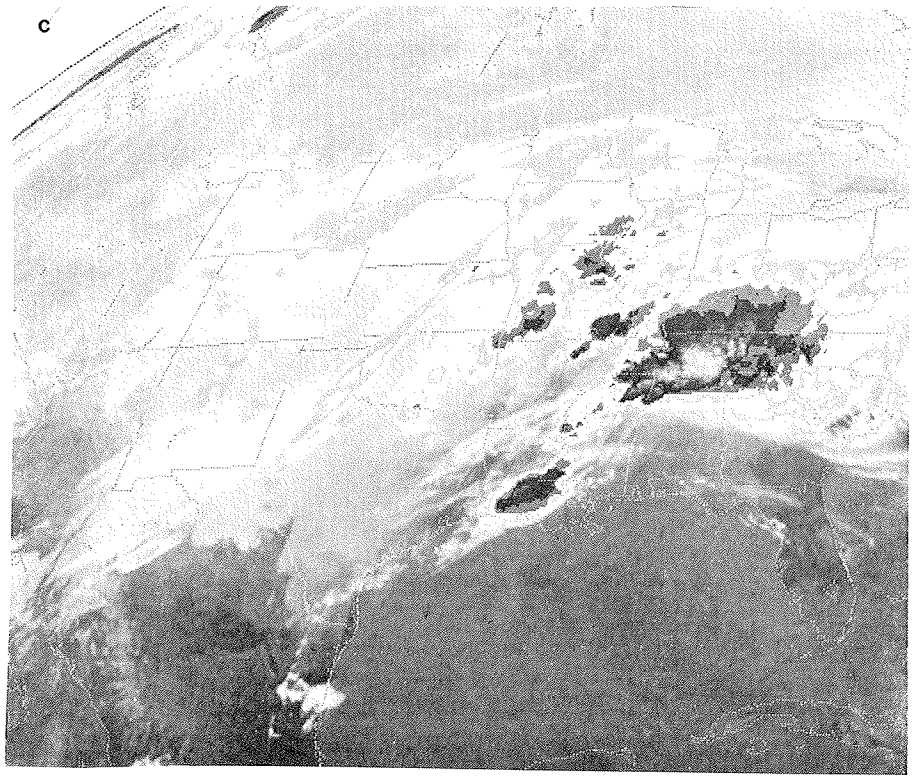
c

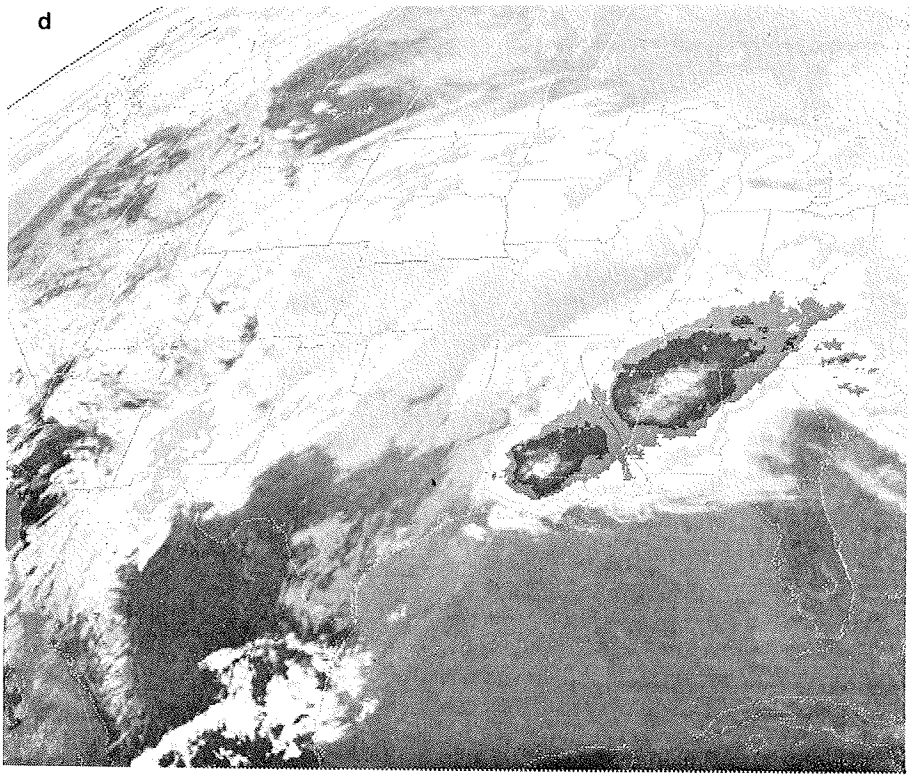
d

e

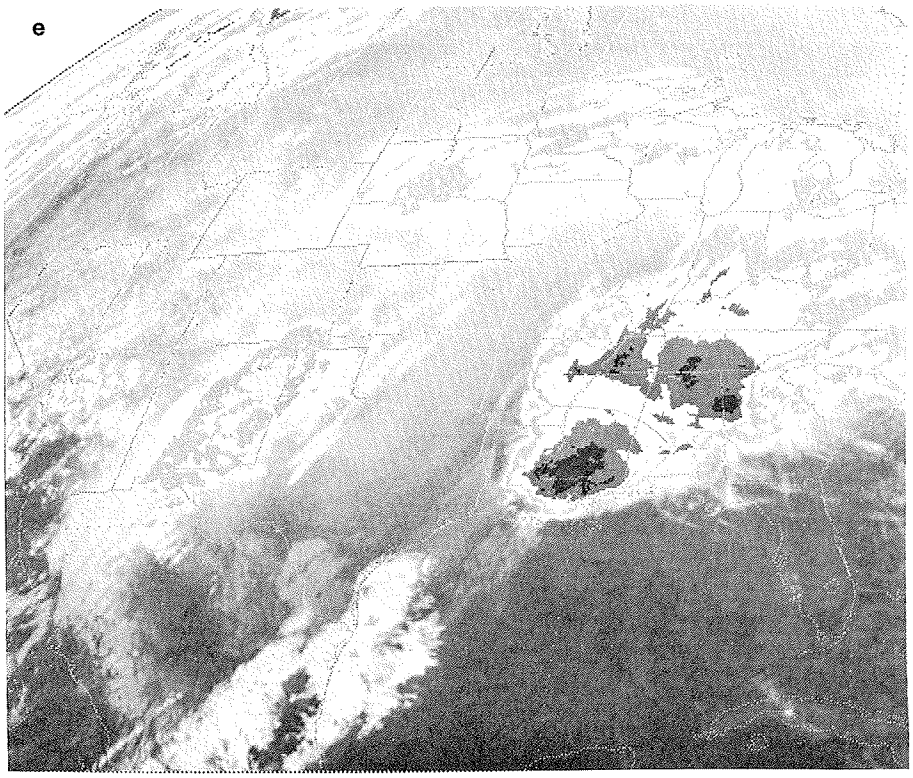

f

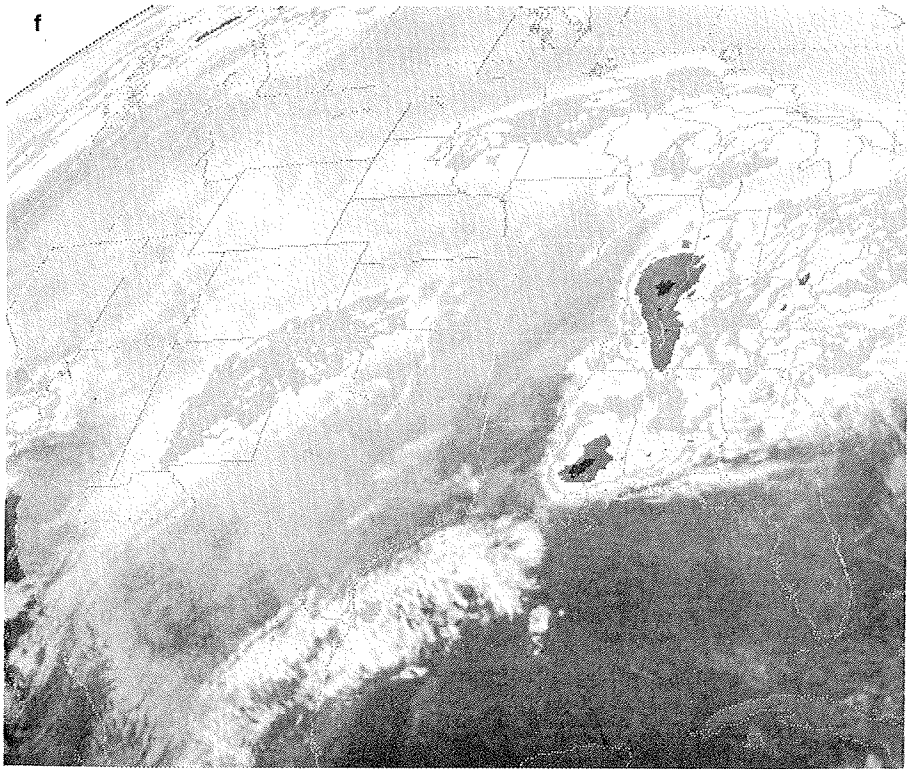

g

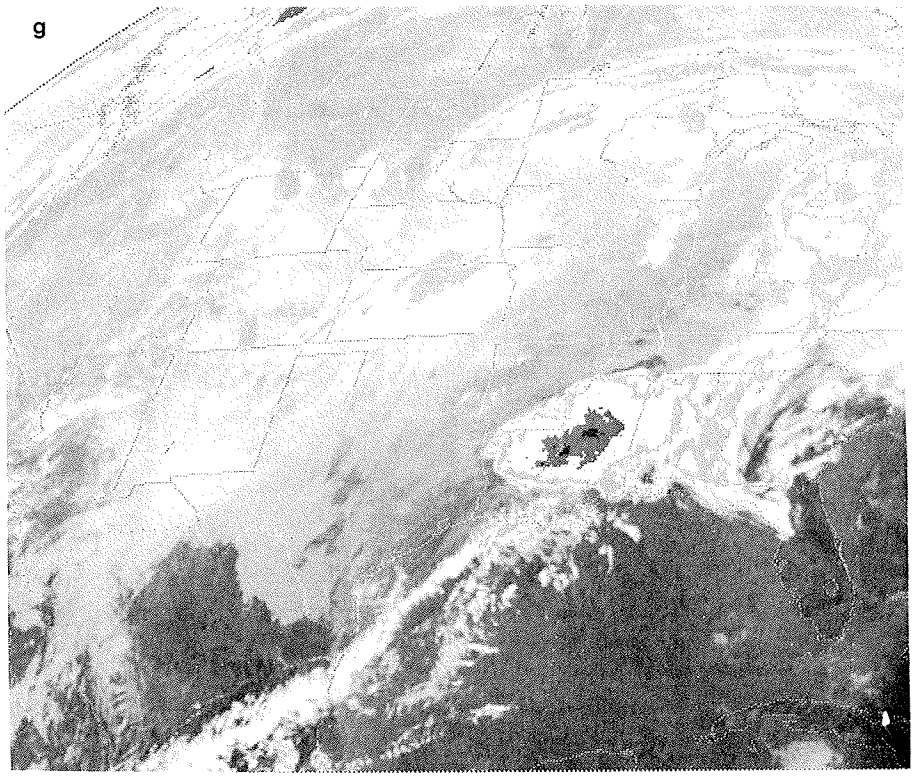

h

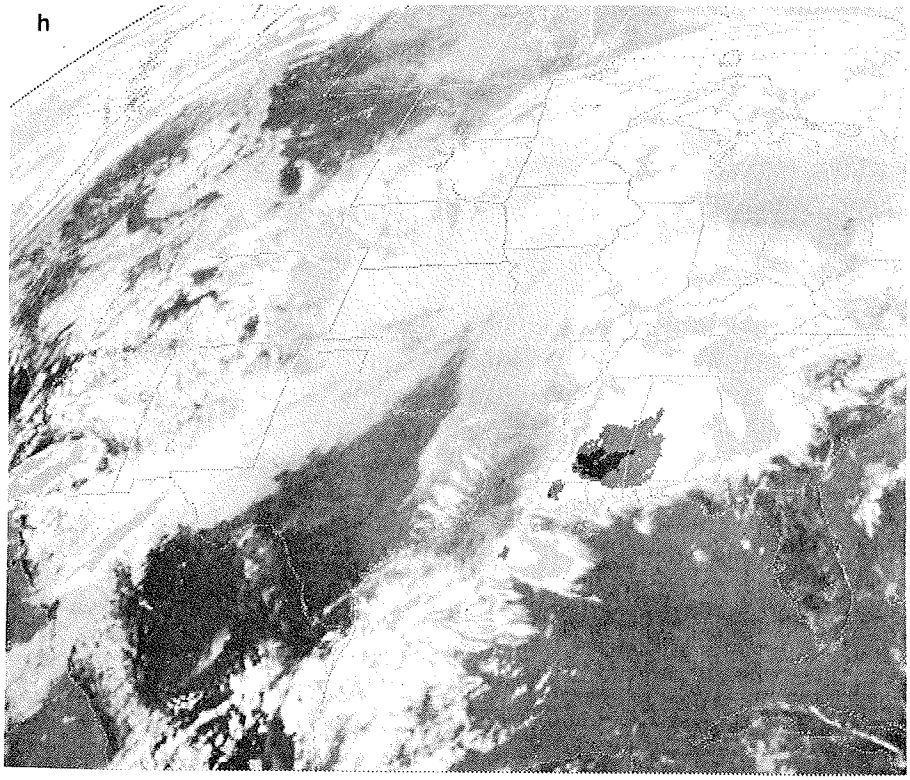

i

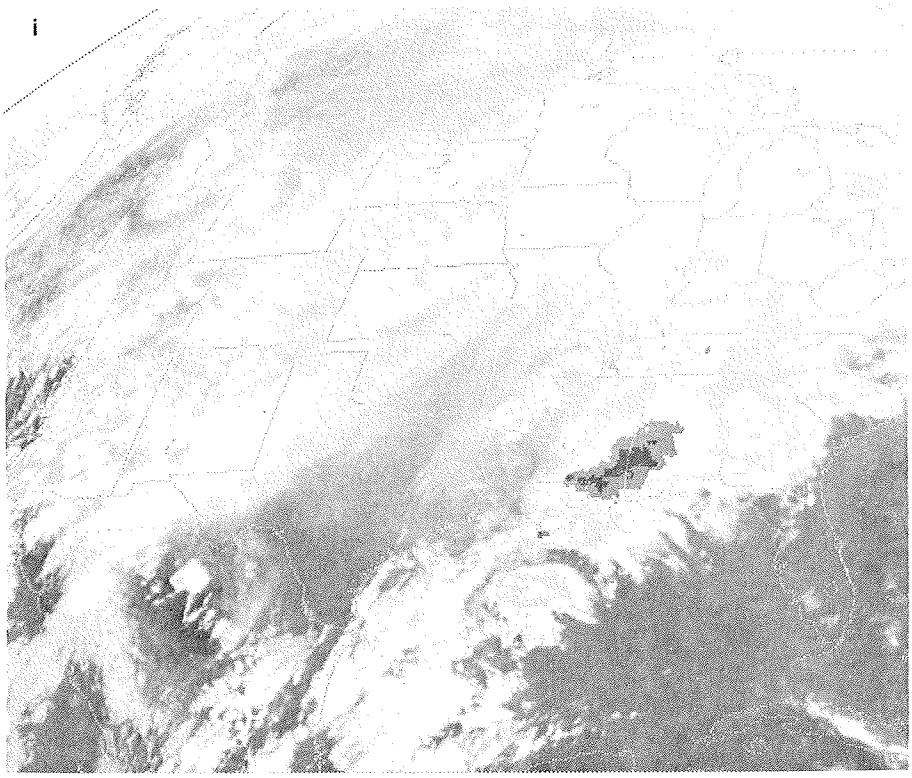

j

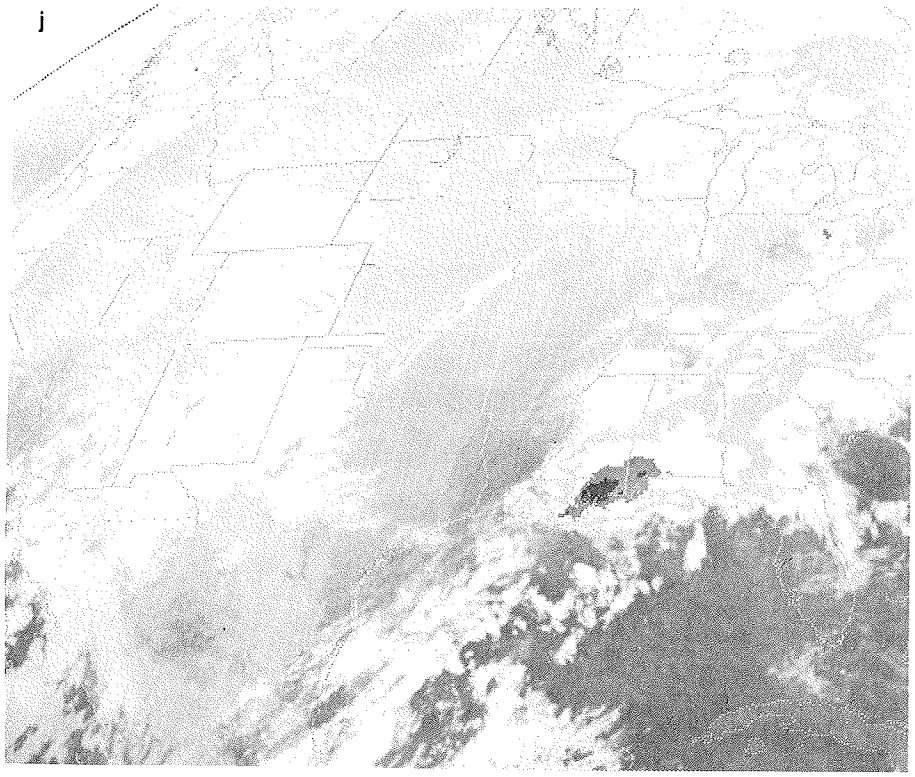

shortwave troughs moving east-northeast from Arizona and New Mexico through the period. As the shortwaves move out, a cold front passes rapidly across Texas and then slows down, becoming quasistationary in Louisiana and Mississippi. Given this situation and the time of the year, it is easy to infer that mid-tropospheric winds are strong but nearly parallel to the front along the Gulf coast.

This situation produced a sequence of convective systems of various types, passing repeatedly over Louisiana and Mississippi. **Storm Data** reveals that flash flooding, river flooding, and severe weather (including tornadoes, hail, and high winds) resulted, with four fatalities from flash flooding in Mississippi. There were 15 counties in Mississippi declared disaster areas.

Thus, even when the component MCSs are relatively fast-moving, the setting can create a quasistationary event. Clearly, the slow-moving synoptic scale front interacted with outflow boundaries laid down by the pre-frontal convection. Strong flow of moist, high-CAPE air off the Gulf of Mexico supplied prodigious amounts of moisture for widespread heavy rain, with local amounts reported up to 14 in as embedded MCSs passed through the overall system.

Such systems can be thought of as a sort of "super MCS," although a detailed study of this class of event has not yet been done. Belville and Stewart (1983) have discussed a localized pattern which appears to fit this model. The example in Fig. 5.5 serves to illustrate the opposite extreme from the rather innocuous synoptic scale setting of a classical MCC. It is not hard to imagine various intermediate forms and variations on the theme. Some of these are mentioned briefly in the next section.

D. Other Types of Quasistationary Convective Events

Some schematic examples of synoptic patterns conducive to slow-moving convective systems are provided by Chappell (1984), although it is not an exhaustive classification. One factor which may be an important controlling influence in producing slow-moving convective systems is topography. There are numerous well-documented examples of this (see, e.g., Maddox **et al.**, 1978; Caracena and Fritsch, 1983; Huang and Schroeder, 1983). It may be proper to consider the role of topography to be one of providing a fixed source of lift which, under the right circumstances, produces the propagation needed to make systems quasistationary. Clearly, topography may be the single most important factor, as perhaps is the case for flash flood events along the Pacific Coast (which may not even be characterized by much CAPE in some situations), and in mountainous terrain.

As pointed out by Grice and Ward (1983), tropical cyclones can create the right environment for heavy precipitation, providing the synoptic pattern which is appropriate in the sense we have described. The case presented by Caracena and Fritsch (1983) is one which includes the effects of a tropical cyclone, as well as being influenced by topography.

Scofield and Spayd (1983) have pointed out that the majority of flash flood events in the eastern U.S. are not associated with classical MCC events. Their classification system suggests that extratropical weather systems are often present, but clearly the resulting MCSs are not fast-moving despite the relatively strong synoptic situation. Topography may well be an important factor, as well as the occasional tropical cyclone.

E. Some Climatological Speculations

Although data exist to produce it, a study comparable to those done for severe thunderstorms providing a climatological evaluation of flash flood events does not yet exist. The available climatological information tends to be rather region-specific (e.g., Maddox **et al.**, 1980b; Guttman and Ezell, 1980). In many such studies, the climatological data base is rather limited, since the historical record is not usually the main thrust. Of course, numerous statistical examinations of rainfall exist (e.g., Rao, 1981), but these tend to be rather esoteric applications of statistical models, especially concerned with mean recurrence intervals (e.g., the so-called "100-year event").

Further, the climatology of **heavy precipitation** is not necessarily identical to that of **flash floods**, owing to a variety of factors (e.g., rainfall rates, topography of the basins, prior rainfall history, etc.). What is even more distressing is the rather arbitrary boundary drawn between flash floods and river floods (Barrett, 1983). Clearly, as the example of a "super MCS" (above) shows, both river floods and flash floods can occur in the same event.[2] Finally, many of the problems with climatological data for severe thunderstorm events also plague the record of flash flood events (i.e., population density biases, uneven reporting procedures, improper perception of the event, etc.).

In any case, we can speculate a bit about the national picture of flash flood climatology, based on the rather uneven climatological analyses available. It is tempting to suggest that the seasonal variation of flash flood events is roughly comparable to that of convection itself. Naturally, there are some obvious cautions to be stated in using this concept. There is reason to believe that regional variations in the climatology exist. For example, on the Pacific Coast, convection is far more common in the cool season, at least in a relative sense, so synoptically-driven convection, with flash flood potential, may depart from the national trend (Dias **et al.**, 1980). As suggested above, the Gulf of Mexico coastal region may have more persistent, slow-moving, intense rainfall events in the spring and fall. The mountainous areas of the country are most likely to have heavy rain events in the summer, or early fall. These do reflect regional variations in the seasonal frequency of convection, to some extent.

Where warm season convection predominates, the tendency for nocturnal heavy rain is well known (Maddox **et al.**, 1979). When convection is driven by synoptic-scale processes, the predominance of nocturnal events is usually less clear. Complicating the study of the diurnal variation is the fact that the rainfall is spread out over a period of hours, with fluctuations in rainfall rate superimposed on the overall storm intensity, whereas severe storm events are usually brief enough to be considered instantaneous, for climatological purposes. It is the combination of rainfall rate and duration which creates flash flood potential, so an event which begins during daylight may proceed well into the night (and perhaps into the next day!).

---

[2] The normal situation is for flash floods to develop in the tributaries, with river flooding resulting from widespread heavy rain, which includes the localized flash flooding.

VI. Computer Simulations of Convective Storms

> The principle of science, the definition, almost, is the following: The test of all knowledge is experiment....Experiment, itself, helps to produce these laws [to be tested], in the sense that it gives us hints....The third way to tell whether our ideas are right is relatively crude but probably the most powerful of them all. That is, by rough approximation.
>
> -- Richard Feynman, **Lectures on Physics**

With the advent of digital computers in the 1950s, it became possible to solve detailed mathematical models of processes involving convection, as well as large-scale weather systems. The major value in developing computer solutions to a set of equations related to convection is the ability to control the conditions. Real clouds are far more complex than even our mathematics can describe, but we derive value from the process by being able to test our hypotheses about clouds in a controlled, even if simulated, "environment". The models are not real clouds, but contain **enough** reality to teach us about convection.

In essence, parcel theory is a simple mathematical convection model, for which non-numerical solutions can be obtained. Prior to the development of computers, it was simply impossible to solve the equations applicable to more complex models than parcel theory. Numerical solutions to the equations are, in actuality, only approximations (as is the case with large-scale forecast models!), but these approximations can, in principle, be made arbitrarily close to an actual solution of the equations. One should also be aware that the equations are approximations, as well. Our physics and mathematics do not yet contain all of reality -- for example, there is no known mathematical description of turbulence. Yet, turbulence is so important in the physics that models must include some sort of approximation to the process in order to work at all realistically. The most essential element of any model (numerical, mathematical, conceptual) is **simplification** -- to contain all of reality is, in some sense, to **be** reality.

It is beyond the scope of this work to provide a comprehensive review of numerical convection models. We provide only a brief sketch of how the numerical simulations have evolved and make some guesses about where they are headed in the near future. A detailed treatment of convection models can be found in Anthes **et al.** (1982).

Broadly speaking, convection models can be grouped by the number of spatial dimensions explicitly used in the simulation, by whether or not the model assumes steady-state conditions, and by what physical aspects of the convection process are emphasized. No complete description, incorporating all the elements involved in convection, is being attempted. Nor is such an all-encompassing model feasible in the foreseeable future. Instead, convection models are designed to consider some specific, limited set of elements. The choices made as to what elements are to be incorporated depend on the modeller's interests and, especially, the modeller's resources.

A. One-Dimensional Models

The first convection (or "cloud") models were not particularly far removed from pure parcel theory. That is, they considered only the vertical equation of motion. In order to reduce the problem of convection to one dimension (i.e., "1-d"), a host of restrictive assumptions must be made. The 1-d cloud models have been mentioned in II.A.2 to a limited extent, during the discussion of "bubble" versus "plume" convection. Both are steady-state models, which consider the forces following a rising parcel of air (i.e., Lagrangian), but each parcel is treated the same as any other. In such models, entrainment is usually made inversely proportional to the cloud radius (where radius is a

variable carried by the model, rather than an actual physical dimension). Examples in addition to those already mentioned can be found in Weinstein (1970), Simpson and Wiggert (1969), and Warner (1970).

Those 1-d models which are time-dependent usually take an Eulerian viewpoint, in which motions are followed along a line of vertically distributed (but fixed) grid points. In such approaches, the governing equations are horizontally averaged to eliminate the other spatial dimensions -- such models are referred to as "1 1/2-d models". Entrainment in these models is treated somewhat differently, since the averaged horizontal motion (allowing for relative inflow/outflow) is included, as well as lateral mixing at the boundary of the cloud. Examples include the models described by Wang (1968), Weinstein (1970), and Lee (1972).

One might be inclined to consider 1-d models of only limited usefulness, owing to the extremely restrictive nature of the necessary assumptions. In many senses, this is true. However, by creating a cloud model which has many essential dynamical characteristics of convection within a very economical framework, it is possible to concentrate on other aspects of convective physics in great detail. For example, Danielson **et al.** (1972) and Ogura and Takahashi (1971) have used 1-d cloud models which include very sophisticated cloud microphysical effects. Also, Kreitzberg and Perkey (1976) have used a 1-d model to account for convective effects embedded within a regional (mesoscale) forecast model. Thus, the 1-d model has a continuing use, in spite of its obvious limitations in convective simulations, proper. See Simpson (1983d) for a recent review of problems and applications of 1-d cloud models.

B. Two-Dimensional Models

The next logical step in convection modeling is to two spatial dimensions (2-d). Such models can also be broken down into steady-state (or, "diagnostic") and time-dependent models. However, since relatively few diagnostic models have been developed (examples include Moncrieff and Green, 1972; Kessler, 1969), this distinction is of less importance. The most significant characteristic of 2-d models is how the second horizontal dimension is suppressed. This is done by assuming symmetry, in two different ways. One is called **slab symmetry**, the other is called **cylindrical symmetry** -- these are illustrated in Fig. 6.1. As shown in Fig. 6.1a, the slab-symmetric model is assumed to lie in an (x,z) coordinate framework, and to have no variation along the y-direction. This symmetry assumption is probably most appropriate for squall lines (see Sasaki, 1959; Hane, 1973) but has been used in a wide variety of other contexts (e.g., Liu and Orville, 1969; Takeda, 1971; Schaefer, 1974; Williams, 1967).

Cylindrical symmetry, as shown in Fig. 6.1b, assumes no variation in properties with azimuth angle (θ), so it is in a (R,z) coordinate system. Models cast in this framework are probably most valid for cumulus clouds (e.g., Ogura, 1963; Lilly, 1964; Ogura and Takahashi, 1971; Wilkins **et al.**, 1974). Naturally, such a system has also been used in other contexts, notably hurricanes (see e.g., Ooyama, 1969; Rosenthal, 1978). Schlesinger (1983a) has compared cylindral and slab symmetric models with respect to their weak and strong points.

In applications, 2-d models are especially useful for situations where their symmetry assumptions are most applicable. Since the assumptions are less restrictive than for 1-d simulations, a broad range of useful applications is possible. However, perhaps the most common recent use for 2-d models is as a testbed for ideas to be explored more fully with 3-d models. As with 1-d models, since the 2-d framework is computationally economical, complexities such as microphysics, entrainment hypotheses, viscous parameterizations, etc., can be tested in a rather realistic model situation

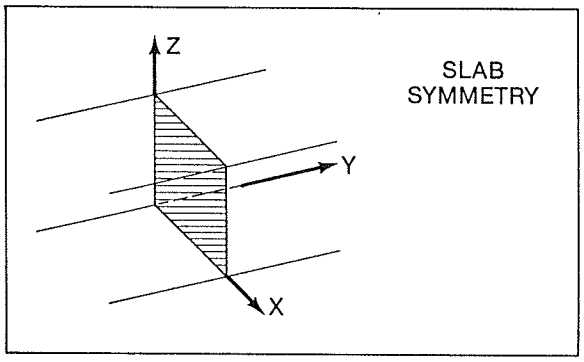

Figure 6.1a Illustration of slab symmetry concept. All variation in the y-direction is suppressed, so simulation in the x-z plane (hatched) applies equally well anywhere on the y-axis.

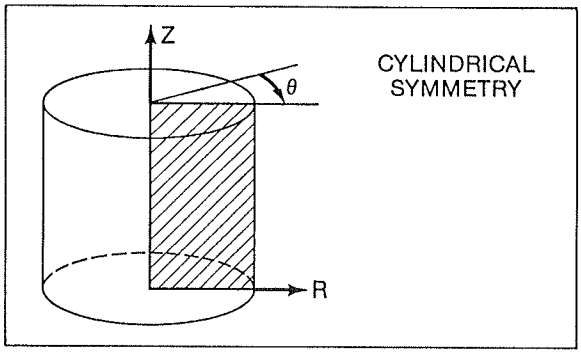

Figure 6.1b Illustration of cylindrical symmetry concept. All variation in the θ-direction is suppressed, so simulation in the R-z plane (hatched) applies equally well for any θ.

without involving all the computer resources needed in a 3-d model. For examples, see Orville and Chen (1982), Schlesinger (1973), Wilhelmson and Ogura (1972), or List and Clark (1973).

In addition, certain exploratory studies dealing with basic concepts of convective storms were done first via 2-d models. For example, Takeda (1971) was among the first to achieve a quasi-steady state cloud simulation, a milestone in studying severe storms. Miller (1974) has examined the validity and applicability of hydrostatic balance in convection with a slab-symmetric 2-d model. Microphysical interactions with 2-d convective circulations have already been mentioned. The influence of terrain has been studied in a 2-d system by Orville and Sloan (1970). The numerical simulation of squall lines continues to be quite productive within the 2-d framework, as seen in Thorpe **et al.** (1982).

C. Three-Dimensional Models

Many of the aspects of convection require a fully 3-dimensional simulation. As we have seen (III.F.2.e, above), supercells most frequently occur within environments having both directional and speed shear. Deduced circulations in such storms are clearly asymmetric, as are the spatial distributions of all the variables. Thus, it has been a long-awaited goal of convection modelling to achieve a full 3-d simulation. During the past decade, this goal finally has been realized. Schlesinger (1982, 1983a) has given an excellent summary of 3-d modeling and some of the motivations for adding the third spatial dimension (i.e., weaknesses of 2-d models).

While computer resources to develop a 1-d or 2-d model are within the grasp of most research facilities, a 3-d simulation requires much more computing power than most facilities possess. Thus, 3-d modelling has been done by relatively few. Even with

the enormous power of today's supercomputers, 3-d model runs are barely capable of simulating convection in a near-real time fashion -- i.e., it takes on the order of an hour to simulate a thunderstorm process of, say, 2 h real duration. Two major efforts in 3-d storm modeling are at the University of Wisconsin (Schlesinger, 1975, 1978, 1980, 1983b) and jointly at the University of Illinois and the National Center for Atmospheric Research (Wilhelmson, 1974; Klemp and Wilhelmson, 1978a,b; Weisman and Klemp, 1982; Droegemeier and Wilhelmson, 1983).

To summarize the state of convective simulations to date, it is safe to say that considerable progress has been made. When comparing model storms with observations (Schlesinger, 1982; Klemp and Wilhelmson, 1978b; Klemp and Rotunno, 1983; etc.), the models have become remarkably realistic. Such processes as mesocyclone development, storm splitting, and re-development of new convection have all been demonstrated in the simulations.

To illustrate how far the simulations have advanced, consider Figs. 6.2-6.7, which show some of the variety of solutions obtained, as a function of the wind profile characteristics. All these model runs have the same CAPE, and are initialized in the same fashion. Figure 6.2 is for a weak-shear environment, which produces a short-lived multicell storm.

In Fig. 6.3, the hodograph has twice the shear strength of that in Fig. 6.2, and the result is a storm closely resembling a supercell at the end of a line of multicellular storms. When the hodograph is a straight line between 2.5 and 5.0 km, as in Fig. 6.4, the simulation resembles a splitting storm pair, with the right-moving cell slightly dominant. This trend continues in Fig. 6.5, where the straight-line hodograph extends to 7.5 km.

For Fig. 6.6, the shear is strong, but only in a shallow layer (to 2.5 km). This yields an evolution which looks like a squall line. Note that the surface gust front ends up well in front of the echoes. With the same profile as in Fig. 6.6, but with 50% more shear strength, a squall line develops which is substantially stronger, and is beginning to show some "bow echo"-like features (Fig. 6.7). In this latter case, the gust front is much closer to the storm cores.

Numerical storm models allow researchers to learn more about how the basic factors present in convective weather interact to produce observed effects. Concepts of how these interactions proceed can be tested and revised. Further, it has recently been proposed that Doppler wind observations can be combined with model equations (e.g., Bonesteele and Lin, 1978; Gal-Chen, 1978; Hane **et al.**, 1981) to yield information about unobserved variables within the storm, like pressure and temperature. This may allow scientists to understand how the pressure and temperature fields inside a thunderstorm evolve and produce the observed changes in the flow field.

As progress in the technology of computers proceeds, it should be possible to include more and more realistic physics into the models. For example, most model storms are "kicked off" by physically unrealistic initial conditions -- usually a warm (and/or moist) "bubble" at low levels. This may eventually give way to a more realistic initiation by low-level convergence on a scale much larger than the storm itself. Thus, it may be possible to calculate more explicitly how the storm is influenced by its complex mesoscale environment (and vice-versa). Since it often is observed that storms are modified by pre-existing mesoscale phenomena (not just those produced by other convective storms), this is an important facet of the simulation process, but which has yet to be explored.

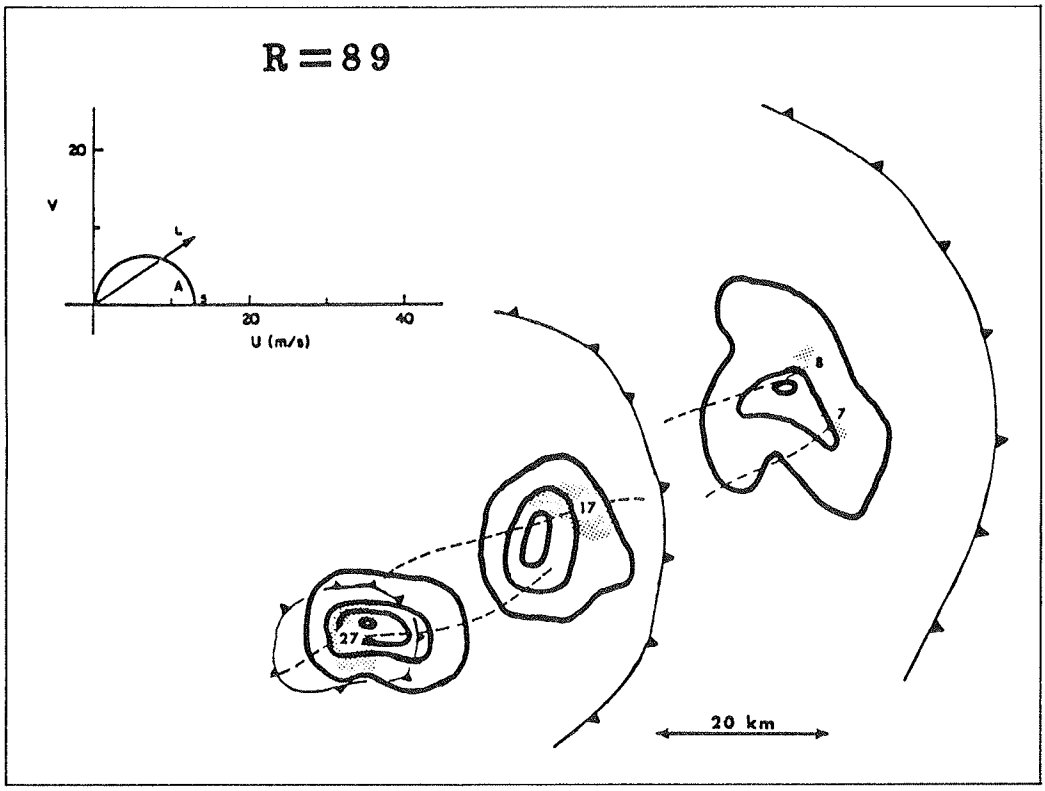

Figure 6.2 Numerical simulation of convective storms developing in an environment with a hodograph as indicated in upper left. Successive pictures of the storm are at 40, 80, and 120 min into the simulation. Solid contours are of rainwater (roughly akin to radar reflectivity) at 2 g kg^{-1} intervals, shading indicates mid-level (4.6 km) updraft exceeding 5 m s^{-1}, while the frontal symbols are applied to the gust front (defined in the model by the -1 °C temperature perturbation). The path of each updraft is indicated by a dashed line, while the numbers plotted at the updraft centers represent the maximum vertical velocity with the cell at the given time (from Weisman and Klemp, 1984b)

Further, many details of the tornadogenesis process remain only poorly understood. Observations (e.g., Lemon and Doswell, 1979) have been unable to resolve which, if any, of the crop of currently existing theories are valid, or upon what circumstances their validity depends. Newer, more complex 3-d models may provide important clues (see e.g., Klemp and Rotunno, 1982).

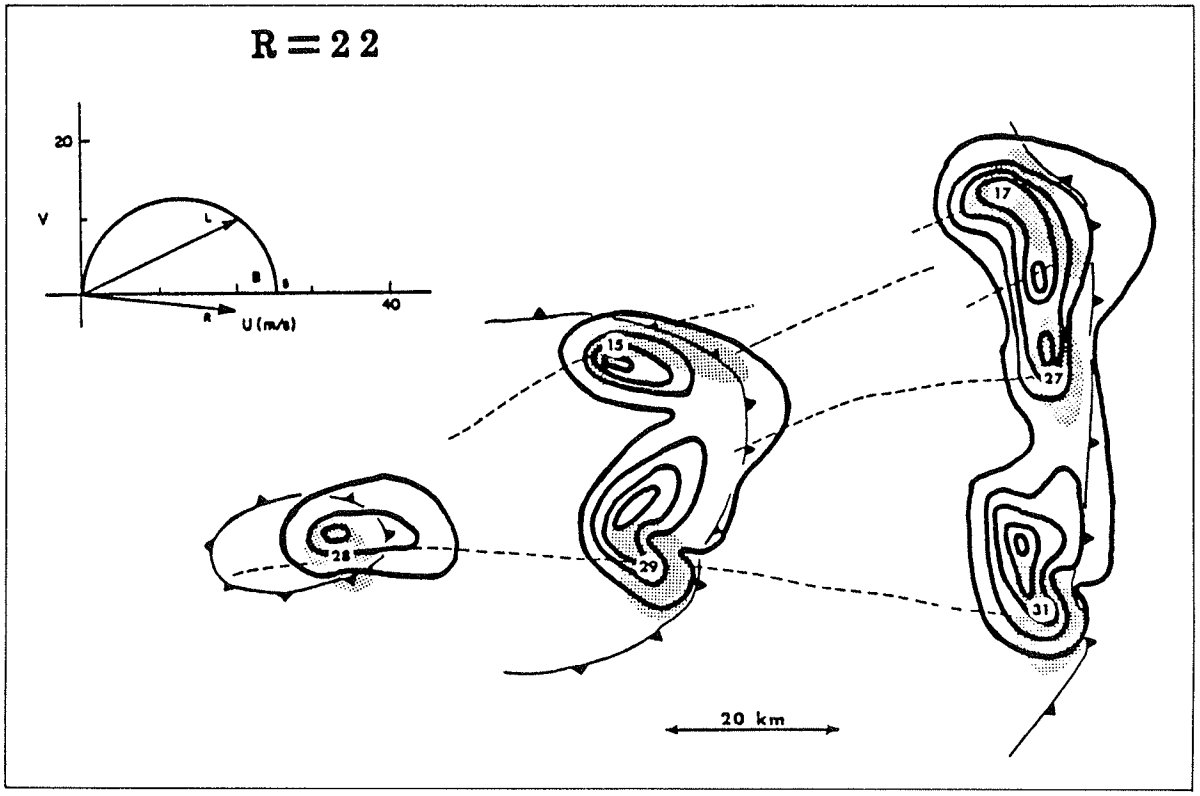

Figure 6.3 As in Fig. 6.2, with a different hodograph, as indicated in upper left corner.

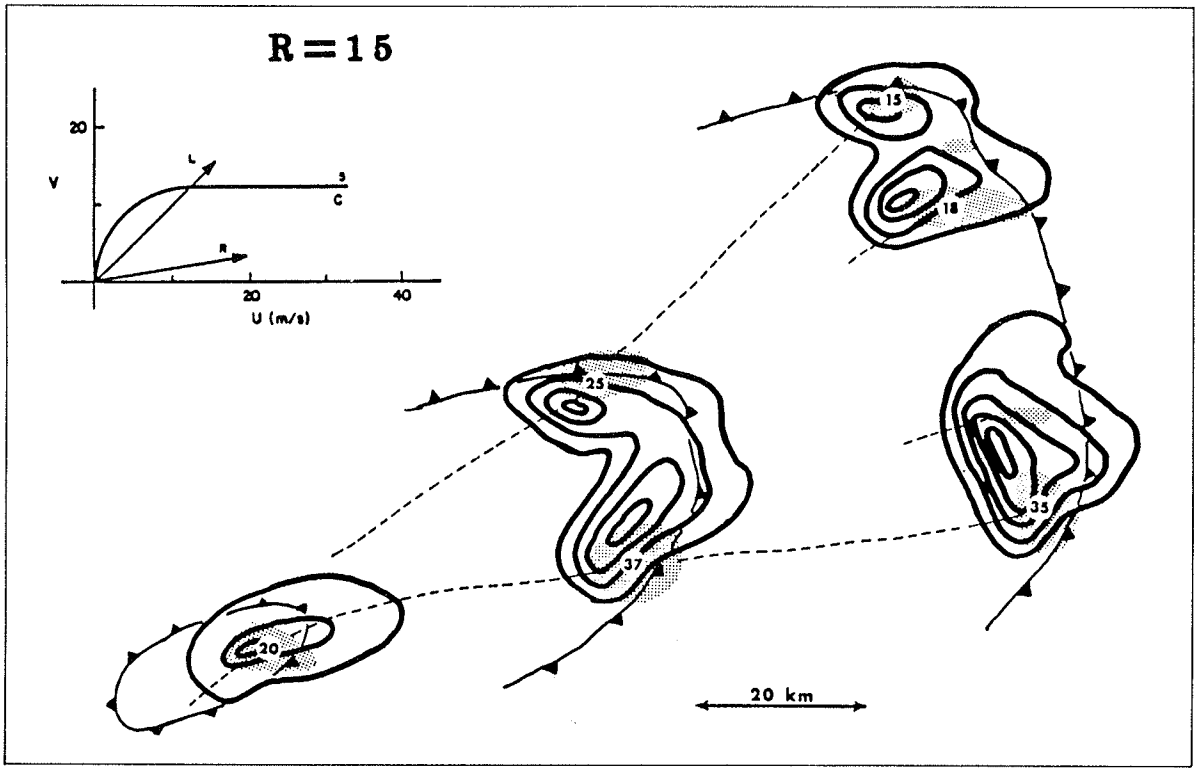

Figure 6.4 As in Fig. 6.3.

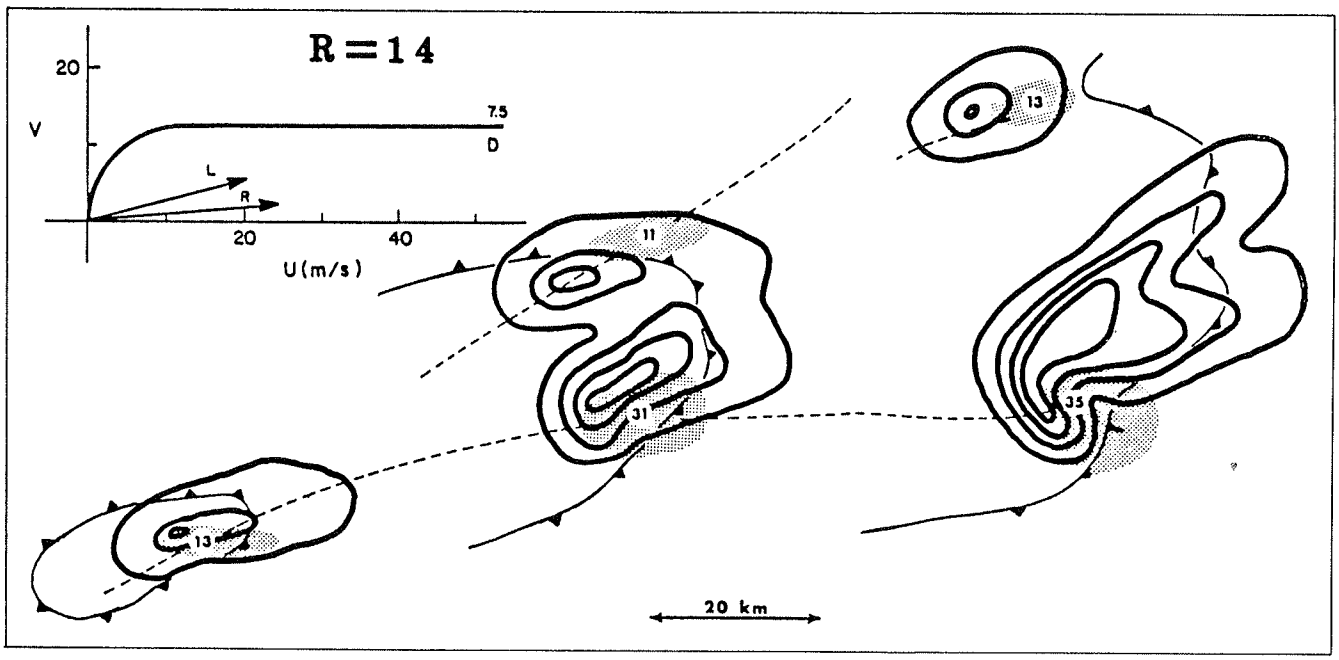

Figure 6.5 As in Fig. 6.3.

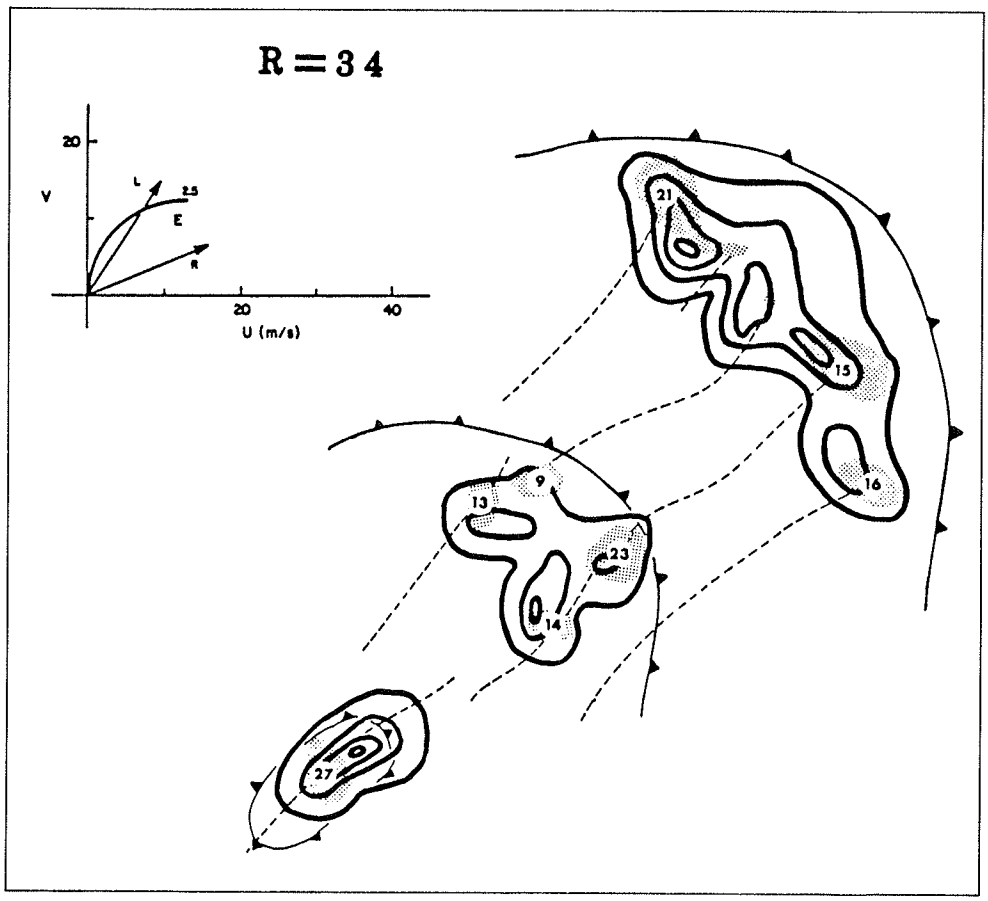

Figure 6.6 As in Fig. 6.3.

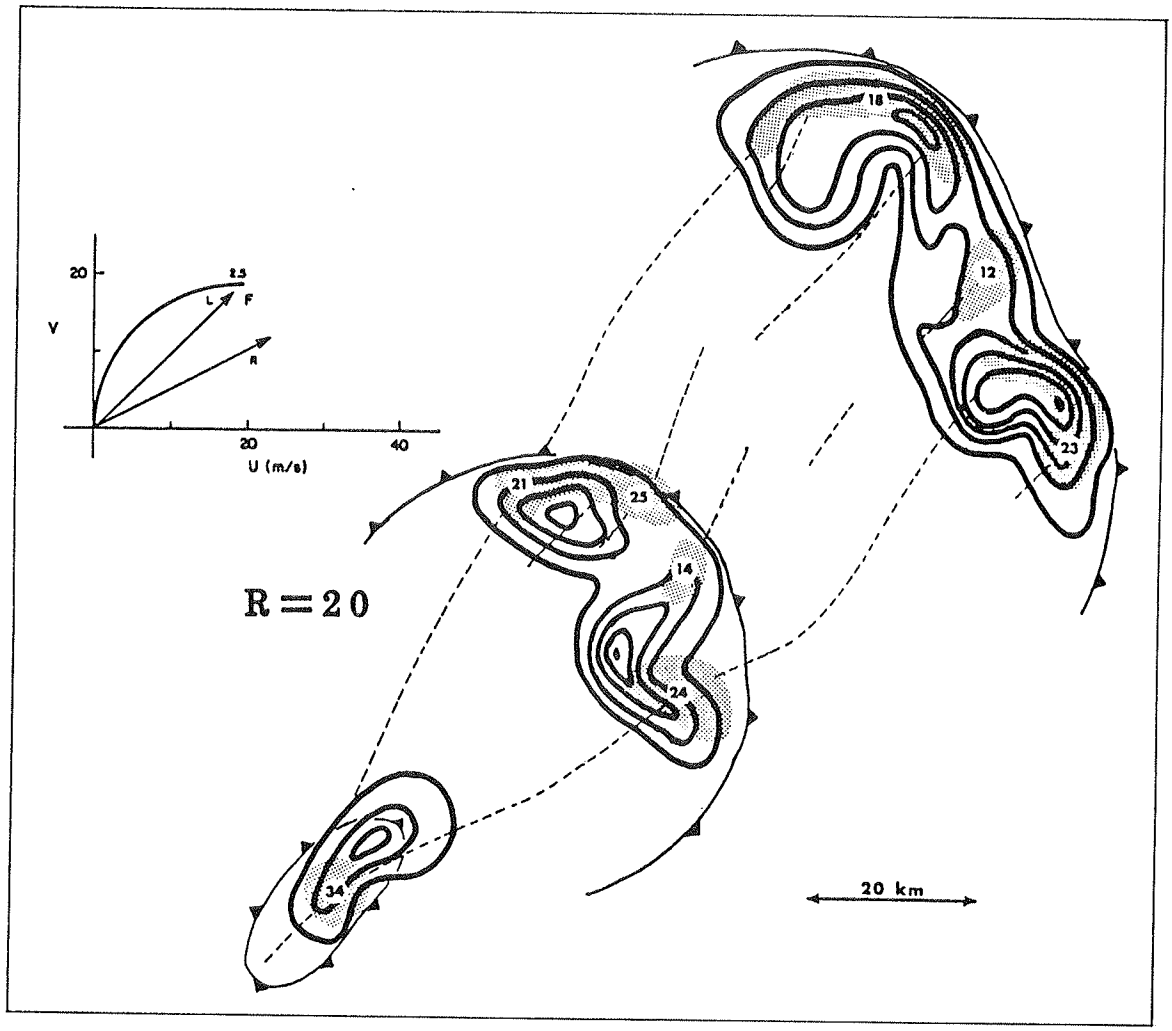

Figure 6.7 As in Fig. 6.3.

D. Discussion of Modeling Results

Several times in the chapters above, attention has been drawn to aspects of convection which have been especially difficult to resolve without numerical simulation. These include: origins of tornadic vorticity, storm motion, and interactions between the convective circulations and their immediate environment. The nature of these issues (and others, of course) makes it very difficult to use "thought experiments" to provide answers to the questions. The reason that thought experiments have proven so ineffective is that the physical processes involve complicated, nonlinear interactions.

As an example, consider the pressure effects within convective systems. These have proven quite difficult to observe, so we have little direct evidence about how pressure is distributed within and near convection. It is tempting to "assume the problem away" -- i.e., to assume that the nasty things we don't observe aren't important. Yet, we have indirect evidence (e.g., the lifting of negatively buoyant air at low levels in a supercell) that such an assumption is not always valid. Weisman and Klemp (1984a) have found, for instance, that in supercell-like storm simulations, the dynamic pressure effects can contribute more to parcel vertical motion than buoyancy! It is difficult to imagine how quantitative evidence of this important process could have been obtained without numerical simulations.

Notions of how storms move have been profoundly changed by having realistic convection models. We have drawn attention to the "obstacle" model and suggested that it is not entirely satisfactory. Once again, just thinking about the problem has not provided us with the quantitative justification (or refutation) of the obstacle model. By using the simulations to evaluate the quantitative impact of the various physical processes, it has been possible to replace the obstacle model with one which is consistent with the observations but which is also physically plausible. This improved model has been presented by Rotunno and Klemp (1982, 1985). By moving parcels vertically, the convection sets up momentum gradients which, in turn, produce dynamic pressure forces. At certain levels in the storm, the result is flows which look like flow around an obstacle, but which arise in a rather different manner.

Similarly, the numerical simulations have suggested that the **rotating** obstacle model also has limitations in explaining deviate storm motion. Once again, the behavior of simulated storms suggests that the coupling of rotation and verical motion can induce dynamic processes which give storm motions appearing to result from "lift" owing to a rotating obstacle.

Finally, theories of tornadogenesis have evolved considerably in recent times as a result of modelling efforts. Once scientific thought moved beyond the simple convergence of ambient vorticity model, the range of possibilities became rather wide. While the visual and Doppler radar observations could be used to make suggestions, it has been the numerical simulations which have allowed a gradual sifting and winnowing of those ideas. The process of establishing a completely satisfactory theory of tornadogenesis is not yet finished, and may never be, of course.

Interestingly, once theories have been tested via numerical simulations which include complex, nonlinear processes, it often is possible to construct relatively simple new theories. That linear theory can evolve from nonlinear computations is an important side benefit of numerical simulation. It is hard to think in nonlinear terms -- that is why the "thought experiment" can be misleading (although not without value). Given a better understanding gained from the quantitative experiments, it may be possible to capture the essence with a linear theory and so provide new insights. Naturally, the whole process can work the opposite way, going from simple theory to the more complex.

Numerical models are probably most wisely used in an **interactive** mode. That is, they can be employed to test theories and to imply how to go about making observations to verify those theories (e.g., see Schlesinger, 1983b). Then, with the theories in mind and the model simulations in hand, new observations can lead to improvements and modifications in the numerical models. This is, in effect, how the scientific method works -- a constant interplay between models (numerical, theoretical, conceptual, etc.) and observations which allows the continuing refinement of both to produce ever deeper understanding.

VII. Thunderstorm Electricity

> A dark and most dismal cloud...occasioned the most awful sensations in the minds of the most hardy and courageous; our zenith and horizon was almost as dark as at midnight, the lightning streaking the clouds and frequently piercing the earth....The lightning struck a number of buildings, set fire to a barn or two and consumed them to the ground; a dwelling house belonging to Mr. Bower, was pierced by the lightning and considerably injured; Mr. Bower very narrowly escaped the flash; the shock struck him down, unfortunately falling on a wash tub, was considerably hurt....It is earnestly hoped that the inhabitants of this village, will take warning and guard themselves against lightning, that dreadful element, by furnishing their buildings with lightning rods....
>
> -- **New York Post**, 11 July 1808

A. Charge Production and Separation

Lightning, and the thunder which results from it, are the basic elements which distinguish a thunderstorm from a shower.[1] Electrical effects can be seen under a wide variety of circumstances (dust storms, volcanic eruptions, static discharges when walking across a rug, etc.). However, by far the most common form of significant atmospheric electricity is lightning produced by thunderstorms. Large static charges are developed in association with the processes involved in convection. These static charges result in large electrical fields. Once the gradients become strong enough, the normally insulating properties of the atmosphere break down and a lightning flash occurs.

Why do such large charge build-ups occur almost exclusively in convective storms? This is equivalent to asking how convection produces such concentrations of electrical charge. Perhaps somewhat surprisingly, a completely satisfactory explanation remains elusive. There is a variety of competing theories which seem to apply under certain circumstances (Lhermitte and Williams, 1983) and it may well be that most, if not all, such theories are valid under appropriate conditions.

It is neither possible nor desirable to detail here these competitive theories for thunderstorm electrification. Rather, this work outlines briefly what is observed and takes what is hoped to be a reasonable middle ground in explaining the observations. Review articles concerning thunderstorm electrification can be found in Moore and Vonnegut (1977), Uman (1969) and Lhermitte and Williams (1983).

The logical place to begin is the so-called "fair weather electrical field". Even in the absence of convection, there exists an atmospheric electrical field. Basically, the earth's surface is negatively charged with respect to the atmosphere, so by convention the field points downward (from positive to negative). A weak electrical current results from this field. It is weak because the atmosphere is a good insulator (low conductivity). Near the surface, the electric field is over 100 v m^{-1}, decreasing to about 5 volts m^{-1} at 10 km heights. The fair-weather current stays roughly constant with height since the conductivity increases with height while the electric field decreases. These findings are shown schematically in Fig. 7.1.

---

[1] The use of the term "thundershower" is hard to understand. Huschke (1959) does not include it and it is not at all obvious how it differs from "thunderstorm". It is widely perceived as a **weak** thunderstorm, but the distinction is not clearly defined. Its use is heartily discouraged.

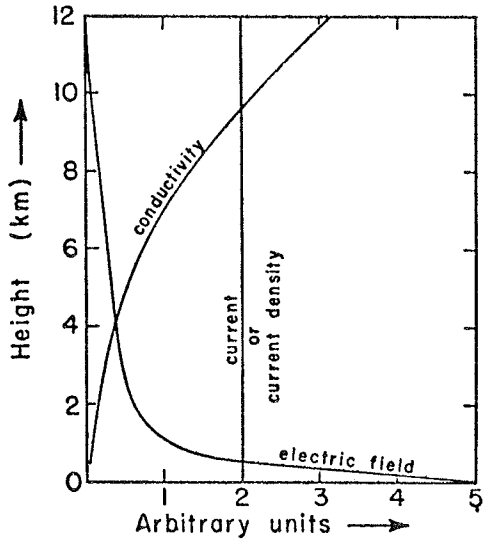

Figure 7.1 Schematic representation of the various parameters of the atmosphere's fair weather electrical state as a function of elevation (from Johnson, 1954, p. 290).

As convection develops, clouds are observed to become electrified near the time precipitation forms (Moore and Vonnegut, 1977). Visible flashes usually commence near the same time, late in the towering cumulus stage in cell growth. Note that some time (several minutes) may elapse before the onset of precipitation at the surface, so flashes often begin before surface precipitation is observed. This suggests that the mechanisms of charge separation which produce the large electrical fields in thunderstorms depend in some way on the precipitation particles within the cloud. It is also noteworthy that stable precipitation associated with synoptic-scale (weak) vertical motions normally is not accompanied by lightning and thunder. That is, the strong up- and downdrafts in convective storms must somehow enhance the charge separation process accompanying the formation of precipitation. On the other hand, intense precipitation is not **always** accompanied by lightning activity.

Convection in the tropics, where the entire depth of the cloud may be at temperatures above freezing, also can produce lightning. However, the most electrically active convection seems to occur with mid-latitude thunderstorms, where the upper portions of the cloud are well above the freezing level. Observations of the charge distribution in a thundercloud are summarized in Fig. 7.2. The upper portion generally is positively charged while the lower is mostly negative. There are some limited observations of a low-level center of positive charge in (or near) the area of heaviest precipitation.

Recently, Rust **et al.** (1981) have documented the occurrence of cloud-to-ground (CG) lightning strokes that carry positive charge to ground, in contrast to the more normal CG strokes that lower negative charge. Their observations in severe storms are that the CG flashes in the rain area are almost invariably negative, but that positive CG's can occur from the wall cloud (which is often near the precipitation core), and from the anvil. Figure 7.3 summarizes these findings. Such observations suggest that the charge distribution can be considerably more complex than implied by Fig. 7.2.

Upon examination of Fig. 7.2, one notes that the ground takes on the opposite charge to that at the storm's base. The presence of the charges at cloud base (usually negative) repels the same charge at the surface, leaving a surplus of the opposite charge at the ground. This is called charging by **induction.** That is, the presence of a charged body induces a region of opposite charge (by repulsion of similar charges), when the bodies are brought together.

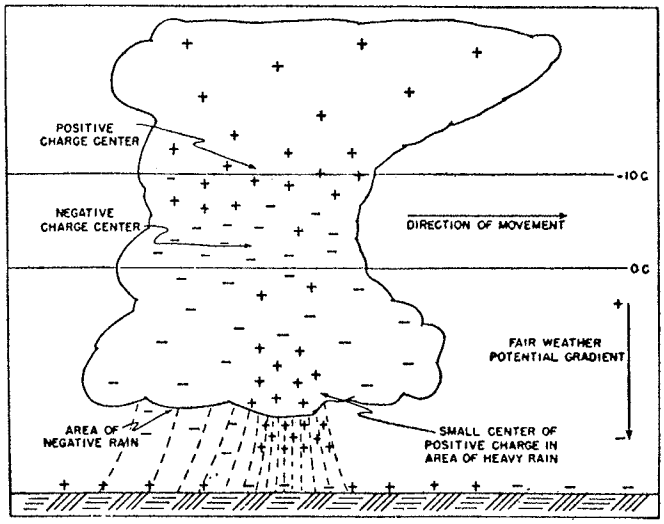

Figure 7.2 The distribution of electrical charges in a mature thunderstorm cell (from Byers and Braham, 1949).

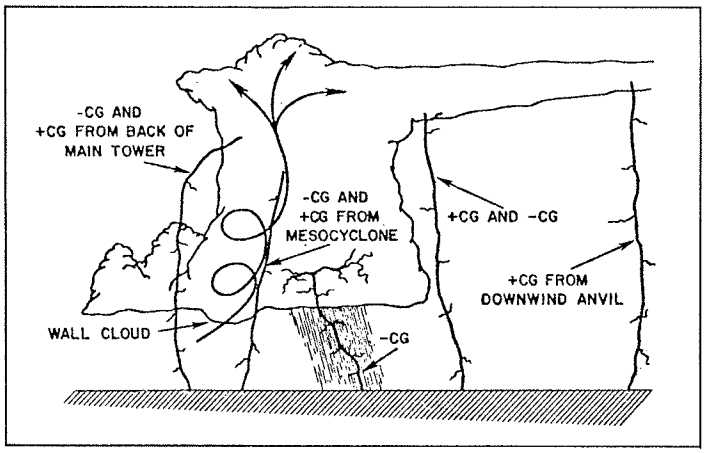

Figure 7.3 Sketch of observed locations and polarities of CG flashes from severe thunderstorms. The spiral denotes the region of intense updraft and rotation. Only negative CG flashes have been observed in the precipitation core. The +CG flashes seem to constitute only a very small percentage of the total flashes to ground (from Rust ***et al.****, 1981).*

It is generally accepted that the net negative charge at the surface and the fair weather field are the result of world-wide thunderstorm activity. This activity is dominated by CG strokes which carry negative charge to ground. One hypothesis about the mechanism of charge separation in a thundercloud is that the fair weather field induces charges on precipitation particles, which are then separated by collisions and particle shattering in the cloud. This is the induction hypothesis.

The main competing theory to induction is a **non-inductive** one. Charge separation in a non-inductive process requires the existence of ice phase precipitation particles. While the details are not described here, non-inductive charging depends on the physical properties of ice, especially as ice particles interact with liquid water or other ice particles.

So which one is responsible? As with many questions of this sort, the answer (as proposed by Kuettner **et al.**, 1981; see also Latham, 1981) seems to be that both are correct. Certainly, the non-inductive process cannot produce thunderstorms in clouds which remain below the freezing level. Further, the non-inductive mechanism alone seems incapable of producing fields strong enough to result in lightning discharges. Rather, it appears that in cold clouds (i.e., those which penetrate the freezing level) the inductive process operates on charges produced in part by the non-inductive mechanism. This explanation seems to allow fields of the observed strength to develop in time periods comparable to what is seen in real storms. Combining the inductive with the non-inductive charging mechanisms seems to be a reasonable hypothesis. However, charge production in warm clouds (those **without** ice phase particles) is not accounted for by this hypothesis. Clarification awaits further research in this area.

B. The Cloud-to-Ground Lightning Stroke

The actual discharge of electricity which relieves the very large charge build-ups is a fairly complicated process. Krider and Alejandro (1983) have given an excellent summary of the process. It has been noted that air is not a very good conductor of electricity. The very strong voltage gradient literally seeks the proverbial "path of least resistance". Consider the typical situation of a negatively charged cloud base over flat terrain with a positive charge. When the electric field reaches breakdown strength (about 10^6 v m^{-1}!), a **step leader** (Fig. 7.4) begins.

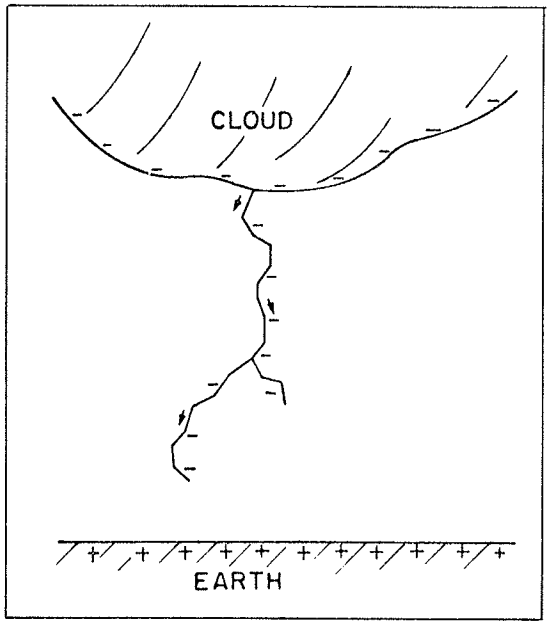

*Figure 7.4 The formation of the "step leader" (from Feynman **et al.**, 1964).*

The step leader is essentially a cascade of charged particles (called a "plasma" by physicists), which moves downward rather quickly -- roughly 2×10^5 m s^{-1}. However, its downward movement is in fits and starts. Typically, the step leader travels about 50 m at a time, pausing for about 50×10^{-6} s (50 μs) before starting again. This process is generally invisible to the naked eye, in part because of its speed and also because the step leader is not very bright -- the total charge carried by the step leader is not great. The step leader may branch several times, seeking a path of minimal electrical resistance. Most of these branches never reach the ground.

As it approaches the ground, a surface-based leader rises up to meet the step leader. There may be more than one such surface-based leader and it is not obvious which may be the one to join the step leader (Krider and Alejandro, 1983). When they meet a short distance above the surface, the circuit is completed. Then, the **return stroke** can occur (Fig. 7.5) and the enormous potential is released by charge running along the path created by the step leader. The return stroke propagates along the path very quickly -- roughly 10^8 m s^{-1}. Owing to the huge voltages involved, this creates tremendous heat and light. In physical terms, the return stroke is a **wavefront** with very high field strength, which carries ground potential (+) up the step leader path. The excess negative charge of the leader channel is lowered to earth in the conducting channel left in the wake of the return stroke (see Uman, 1969, p. 8).

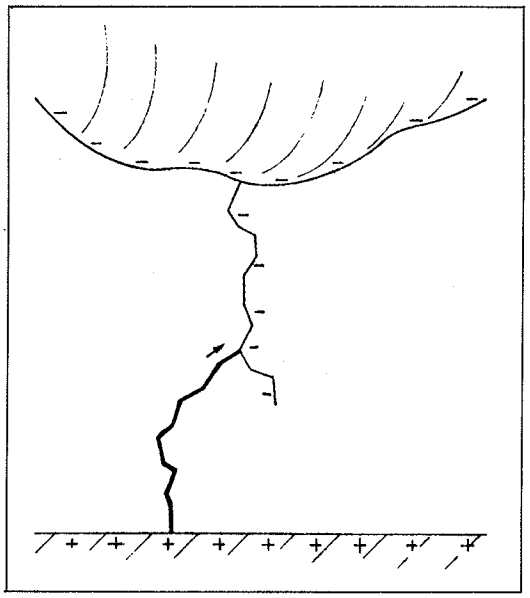

Figure 7.5 The return lightning stroke runs back up the path made by the leader (from Feynman ***et al.****, 1964).*

In many lightning strokes, there are several flashes along the same path, sometimes as many as 20 or so, but usually around 2 to 5 times. In multiple strokes, a **dart leader** comes down after the first return stroke. It travels very quickly because the path created by the step leader and first return stroke is still the easiest path. When this dart leader touches the surface, another return stroke flashes along the path. The time between these strokes varies from 20 to 200 ms. If the intervals are long enough and there are several strokes, the unaided eye can see the lightning flicker.

Naturally, lightning discharges also take place from one part of the cloud to another, from within the cloud out into the air surrounding it, and often spectacularly within and from the anvil cloud. All of these result from complexities in the charge distribution. Intracloud flashes do not appear to involve currents as large as those to ground.

C. Storms and Lightning

1. Observations

The following represents the accumulation of many years of my personal storm observations. As such, it is not intended to represent any conclusive scientific

viewpoint. Rather, the discussions are intended to familiarize the readers with these observations. I have been interested in lightning photography, which allows one to document the gross observations of how lightning is distributed in thunderstorms. Of course, the internal flashes (or the intracloud portions of flashes) are not precisely located with respect to the storm, compared with flashes exterior to the cloud. Basically, lightning photography is accomplished by holding the camera's shutter open until one or more flashes are recorded -- exposure factors are determined by experience.[2]

A developing thunderstorm is relatively inactive with lightning -- it is not until the early mature stage that lightning becomes frequent. Usually, the first lightning is within the cloud at relatively great heights. These flashes are useful in that they reveal the cloud structure, but flashes outside the cloud are infrequent, as are CG strokes.

After attaining the mature stage, CG flashes increase rapidly. They tend to cluster within and near the precipitation region. When observing the storm from relatively great distances, CG strokes may be observed to leave the cumulonimbus storm tower at fairly high levels, travelling downward mostly outside the cloud (Fig. 7.6). They can also reach

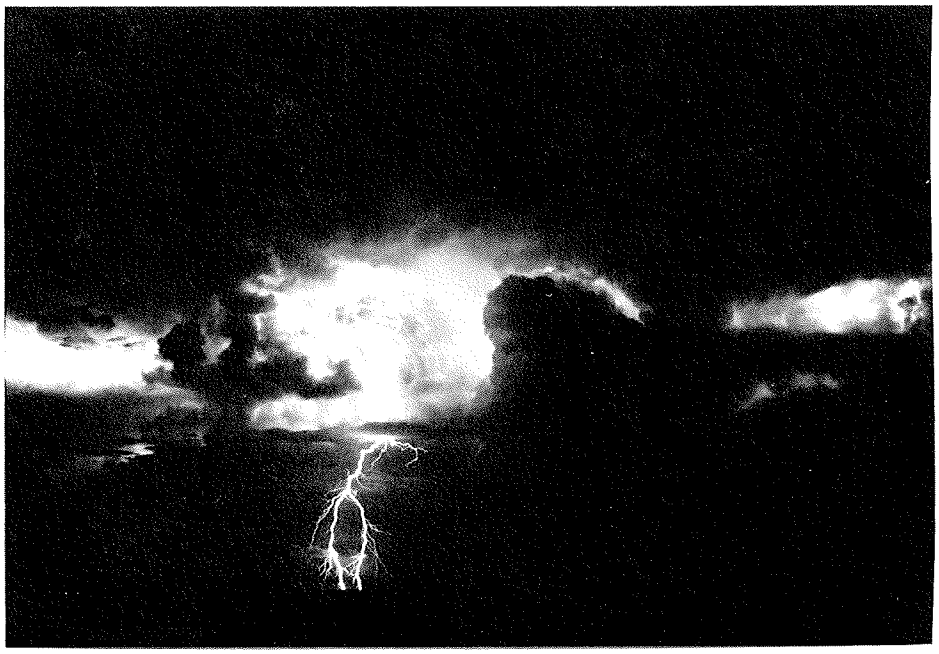

Figure 7.6 Cloud-to-ground lightning bolt from upper portion of cumulonimbus tower, striking well behind the precipitation area. View is toward the east at a retreating line of storms — note new, dark tower to the right of the lightning stroke, which has yet to produce any visible flashes.

---

[2] With ASA 64 film, a good starting point for CG strokes at a distance of a few miles is f4.0. Inexperienced photographers should bracket their exposures over a wide range, until their experience level increases to the point where they can estimate the exposure to within about one and one-half stops. Such an estimate is within the exposure latitude of ASA 64 film. When the flashes are at great distance, tungsten-balanced film can be used to compensate for haze reddening.

from the anvil to the ground, even well ahead of the precipitation area. In severe storms with wall clouds, there may be relatively frequent CG flashes near or from the wall cloud or along the flanking line. Experience suggests that strokes which appear as extremely bright, short duration strokes often have considerable branching in the photographs (Fig. 7.7). Such flashes are called "staccato" flashes by Arnold and Rust, 1979).[3] Regions of the storm where CG stroke activity begins tend to remain active for periods of 10 min or more.

As the storm enters late maturity, the CG activity tends to diminish. Intracloud flashes tend to maintain a more or less constant rate through the mature phase, so intracloud activity tends to dominate the latter stages of storm maturity. A fairly reliable (but not infallible) sign of the entrance into the dissipating stage is the occurrence of long-duration lightning flashes which propagate great distances entirely within the anvil region. These can be quite spectacular (Fig. 7.8), but tend to be relatively infrequent. On occasion, an extension of these long flashes within the anvil may reach down to the ground.

Because of the relatively unadvanced nature of the science of atmospheric electricity, amateur observations can still be of value (e.g., see Krider and Alejandro, 1983). This is especially true when those observations can be documented with photographs.

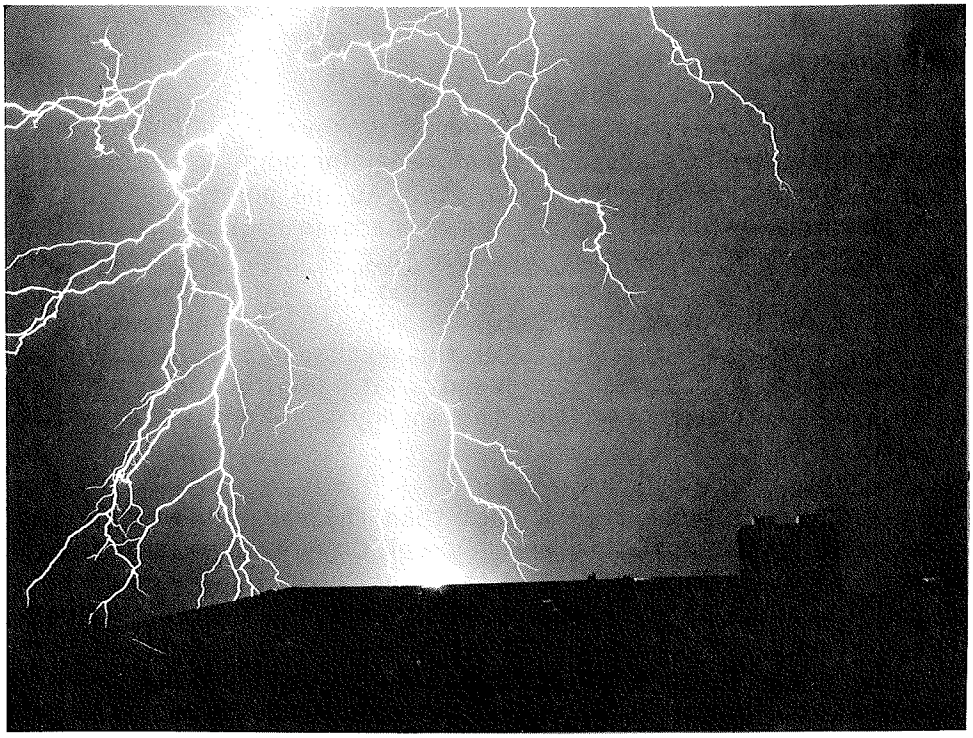

Figure 7.7 Example of a cloud-to-ground lightning stroke with considerable branching. The main channel is much brighter than the others. This was a "staccato" flash (see text).

[3] Those strokes which "flicker" over relatively long periods (as described above) usually photograph as a single main channel with little branching evident.

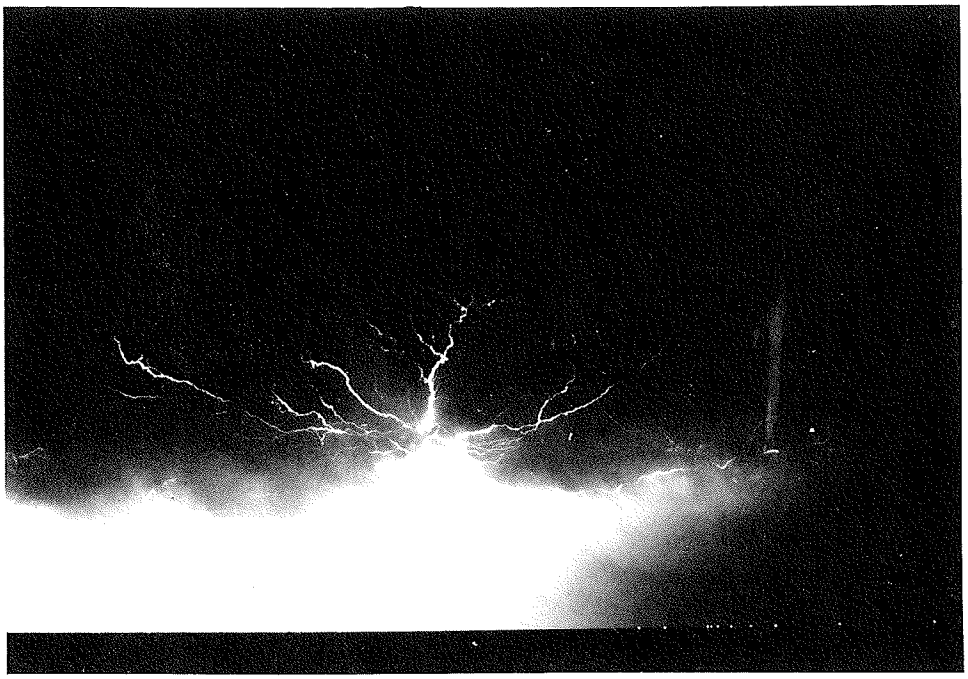

Figure 7.8 Lightning within the downstream anvil, late in the storm's life cycle.

2. Relationship to Storm Severity

There has been considerable speculation that severe thunderstorms, especially tornadic ones, display unusual electrical phenomena, including more frequent lightning strokes, corona discharges, colored lightning, etc. At one point, there was some belief that electrical phenomena actually drove the tornado (see IV.E.4). Davies-Jones and Golden (1975a) have discussed this issue and have "...cast doubt on theories which depend directly on electrical energy for tornado production and maintenance." This discussion prompted comments by Vonnegut (1975) and Colgate (1975) -- with replies by Davies-Jones and Golden (1975b,c). Somewhat after this exchange of views, Vonnegut and his colleagues (Watkins **et al.**, 1978) concluded that "...although continuous current discharges may occur in tornado vortices, the energy supplied...would not constitute a major power source."

It is noteworthy that more recent data than that available to Davies-Jones and Golden have suggested that the flash rates may well be quite high near the tornado/wall cloud. This observation does **not** contradict the conclusions of Davies-Jones and Golden, since tornadic wall clouds also are observed without this enhanced lightning activity. If unusually high flash rates are to be a **necessary** condition for tornadoes, they invariably must appear. Therefore, it probably remains safe to say that any unusual electrical activity associated with a tornadic storm is the result of the storm's character and not a controlling factor in storm behavior -- i.e., an "effect" rather than a "cause".

However, this does not answer the question concerning the quality and/or quantity of storm electricity versus the severity of the storm. Is there, in fact, any such relationship? If one reviews what has been learned about storm electricity, one fact emerges: the electrification of the cloud depends heavily on updraft strength. For example, synoptic scale vertical motion almost never produces thundering forms of precipitation. Further, the existence of ice seems to be important in storm

electrification, so the updraft has to be strong enough to penetrate the freezing level. Also, the process of particle collision, which seems to be important in charge production, is enhanced by the strong drafts in a severe storm. Finally, strong updrafts condense a lot of water. The more precipitation particles available, the more effective the charging mechanism (non-inductive, recall) which depends on those particles.

There are observations which support this, both quantitative and qualitative. Rust **et al.** (1981) have pointed out the apparent differences in severe versus non-severe storm electrical effects (Fig. 7.9). Thus, in the typical case, there is evidence in favor of severe storms having enhanced electrical effects, and unusual phenomena certainly are possible in the severe storm situation.

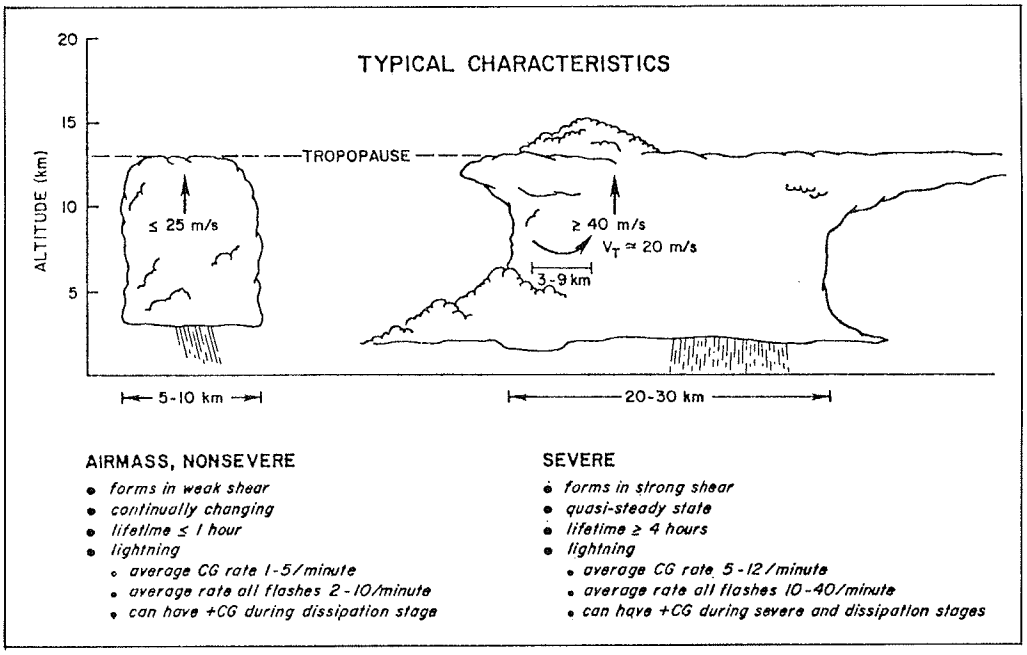

Figure 7.9 Oversimplified depiction of apparent differences between very small ("airmass", nonsevere) storms and supercell, severe storms. Other differences are likely (from Rust ***et al.****, 1981).*

Having said all this, one should balance it with some words of caution. It is my own observation that there seems to be some seasonal dependence in the level of electrical activity. Storms in early spring may be quite severe and yet produce relatively little lightning. From late spring into fall, both severe and non-severe thunderstorms have a tendency to produce frequent and/or intense electrical effects. Reasons for this are not entirely clear and the quantitative measurements of the apparent seasonal variation have yet to be done. Technology to do this is becoming available, and is mentioned below. Assuming that this apparent seasonal dependence is real, then a given amount of electrical activity is a poor measure of storm severity, except perhaps in an average sense.

Further, non-severe (in the official sense: see III.B.1.) heavy rainstorms are often quite prolific lightning producers. Some distinctly non-severe storms (including high-based storms in mountainous terrain) can also produce spectacular lightning.

Some recent results (Holle **et al.**, 1983) for storms in Florida show that CG lightning frequency [4] is not simply related to radar reflectivity. As seen in Fig. 7.10, the frequency drops essential to zero above 56 dBz. This is a rather surprising result. There is much work yet to be done, especially repeating the experiment in different geographical areas.

Therefore, in summary, it can be said that storm electricity seems to have some rough relationship to storm severity. However, such a statement must be tempered by saying that considerable evidence exists for frequent exceptions to that rule. Thus, "severe storm detectors" based solely on lightning activity are probably not to be relied upon exclusively.

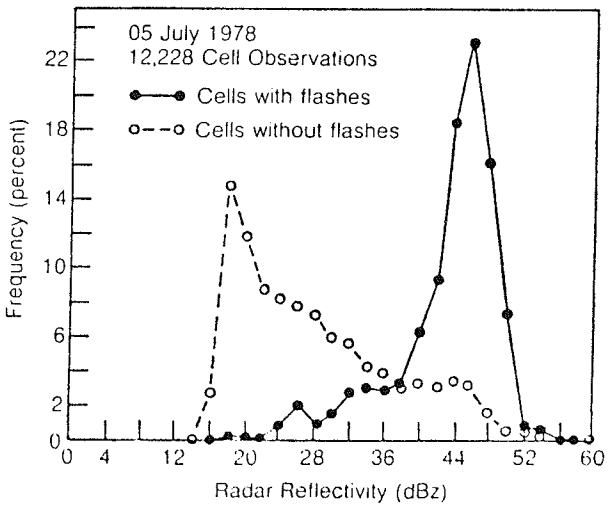

Figure 7.10 Distribution of radar cells on 5 July 1978 according to the maximum reflectivity (dBz) in the cell. Solid curve shows the distribution when cells had at least one CG flash in the area of the cell within 2 1/2 minutes of the radar scan, while the dashed plot shows the distribution without flashes. Note that these data are for CG flashes only (from Holle ***et al.****, 1983).*

3. Detection Techniques

As discussed, the thunderstorm cloud charging mechanism is still not completely understood. Perhaps even more unsettling is the lack of factual information about the spatial and seasonal distribution of electrical activity. What historical data we do have depends on an observer actually seeing lightning and/or hearing thunder. Such an observer does not provide quantitative data about flash frequency, but merely a subjective assessment: occasional, frequent, or continuous lightning. Further, no quantitative value is provided for how often CG strokes occur versus intracloud flashes. Finally, the observer's ability to see lightning is limited by low-level clouds, haze, trees or other obstructions to vision. Since many offices are located at airports, the observer may miss hearing thunder because of aircraft or automobile traffic. Light from habitation near the site can limit the observer's capability to see flashes.

This situation is compounded by an ever-dwindling array of surface sites, and by station closings after dark. There have never been very many sites over the vast portions of the world covered by large bodies of water (oceans, the Great Lakes, etc.). Even on land, large areas have such sparse populations that observations are not available (for example, in mountain or desert regions, and rural areas).

---

[4] It is worth noting that **CG flashes are not the whole story** of convective electrical activity. This is especially important to remember since much of the new ground-based sensor technology is limited (as of this writing) to CG detection.

In short, the actual distribution of thunderstorm activity is only dimly sensed. This creates myriad problems and large gaps in our understanding as well as forecast errors. It has been hinted already that there may well be a seasonal variation in the electrical activity level in thunderstorms. Are there year-to-year variations? What differences exist in electrical activity in storms over high terrain, versus those occurring in the plains, versus thunderstorms at sea? We have few answers to these and other questions (see Orville and Spencer, 1979).

What is needed is a means to detect lightning flashes in a quantitative fashion, at a distance -- i.e., remote sensing. Preferably, such a technique would be able to sense the difference between CG strokes and the other varieties, since CG flashes have the greatest potential for damaging effects. Also, the method should account separably for positive- and negative-to-ground strokes. Perhaps not well-known is the fact that the technology to accomplish these objectives may already exist (Krider **et al.**, 1980; Davis **et al.**, 1983; Christian **et al.**, 1983). For example, an operational network (ground-based) of CG lightning detection devices has been developed for Alaska and the western third of the United States (Vance, 1979). This system detects the electromagnetic radiation emitted by CG lightning strokes in the radio frequency range (called "sferics"). Since most CG strokes transfer negative charge to ground and, since the system can detect such strokes, it can provide information about the distribution of such CG strokes. It has become possible to distinguish those relatively infrequent positive CG strokes, as well.

Using optical wavelengths, satellite-borne lightning sensors may soon be available (Turman, 1979; Davis **et al.**, 1983). Interestingly, such devices are capable of operating effectively even in daylight! By virtue of their operation on satellites, it is entirely possible that world-wide coverage shall one day be available.

The ideal system may combine information from **both** satellite-carried and ground-based sensors. By doing so, it is possible that a really complete picture of lightning occurrence distribution will be available within the next several years. Immediate and practical applications, as well as whole new fields of research are possible. Aviation and agricultural interests are likely to be the immediate beneficiaries, but the whole field of thunderstorm meteorology will eventually benefit from such observations.

Some exciting preliminary results are already available (e.g., Lopez **et al.**, 1983; Orville **et al.**, 1983). Such studies have the potential to relate CG lightning occurrence, frequency, and type to large-scale environmental conditions, as well as to details about the storm(s) producing the activity. It should be anticipated that much new material will result from the new lightning occurrence data. For example, just having reliable, complete data about lightning could have a profound effect on thunderstorm forecasting, since verification of thunderstorm forecasts has been keyed to questionable data (or hypotheses about the data --e.g., thunder is uniquely associated with some threshold radar reflectivity) in the past. Clearly, the future in this area looks very exciting.

VIII. Concluding Remarks

> The mark of the true professional in any field is a rich vocabulary of patterns, developed through years of formal education and especially through years of practical experience....The vocabulary-of-patterns notion ought to...encourage all of us to think hard about the value of experimenting as opposed to merely detached study.
>
> -- T.J. Peters and R.H. Waterman, Jr., **In search of Excellence**

This volume, like the preceding one, has dealt primarily with fundamental aspects of convective meteorology. In order to present storm-scale meteorology, a wide range of topics has been considered. Certain subjects, like precipitation physics, have been examined at some length in order to provide the basic physical understanding of how thunderstorms work. A classification scheme has been introduced for convective storms -- this scheme allows the reader to make certain physical distinctions in the way storms are organized. Hopefully, this allows one to infer how the storms behave.

It should be emphasized that convective storms the world over are governed by the same basic physics. Since the reasons for a particular storm's organization depend on local conditions, the frequency of storm types varies considerably over space and/or time. Nevertheless, the processes which occur in thunderstorms and the resulting organization do not recognize any artificial boundaries. If conditions warrant, a supercell which develops in a region where supercells are infrequent retains the basic characteristics of a supercell. In fact, the supercell concept was first developed in Great Britain, where such storms are decidedly rare.

Storm-scale analysis hinges predominantly on remote sensing, since conventional networks don't provide the density of observations needed to define storm-scale structures. The key to using conventional data for storm-scale analysis is **basic physical understanding** -- the sparse conventional data provide checks and clues about how the storm is organized. These should be compared with remotely-sensed data, keeping in mind the models of storm structure we have developed.

The final step of operational meteorology is to put the material contained in these first two volumes into a coherent picture, applicable to the current weather events. Do not be deceived into thinking that that picture is going to be complete, or that the process of blending the science with the data is effortless. Many aspects of how the scales interact remain mysterious. Nevertheless, it is possible to integrate these ideas into the operational forecast/analysis routine. It is to this end that Volume **III**, Applications and Case Studies, is directed.

REFERENCES

Achtemeier, G.L., 1969: Some observations of splitting thunderstorms over Iowa on August 25-26, 1965. **Preprints, 6th Conf. Severe Local Storms** (Chicago, IL), Amer. Meteor. Soc., 89-94.

Adler, R.F., and D.D. Fenn, 1977: Satellite-based thunderstorm intensity parameters. **Preprints, 10th Conf. Severe Local Storms** (Omaha, NE), Amer. Meteor. Soc., 8-15.

Agee, E.M., and T.S. Chen, 1973: A model for investigating eddy viscosity effects on mesoscale cellular convection. **J. Atmos. Sci., 30,** 180-189.

_____, J.T. Snow, and P.R. Clare, 1976: Multiple vortex features in the tornado cyclone and the occurrence of tornado families. **Mon. Wea. Rev., 104,** 552-563.

_____, _____, F.S. Nickerson, P.R. Clare, C.R. Church, and L.A. Schaal, 1977: An observational study of the West Lafayette, Indiana, tornado of 20 March 1976. **Mon. Wea. Rev., 105,** 893-907.

*Alberty, R.L., 1969: A proposed mechanism for cumulonimbus persistence in the presence of strong vertical shear. **Mon. Wea. Rev., 97,** 590-596.

Anderson, C.E., 1960: A technique for classifying cumulus clouds based on photogrammetry. **Cumulus Dynamics,** Pergamon Press, Oxford, England, 50-59.

Anthes, R.A., H.D. Orville, and D.J. Raymond, 1982: Mathematical modeling of convection. **Thunderstorms: A Social, Scientific and Technological Documentary. Vol. 2: Thunderstorm Morphology and Dynamics** (E. Kessler, Ed.), NOAA/ERL, 495-579.

Anthony, R.W., W.E. Carle, J.T. Schaefer, R.L. Livingston, A.L. Siebers, F.L. Mosher, J.T. Young, and T.M. Whittaker, 1982: The Centralized Storm Information System at the NOAA Kansas City Complex. **Preprints, 9th Conf. Wea. Forecasting and Analysis** (Seattle, WA), Amer. Meteor. Soc., 40-43.

Arnold, R.T., and W.D. Rust, 1979: Initial attempt to make electrical measurements on tornadic storms by surface intercept. **Preprints, 11th Conf. Severe Local Storms** (Kansas City, MO), Amer. Meteor. Soc., 320-325.

Asai, T., 1970: Stability of a plane parallel flow with variable vertical shear and unstable stratification. **J. Meteor. Soc. Japan, 48,** 129-138.

Asp, M.O., 1963: History of tornado observations and data sources. Key to Meteorological Records Documentation, No. 3.131, U.S. Wea. Bur., 25 pp.

Atlas, D.A., 1963: Radar analysis of severe storms. **Meteor. Monogr., 5,** No. 27, Amer. Meteor. Soc., Boston, MA, 177-220.

* denotes key references

_____, K.A. Browning, R.J. Donaldson, Jr., and H.J. Sweeney, 1963: Automatic digital radar reflectivity analysis of a tornadic storm. **J. Appl. Meteor., 2,** 574-581.

*Auer, A.H., Jr., and J.D. Marwitz, 1968: Estimates of air and moisture flux into hailstorms on the high plains. **J. Appl. Meteor., 7,** 196-198.

Austin, J.M., and A. Fleisher, 1948: A thermodynamic analysis of cumulus convection. **J. Meteor., 5,** 240-243.

Barge, B.L., and R.G. Humphries, 1980: Identification of rain and hail with polarization and dual-wavelength radar. **Preprints, 19th Conf. Radar Meteorology** (Miami Beach, FL), Amer. Meteor. Soc., 507-516.

Barnes, G.M., and K. Seickman, 1984: The environment of fast- and slow-moving tropical mesoscale cloud lines. **Mon. Wea. Rev., 112,** 1782-1794.

Barnes, S.L., 1968: On the source of thunderstorm rotation. ESSA Tech. Memo. ERLTM-NSSL 38 [NTIS Accession No. PB-178990], 28 pp.

*_____, 1970: Some aspects of a severe, right-moving thunderstorm deduced from mesonetwork rawinsonde observations. **J. Atmos. Sci., 27,** 634-648.

*_____, 1976: Severe local storms: Concepts and understanding. **Bull. Amer. Meteor. Soc., 57,** 412-419.

*_____, and C.W. Newton, 1982: Thunderstorms in the synoptic setting. **Thunderstorms: A Social, Scientific and Technological Documentary. Vol. 2: Thunderstorm Morphology and Dynamics** (E. Kessler, Ed.), NOAA/ERL, 109-173.

Barrett, C.B., 1983: The NWS flash flood program. **Preprints, 5th Conf. Hydrometeorology** (Tulsa, OK), Amer. Meteor. Soc., 9-16.

Bartels, D.L., and A.A. Rockwood, 1983: Internal structure and evolution of a dual mesoscale convective complex. **Preprints, 5th Conf. Hydrometeorology** (Tulsa, OK), Amer. Meteor. Soc., 97-102.

Bartlett, J.T., 1965: The growth of cloud droplets by coalescence. **Quart. J. Roy. Meteor. Soc., 91,** 93-104.

*Bates, F.C., 1963: An aerial observation of a tornado and its parent cloud. **Weather, 18,** 12-18.

Battan, L.J., 1973: **Radar Observation of the Atmosphere.** Univ. of Chicago Press, Chicago, IL, 324 pp.

_____, 1980: Observations of two Colorado thunderstorms by means of a zenith-pointing Doppler radar. **J. Appl. Meteor., 19,** 580-592.

*Beebe, R.G., 1958: Tornado proximity soundings. **Bull. Amer. Meteor. Soc., 39,** 195-201.

Belville, J.D., G.A. Johnson, A.R. Moller, and J.D. Ward, 1980: A synoptic and mesoscale analysis of the Palo Duro Canyon flash flood and associated severe weather. **Preprints, 2nd Conf. Flash Floods** (Atlanta, GA), Amer. Meteor. Soc., 30-

_____, and N.O. Stewart, 1983: Extreme rainfall events in Louisiana: The "New Orleans" type. **Preprints, 5th Conf. Hydrometeorology** (Tulsa, OK), Amer. Meteor. Soc., 284-290.

*Bergeron, T., 1933: On the physics of cloud and precipitation. **Mem. de l'Union Geod. Geophys. Int.**, Lisbon.

_____, 1954: The problem of tropical hurricanes. **Quart. J. Roy. Meteor. Soc., 80,** 131-164.

Berry, E.X., 1967: Cloud droplet growth by collection. **J. Atmos. Sci., 24,** 688-701.

Biter, C.J., T.W. Cannon, E.L. Crow, C.A. Knight, and P.M. Roskowski, 1983: Improvements in cloud photogrammetry using airborne, side-looking time-lapse cameras. **J. Clim. Appl. Meteor., 22,** 1047-1055.

Bjerknes, J., 1938: Saturated ascent of air through a dry-adiabatically descending environment. **Quart. J. Roy. Meteor. Soc., 64,** 325-330.

Blanchard, D.O., and R.E. Lopez, 1984: Spatial and temporal variations of the convective field pattern in south Florida and its relationship to the synoptic flow. **Postprints, 15th Conf. Hurricanes and Tropical Meteor.** (Miami, FL), Amer. Meteor. Soc., (493-499).

Bluestein, H.B., and A.J. Bedard, Jr., 1982: Surface meteorological measurements in severe thunderstorms: Field measurements and design detail of TOTO. **Preprints, 12th Conf. Severe Local Storms** (San Antonio, TX), Amer. Meteor. Soc., 383-395.

*_____, and M.H. Jain, 1985: The formation of mesoscale lines of precipitation: Severe squall lines in Oklahoma during spring. **J. Atmos. Sci., 42**(in press).

*_____, and C.R. Parks, 1983: A synoptic and photographic climatology of low-precipitation severe thunderstorms in the southern plains. **Mon. Wea. Rev., 111,** 2034-2046.

Bonesteele, R.G., and Y.J. Lin, 1978: A study of updraft-downdraft interaction based upon perturbation pressure and single-Doppler radar data. **Mon. Wea. Rev., 106,** 62-68.

Braham, R.R., Jr., 1952: The water and energy budgets of the thunderstorm and their relation to thunderstorm development. **J. Meteor., 9,** 227-242.

*Brandes, E.A., 1978: Mesocyclone evolution and tornadogenesis: Some observations. **Mon. Wea. Rev., 106,** 995-1011.

_____, 1981: Finestructure of the Del City-Edmond tornadic mesocirculation. **Mon. Wea. Rev., 109,** 635-647.

_____, 1984: Vertical vorticity generation and mesocyclone sustenance in tornadic thunderstorms: The observational evidence. **Mon. Wea. Rev., 112,** 2253-2269.

Brooks, E.M., 1949: The tornado cyclone. **Weatherwise, 2,** 32-33.

Brown, J.M., K.R. Knupp, and F. Caracena, 1982: Destructive winds from shallow, high-based cumulonimbi. **Preprints, 12th Conf. Severe Local Storms** (San Antonio, TX), Amer. Meteor. Soc., 272-275.

Brown, R.A., 1972: On the inflection point instability of a stratified Ekman boundary layer. **J. Atmos. Sci., 29,** 850-859.

*Brown, R.A., and K.C. Crawford, 1972: Doppler radar evidence of severe storm high-reflectivity cores acting as obstacles to airflow. **Preprints, 15th Conf. Radar Meteor.** (Boston, MA), Amer. Meteor. Soc., 16-21.

_____, and L.R. Lemon, 1976: Single Doppler radar vortex recognition: Part II--Tornadic vortex signatures. **Preprints, 17th Conf. Radar Meteor.** (Seattle, WA), Amer. Meteor. Soc., 104-109.

_____, D.W. Burgess, and K.C. Crawford, 1973: Twin tornado cyclones within a severe thunderstorm: Single Doppler radar observations. **Weatherwise, 26,** 63-69.

*_____, L.R. Lemon, and D.W. Burgess, 1978: Tornado detection by pulsed Doppler radar. **Mon. Wea. Rev., 106,** 29-38.

_____, C.R. Safford, S.P. Nelson, D.W. Burgess, W.C. Baumgarner, M.L. Weible, and L.C. Fortner, 1981: Multiple Doppler analysis of severe thunderstorms: Designing a general analysis system. NOAA Tech. Memo. ERL NSSL-92 [NTIS Accession No. PB82-114117], 21 pp.

*Browning, K.A., 1964: Airflow and precipitation trajectories within severe local storms which travel to the right of the winds. **J. Atmos. Sci., 21,** 634-639.

*_____ (Ed.), 1965a: "A Family Outbreak of Severe Local Storms -- A Comprehensive Study of the Storms in Oklahoma on 26 May 1963. Part I." Report No. AFCRL-65-695(I), Office of Aerospace Research, U.S. Air Force, Bedford, MA [NTIS Accession No. AD 623787], 346 pp.

_____, 1965b: Some inferences about the updraft within a severe local storm. **J. Atmos. Sci., 22,** 669-677.

*_____, 1965c: The evolution of tornadic storms. **J. Atmos. Sci., 22,** 664-668.

*_____, 1965d: Some inferences about the updraft within a tornadic storm. **J. Atmos. Sci., 22,** 669-677.

*_____, 1977: The structure and mechanism of hailstorms. **Meteor. Monogr.,** No. 38, 1-39.

_____, 1982: General circulation of middle-latitude thunderstorms. **Thunderstorms: A Social, Scientific and Technological Documentary. Vol. 2: Thunderstorm Morphology and Dynamics** (E. Kessler, Ed.), NOAA/ERL, 211-248.

*_____, and R.J. Donaldson, Jr., 1963: Airflow and structure of a tornadic storm. **J. Atmos. Sci., 20,** 533-545.

_____, and _____, 1965: Surface weather associated with the severe storms. "A Family Outbreak of Severe Local Storms -- A Comprehensive Study of the Storms in Oklahoma on 26 May 1963, Part I" (K.A. Browning, Ed.), Report No. AFCRL-65-695(I), Office of Aerospace Research, U.S. Air Force, Bedford, MA [NTIS Accession No. AD 623787], 99-108.

*_____, and G.B. Foote, 1976: Airflow and hail growth in supercell storms and some implications for hail suppression. **Quart. J. Roy. Meteor. Soc., 102,** 499-534.

_____, and C.R. Landry, 1963: Airflow within a tornadic storm. **Proceedings, 10th Wea. Radar Conf.** (Washington, D.C.), Amer. Meteor. Soc., 116-122.

_____, and F.H. Ludlam, 1960: Radar analysis of a hailstorm. Tech. Note 5, Dept. of Meteorology, Imperial College, London.

*_____, and _____, 1962: Airflow in convective storms. **Quart. J. Roy. Meteor. Soc., 88,** 117-135.

Burgess, D.W., 1981: Evidence for anticyclonic rotation in left-moving thunderstorms. **Preprints, 20th Conf. Radar Meteor.** (Boston, MA), Amer. Meteor. Soc., 52-54.

*_____, and R.P. Davies-Jones, 1979: Unusual tornadic storms in eastern Oklahoma on 5 December 1975. **Mon. Wea. Rev., 107,** 451-457.

_____, and R.J. Donaldson, Jr., 1979: Contrasting tornadic storm types. **Preprints, 11th Conf. Severe Local Storms** (Kansas City, MO), Amer. Meteor. Soc., 189-192.

_____, and P.S. Ray, 1984: Principles of radar. In Vol. I, AMS Short Course on Mesoscale Meteorology, Amer. Meteor. Soc. (in press).

_____, L.R. Lemon, and R.A. Brown, 1975a: Evolution of a tornado signature and parent circulation as revealed by single Doppler radar. **Preprints, 16th Conf. Radar Meteor.** (Houston, TX), Amer. Meteor. Soc., 99-106.

_____, _____, and _____, 1975b: Tornado characteristics revealed by Doppler radar. **Geophys. Res. Lett., 2,** 183-184.

_____, R.A. Brown, L.R. Lemon, and C.R. Safford, 1977: Evolution of a tornadic thunderstorm. **Preprints, 10th Conf. Severe Local Storms** (Omaha, NE), Amer. Meteor. Soc., 84-89.

_____, R.J. Donaldson, T. Sieland, and J. Hinkelman, 1979: Part I: Meteorological applications. In Final Report on the Joint Doppler Operational Project (JDOP), NOAA Tech. Memo. ERL NSSL-86 [NTIS Accession No. PB80-107188/AS], 84 pp.

*_____, V.T. Wood, and R.A. Brown, 1982: Mesocyclone evolution statistics. **Preprints, 12th Conf. Severe Local Storms** (San Antonio, TX), Amer. Meteor. Soc., 422-424.

Byers, H.R.,1959: **General Meteorology.** McGraw-Hill, New York, NY, 540 pp.

_____, 1965: **Elements of Cloud Physics.** University of Chicago Press, Chicago, IL, 191 pp.

_____, 1974: History of weather modification. **Weather and Climate Modification** (W.N. Hess, Ed.), John Wiley & Sons, New York, NY, 3-44.

*_____, and R.R. Braham, Jr., 1949: **The Thunderstorm.** U.S. Government Printing Office, Washington, D.C., 287 pp.

Caracena, F., and J.M. Fritsch, 1983: Focusing mechanisms in the Texas Hill Country flash floods of 1978. **Mon. Wea. Rev., 111,** 2319-2332.

*_____, R.A. Maddox, L.R. Hoxit, and C.F. Chappell, 1979: Mesoanalysis of the Big Thompson storm. **Mon. Wea. Rev., 107,** 1-17.

_____, J. McCarthy, and J. Flueck, 1983a: Forecasting the likelihood of microbursts along the front range of Colorado -- Results of the JAWS project. **Preprints, 13th Conf. Severe Local Storms** (Tulsa, OK), Amer. Meteor. Soc., Boston, 262-264.

_____, _____, J.F.W. Purdom, J.F. Weaver, and R.N. Green, 1983b: Multi-scale analyses of conditions affecting Pan American World Airways Flight 759. NOAA Tech. Memo. ERL ESG-2 [NTIS Accession No. PB83-222562], 45 pp.

Carbone, R.E., 1982: A severe frontal rainband. Part I: Stormwide hydrodynamic structure. **J. Atmos. Sci., 39,** 258-279.

_____, 1983: A severe frontal rainband. Part II: Tornado parent vortex circulation. **J. Atmos. Sci., 40,** 2639-2654.

_____, D.M. Takenchi, and S.M. Howard, 1976: Some characteristics of convective showers in Texas as deduced from conventional radar and instrumented aircraft measurements. **Preprints, 17th Conf. Radar Meteor.** (Seattle, WA), Amer. Meteor. Soc., 143-150.

*Carlson, T.N., and F.H. Ludlam, 1968: Conditions for the occurrence of severe local storms. **Tellus, 20,** 203-226.

Carrier, C., and R.G.Reebe, 1960: "Tornadoes and What To Do About Them." Aircon Co., Wichita, KS, 41 pp.

Changnon, S.A., 1981: The American Association of State Climatologists. **Bull. Amer. Meteor. Soc., 62,** 620-622.

_____, 1982: User beware: The upward trend in tornado frequencies. **Weatherwise, 35,** 64-69.

_____, **et al.,** 1977: "Hail Suppression: Impacts and Issues." Illinois State Water Survey Rept. No. ERP75-09980, Urbana, IL, p. 10 (Fig. 4).

Chappell, C.F., 1984: Quasi-stationary convective events. In Vol. 2, AMS Short Course on Mesoscale Meteorology, Amer. Meteor. Soc. (in press).

Charba, J., 1972: Gravity current model applied to analysis of squall-line gust front. NOAA Tech. Memo. ERL NSSL-61 [NTIS Accession No. COM-73-10410], 58 pp.

*_____, 1974: Application of the gravity current model to analysis of squall-line gust fronts. **Mon. Wea. Rev., 102,** 140-156.

*_____, and Y. Sasaki, 1971: Structure and movement of the severe thunderstorms of 3 April 1964 as revealed from radar and surface mesonetwork data analysis. **J. Meteor. Soc. Japan, 49,** 191-213.

Chisholm, A.J., 1973: Alberta hailstorms, Part I: Radar case studies and airflow models. **Meteor. Monogr., 14,** Boston, Amer. Meteor. Soc., 1-36.

*_____, and J.H. Renick, 1972: The kinematics of multicell and supercell Alberta hailstorms. "Alberta Hail Studies, 1972," Research Council of Alberta Hail Studies, Report No. 72-2, 24-31.

Christian, H.J., R.L. Frost, P.H. Gillaspy, S.J. Goodman, O.H. Vaughn, Jr., M. Brook, B. Vonnegut, and R.E. Orville, 1983: Observations of optical lightning emissions from above thunderstorms using U-2 aircraft. **Bull. Amer. Meteor. Soc., 64,** 120-123.

Colgate, S.A., 1967: Tornadoes: Mechanism and control. **Science, 157,** 1431-1432.

_____, 1975: Comment on "On the relation of electrical activity to tornadoes." **J. Geophys. Res., 80,** 4556.

_____, 1982: Small rocket tornado probe. **Preprints, 12th Conf. Severe Local Storms** (San Antonio, TX), Amer. Meteor. Soc., 396-400.

Cooley, J.R., 1978: Cold air funnel clouds. **Mon. Wea. Rev., 106,** 1368-1372.

Danielson, E.F., R. Bleck, and D.A. Morns, 1972: Hail growth by stochastic collection in a cumulus model. **J. Atmos. Sci., 29,** 135-155.

*Darkow, G.L., and D.W. McCann, 1977: Relative environmental winds for 121 tornado bearing storms. **Preprints, 10th Conf. Severe Local Storms** (Omaha, NE), Amer. Meteor. Soc., 413-417.

*Davies-Jones, R.P., 1973: The dependence of core radius on swirl ratio in a tornado simulation. **J. Atmos. Sci., 30,** 1427-1430.

_____, 1976: Laboratory simulations of tornadoes. **Proc., Symposium on Tornadoes** (R.E. Peterson, Ed.), Inst. for Disaster Research, Texas Tech. Univ., Lubbock, TX, 151-174.

_____, 1982a: Tornado dynamics. **Thunderstorms: A Social, Scientific and Technological Documentary, Vol. 2, Thunderstorm Morphology and Dynamics** (E. Kessler, Ed.), NOAA/ERL, 297-361.

_____, 1982b: Observational and theoretical aspects of tornadogenesis. **Topics in Atmospheric and Oceanographic Sciences: Intense Atmospheric Vortices** (Bengtsson/Lighthill, Ed's), Springer-Verlag, Berlin, 175-189.

*_____, 1984: Streamwise vorticity: The origin of updraft rotation. **J. Atmos. Sci., 41,** 2991-3006

*_____, D.W. Burgess, and L.R. Lemon, 1976: An atypical tornado-producing cumulonimbus. **Weather, 31,** 336-347.

_____, _____, _____, and D. Purcell, 1978: Interpretation of surface marks and debris patterns from the 24 May 1973 Union City, Oklahoma tornado. **Mon. Wea. Rev., 106,** 12-21.

*_____, and J.H. Golden, 1975a: On the relation of electrical activity to tornadoes. **J. Geophys. Res., 80,** 1614-1616.

_____, and _____, 1975b: Reply to comment on "On the relation of electrical activity to tornadoes." **J. Geophys. Res., 80,** 4557-4558.

_____, and _____, 1975c: Reply to comment on "On the relation of electrical activity to tornadoes." **J. Geophys. Res., 80,** 4561-4562.

*_____, and J.H. Henderson, 1975: Updraft properties deduced statistically from rawin soundings. **Pure Appl. Geophys., 113,** 787-801.

_____, and E. Kessler, 1974: Tornadoes. **Weather and Climate Modification** (W.N. Hess, Ed.), John Wiley and Sons, 552-595.

Davis, M.H., M. Brook, H. Christian, B.G. Heikes, R.E. Orville, C.G. Park, R.G. Noble, and B. Vonnegut, 1983: Some scientific objectives of a satellite-borne lightning mapper. **Bull. Amer. Meteor. Soc., 64,** 114-119.

*Dennis, A.S., C.A. Schock, and A. Koscielski, 1970: Characteristics of hailstorms of western South Dakota. **J. Appl. Meteor., 9,** 127-135.

Dias, M.A., L.R. Hoxit, and C.F. Chappell, 1980: Meteorological analyses of the Los Angeles-Tujunga Canyon flash flood of 10 February 1978. **Preprints, 2nd Conf. Flash Floods** (Atlanta, GA), Amer. Meteor. Soc., 45-52.

*Donaldson, R.J., Jr., 1970: Vortex signature recognition by a Doppler radar. **J. Appl. Meteor., 9,** 661-670.

Doswell, C.A. III, 1977: Obtaining meteorologically significant surface divergence fields through the filtering property of objective analysis. **Mon. Wea. Rev., 105,** 885-892.

_____, 1980: Synoptic-scale environments associated with high plains severe thunderstorms. **Bull. Amer. Meteor. Soc., 61,** 1388-1400.

_____, 1983: Comments on "Photographic documentation of some distinctive cloud forms observed beneath a large cumulonimbus." **Bull. Amer. Meteor. Soc., 64,** 1389-1390.

_____, 1984: A kinematic analysis of frontogenesis associated with a nondivergent vortex. **J. Atmos. Sci., 41,** 1241-1248.

*_____, and L.R. Lemon, 1979: An operational evaluation of certain kinematic and thermodynamic parameters associated with severe thunderstorm environments. **Preprints, 11th Conf. Severe Local Storms** (Kansas City, MO), Amer. Meteor. Soc., 397-402.

_____, and A.R. Moller, 1985: Scientific impact of southern Great Plains severe storm intercept operations -- 1972 to the present. Manuscript submitted to **Bull. Amer. Meteor. Soc.**

_____, D.L. Kelly, and J.T. Schaefer, 1983: Preliminary climatology of non-tornadic severe thunderstorm events. **Preprints, 13th Conf. Severe Local Storms** (Tulsa, OK), Amer. Meteor. Soc., 25-28.

Doviak, R.J., and D.S. Zrnic', 1984: **Doppler Radar and Weather Observations.** Academic Press, Orlando, FL, 480 pp.

Drazin, P.G., and L.N. Howard, 1966: Hydrodynamic stability of parallel flow of inviscid fluids. **Adv. Appl. Mech., 9,** 1-89.

Drogemeier, K.K., and R.B. Wilhelmson, 1983: Three dimensional numerical simulation of the interaction between a shallow cumulus field and a thunderstorm outflow boundary. **Preprints, 13th Conf. Severe Local Storms** (Tulsa, OK), Amer. Meteor. Soc., 245-248.

Eccles, P.J., and D. Atlas, 1973: A dual-wavelength hail detector. **J. Appl. Meteor., 12,** 847-854.

Elsom, D.M., and G.T. Meaden, 1982: Suppression and dissipation of weak tornadoes in metropolitan areas: A case study of greater London. **Mon. Wea. Rev., 110,** 745-756.

Emanuel, K.A., 1981: A similarity theory for unsaturated downdrafts within clouds. **J. Atmos. Sci., 38,** 1541-1557.

*Fankhauser, J.C., 1971: Thunderstorm-environment interactions determined from aircraft and radar observations. **Mon. Wea. Rev., 99,** 171-192.

_____, and C.G. Mohr, 1977: Some correlations between various sounding parameters and hailstorm characteristics in northeast Colorado. **Preprints, 10th Conf. Severe Local Storms** (Omaha, NE), Amer. Meteor. Soc., 218-225.

_____, G.M. Barnes, L.J. Miller, and P.M. Roskowski, 1983: Photographic documentation of some distinctive cloud forms observed beneath a large cumulonimbus. **Bull. Amer. Meteor. Soc., 64,** 450-462.

Feynman, R.P., R.B. Leighton, and M. Sands, 1964: Electricity in the atmosphere. **The Feynman Lectures on Physics. Vol. II: Mainly Electromagnetism and Matter.** Addison-Wesley, Reading, MA, 11 pp.

Findeisen, W., 1938: Die kolloid meteorologischen Vorgange der Niederschlagsbildung. **Meteor. Z., 55,** 121-133.

Fletcher, N.H., 1966: **The Physics of Rainclouds.** Cambridge University Press, Cambridge, England, 390 pp.

Flora, S.D., 1956: **Hailstorms of the United States.** University of Oklahoma Press, Norman, OK, 201 pp.

*Foote, G.B., and J.C. Fankhauser, 1973: Airflow and moisture budget beneath a northeast Colorado hailstorm. **J. Appl. Meteor., 12,** 1330-1353.

_____, and H.W. Frank, 1983: Case study of a hailstorm in Colorado. Part III: Airflow from triple Doppler measurements. **J. Atmos. Sci., 40,** 686-707.

_____, and C.G. Wade, 1981: The 22 July 1976 case study: Radar echo structure and evolution. Ch. 16 in **Hailstorms of the Central High Plains, Vol. 1** (C.A. Knight and P. Squires, Ed's), Colorado Associated University Press, Boulder, CO, 93-114.

Forbes, G.S., 1975: Relationship between tornadoes and hook echoes on April 3, 1974. **Preprints, 9th Conf. Severe Local Storms** (Norman, OK), Amer. Meteor. Soc., 280-285.

_____, 1978: Three scales of motion associated with tornadoes. Nuclear Regulatory Commission Report NUREG/CR-0363, 359 pp.

*_____, 1981: On the reliability of hook echoes as tornado indicators. **Mon. Wea. Rev., 109,** 1457-1466.

*_____, and R.M. Wakimoto, 1983: A concentrated outbreak of tornadoes, downbursts and microbursts, and implications regarding vortex classification. **Mon. Wea. Rev., 111,** 220-235.

Fritsch, J.M., and C.F. Chappell, 1980: Numerical prediction of convectively driven mesoscale pressure systems. Part I: Convective parameterization. **J. Atmos. Sci., 37,** 1722-1733.

*_____, and R.A. Maddox, 1981: Convectively driven mesoscale weather systems aloft. Part I: Observations. **J. Appl. Meteor., 20,** 9-19.

*Fujita, T., 1958a: Mesoanalysis of the Illinois tornadoes of April 9, 1953. **J. Meteor., 16,** 454-466.

_____, 1958b: Structure and movement of a dry front. **Bull. Amer. Meteor. Soc., 39,** 574-582.

*_____, 1960: A detailed analysis of the Fargo tornadoes of June 20, 1957. U.S. Weather Bureau Res. Pap. No. 42, 67 pp.

_____, 1965: Formation and steering mechanisms of tornado cyclones and associated hook echoes. **Mon. Wea. Rev., 93,** 67-78.

*_____, 1970: The Lubbock tornadoes: A study of suction spots. **Weatherwise, 23,** 160-173.

_____, 1971: A proposed characterization of tornadoes and hurricanes by area and intensity. Satellite and Mesometeorology Research Project Report No. 91, Univ. of Chicago, 42 pp.

_____, 1973: Proposed mechanism of tornado formation from rotating thunderstorm. **Preprints, 8th Conf. Severe Local Storms** (Denver, CO), Amer. Meteor. Soc., 191-196.

_____, 1974: Jumbo tornado outbreak of 3 April 1974. **Weatherwise, 27,** 116-126.

_____, 1976: Graphic examples of tornadoes. **Bull. Amer. Meteor. Soc., 57,** 401-412.

_____, 1978a: Manual of downburst identification for Project NIMROD. SMRP Res. Pap. No. 156, Univ. of Chicago, Chicago, IL [NTIS Accession No. PB-286048], 104 pp.

_____, 1978b: Workbook of tornadoes and high winds for engineering applications. SMRP Res. Paper No. 165, Univ. of Chicago, Chicago, IL, 142 pp.

_____, 1981: Tornadoes and downbursts in the context of generalized planetary scales. **J. Atmos. Sci., 38,** 1511-1534.

_____, and J. Arnold, 1963: Development of a cumulonimbus under the influence of strong vertical shear. **Proceedings, 10th Wea. Radar Conf.** (Washington, D.C.), Amer. Meteor. Soc., 178-186.

*_____, and H.R. Byers, 1977: Spearhead echo and downburst in the crash of an airliner. **Mon. Wea. Rev., 105,** 129-146.

*_____, and F. Caracena, 1977: An analysis of three weather-related aircraft accidents. **Bull. Amer. Meteor. Soc., 58,** 1164-1181.

*_____, and H. Grandoso, 1968: Split of a thunderstorm into anticyclonic and cyclonic storms and their motion as determined from numerical model experiments. **J. Atmos. Sci., 25,** 416-439.

_____, and R. Stuhmer, 1965: Hourly mesosynoptic analyses. "A Family Outbreak of Severe Local Storms -- A Comprehensive Study of the Storms in Oklahoma on 26 May 1963, Part I" (K.A. Browning, Ed.), Report No. AFCRL-65-695(I), Office of Aerospace Research, U.S. Air Force, Bedford, MA [NTIS Accession No. AD 623787], 63-72.

*_____, and R.M. Wakimoto, 1981: Five scales of airflow associated with a series of downbursts on 16 July 1980. **Mon. Wea. Rev., 109,** 1438-1456.

Gage, K.S., and B.B. Balsley, 1978: Doppler radar probing of the clear atmosphere. **Bull. Amer. Meteor. Soc., 59,** 1074-1093.

Gal-Chen, T., 1978: A method for the initialization of the anelastic equations: Implications for matching models with observations. **Mon. Wea. Rev., 106,** 587-606.

Gall, R.L., 1983: A linear analysis of the multiple vortex phenomenon in simulated tornadoes. **J. Atmos. Sci., 40,** 2010-2024.

Galway, J.G., 1975: Relationship of tornado deaths to severe weather watch areas. **Mon. Wea. Rev., 103,** 737-741.

*_____, 1977: Some climatological aspects of tornado outbreaks. **Mon. Wea. Rev., 105,** 477-484.

_____, 1983: Tornado track characteristics of killer tornadoes. **Preprints, 13th Conf. Severe Local Storms** (Tulsa, OK), Amer. Meteor. Soc., 117-119.

_____, and J.T. Schaefer, 1979: Fowl play -- An undeniably true tornado oddity. **Weatherwise, 32,** 116-118.

Gamache, J.F., and R.A. Houze, Jr., 1982: Mesoscale air motions associated with a tropical squall line. **Mon. Wea. Rev., 110,** 118-135.

*Garrett, R.A., and V.D. Rockney, 1962: Tornadoes in northeastern Kansas, May 19, 1960. **Mon. Wea. Rev., 90,** 231-240.

Godske, C.L., T. Bergeron, J. Bjerknes, and R.C. Bundgaard, 1957: **Dynamic Meteorology and Weather Forecasting.** Amer. Meteor. Soc., Boston, 800 pp.

*Goff, R.C., 1976: Vertical structure of thunderstorm outflows. **Mon. Wea. Rev., 104,** 1429-1440.

*Golden, J.H., 1974: The lifecycle of Florida Keys' waterspouts, I. **J. Appl. Meteor., 13,** 676-692.

_____, 1976: An assessment of windspeeds in tornadoes. **Proceedings, Symposium on Tornadoes** (R.E. Peterson, Ed.), Inst. for Disaster Research, Texas Tech. Univ., Lubbock, TX, 5-42.

_____, and D. Purcell, 1977: Photogrammetric velocities for the Great Bend, Kansas tornado of 30 August 1974: Accelerations and asymmetries. **Mon. Wea. Rev., 105,** 485-492.

*_____, and _____, 1978a: Life cycle of the Union City, Oklahoma tornado and comparison with waterspouts. **Mon. Wea. Rev., 106,** 3-11.

*_____, and _____, 1978b: Airflow characteristics around the Union City tornado. **Mon. Wea. Rev., 106,** 22-38.

Goody, R., and P. Gierasch, 1974: The influence of vorticity on free convection. **J. Atmos. Sci., 31,** 1021-1027.

Grazulis, T.P., and R.F. Abbey, Jr., 1983: 103 years of violent tornadoes...Patterns of serendipity, population, and mesoscale topography. **Preprints, 13th Conf. Severe Local Storms** (Tulsa, OK), Amer. Meteor. Soc., 124-127.

Grice, G.K., and R.A. Maddox, 1983: Significant radar characteristics of the Austin, Texas, flash flood. **Preprints, 5th Conf. Hydrometeorology** (Tulsa, OK), Amer. Meteor. Soc., 103-110.

_____, and J.D. Ward, 1983: Synoptic conditions of heavy rain and non-heavy rain events over south Texas associated with tropical cyclones. **Preprints, 5th Conf. Hydrometeorology** (Tulsa, OK), Amer. Meteor. Soc., 130-137.

Guttman, N.B., and D.S. Ezell, 1980: Flash flood climatology for Appalachia. **Preprints, 2nd Conf. Flash Floods** (Atlanta, GA), Amer. Meteor. Soc., 70-72.

Haglund, G.T., 1969: A study of severe local storm of 16 April 1967. ESSA Tech. Memo. ERLTM-NSSL 44, [NTIS Accession No. PB-188315], 54 pp.

Hales, J.E., 1978: The Kansas City flash flood of 12 September 1977. **Bull. Amer. Meteor. Soc., 59,** 706-710.

*_____, 1982: Relationship of selected synoptic scale parameters to significant tornado occurrences in 1980. **Preprints, 12th Conf. Severe Local Storms** (San Antonio, TX), Amer. Meteor. Soc., 139-142.

Haltiner, G.J., and F.L. Martin, 1957: **Dynamical and Physical Meteorology.** McGraw-Hill, New York, 470 pp.

Hammond, G.R., 1967: Study of a left-moving thunderstorm of 23 April 1964. ESSA Tech. Memo. ERLTM-NSSL 31, [NTIS Accession No. PB-174681], 75pp.

Hane, C.E., 1973: The squall line thunderstorm: Numerical experimentation. **J. Atmos. Sci., 30,** 1672-1690.

_____, R.B. Wilhelmson, and T. Gal-Chen, 1981: Retrieval of thermodynamic variables within deep convective clouds: Experiments in three dimensions. **Mon. Wea. Rev., 109,** 564-576.

Hartsell, C., 1970: Case study of a travelling hailstorm. Report No. 70-1, Inst. Atmos. Sci., S. Dakota School of Mines and Tech., Rapid City, SD, 72 pp.

Hennington, L., D. Zrnic', and D. Burgess, 1982: Doppler spectra of a maxi-tornado. **Preprints, 12th Conf. Severe Local Storms** (San Antonio, TX), Amer. Meteor. Soc., 433-436.

Hess, S.L., 1959: **Introduction to Theoretical Meteorology.** Holt, Rinehart and Winston, New York, NY, 362 pp.

Hexter, P.L., Jr., 1962: An observation of arcus and funnel clouds over Chesapeake Bay. **Mon. Wea. Rev., 90,** 225-230.

*Heymsfield, A.J., P.N. Johnson, and J.E. Dye, 1978: Observations of moist adiabatic ascent in northeast Colorado cumulus congestus clouds. **J. Atmos. Sci., 35,** 1689-1703.

_____, A.R. Jameson, and H.W. Frank, 1980: Hail growth mechanisms in a Colorado storm. Part II: Hail formation processes. **J. Atmos. Sci., 37,** 1779-1807.

Heymsfield, G.M., 1981: Evolution of downdrafts and rotation in an Illinois storm. **Mon. Wea. Rev., 109,** 1969-1988.

Hitschfield, W., 1960: Plume formation in thunderstorms. **Physics of Precipitation** (H. Weickman, Ed.), Amer. Geophys. Union, Washington, D.C., 94-103.

*Hoecker, W.H., 1960: Windspeed and air flow patterns in the Dallas tornado of April 2, 1957. **Mon. Wea. Rev., 88,** 167-180.

Holle, R.L., 1982: Photogrammetry of thunderstorms. **Thunderstorms: A Social, Scientific and Technological Documentary. Vol. 3: Instruments and Techniques for Thunderstorm Observation and Analysis** (E. Kessler, Ed.), NOAA/ERL, 77-98.

_____, and M.W. Maier, 1980: Tornado formation from downdraft interaction in the FACE network. **Mon. Wea. Rev., 108,** 1010-1028.

_____, and A.I. Watson, 1983: Duration of convective events related to visible cloud, convergence, radar and rain gage parameters in south Florida. **Mon. Wea. Rev., 111,** 1046-1051.

_____, R.E. Lopez, and W.L. Hiscox, 1983: Relationships between lightning occurrences and radar echo characteristics in south Florida. **Proceedings, Int. Aerosp. and Ground Conf. on Lightning and Static Electricity** (Fort Worth, TX), 14.1-14.9.

Holton, J.R., 1979: **An Introduction to Dynamic Meteorology.** Academic Press, New York, 391 pp.

Houze, R.A., Jr., 1977: Structure and dynamics of a tropical squall-line system observed during GATE. **Mon. Wea. Rev., 105,** 1540-1567.

Howard, K.W., and C.A. Doswell III, 1983: A comparison of severe thunderstorm cases with and without widespread heavy precipitation. **Preprints, 13th Conf. Severe Local Storms** (Tulsa, OK), Amer. Meteor. Soc., 304-307.

Hoxit, L.R., R.A. Maddox, C.F. Chappell, F.L. Zuckerberg, H.M. Mogil, and I. Jones, 1978: **Meteorological analysis of the Johnstown, Pennsylvania, flash flood, 19-20 July 1977.** NOAA Tech. Rept. ERL 401-APCL 43, 71 pp.

Huang, W.-G., and T.A. Schroeder, 1983: Aspects of torrential rains in China. **Preprints, 5th Conf. Hydrometeorology** (Tulsa, OK), Amer. Meteor. Soc., 138-141.

Huff, F.A., H.W. Hiser, and S.G. Bigler, 1954: Study of an Illinois tornado using radar, synoptic weather and field survey data. Rept of Investigation No. 22, Illinois State Water Survey, 73 pp.

Huschke, R.E., 1959: **Glossary of Meteorology.** Amer. Meteor. Soc., Boston, 639 pp.

Jameson, A.R., and A.J. Heymsfield, 1980: Hail growth mechanisms in a Colorado storm. Part I: Dual-wavelength radar observations. **J. Atmos. Sci., 37,** 1768-1778.

JDOP Staff, 1979: Final report on the Joint Doppler Operational Project (JDOP). NOAA Tech. Memo. ERL NSSL-80 [NTIS Accession No. PB80-107188], 84 pp.

Jensen, B., T.P. Marshall, M.A. Makey, and E.N. Rasmussen, 1983: Storm scale structure of the Pampa storm. **Preprints, 13th Conf. Severe Local Storms** (Tulsa, OK), Amer. Meteor. Soc., 85-88.

Jischke, M.C., and M. Parang, 1974: Properties of simulated tornado-like vortices. **J. Atmos. Sci., 31,** 506-512.

*Johns, R.H., 1982: A synoptic climatology of northwest flow severe weather outbreaks. Part I: Nature and significance. **Mon. Wea. Rev., 110,** 1653-1663.

Johnson, R.C., 1983: The heatburst of 29 May 1976. **Mon. Wea. Rev., 111,** 1776-1792.

Johnson, D.B., and M.J. Dungey, 1978: Microphysical interpretation of radar first echoes. **Preprints, 18th Conf. Radar Meteor.** (Atlanta, GA), 117-120.

Johnson, J.C., 1954: **Physical Meteorology.** M.I.T. Press, Cambridge, MA, 393 pp.

*Kamburova, P.L., and F.H. Ludlam, 1966: Rainfall evaporation in thunderstorm downdraughts. **Quart. J. Roy. Meteor. Soc., 92,** 510-518.

Kelly, D.L., J.T. Schaefer, and C.A. Doswell III, 1985: The climatology of non-tornadic severe thunderstorm events. **Mon. Wea. Rev., 113,** (in press).

*_____, _____, R.P. McNulty, C.A. Doswell III, and R.F. Abbey, Jr., 1978: An augmented tornado climatology. **Mon. Wea. Rev., 106,** 1172-1183.

Kessler, E., 1969: On the distribution and continuity of water substance in atmospheric circulation. **Meteor. Monogr., 10,** No. 32, Amer. Meteor. Soc., Boston, MA, 84 pp.

*Klemp, J.B., and R. Rotunno, 1982: High resolution numerical simulations of the tornadic region within a mature thunderstorm. **Topics in Atmospheric and Oceanographic Sciences: Intense Atmospheric Vortices** (Bengtsson/Lighthill, Ed's), Springer-Verlag, Berlin, 191-203.

*_____, and _____, 1983: A study of the tornadic region within a supercell thunderstorm. **J. Atmos. Sci., 40,** 359-377.

_____, and R.B. Wilhelmson, 1978a: The simulation of three-dimensional convective storm dynamics. **J. Atmos. Sci., 35,** 1070-1096.

*_____, and _____, 1978b: Simulations of right- and left-moving storms produced through storm splitting. **J. Atmos. Sci., 35,** 1097-1110.

_____, and P.S. Ray, 1981: Observed and numerically simulated structure of a mature supercell thunderstorm. **J. Atmos. Sci., 38,** 1558-1580.

Knight, C.A., and W.D. Hall, and P.M. Roskowski, 1983: Visual cloud histories related to first radar echo formation in northeast Colorado cumulus. **J. Clim. Appl. Meteor., 22,** 1022-1040.

_____, and N.C. Knight, 1970: Hailstone embryos. **J. Atmos. Sci., 27,** 659-666.

_____, and _____, 1974: Drop freezing in clouds. **J. Atmos. Sci., 31,** 1174-1176.

_____, P. Smith, and C. Wade, 1981: Storm types and some radar reflectivity characteristics. Ch. 5 in **Hailstorms of the Central High Plains, Vol. 1** (C.A. Knight and P. Squires, Ed's), Colorado Assoc. Univ. Press, Boulder, CO, 81-93.

Knight, N.C., 1981: The climatology of hailstone embryos. **J. Appl. Meteor., 20,** 750-755.

Kreitzberg, C.W., and D.J. Perkey, 1976: Release of potential instability. Part I: A sequential plume model within a hydrostatic primitive equation model. **J. Atmos. Sci., 33,** 456-475.

Krider, E.P., and S.B. Alejandro, 1983: Lightning: An unusual case study. **Weatherwise, 36**, 71-75.

_____, R.C. Noggle, A.E. Pifer, and D.L. Vance, 1980: Lightning direction-finding systems for forest fire detection. **Bull. Amer. Meteor. Soc., 61**, 980-986.

Krumm, W.R., 1975: On the cause of downdrafts from dry thunderstorms over the plateau area of the United States. **Bull. Amer. Meteor. Soc., 35**, 122-126.

Kuettner, J.P., 1971: Cloud bands in the earth's atmosphere -- Observations and theory. **Tellus, 23**, 404-426.

_____, Z. Levin, and J.D. Sartor 1981: Thunderstorm electrification -- Inductive or non-inductive? **J. Atmos. Sci., 38**, 2470-2484.

Kuo, H.-L., 1966: On the dynamics of convective atmospheric vortices. **J. Atmos. Sci., 23**, 25-42.

Langmuir, I., 1948: The production of rain by a chain reaction in clouds at temperatures above freezing. **J. Meteor., 5**, 175-192.

Latham, J., 1981: The electrification of thunderstorms. **Quart. J. Roy. Meteor. Soc., 107**, 277-298.

Lee, J.L., 1972: A numerical study of shallow convection. Rept. No. 19, NSF GA 13818, Dept. of Meteorology, Penn. St. Univ., University Park, PA, 93 pp.

Lee, J.T., R.P. Davies-Jones, D.S. Zrnic', and J.H. Golden, 1981: Summary of AEC-ERDA-NRC supported research at NSSL 1973-1979. NOAA Tech. Memo. ERL NSSL-90 [NTIS Accession No. PB81-220162], 93 p.

Leichter, I., and A.S. Dennis, 1974: Moisture flux and precipitation studies of convective storms in western South Dakota using pibal and radar data. **Preprints, Conf. Cloud Physics** (Tucson, AZ), 438-441.

*Lemon, L.R., 1976a: The flanking line, a severe thunderstorm intensification source. **J. Atmos. Sci., 33**, 686-694.

_____, 1976b: Wake vortex structure and aerodynamic origin in severe thunderstorms. **J. Atmos. Sci., 33**, 678-685.

*_____, 1977: New severe thunderstorm radar identification techniques and warning criteria: A preliminary report. NOAA Tech. Memo. NWS NSSFC-1, [NTIS Accession No. PB-273049], 60 pp.

_____, 1978: On the use of storm structure for hail identification. **Preprints, 18th Conf. Radar Meteorology** (Atlanta, GA), Amer. Meteor. Soc., 203-206.

_____, 1979: On improving National Weather Service severe thunderstorm and tornado warnings. **Preprints, 11th Conf. Severe Local Storms** (Kansas City, MO), Amer. Meteor. Soc., 569-572.

_____, and D.W. Burgess, 1980: Magnitude and implications of high speed outflow of severe storm summits. **Preprints, 19th Conf. Radar Meteor.** (Miami, FL), Amer. Meteor. Soc., 364-368.

*_____, and C.A. Doswell III, 1979: Severe thunderstorm evolution and mesocyclone structure as related to tornadogenesis. **Mon. Wea. Rev., 107,** 1184-1197.

_____, D.W. Burgess, and R.A. Brown, 1978: Tornadic storm airflow and morphology derived from single-Doppler radar measurements. **Mon. Wea. Rev., 106,** 48-61.

_____, _____, and L.D. Hennington, 1982: A tornado extending to extreme heights as revealed by Doppler radar. **Preprints, 12th Conf. Severe Local Storms** (San Antonio, TX), Amer. Meteor. Soc., 430-432.

*_____, R.J. Donaldson, Jr., D.W. Burgess, and R.A. Brown, 1977: Doppler radar application to severe thunderstorm study and potential real-time warning. **Bull. Amer. Meteor. Soc., 58,** 1187-1193.

_____, C.A. Doswell III, A.R. Moller, and D.K. Hoadley, 1980: A slide series supplement to "Tornado: A Spotter's Guide". Available from National Audio-Visual Center, Order Section, General Services Admin., Washington, D.C. 20409.

LeMone, M.A., 1973: The structure and dynamics of horizontal roll vortices in the planetary boundary layer. **J. Atmos. Sci., 30,** 1077-1091.

_____, and E.J. Zipser, 1980: Cumulonimbus vertical velocity events in Gate. Part I: Diameter, intensity, and mass flux. **J. Atmos. Sci., 37,** 2444-2457.

_____, G.M. Barnes, and E.J. Zipser, 1984: Momentum flux by lines of cumulonimbus over the tropical oceans. **J. Atmos. Sci., 41,** 1914-1932.

Leslie, F.W., 1977: Surface roughness effects on suction vortex formation: A laboratory simulation. **J. Atmos. Sci., 34,** 1022-1027.

Leverson, V.H., P.C. Sinclair, and J.H. Golden, 1977: Waterspout wind, temperature and pressure structure deduced from aircraft measurements. **Mon. Wea. Rev., 105,** 725-733.

Lewellen, W.S., 1976: Theoretical models of the tornado vortex. **Proceedings, Symposium on Tornadoes** (R.E. Peterson, Ed.), Inst. for Disaster Research, Texas Tech. Univ., Lubbock, TX, 107-143.

Lhermitte, R., and E. Williams, 1983: Cloud electrification. **Rev. Geophys. Space Phys., 21,** 984-992.

Ligda, M.G.H., 1951: Radar storm observation. **Compendium of Meteorology** (T.F. Malone, Ed.), Amer. Meteor. Soc., Boston, MA, 1265-1282.

Lilly, D.K., 1964: Numerical solutions for the shape-preserving, two-dimensional thermal convection element. **J. Atmos. Sci., 21,** 83-98.

_____, 1966: On the instability of Ekman boundary flow. **J. Atmos. Sci., 23,** 481-494.

_____, 1983: Helicity as a stabilizing effect on rotating convective storms. **Preprints, 13th Conf. Severe Local Storms** (Tulsa, OK), Amer. Meteor. Soc., 219-222.

Lindzen, R.S., 1974: Stability of a Helmholtz velocity profile in a continuously stratified, infinite Boussinesq fluid -- Applications to clear air turbulence. **J. Atmos. Sci., 31,** 1507-1514.

List, R., and T.L. Clark, 1973: The effect of particle size distribution on the dynamics of falling precipitation zones. **Atmosphere, 11,** 179-188.

Liu, J.Y., and H.D. Orville, 1969: Numerical modelling of precipitation and cloud shadow effects on mountain-induced cumuli. **J. Atmos. Sci., 26,** 1283-1298.

Livingston, R.L., 1971: An unusual arcus cloud. **Mon. Wea. Rev., 100,** 817-818.

Lopez, R.E., R.L. Holle, W.L. Hiscox, 1983: Climatological characteristics of lightning over south Florida and their correlation with radar activity. **Proceedings, Int'l Aerosp. and Ground Conf. on Lightning and Static Electricity** (Fort Worth, TX), 15.1-15.16.

Lott, G.A., 1974: The world record 42-minute Holt, Missouri rainstorm. **Mon. Wea. Rev., 82,** 50-59.

Lowe, A.B., 1963: Temperature flashes at Gretna, Manitoba. **Weatherwise, 16,** 172-174.

Ludlam, F.H., 1958: The hail problem. **Nubila, 1,** 13-96.

*_____, 1963: Severe local storms: A review. **Meteor. Monogr., 5,** No. 27, Amer. Meteor. Soc., Boston, MA, 1-30.

_____, 1976: Aspects of cumulonimbus study. **Bull. Amer. Meteor. Soc., 57,** 774-779.

*_____, 1980: **Clouds and Storms.** Pennsylvania State niversity Press, University Park, PA, 405 pp.

_____, and W.C. Macklin, 1959: Some aspects of a severe storm in S.E. England. **Nubila, 2,** 38-50.

MacDonald, A.E., 1976: Gusty surface winds and high level thunderstorms. NOAA NWS-Western Region Tech. Attachment No. 76-14, 5 pp.

Mack, R.A., and D.P. Wylie, 1982: An estimation of the condensation rates in three severe storm systems from satellite observations of the convective mass flux. **Mon. Wea. Rev., 110,** 725-744.

*Maddox, R.A., 1980: Mesoscale convective complexes. **Bull. Amer. Meteor. Soc., 61,** 1374-1387.

*_____, 1983: Large-scale meteorological conditions associated with mid-latitude, mesoscale convective complexes. **Mon. Wea. Rev., 111,** 1475-1493.

_____, and W. Dietrich, 1981: Synoptic conditions associated with the simultaneous occurrence of significant severe thunderstorms and flash floods. **Preprints, 4th Conf. Hydrometeorology** (Reno, NV), Amer. Meteor. Soc., 181-187.

*_____, and C.A. Doswell III, 1982: An examination of jet stream configurations, 500 mb vorticity advection and low level thermal advection patterns during extended periods of intense convection. **Mon. Wea. Rev., 110,** 184-197.

*_____, C.F. Chappell, L.R. Hoxit, and F. Caracena, 1978: Comparison of meteorological aspects of the Big Thompson and Rapid City flash floods. **Mon. Wea. Rev., 106,** 375-389.

*_____, _____, and _____, 1979: Synoptic and mesoscale aspects of flash flood events. **Bull. Amer. Meteor. Soc., 60,** 115-123.

*_____, L.R. Hoxit, and C.F. Chappell, 1980a: A study of tornadic thunderstorm interactions with thermal boundaries. **Mon. Wea. Rev., 108,** 322-336.

_____, F. Canova, and L.R. Hoxit, 1980b: Meteorological characteristics of flash flood events over the western United States. **Mon. Wea. Rev., 108,** 1866-1877.

_____, D.J. Perkey, and J.M. Fritsch, 1981: Evolution of upper tropospheric features during the development of a mesoscale convective complex. **J. Atmos. Sci., 38,** 1664-1674.

*Magor, B.W., 1959: Meso-analysis: Some operational analysis techniques utilized in tornado forecasting. **Bull. Amer. Meteor. Soc., 40,** 499-511.

*Mahrt, L., 1977: Influence of low-level environment on severity of High Plains moist convection. **Mon. Wea. Rev., 105,** 1315-1329.

_____, and D. Pierce, 1980: Relationship of moist convection to boundary-layer properties: Application to a semiarid region. **Mon. Wea. Rev., 108,** 1810-1815.

Malkus, J.S., and R.S. Scorer, 1955: The erosion of cumulus towers. **J. Meteor., 12,** 43-57.

Marshall, T.P., and E.N. Rasmussen, 1982: The mesocyclone evolution of the Warren, Oklahoma tornadoes. **Preprints, 12th Conf. Severe Local Storms** (San Antonio, TX), Amer. Meteor. Soc., 375-378.

_____, and J.R. McDonald, 1983: An engineering assessment of structural damage in the Altus, OK tornado: May 11, 1982. **Preprints, 13th Conf. Severe Local Storms** (Tulsa, OK), Amer. Meteor. Soc., 66-69.

_____, _____, and K.C. Mehta, 1983: Utilization of load and resistance statistics in a wind speed assessment. Institute for Disaster Research, doc. #67D, Texas Tech. Univ., Lubbock, TX, 91 pp.

*Marwitz, J.D., 1972a: The structure and motion of severe hailstorms. Part I: Supercell storms. **J. Appl. Meteor., 11,** 166-179.

*_____, 1972b: The structure and motion of severe hailstorms. Part II: Multicell storms. **J. Appl. Meteor., 11,** 180-188.

*_____, 1972c: The structure and motion of severe hailstorms. Part III: Severely sheared storms. **J. Appl. Meteor., 11,** 189-201.

_____, 1972d: Precipitation efficiency of thunderstorms on the High Plains. **J. Rech. Atmos., 6,** 367-370.

Mason, B.J., 1959: The formation of rain by coalescence in very shallow cumulus. **Tellus, 11,** 216-219.

McCann, D.W., 1983: Synoptic patterns associated with splitting thunderstorms. **Preprints, 13th Conf. Severe Local Storms** (Tulsa, OK), Amer. Meteor. Soc., J1-J4.

McCarthy, J., 1974: Field verification of the relationship between entrainment rate and cumulus cloud diameter. **J. Atmos. Sci., 31,** 1028-1039.

_____, and D.L. Veal, 1982: Observations from instrumented aircraft. **Thunderstorms: A Social, Scientific and Technological Documentary. Vol. 3: Instruments and Techniques for Thunderstorm Observation and Analysis** (E. Kessler, Ed.), NOAA/ERL, 47-76.

McDonald, J.E., 1958: The physics of cloud modification. **Adv. Geophys., 5,** 223-303.

McGuire, E.L., 1962: The vertical structure of three drylines as revealed by aircraft traverses. National Severe Storms Lab. Report No. 7, [NTIS Accession No. PB-168213], 10 pp.

McNulty, R.P., D.L. Kelly, and J.T. Schaefer, 1979: Frequency of tornado occurrence. **Preprints, 11th Conf. Severe Local Storms** (Kansas City, MO), Amer. Meteor. Soc., 222-226.

Merritt, L.P., K.E. Wilk, and M.L. Weible, 1974: Severe rainstorm at Enid, Oklahoma -- October 10, 1973. NOAA Tech. Memo. ERL NSSL-73 [NTIS Accession No. COM-75-10583/AS], 50 pp.

Miller, L.J., and J.C. Fankhauser, 1983: Radar echo structure, air motion and hail formation in a large stationary multicellular thunderstorm. **J. Atmos. Sci., 40,** 2399-2418.

Miller, M.J., 1974: On the use of pressure as a vertical co-ordinate in modelling convection. **Quart. J. Roy. Meteor. Soc., 100,** 155-162.

*Minor, J.E., J.R. McDonald, and K.C. Mehta, 1977: The tornado: An engineering-oriented perspective. NOAA Tech. Memo. ERL NSSL-82 [NTIS Accession No. PB-281860/AS], 196 pp.

Mitchell, D.L., and E.M. Agee, 1977: A theoretical investigation of atmospheric convective modes as a function of Rayleigh number, Prandtl number and eddy anisotropy. **J. Meteor. Soc. Japan, 55,** 341-363.

Mitchell, K.E., and J.B. Hovermale, 1977: A numerical investigation of the severe thunderstorm gust front. **Mon. Wea. Rev., 105,** 657-675.

Mogil, H.M., 1977: Lightning -- An update. **Preprints, 10th Conf. Severe Local Storms** (Omaha, NE), Amer. Meteor. Soc., 226-230.

Moller, A.R., 1979: The climatology and synoptic meteorology of southern plains' tornado outbreaks. Master's Thesis, Univ. of Oklahoma, Norman, OK, 70 pp.

_____, C. Doswell, J. McGinley, S. Tegtmeier, and R. Zipser, 1974: Field observations of the Union City tornado in Oklahoma. **Weatherwise, 27,** 68-77.

_____, and C. A. Doswell III, 1985: Observational evidence for a type of modified supercell thunderstorm. **Mon. Wea. Rev., 113** (manuscript in preparation).

*Moncrieff, M.W., and J.S.A. Green, 1972: The propagation of steady convective overturning in shear. **Quart. J. Roy. Meteor. Soc., 98,** 336-352.

Mooney, L.E., 1983: Application and implications of fatality statistics to the flash flood problem. **Preprints, 5th Conf. Hydrometeorology** (Tulsa, OK), Amer. Meteor. Soc., 127-129.

Moore, C.B., and B. Vonnegut, 1977: The thundercloud. **Lightning. Vol I: The Physics of Lightning** (R.H. Golde, Ed.), Academic Press, New York, 51-98.

Mordy, W., 1959: Computations of the growth by condensation of a population of cloud droplets. **Tellus, 11,** 16-44.

*Morton, B.R., 1966: Geophysical vortices. **Progress in Aeronautical Sciences, 7,** Pergamon Press, New York, NY, 145-193.

Nelson, S.P., 1976: Characteristics of multicell and supercell hailstorms in Oklahoma. **Proceedings, 2nd WMO Conf. on Wea. Modification,** WMO-443 (Boulder, CO), 335-340.

_____, 1977: Rear flank downdraft: A hailstorm intensification mechanism. **Preprints, 10th Conf. Severe Local Storms** (Omaha, NE), Amer. Meteor. Soc., 521-525.

_____, 1980: A study of hail production in a supercell storm using a Doppler derived wind field and a numerical hail growth model. NOAA Tech. Memo. ERL NSSL-89 [NTIS Accession No. PB81-178220], 90 pp.

* _____, 1983: The influence of storm flow structure on hail growth. **J. Atmos. Sci., 40,** 1965-1983.

_____, and R.A. Brown, 1982: Multiple Doppler radar derived vertical velocities in thunderstorms. NOAA Tech. Memo. ERL NSSL-94 [NTIS Accession No. PB83-152553], 21 pp.

_____, and N.C. Knight, 1982: Variations in hailstone growth in a supercell storm. **Preprints, 12th Conf. Severe Local Storms** (San Antonio, TX), Amer. Meteor. Soc., 5-8.

_____, and S.K. Young, 1979: Characteristics of Oklahoma hailfalls and hailstorms. **J. Appl. Meteor., 18,** 339-347.

*Newton, C.W., 1950: Structure and mechanism of the pre-frontal squall line. **J. Meteor., 7,** 210-222.

* _____, 1963: Dynamics of severe convective storms. **Meteor. Monogr., 5,** No. 27, Amer. Meteor. Soc., Boston, MA, 33-58.

_____, 1966: Circulations in large sheared cumulonimbus. **Tellus, 18,** 699-712.

*_____, and J.C. Fankhauser, 1975: Movement and propagation of multicellular convective storms. **Pure Appl. Geophys., 113,** 748-764.

*_____, and H.R. Newton, 1959: Dynamical interactions between large convective clouds and environment with vertical shear. **J. Meteor., 16,** 483-496.

Nolen, R.H., 1959: A radar pattern associated with tornadoes. **Bull. Amer. Meteor. Soc., 40,** 277-279.

*Ogura, Y., 1963: The evolution of a moist convective element in a shallow, conditionally unstable atmosphere: A numerical calculation. **J. Atmos. Sci., 20,** 407-424.

_____, and T. Takahashi, 1971: Numerical simulation of the life cycle of a thunderstorm cell. **Mon. Wea. Rev., 99,** 895-911.

Ooyama, K., 1969: Numerical simulation of the life cycle of tropical cyclones. **J. Atmos. Sci., 26,** 3-40.

Orville, H.D., and J.-M. Chen, 1982: Effects of cloud seeding, latent heat of fusion, and condensate loading on cloud dynamics and precipitation evolution: A numerical study. **J. Atmos. Sci., 39,** 2807-2827.

_____, and L.J. Sloan, 1970: A numerical simulation of the life history of rainstorms. **J. Atmos. Sci., 27,** 1148-1159.

Orville, R.E., and D.W. Spencer, 1979: Global lightning flash frequency. **Mon. Wea. Rev., 107,** 934-943.

_____, R.W. Henderson, and L.F. Bosart, 1983: An east coast lightning detection network. **Preprints, 5th Symp. Meteor. Observations and Instrumentation** (Toronto, Ont. Canada), Amer. Meteor. Soc., 520-525.

Palmén, E., and C.W. Newton, 1969: **Atmospheric Circulation Systems.** Academic Press, 603 pp.

*Paluch, I.R., 1979: The entrainment mechanism in Colorado cumuli. **J. Atmos. Sci., 36,** 2462-2478.

Pearson, A.D., and J.A. Miller, 1971: The tornado season of 1970. **Weatherwise, 24,** 12-17.

Petersen, R.A., L.W. Uccellini, D. Chesters, A. Mostek, and D. Keyser, 1982: The use of VAS satellite data in weather analysis, prediction and diagnosis. **Preprints, 9th Conf. Wea. Forecasting and Analysis** (Seattle, WA), Amer. Meteor. Soc., 219-226.

Peterson, R.E., 1976: In pursuit of dust devils. **Weatherwise, 29,** 184-189.

Prandtl, L., and O.G. Tietjens, 1934: **Fundamentals of Hydro- and Aeromechanics.** Dover Publications (1957), New York, 270 pp.

*Porter, J.M., L.L. Means, J.E. Hovde, and W.B. Chappell, 1955: A synoptic study on the formation of squall lines in the North Central United States. **Bull. Amer. Meteor. Soc., 36,** 390-396.

Prosser, N.E., 1964: Aerial photographs of a tornado path in Nebraska, May 5, 1964. **Mon. Wea. Rev., 92,** 593-598.

Purdom, J.F.W., 1971: Satellite imagery and severe weather warnings. **Preprints, 7th Conf. Severe Local Storms** (Kansas City, MO), Amer. Meteor. Soc., 120-137.

Rao, D.V., 1981: Predicting precipitation events: Gumbel vs. Log Pearson. **Preprints, 4th Conf. Hydrometeorology** (Reno, NV), 56-63.

Rasmussen, E.N., 1982: The Tulia outbreak storm: Mesoscale evolution and photogrammetric analysis. M.S. Thesis, Texas Tech. Univ., Lubbock, TX, 180 pp.

_____, and R.B. Wilhelmson, 1983: Relationships between storm characteristics and 1200 GMT hodographs, low-level shear, and stability. **Preprints, 13th Conf. Severe Local Storms** (Tulsa, OK), Amer. Meteor. Soc., J5-J8.

Ray, P.S., J. Weaver, and NSSL Staff, 1977: 1977 Spring program summary. NOAA Tech. Memo. ERL NSSL-84 [NTIS Accession No. PB-2849531AS], 173 pp.

_____, B.C. Johnson, K.W. Johnson, J.S. Bradberry, J.T. Stephens, K.K. Wagner, R.B. Wilhelmson, and J.B. Klemp, 1981: The morphology of several tornadic storms on 20 May 1977. **J. Atmos. Sci., 38,** 1643-1663.

Raymond, D.J., 1975: A model for predicting the movement of continuously propagating convective storms. **J. Atmos. Sci., 32,** 1308-1317.

_____, 1979: A two-scale model of moist, non-precipitating convection. **J. Atmos. Sci., 36,** 816-831.

Resnick, R., and D. Halliday, 1966: **Physics (Part I).** John Wiley and Sons, Inc., New York, 646 pp.

Reynolds, D.W., 1982: Prototype workstation for mesoscale forecasting: A look to the 1990's. **Preprints, 9th Conf. Wea. Forecasting and Analysis** (Seattle, WA), Amer. Meteor. Soc., 65-71.

Robb, A.D., 1959: Severe hail, Selden, Kansas, June 3, 1959. **Mon. Wea. Rev., 87,** 301-303.

Rooth, C., 1960: A statistical study of cloud droplet growth by condensation. **Physics of Precipitation** (H. Weickman, Ed.), Amer. Geophys. Union, Washington, D.C., 220-225.

Rosenthal, S.L., 1978: Numerical simulation of tropical cyclone development with latent heat release by the resolvable scales. I: Model description and preliminary results. **J. Atmos. Sci., 35,** 258-271.

Rotunno, R., 1979: A study on tornado-like vortex dynamics. **J. Atmos. Sci., 36,** 140-155.

_____, 1981: On the evolution of thunderstorm rotation. **Mon. Wea. Rev., 109,** 577-586.

*_____, 1982: A numerical simulation of multiple vortices. **Topics in Atmospheric and Oceanographic Sciences: Intense Atmospheric Vortices** (Bengtsson/Lighthill, Eds.), Springer-Verlag, Berlin, 215-227.

_____, 1984: Tornadoes and tornadogenesis. In Vol. 3, AMS Short Course on Mesoscale Meteorology, Amer. Meteor. Soc., Boston (in press).

*_____, and J.B. Klemp, 1982: The influence of the shear-induced pressure gradient on thunderstorm motion. **Mon. Wea. Rev., 110,** 136-151.

_____, and _____, 1983: A theory for the wall cloud. **Preprints, 13th Conf. Severe Local Storms** (Tulsa, OK), Amer. Meteor. Soc., 241-244.

*_____, and _____, 1985: On the rotation and propagation of simulated supercell thunderstorms. **J. Atmos. Sci., 42** (in press).

Roys, G.P., and E. Kessler, 1966: Measurements by aircraft of condensed water in Great Plains thunderstorms. ESSA Tech. Note 49-NSSP-19 [NTIS Accession No. PB-173048], 17 pp.

*Rust, W.D., W.L. Taylor, D.R. MacGorman, and R.T. Arnold, 1981: Research on electrical properties of severe thunderstorms in the Great Plains. **Bull. Amer. Meteor. Soc., 62,** 1286-1293.

Sasaki, Y., 1959: A numerical experiment for squall line formation. **J. Meteor., 16,** 347-353.

Schaefer, J.T., 1974: A simulative model of dryline motion. **J. Atmos. Sci., 31,** 956-964.

_____, 1975: Moisture stratification in the "well-mixed" boundary layer. **Preprints, 9th Conf. Severe Local Storms** (Norman, OK), Amer. Meteor. Soc., 45-50.

*_____, 1976: Moisture features of the convective boundary layer in Oklahoma. **Quart. J. Roy. Meteor. Soc., 102,** 447-451.

_____, and J.G. Galway, 1982: Population biases in the tornado climatology. **Preprints, 12th Conf. Severe Local Storms** (San Antonio, TX), Amer. Meteor. Soc., 51-54.

_____, D.L. Kelly, and R.F. Abbey, Jr., 1980a: Tornado track characteristics and hazard probabilities. **Wind Engineering** (J.E. Cermak, Ed.), Pergamon Press, New York, NY, 95-109.

_____, _____, C.A. Doswell III, J.G. Galway, R.J. Williams, R.P. McNulty, L.R. Lemon, and B.D. Lambert, 1980b: Tornadoes: When--Where--How Often. **Weatherwise, 33,** 52-59.

Schaefer, V.J., 1946: The production of ice crystals in a cloud of super-cooled water droplets. **Science, 104,** 457-459.

Schlesinger, R.E., 1973: A numerical model of moist deep convection. Part I: Comparative experiments for variable ambient moisture and wind shear. **J. Atmos. Sci., 30,** 835-850.

_____, 1975: A three-dimensional numerical model of an isolated deep convective cloud: Preliminary results. **J. Atmos. Sci., 32,** 934-957.

*_____, 1978: A three-dimensional numerical model of an isolated thunderstorm. Part I: Comparative experiments for variable ambient wind shear. **J. Atmos. Sci., 35,** 690-713.

*_____, 1980: A three-dimensional numerical model of an isolated thunderstorm. Part II: Dynamics of updraft splitting and mesovortex couplet evolution. **J. Atmos. Sci., 37,** 395-420.

*_____, 1982: Three-dimensional numerical modeling of convective storms: A review of milestones and challenges. **Preprints, 12th Conf. Severe Local Storms** (San Antonio, TX), Amer. Meteor. Soc., 506-515.

_____, 1983a: The anelastic pressure perturbation in strongly sheared convective storms: Two versus three dimensions. **Preprints, 13th Conf. Severe Local Storms** (Tulsa, OK), Amer. Meteor. Soc., 227-230.

_____, 1983b: Mature thunderstorm cloud top structure: Three-dimensional numerical simulation versus satellite observations. **Preprints, 13th Conf. Severe Local Storms** (Tulsa, OK), Amer. Meteor. Soc., 512-515.

Schwiesow, R.L., R.E. Cupp, M.J. Post, R.F. Abbey, Jr., and P.C. Sinclair, 1977: Velocity structures of waterspouts and dust devils as revealed by Doppler lidar measurements. **Preprints, 10th Conf. Severe Local Storms** (Omaha, NE), Amer. Meteor. Soc., 116-119.

Scofield, R.A., and L.E. Spayd, Jr., 1983: Operationally detecting flash flood producing thunderstorms which have subtle heavy rainfall signatures in GOES imagery. **Preprints, 5th Conf. Hydrometeorology** (Tulsa, OK), Amer. Meteor. Soc., 190-197.

Scorer, R.S., 1957: Experiments on convection of isolated masses of buoyant fluid. **J. Fluid Mech., 2,** 583-594.

_____, and F.H. Ludlam, 1953: The bubble theory of penetrative convection. **Quart. J. Roy. Meteor. Soc., 79,** 96-103.

_____, and C. Ronne, 1956: Experiments with convective bubbles. **Weather, 11,** 151-154.

Scott, W.T., 1968: Analytical studies of cloud droplet coalescence. **J. Atmos. Sci., 25,** 54-65.

Seitter, K.L., and H.-L. Kuo, 1983: The dynamical structure of squall-line type thunderstorms. **J. Atmos. Sci., 40,** 2831-2854.

Simpson, J., 1983a: Cumulus clouds: Early aircraft observations and entrainment hypotheses. **Mesoscale Meteorology -- Theories, Observations and Models** (D.K. Lilly and T. Gal-Chen, Ed's.), D. Reidel Publishing Co., Hingham MA, 355-373.

_____, 1983b: Cumulus role in tropical circulations. **Mesoscale Meteorology — Theories, Observations and Models** (D.K. Lilly and T. Gal-Chen, Ed's.), D. Reidel Publishing Co., Hingham MA, 375-398.

_____, 1983c: Cumulus clouds: Interactions between laboratory experiments and observations as foundations for models. **Mesoscale Meteorology — Theories, Observations and Models** (D.K. Lilly and T. Gal-Chen, Ed's.), D. Reidel Publishing Co., Hingham MA, 399-412.

_____, 1983d: Cumulus clouds: Numerical models, observations and entrainment. **Mesoscale Meteorology — Theories, Observations and Models** (D.K. Lilly and T. Gal-Chen, Ed's.), D. Reidel Publishing Co., Hingham MA, 413-445.

_____, and V. Wiggert, 1969: Models of precipitating cumulus towers. **Mon. Wea. Rev., 97,** 471-489.

Skolnik, M.I., 1970: **Radar Handbook.** McGraw-Hill, New York, NY.

Snow, J.T., 1978: On inertial instability as related to the multiple vortex phenomenon. **J. Atmos. Sci., 35,** 1660-1671.

*_____, 1982: A review of recent advances in tornado vortex dynamics. **Rev. Geophys. Space Phys., 20,** 953-964.

_____, 1984: The tornado. **Sci. Amer., 250,** 86-96.

Squires, P., 1958a: The spatial variation of liquid water and droplet concentration in cumuli. **Tellus, 10,** 372-380.

*_____, 1958b: Penetrative downdraughts in cumuli. **Tellus, 10,** 381-389.

*_____, and J.S. Turner, 1962: An entraining jet model for cumulonimbus updraughts. **Tellus, 14,** 422-434.

Srivastava, R.C., and A.R. Jameson, 1977: Radar detection of hail. **Meteor. Monogr., 16,** No. 38, 269-277.

Staff, RFC, Tulsa, OK and DMO, Kansas City, MO, 1964: Cloudburst at Tulsa, Oklahoma, July 27, 1963. **Mon. Wea. Rev., 92,** 345-351.

Stommel, H., 1947: Entrainment of air into a cumulus cloud. **J. Meteor., 4,** 91-94.

Szoke, E.J., and E.J. Zipser, 1985: A radar study of convective cells in mesoscale systems in GATE. Part 2: Life cycles of convective cells. Manuscript submitted to **J. Atmos. Sci.**

_____, _____, and D.P. Jorgensen, 1985: A radar study of convective cells in mesoscale systems in GATE. Part 1: Vertical profile statistics and comparison with hurricane cells. Manuscript submitted to **J. Atmos. Sci.**

*Takeda, T., 1971: Numerical simulation of a precipitating convective cloud: The formation of a "long-lasting" cloud. **J. Atmos. Sci., 28,** 350-376.

Tennekes, H., 1978: Turbulent flow in two and three dimensions. **Bull. Amer. Meteor. Soc., 59,** 22-28.

_____, and J.L. Lumley, 1972: **A First Course in Turbulence.** MIT Press, Cambridge, 300 pp.

*Tepper, M., 1950: A proposed mechanism of squall lines: The pressure jump line. **J. Meteor., 7,** 21-29.

Thorpe, A.J., M.J. Miller, and M.W. Moncrieff, 1982: Two-dimensional convection in non-constant shear: A model of mid-latitude squall lines. **Quart. J. Roy. Meteor. Soc., 108,** 739-762.

Turman, B.N., 1979: A review of satellite lightning experiments. **Proceedings, Workshop on the Need for Lightning Observations from Space** (Tullahoma, TN), National Aeronautics and Space Administration (NASACP-1095), 61-80.

Turner, J.S., 1962: The "starting plume" in neutral surroundings. **J. Fluid Mech., 13,** 351-368.

_____, 1973: **Buoyancy Effects in Fluids.** Cambridge University Press, Cambridge, England, 367 pp.

Uccellini, L.W., 1975: A case study of apparent gravity wave initiation of severe convective storms. **Mon. Wea. Rev., 103,** 497-513.

Uman, M.A., 1969: **Lightning.** McGraw-Hill, New York, 264pp.

Vance, D.L., 1979: The geographical distribution of lightning -- Forestry and range requirements and interests. **Proceedings, Workshop on the Need for Lightning Observations from Space** (Tullahoma, TN), National Aeronautics and Space Administration (NASACP-1095), 110-114.

Velarde, M.G., and C. Normand, 1980: Convection. **Sci. Amer., 243,** 92-109.

Vonnegut, B., 1949: Nucleation of supercooled water clouds by silver iodide smokes. **Chem. Rev., 44,** 177-289.

*_____, 1960: Electrical theory of tornadoes. **J. Geophys. Res., 65,** 203-212.

_____, 1975: Comment on "On the relation of electrical activity to tornadoes." **J. Geophys. Res., 80,** 4559-4560.

Wakimoto, R.M., 1982: The life cycle of thunderstorm gust fronts as viewed with Doppler radar and rawinsonde data. **Mon. Wea. Rev., 110,** 1060-1082.

Wang, J.Y.C., 1968: On the formation and development of orographic shallow cumulus cloud. Rept. No. 11, CWB-WBG-71, Dept. of Geophys. Sci., Univ. of Chicago, Chicago, IL.

*Ward, N.B., 1972: The exploration of certain features of tornado dynamics using a laboratory model. **J. Atmos. Sci., 29,** 1194-1204.

Warner, J., 1970: On steady-state one-dimensional models of cumulus convection. **J. Atmos. Sci., 27,** 1035-1040.

Watkins, D.C., J.D. Cobine, and B. Vonnegut, 1978: Electric discharges inside tornadoes. **Science, 199,** 171-174.

*Weaver, J.F., 1979: Storm motion as related to boundary-layer convergence. **Mon. Wea. Rev., 107,** 612-619.

_____, and S.P. Nelson, 1982: Multiscale aspects of thunderstorm gust fronts and their effects on subsequent storm development. **Mon. Wea. Rev., 110,** 707-718.

Weinstein, A.I., 1970: A numerical model of cumulus dynamics and microphysics. **J. Atmos. Sci., 27,** 246-255.

*Weisman, M.L., and J.B. Klemp, 1982: The dependence of numerically simulated convective storms on vertical wind shear and buoyancy. **Mon. Wea. Rev., 110,** 504-520.

*_____, and _____, 1984a: The structure and classification of numerically simulated convective storms in directionally varying wind shears. **Mon. Wea. Rev., 112** (in press).

*_____, and _____, 1984b: Characteristics of isolated convection. In Vol. 2, AMS Short Course on Mesoscale Meteorology, Amer. Meteor. Soc., Boston (in press).

_____, _____, and L.J. Miller, 1983a: Modeling and Doppler analysis of the CCOPE 2 August supercell storm. **Preprints, 13th Conf. Severe Local Storms** (Tulsa, OK), Amer. Meteor. Soc., 223-226.

_____, _____, and J.W. Wilson, 1983b: Dynamic interpretation of notches, BWERs, and mesocyclones simulated in a numerical cloud model. **Preprints, 21st Conf. Radar Meteor.** (Edmonton, Alta), Amer. Meteor. Soc., 39-43.

*Wilhelmson, R.B., 1974: The life cycle of a thunderstorm in three dimensions. **J. Atmos. Sci., 31,** 1629-1651.

_____, and Y. Ogura, 1972: The pressure perturbation and the numerical modeling of a cloud. **J. Atmos. Sci., 29,** 1295-1307.

_____, and J.B. Klemp, 1983: Numerical simulation of severe storms within lines. **Preprints, 13th Conf. Severe Local Storms** (Tulsa, OK), Amer. Meteor. Soc., 231-234.

Wilk, K.E., and J.T. Dooley, 1980: FAA radars and their display of severe weather (thunderstorms). FAA Tech. Report No. FAA-RD-80-65, Washington, D.C., 38 pp.

_____, and S.L. Barnes, 1982: Station networks for storm observation. **Thunderstorms: A Social, Scientific and Technological Documentary. Vol. 3: Instruments and Techniques for Thunderstorm Observation and Analysis** (E. Kessler, Ed.), NOAA/ERL, 1-31.

_____, L.R. Lemon, and D.W. Burgess, 1979: Interpretation of radar echoes from severe thunderstorms: A series of illustrations with extended captions. Prepared for training FAA ARTCC Coordinators, National Severe Storms Laboratory, Norman, OK [available from authors on request], 55 pp.

_____, K. Gray, C. Clark, D. Sirmans, J. Dooley, J. Carter, and W. Bumgarner, 1976: Objectives and accomplishments of the NSSL 1975 spring program. NOAA Tech. Memo. ERL NSSL-78 [NTIS Accession No. PB-263813/AS], 47 pp.

Wilkins, E.M., Y. Sasaki, R.L. Inman, and L.T. Terrell, 1974: Vortex formation in a friction layer: A numerical simulation. **Mon. Wea. Rev., 102,** 99-114.

Williams, D.T., 1960: The role of a subsidence layer. In "The Tornadoes at Dallas, Tex., April 2, 1957," Wea. Bur. Res. Paper No. 41, 143-158,

_____, 1963: The thunderstorm wake of May 4, 1961. National Severe Storms Project Rep. No. 18, [NTIS Accession No. PB-168223], 23 pp.

Williams, R.T., 1967: Atmospheric frontogenesis: A numerical experiment. **J. Atmos. Sci., 24,** 627-641.

*Wilson, J., R. Carbone, H. Baynton, and R. Serafin, 1980: Operational application of meteorological Doppler radar. **Bull. Amer. Meteor. Soc., 61,** 1154-1168.

Wilson, J.W., and T.T. Fujita, 1979: Vertical cross section through a rotating thunderstorm by Doppler radar. **Preprints, 11th Conf. Severe Local Storms** (Kansas City, MO), Amer. Meteor. Soc., 447-452.

Wilson, T., and R. Rotunno, 1982: Numerical simulation of a laminar vortex flow. **Proceedings, Int. Conf. Computational Methods and Experimental Measurements** (Washington, D.C.), Int. Soc. for Computation Methods and Engr., 203-215.

Young, R.G.E., and K.A. Browning, 1967: Wind tunnel tests of simulated spherical hailstones with variable roughness. **J. Atmos. Sci., 24,** 58-62.

Zamora, R.J., and M.A. Shapiro, 1984: Diagnostic divergence and vorticity calculations using a network of mesoscale wind profilers. **Preprints, 10th Conf. Wea. Forecasting and Analysis** (Clearwater Beach, FL), Amer. Meteor. Soc., 386-391.

Zehr, R.M., and J.F.W. Purdom, 1982: Examples of a wide variety of thunderstorm propagation mechanisms. **Preprints, 12th Conf. Severe Local Storms** (San Antonio, TX), Amer. Meteor. Soc., 499-502.

Zeman, O., and H. Tennekes, 1977: Parameterization of the turbulent energy budget at the top of the daytime atmospheric boundary layer. **J. Atmos. Sci., 34,** 111-123.

*Zipser, E.J., 1977: Mesoscale and convective-scale downdrafts as distinct components of squall-line structure. **Mon. Wea. Rev., 105,** 1568-1589.

_____, and M.A. Lemone, 1980: Cumulonimbus vertical velocity events in GATE. Part II: Synthesis and model core structure. **J. Atmos. Sci., 37,** 2458-2469.

Zrnic', D.S., and R.J. Doviak, 1975: Velocity spectra of vortices scanned with a pulse-Doppler radar. **J. Appl. Meteor., 14,** 1531-1539.

_____, and M. Istok, 1980: Wind speeds in two tornadic storms and a tornado, deduced from Doppler spectra. **J. Appl. Meteor., 19,** 1405-1415.

APPENDIX

LOGGING PROCEDURES

I. The following events will be considered as "severe weather events" and will be coded and logged on the activity chart by sequential number:

A. Hail

1. Any report of hail 3/4" in diameter or larger occurring either at the surface or aloft [e.g., 1 1/2" HAIL or 1 1/2" HAIL ALF]

2. Hail breaking out windows or windshields, or damaging roofs [e.g., HAIL DAMAGE]

3. Hail the size of the following objects:

   a. Penny - 3/4" diameter
   b. Dime - 3/4"diameter
   c. Nickel - 1" diameter
   d. Quarter - 1" diameter
   e. Anthony dollar - 1 1/4" diameter
   f. Half dollar - 1 1/4" diameter
   g. Walnut - 1 1/2" diameter
   h. Golfball - 1 3/4" diameter
   i. Hen egg - 2" diameter
   j. Tennis ball - 2 1/2" diameter
   k. Baseball - 2 3/4" diameter
   l. Tea cup - 3" diameter
   m. Grapefruit - 4" diameter
   n. Softball - 4 1/2" diameter

4. Hail the size of any object that has an estimated diameter of 3/4" or greater

B. Wind (Convective)*

1. Official convective wind gusts of 50 kt or greater

2. Estimated convective wind gusts of 50 kt (58 mph) or greater

---

* For logging purposes, a convective gust is defined as any gust of 50 kt or greater that is associated with thunderstorm activity and is (1) accompanied by thunder at the station or (2) occurs at the station at the same time that lightning is being observed, or (3) thunder occurs at the station within 1/2 hour after the gust occurs. Post-storm depression winds are not logged unless one of the above criteria is met.

3. Specific wind damage (convectively induced), including:

   a. Trees down
   b. Large limbs (branches) down (more than one)
   c. Power lines down from wind
   d. Roof damage
   e. Man-made structures (house, barn, shed, circus tent, etc.) damaged or destroyed
   f. Windows broken by wind
   g. Permanent signs blown down
   h. Radio tower or large antenna blown down
   i. Home TV antenna blown down (more than one)

C. **Tornadoes**, including:

1. Any waterspout that moves ashore
2. Any tornado that is called a "waterspout" because it happens to be over a water body

II. The following events will be logged on the activity chart (without a sequential number) but will **not** be coded for archiving:

A. Funnel cloud
B. Any waterspout associated with warm water sources (i.e., Gulf of Mexico in summer; Great Lakes in fall and winter)

III. The following events will **not** be logged **or** coded:

A. **Hail**

1. Hail smaller than 3/4" in diameter
2. "Large" hail (no size given)
3. Mothball-size hail (considered 1/2")
4. Marble-size hail (considered 1/2")
5. Hail larger than marbles (considered less than 3/4")
6. Hail damage to crops (no size given)

B. **Wind (Convective)**

1. Official convective wind gusts less than 50 kt
2. Estimated convective winds less than 50 kt (58 mph)
3. Wind damage (non-specific)
4. Damaging winds (non-specific)
5. Estimated winds of 50 to 60 mph**
6. Limbs (branches) down
7. Tree damage

C. **Funnel Clouds**

1. "Unconfirmed" funnel cloud
2. "Possible" funnel cloud

** When considering a **range** of **estimated** wind speeds, take an average estimated speed (i.e., 50 to 60 mph = 55 mph avg).

D. Tornado -- "Indicated by radar"

IV. Space and time density of logged severe weather events:

In general, a severe weather event should not be logged within 10 miles of a previously logged event of the same type, if the second event has occurred within 1/2 hour of the previously logged event. Exceptions to this rule would include:

A. Tornadoes documented as separate events (multiple suction vortices should be logged as one event).

B. Significant severe weather events involving injuries, deaths, and/or spectacular damage should be logged regardless of time and distance of earlier event. This may be done by replacing earlier event with more significant event or by adding the significant event notations to the previously logged event.

C. All official convective wind gusts exceeding 50 kt should be logged regardless of space density.

SMOOTHING THE SELS LOG

The object of "smoothing" the NSSFC severe weather data record is to add reports that are not already included in the record, to weed out duplicate and/or erroneous reports, and to correct errors in time of occurrence, location, or type of event.

Starting with the June 1979 data please follow these procedures to "smooth" the severe weather record for the station -- you need to cross-check the following:

SELS rough log summary sheets (lists SELS cards)
SELS activity chart
Storm Data sheets (from WSFO)
FPP Tornado Data Sheet (from WSFO)
Radar Charts

Use the SELS rough log summary sheets as work sheets for changes and comments as you go.

1. The SELS rough log summary sheets should include all reports listed on the activity chart. CROSS CHECK.

2. The FPP Tornado Data Sheets are usually only a partial listing of the reports listed in the states' corresponding **Storm Data** entries. However, the reports that are listed on the FPP Tornado Data Sheets should agree with the entries in **Storm Data.** CROSS CHECK.

3. The FPP Tornado Data Sheets should include all tornadoes listed in **Storm Data.** CROSS CHECK!!! The **Storm Data** entries are the **final** authority on verifying tornadoes. The SELS cards must agree with Storm Data concerning tornadoes. If the SELS rough log lists a tornado and **Storm Data** does not verify it, the SELS card must be either discarded or changed to wind damage -- depending on the evidence at hand (i.e., if damage was indicated at that location either by the activity chart entry or by an entry in **Storm Data,** then the tornado report should be changed to wind damage).

5. Concerning wind damage and hail reports: As a general rule widespread wind damage reports from a single storm should not be logged denser than a ten mile or 20 minutes spacing between reports (similarly for hailstorms). In cases where **Storm Data** gives a list of counties with wind damage (or hail) log a report at each county seat. The western states with large counties would necessitate a different method to approach more closely the "ten mile" density.

☆ U.S. GOVERNMENT PRINTING OFFICE:1988-573-002/80522